

**Oxygen regulation and redox control of
magnetosome biomineralization in
*Magnetospirillum gryphiswaldense***

Dissertation
der Fakultät für Biologie
der
Ludwig-Maximilians-Universität München



Yingjie Li

München
26.02.2014

Erstgutachter: Prof. Dr. Dirk Schüler

Zweitgutachter: PD Dr. Susanne Gebhard

Tag der Einreichung: February 26th 2014

Tag der mündlichen Prüfung: March 25th 2014

Publications and manuscripts originating from this thesis

Chapter 2

Li Y, Katzmann E, Borg S, Schüler D. 2012. The periplasmic nitrate reductase Nap is required for anaerobic growth and involved in redox control of magnetite biomineralization in *Magnetospirillum gryphiswaldense*. *J. Bacteriol.* **194**:4847-4856.

Chapter 3

Li Y, Bali S, Borg S, Katzmann E, Ferguson SJ, Schüler D. 2013. Cytochrome *cd*₁ nitrite reductase NirS is involved in anaerobic magnetite biomineralization in *Magnetospirillum gryphiswaldense* and requires NirN for proper *d*₁ heme assembly. *J. Bacteriol.* **195**:4297-4309.

Chapter 4

Li Y, Sabaty M, Borg S, Silva KT, Pignol D, Schüler D. 2014. The oxygen sensor MgFnr controls magnetite biomineralization by regulation of denitrification in *Magnetospirillum gryphiswaldense*. Submitted.

Chapter 5

Li Y, Raschdorf O, Silva KT, Schüler D. 2014. The terminal oxidase *cbb*₃ functions as an O₂ sensor to control redox balance for magnetite biomineralization in *Magnetospirillum gryphiswaldense*. In preparation.

ABBREVIATIONS

aa	Amino acid
CM	Cytoplasmic membrane
EcFnr	Fnr from <i>Escherichia coli</i>
Fnr	Fumarate and nitrate reductase regulation
Fur	Ferric uptake regulator
HCOs	Heme-copper oxidases
MAI	Magnetosome island
Mam	Magnetosome membrane proteins
MgFnr	Fnr from <i>Magnetospirillum gryphiswaldense</i>
MM	Magnetosome membrane
Mms	Magnetic particle membrane-specific proteins
MSR-1	<i>Magnetospirillum gryphiswaldense</i>
MTB	Magnetotactic bacteria
Nap	Periplasmic nitrate reductase
Nir	Nitrite reductase
Nor	Nitric oxide reductase
Nos	Nitrous oxide reductase
OD	Optical density
OM	Outer membrane
SDS-PAGE	Sodium dodecyl sulphate – polyacrylamide gel electrophoresis
TEM	Transmission electron microscopy
TMBZ	<i>N, N, N', N'</i> -tetramethylbenzidine

SUMMARY

Magnetosomes of many magnetotactic bacteria consist of membrane-enveloped magnetite crystals, which are known to be only synthesized under suboxic conditions with a low redox potential. However, the cellular redox processes governing the biomineralization of the mixed-valence iron oxide magnetite (Fe_3O_4) have remained unknown. Therefore, in this thesis we set out to investigate whether electron transport chains are involved in redox control required for magnetosome formation. First, the relationship between denitrification and magnetite biomineralization in *Magnetospirillum gryphiswaldense* was analyzed. A complete denitrification pathway for nitrate (*nap*), nitrite (*nirS*), nitric oxide (*norCB*), and nitrous oxide reduction (*nosZ*) was identified, and it was shown that nitrate is the only electron acceptor supporting anaerobic growth. Analyses of transcriptional *gusA* reporter fusions revealed that, except for *nap*, highest expression of other denitrification genes coincided with conditions permitting maximum magnetite synthesis. Deletion of *nap* genes encoding a periplasmic nitrate reductase, but not *nirS*, *norCB* or *nosZ*, not only abolished anaerobic growth, but also delayed aerobic growth. Furthermore, magnetite biomineralization was shown to be linked to dissimilatory nitrate reduction. While loss of *nosZ* or *norCB* had no or relatively weak effects on magnetosome synthesis, deletion of *nap* severely impaired magnetite biomineralization and resulted in the biosynthesis of fewer, smaller and irregular crystals during denitrification and also aerobic respiration, probably by disturbing the proper redox balance required for magnetite synthesis. Effective nitrite reduction catalyzed by NirS was also required for the biomineralization of WT crystals, probably by contributing to the oxidation of ferrous iron under oxygen-limited conditions. Loss of *nirS* impaired magnetosome formation and caused the biosynthesis of smaller, fewer and aberrantly shaped magnetite crystals during denitrification.

In *M. gryphiswaldense* a magnetobacterial Fnr-like (Fumarate and nitrate reductase regulation) protein MgFnr was identified and shown to mediate the oxygen-responsive expression of denitrification genes. Deletion of *Mgfnr* not only caused reduced N_2O reductase activity, but also impaired magnetite biomineralization under microaerobic conditions in the presence of nitrate. Overexpression of MgFnr in the WT also caused the synthesis of smaller

magnetite particles under anaerobic and microaerobic conditions in the presence of nitrate. Altogether, these data suggest that proper expression of MgFnr is required for the synthesis of WT-like magnetosomes, which is regulated by MgFnr itself and oxygen.

In addition to denitrification, *M. gryphiswaldense* is also capable of aerobic respiration using oxygen as electron acceptor and possesses multiple terminal oxidases, including two heme-copper oxidases *aa₃* and *cbb₃* and a *bd*-type quinol oxidase. The oxidases *cbb₃* and *bd* were shown to be required for aerobic respiration, while the *aa₃* oxidase had no physiological significance for oxygen reduction under test conditions. Loss of both oxidases *cbb₃* and *bd* completely abolished microaerobic and aerobic growth even in the presence of nitrate, suggesting that aerobic respiration is a prerequisite for microaerobic denitrification. While loss of the *bd* oxidase had no effects on growth and magnetosome synthesis, inactivation of *cbb₃* oxidase caused pleiotropic effects under microaerobic conditions in the presence of nitrate. In addition to causing inability of simultaneous denitrification and aerobic respiration, loss of *cbb₃* oxidase resulted in complex biomineralizing phenotypes and aberrant cell morphologies, probably by disturbing the proper redox balance required for metabolism and magnetite biomineralization.

In conclusion, this work provided evidence that in MSR-1 in addition to the various essential and accessory proteins encoded within the genomic magnetosome island, genes outside the magnetosome island are also involved in magnetite biomineralization. By participating in redox reactions required for magnetite biomineralization, denitrification and aerobic respiration have a key role in the synthesis of WT-like magnetosomes.

ZUSAMMENFASSUNG

Die Magnetosomen vieler magnetotaktischer Bakterien bestehen aus membranumhüllten Magnetitkristallen, deren Synthese durch ein niedriges Redoxpotential gefördert wird. Die zellulären Redox-Prozesse, welche die Biomineralisation des gemischtvalenten Eisenoxids antreiben sind bislang jedoch nicht bekannt. In der vorliegenden Arbeit wurde daher zuerst die Abhängigkeit der Magnetitbiomineralisation von der Denitrifikation in *Magnetospirillum gryphiswaldense* untersucht. Dabei wurde der komplette Denitrifikationsweg für Nitrat (*nap*), Nitrit (*nirS*), Stickstoffmonoxid (*norCB*) und Distickstoffmonoxid (*nosZ*) identifiziert. Wachstum in der Abwesenheit von Sauerstoff als Elektronenakzeptor ermöglicht jedoch nur Nitrat. Durch transkriptionale *gusA*-Fusionen konnte gezeigt werden, dass unter optimalen Magnetosomen-synthesebedingungen mit Ausnahme von *nap* alle Denitrifikationsgene maximal exprimiert werden. Die Deletion der *nap* Gene, die eine periplasmatische Nitratreduktase codieren, aber nicht die Deletion von *nirS*, *norCB* oder *nosZ* verhinderte anaerobes Wachstum und verzögerte aerobes Wachstum. Weiterhin konnte gezeigt werden, dass Magnetitbiomineralisation auch mit der dissimilatorischen Nitratreduktion verbunden ist. Während der Verlust von *nosZ* oder *norCB* keine, bzw. nur eine schwache Auswirkung auf die Magnetosomensynthese zeigte, führte die Deletion von *nap* zu einer starken Beeinträchtigung der Biomineralisation. Sowohl unter anaeroben als auch mikroaeroben Bedingungen bildete die *nap* Deletionsmutante weniger, kleinere und irreguläre Kristalle als der Wildtyp. Dies kann wahrscheinlich mit einer Störung der für die Magnetosomensynthese benötigten Redox-Balance begründet werden. Daneben ist aber auch eine effektive, durch NirS katalysierte, Nitritreduktion für die Biomineralisation von Wildtyp Kristallen essentiell. Eine *nirS* Deletionsmutante bildete während der Nitratreduktion kleinere, weniger und unregelmäßig geformte Magnetitkristalle. Letzteres ist eventuell auf die Beteiligung von NirS an der Eisen(II)oxidation unter sauerstofflimitierenden Bedingungen zurückzuführen.

In *M. gryphiswaldense* wurde ein magnetobakterielles (Fumarate and nitrate reductase regulation) FNR-ähnliches Protein (MgFnr) identifiziert, das an der Sauerstoff-abhängigen Expression der Denitrifikationsgene beteiligt ist. Die Deletion von MgFnr führte nicht nur zu einer verringerten N₂ Bildung aufgrund reduzierter N₂O-Reduktase-Aktivität, sondern unter

mikroaeroben Bedingungen in Gegenwart von Nitrat auch zu einer beeinträchtigten Magnetitbiomineralisation. Überexpression von MgFnr im WT in Gegenwart von Nitrat verursachte die Synthese von kleineren Magnetitpartikeln unter anaeroben als auch mikroaeroben Bedingungen. Diese Daten legen nahe, dass eine balancierte Expression von MgFnr für die Synthese von WT-ähnlichen Magnetosomen erforderlich ist.

Neben der Denitrifikation ist *M. gryphiswaldense* auch in der Lage Sauerstoff als terminalen Elektronenakzeptor zur Energiegewinnung zu verwenden. Dazu besitzt *M. gryphiswaldense* mehrere terminale Oxidasen wie die Häm-Kupfer-Oxidasen *aa₃* und *cbb₃* als auch die Chinoloxidase vom *bd*-Typ. Während die Oxidasen *cbb₃* und *bd* für aerobe Atmung erforderlich sind, hat die *aa₃* Oxidase unter den getesteten Bedingungen keine physiologische Bedeutung für die Sauerstoffreduktion. Die Co-Deletion der *cbb₃* und *bd* Oxidasen führte in Gegenwart von Nitrat zu einem vollständigen Verlust mikroaeroben und aeroben Wachstums, weshalb aerobe Atmung vermutlich eine Voraussetzung für mikroaerobe Denitrifikation ist. Während der Verlust der *bd* Oxidase keine Auswirkungen auf Wachstum und Magnetosomensynthese hatte, verursachte die Inaktivierung der *cbb₃* Oxidase pleiotrophe Effekte unter mikroaeroben Bedingungen in Gegenwart von Nitrat. Neben der Unfähigkeit zur simultanen Denitrifikation und aeroben Atmung, verursachte der Verlust der *cbb₃* Oxidase komplexe Biomineralisations-phänotypen und anormale Zellmorphologien, welche wahrscheinlich durch ein verändertes Redox-Gleichgewicht hervorgerufen wurden.

Zusammenfassend lieferte die vorliegende Studie Hinweise darauf, dass in MSR-1 neben den essentiellen und akzessorischen Proteinen die innerhalb der genomischen Magnetosomeninsel kodiert sind, auch Gene außerhalb der genomischen Magnetosomeninsel an der Magnetitbiomineralisation beteiligt sind. Durch die Teilnahme an Redox-Reaktionen die für Magnetitbiomineralisation erforderlich sind, spielen die aerobe Atmung sowie die Denitrifikation eine wichtige Rolle bei der Synthese von Wildtyp-ähnlichen Magnetosomen.

INDEX

PUBLICATIONS AND MANUSCRIPTS	i
ABBREVIATIONS	ii
SUMMARY	iii
ZUSAMMENFASSUNG	v
INDEX	vii
CHAPTER 1	1
INTRODUCTION	
1.1 <i>The magnetotactic bacterium Magnetospirillum gryphiswaldense</i>	1
1.2 <i>Molecular mechanism of magnetosome formation in MSR-1</i>	2
1.3 <i>Respiratory pathways in magnetospirilla</i>	6
1.4 <i>Regulation of respiration from aerobic to anaerobic conditions</i>	10
1.5 <i>Aims of this work</i>	11
1.6 <i>References</i>	13
CHAPTER 2	21
The periplasmic nitrate reductase Nap is required for anaerobic growth and involved in redox control of magnetite biomineralization in <i>Magnetospirillum gryphiswaldense</i>	
CHAPTER 3	41
Cytochrome <i>cd</i> ₁ nitrite reductase NirS is involved in anaerobic magnetite biomineralization in <i>Magnetospirillum gryphiswaldense</i> and requires NirN for proper <i>d</i> ₁ heme assembly	
CHAPTER 4	65
The oxygen sensor MgFnr controls magnetite biomineralization by regulation of denitrification in <i>Magnetospirillum gryphiswaldense</i>	
CHAPTER 5	93
The terminal oxidase <i>cbb</i> ₃ functions as an O ₂ sensor to maintain redox balance for magnetite biomineralization in <i>Magnetospirillum gryphiswaldense</i>	
CHAPTER 6	123

DISCUSSION

6.1 Denitrification is involved in redox control of magnetite biomineralization 123

6.2 Oxygen respiration is linked to magnetite biomineralization..... 126

6.3 Regulation of respiration and magnetite biomineralization in response to different oxygen concentrations 128

6.4 Open questions and further research..... 132

6.5 References..... 135

ACKNOWLEDGEMENTS 139

CURRICULUM VITAE..... 140

Declaration / Eidesstattliche Versicherung 142

CHAPTER 1

INTRODUCTION

1.1 The magnetotactic bacterium *Magnetospirillum gryphiswaldense*

Although magnetotactic bacteria were already discovered by Salvatore Bellini in 1963 (1), microbiologists have not been aware of them until 1975 when Richard Blackmore rediscovered the magneto-responsive behavior of certain microorganisms containing intracellular crystal-like and iron-rich inclusions, the magnetosomes (2). Individual magnetosomes are aligned into one or multiple chains thereby providing the cell with the capability of orientation in the Earth's magnetic field to facilitate search for growth-favoring suboxic zones of stratified aquatic habitats (3). At present, known representatives of magnetotactic bacteria are affiliated with five major phylogenetic lineages within the domain *Bacteria* including Alpha-, Gamma-, and Delta- subgroups of the *Proteobacteria* phylum, *Nitrospirae* phylum, as well as a candidate division OP3 (4). Despite their high abundance and ubiquitous occurrence in many freshwater and marine habitats, magnetotactic bacteria are notoriously difficult to isolate and cultivate in the laboratory. To date, most magnetotactic bacteria grown in axenic culture are members of alpha-proteobacteria, including three well characterized *Magnetospirillum* species, *M. magnetotacticum* (5), *M. magneticum* (6), and *M. gryphiswaldense* MSR-1 (in the following referred to as MSR-1) which was isolated by D. Schüler from the mud of the eutrophic river Ryck near Greifswald (7, 8). Due to its relative ease of growth in the laboratory and genetic tractability, MSR-1 has been used as the model organism in numerous recent studies and this thesis to understand the mechanism of magnetosome biosynthesis (3). MSR-1 cells are spiral-shaped, with bipolar flagella, and contain up to more than 100 magnetosomes positioned as a single or multiple linear chains (Fig. 1-1) (8). MSR-1 is a microaerophile and grows chemoorganoheterotrophically using several organic acids as sources of carbon and electrons, but is unable to grow by fermentation (9, 10).

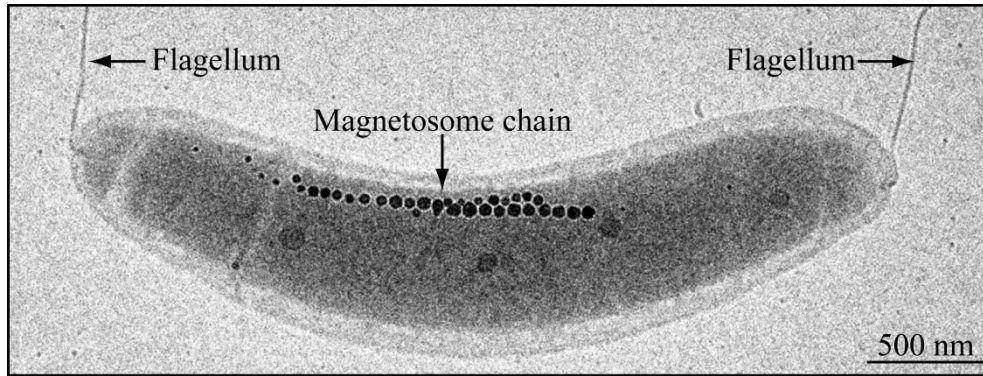


Fig. 1-1 Transmission electron micrograph of MSR-1 (by E. Katzmann). Magnetosome chain and two flagella are indicated by arrows.

1.2 Molecular mechanism of magnetosome formation in MSR-1

Over the past decade significant progress has been made in the identification of magnetosome-associated genes, which are clustered within a more than 100 kb genomic region, magnetosome island (MAI) (11-13). In MSR-1, more than 30 specific proteins have been designated the magnetosome membrane proteins (Mam) and magnetic particle membrane-specific proteins (Mms), respectively (14, 15), which are encoded within four clusters known as *mms6*, *mamGFDC*, *mamAB*, and *mamXY* operons (12). Although the mechanism of magnetite biomineralization so far has not been understood in detail, a stepwise pathway for the formation and assembly of magnetosomes has been suggested: (i) the invagination of magnetosome vesicles from the cytoplasmic membrane, (ii) iron transport, and (iii) magnetite biomineralization and magnetosome assembly into chains (Fig. 1-2). Individual deletions of genes within MAI produced different mutants arrested at various stages of magnetosome formation.

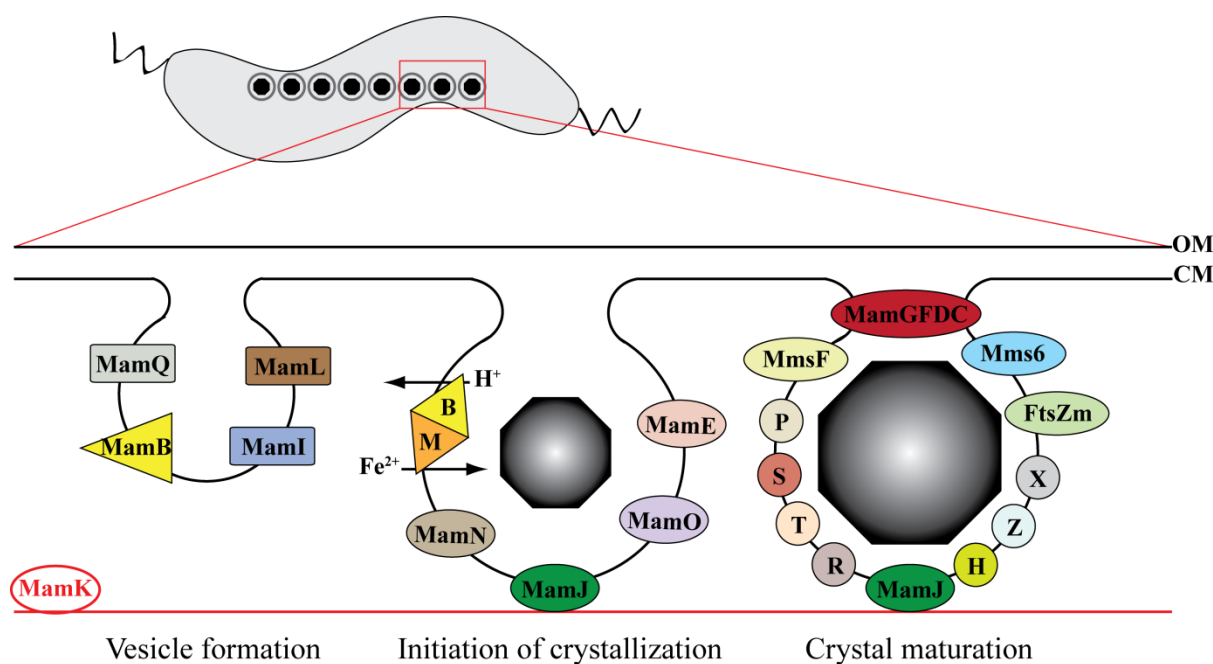


Fig. 1-2 A stepwise pathway of magnetosome formation. MamQ, MamB, MamL, and MamI are required for the formation of magnetosome vesicles; MamM, MamN, MamO, and MamE are essential to initiate magnetite biomineralization; MmsF, MamP (P), MamS (S), MamT (T), MamR (R), MamGFDC, Mms6, FtsZm, MamX (X), MamZ (Z), and MamH (H) are involved in the subsequent crystal maturation; MamJ and MamK are required to assemble magnetosomes into chains. OM, outer membrane; CM, cytoplasmic membrane. Iron uptake and proton efflux for magnetite biomineralization are indicated by arrows.

1.2.1 The biosynthesis of magnetosome vesicles

In MSR-1 the magnetosomes are membrane-enveloped crystals of magnetite. It was originally proposed that the magnetosome membrane is derived from cytoplasmic membrane based on the observation that the composition of fatty acids in magnetosome membrane was similar to that in cytoplasmic membrane but distinct from the outer membrane (16). This suggestion was further confirmed in MSR-1 and *M. magneticum* by electron cryotomography (ECT), which in fact showed that empty vesicles originate from the cytoplasmic membrane by invagination (17, 18). So far, four proteins including MamI, MamL, MamQ, and MamB have been assigned roles in the early stage of vesicle formation (Fig. 1-2) (A. Lohsse and O. Raschdorf, unpublished data) (11, 19). In *M. magneticum* loss of any of these proteins completely abolished the formation of magnetosome vesicles (11). MamI and MamL are inner membrane proteins and do not show homology to any proteins beyond magnetotactic bacteria (11). Although their role in magnetite biomineralization is still unclear, it has been hypothesized that the 15-amino-acid C-terminal tail of MamL, which is rich in positively charged residues, may interact with the cytoplasmic side of the inner membrane and thereby induce local membrane curvature (20). The other two proteins, MamQ and MamB, contain

domains conserved in large families. MamQ is homologous to proteins of the LemA family, for which no function is known (21). But the proteins of this group contain coiled-coil repeat domains which may facilitate interactions of bending the magnetosome membrane (20). MamB belongs to the cation diffusion facilitator (CDF) family of transporters, which plays a role in the transport of divalent cation metals (22). In addition to self-interaction via its C-terminal domain, MamB also interacts with, and in turn is stabilized by a second CDF protein, MamM (19).

1.2.2 Iron transport

Before the biosynthesis of magnetite can take place, the first step is the transport of iron from the extracellular environment into the cell. Early studies of uptake and accumulation of large amounts of iron in magnetotactic bacteria suggested that some regulation is required to sustain a strict iron homeostasis (23). Bioinformatic analysis predicted that a ferric uptake regulator Fur might be involved in iron-responsive regulation of magnetite biomineralization (24). However, deletion of the *fur*-like gene in MSR-1 only caused weak effects on magnetite biomineralization (25, 26), indicating that other regulators might be present and provide contribution to the iron homeostasis for magnetosome formation. Iron transport for magnetite synthesis may occur via two copies of the ferrous iron transporter FeoB that is common to most bacteria, and deletions of *feoB1* and *feoB2* caused reduced magnetite content of MSR-1 (R. Uebe, unpublished data) (27, 28). However, much is still unknown about iron transport for magnetosome formation.

1.2.3 Magnetite biomineralization

There is huge diversity in the size and shape of magnetite nanocrystals produced by different species of magnetotactic bacteria, and in MSR-1, the magnetite crystals are cubo-octohedral with a narrow size distribution (29). The synthesis of mixed-valence iron oxide magnetite (Fe_3O_4) was supposed to occur at high pH by coprecipitation of ferrous and ferric iron in supersaturating concentrations (30). It was first suggested that the process of magnetite crystallization comprises three phases with different iron oxides based on Mössbauer spectroscopy observations on *M. magnetotacticum*: (i) low-density-hydrous ferric oxides, (ii) high-density-hydrous ferric oxides, and (iii) magnetite formed by partial reduction of the high-density-hydrous ferric oxides (31). However, later studies on MSR-1 revealed the

absence of mineral precursors, which indicated that magnetite is synthesized by fast coprecipitation of ferrous and ferric iron inside the magnetosome compartments without any intermediate mineral precursors (32). By X-ray circular magnetic dichroism measurements, hematite (α -Fe₂O₃) was detected on the surface of immature magnetite crystals, and thereby proposed to be a precursor to magnetite in MSR-1 (33). However, very recently, Baumgartner et al. showed that in *M. magneticum* magnetite may be synthesized from a phosphate-rich ferric hydroxide phase via a transient and short-lived ferrihydrite (Fe₂O₃ · nH₂O) phase (34).

Four proteins were identified to be required for the initiation of crystallization (Fig. 1-2). Loss of MamE, a DegP/HtrA serine protease with putative heme-binding domains, resulted in empty vesicles and mislocalization of a number of magnetosome proteins such as MamJ, MamI and MamC (35, 36). Therefore, it was proposed that MamE is essential to the localization of a number of proteins to the magnetosome. MamM is required not only for the initiation of magnetite nucleation, but also for maintaining the stability of MamB, since in MSR-1 the deletion of *mamM* resulted in the formation of empty magnetosome vesicles and loss of MamB protein (19). Although MamO and MamN are also essential to the initiation of biomineralization (11), the mechanism of their role remains unclear.

In addition, a number of players are required for the crystal maturation. A magnetosome membrane protein MmsF in *M. magneticum* was found to be sufficient to restore magnetite synthesis in the absence of other candidates with respect to particle morphology and size (37). Therefore, MmsF was proposed to be a major constituent in controlling magnetite crystal size and morphology (37). MamX, MamZ, and MamH were shown to functionally interact to control redox state of iron within the magnetosome compartments (38). In MSR-1 deletion of any of these genes led to similar defects in magnetite biomineralization, such as WT-like magnetite crystals flanked by poorly crystalline flake-like particles (38). Similarly, an FtsZ-like protein FtsZm also plays a role in poisoning the redox conditions for magnetite biosynthesis and deletion of *ftsZm* resulted in the generation of irregular crystals in the absence of nitrate (39). A recent crystal structure of MamP from magnetotactic ovoidal bacterium MO-1 strain provided first insight in the mechanism of a new class of cytochromes, which share a unique configuration of two close CXXCH heme-binding domains, termed the magnetochrome domain (40, 41). It was suggested that MamP functions as a dimer to bind and further oxidize the iron for magnetite synthesis (40). MamR, MamS, MamT, Mms6, and MamGFDC proteins also exhibit so-far uncharacterized functions to regulate magnetite size and

morphology (11, 42, 43). To maximize their magnetic response, MSR-1 cells position their magnetosomes as one or more chains along the long axis of the cell through the interaction of the actin-like protein MamK and MamJ (18, 44).

1.2.4 Redox control required for magnetite biomineralization

The biosynthesis of mixed-valence iron oxide magnetite [FeII(FeIII)₂O₄] was proposed to occur by coprecipitation of ferrous and ferric iron in supersaturating concentrations, which requires a balanced ratio of ferrous and ferric iron (30, 32, 45). Nitrite and oxygen have been shown to be potent oxidants for ferrous iron and used for the preparation of inorganic magnetite films, ferrite plating (46). Faivre et al. also found that the formation of abiotic magnetite required a rather high pH and high concentration of iron (30). In addition, the redox state required for magnetite synthesis is also possible to be affected by proteins via biological process. For example, as mentioned above, in MSR-1 several proteins such as MamX, MamZ, MamH, and FtsZm have been found to play a role in maintaining the redox balance of Fe²⁺/Fe³⁺ for magnetite biomineralization (38, 39). Maximum biomineralization of magnetite in MSR-1 occurred in low oxygen tensions and the presence of nitrate, while aerobic conditions completely inhibited magnetosome formation (47, 48). Therefore, the redox state required for magnetite biosynthesis is also likely regulated by denitrification and aerobic respiration, during which nitrate and oxygen are used as respective electron acceptors. Thus, besides the highly specific proteins encoded within the genomic magnetosome island, genes used for common metabolic functions such as respiration might be also involved in controlling the redox potential for magnetite synthesis.

1.3 Respiratory pathways in magnetospirilla

1.3.1 Aerobic respiration

Although MSR-1 is a microaerophile and magnetosome formation was only induced when the oxygen concentration was below threshold value of 2,000 Pa (47), oxygen is a preferred electron acceptor for respiration and energy generation. It was initially proposed that oxygen is required for Fe₃O₄ biosynthesis (49). However, later isotope experiment demonstrated that the oxygen molecules bound in biologically synthesized Fe₃O₄ are derived from water but not

O₂ (50). To understand the role of oxygen in magnetite biomineralization, aerobic respiration was studied in *M. magnetotacticum*. By spectral analyses, six types of cytochrome were identified including *a*-, *a*₁-, *b*-, *c*-, *cd*₁-, and *o*-type hemes (51). Among them, more than 85% of the total cytochromes were of the *c*-type, which were mainly soluble. However, the *a*- and *b*-type cytochromes were mostly detected in cell membranes. Since *a*₁ hemes (usually part of the 'low aeration' cytochrome oxidase) and *o* hemes (usually part of the 'high aeration' cytochrome oxidase) were simultaneously observed in *M. magnetotacticum*, O'Brien et al. suggested that the oxygen respiration chain is branched (51). Subsequently, a new 'cytochrome *a*₁-like' hemoprotein was found to display poor cytochrome *c* oxidase activity and be present in higher amounts in magnetic cells of *M. magnetotacticum* compared to nonmagnetic cells, indicating that this protein might be involved in magnetosome formation (52). In 1994, Tamegai and Fukumori reported a novel *cbb*-type cytochrome *c* oxidase, which displayed cytochrome *c* oxidase activity and thus was assumed to function as the terminal oxidase for microaerobic respiration (53). ***However, no genetic evidence has been available to elucidate which proteins function for aerobic respiration, and whether aerobic respiration is implicated in magnetite biomineralization by maintaining the redox balance of ferrous and ferric iron.***

In bacteria the electron transport chain for O₂ reduction contains several terminal oxidases. Based on the substrates used as electron donors, they are grouped into two main types: cytochrome *c* oxidases and quinol oxidases (Fig. 1-3). Cytochrome *c* oxidases are proteins receiving electrons from cytochrome *c* and transferring them to the reactions coupled to H⁺ to produce H₂O (54). All of them are members of heme-copper oxidases (HCOs). Based on the evolutionary relationships, the HCO enzymes are categorized into three different types: (i) type A oxidases, classified as cytochrome oxidases *aa*₃, which are homologous to the mitochondrial oxidases (55), (ii) type B oxidases, grouped as quinol oxidases *bo*₃, in which the catalytic subunit and two other subunits are analogous to the subunits of *aa*₃-type cytochrome *c* oxidases (56), and (iii) type C oxidases, the cytochrome oxidases *cbb*₃. Although the terminal oxidases *aa*₃ and *bo*₃ receive electrons from different donors, their proton pumps probably operate in a similar manner (57). However, *cbb*₃ oxidases are quite distinct from other HCO enzymes in terms of its strategy for accepting electrons, the heme prosthetic group present in the active site, and its affinity for oxygen (58).

Quinol oxidases provide an alternative route of electron transfer from quinols to oxygen other than via a bc_1 complex, which is to accept electrons directly from quinol and further use them for oxygen reduction (Fig. 1-3). Quinol oxidases contain various types of cytochrome and can be grouped into HCOs and cytochrome d -containing oxidases (54). Similar to cbb_3 -type oxidases, bd -type quinol oxidases do not share any homology with HCO members. Compared to HCOs, bd quinol oxidases are less efficient at creating the charge gradient for ATP synthesis since they do not pump protons (59). However, they have been found to have a higher affinity for O_2 than other cytochrome oxidases, and it was therefore proposed that bd oxidases function for aerobic respiration under low O_2 conditions (60).

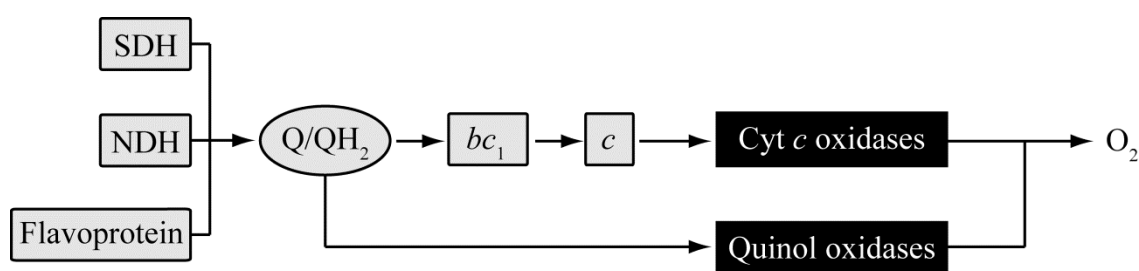


Fig. 1-3 Schematic representation of aerobic respiration pathway in bacteria. Q/QH_2 , quinone/quinol pool in the membrane; SDH, succinate dehydrogenase; NDH, NADH dehydrogenase; bc_1 , cytochrome bc_1 ; c , cytochrome c . Electron transfer is indicated by arrows. This figure is adapted from (54).

1.3.2 Denitrification and magnetite biomineralization

MSR-1 and related magnetospirilla were considered denitrifying bacteria with nitrate as an alternative terminal electron acceptor but not with Fe(III), sulfate, or fumarate as terminal electron acceptors (4, 61, 62). In agreement with this, genomic analysis predicted a complete denitrification pathway in magnetospirilla, which includes genes functioning for nitrate, nitrite, nitric oxide, and nitrous oxide reduction (62). However, before this thesis no evidence was available to prove that MSR-1 is able to grow anaerobically with nitrate as the only electron acceptor in the absence of oxygen.

Bacterial denitrification is a respiratory process in which nitrate is reduced stepwise to N_2 ($NO_3^- \rightarrow NO_2^- \rightarrow NO \rightarrow N_2O \rightarrow N_2$) (63). Two types of dissimilatory nitrate reductase catalyze the reduction of nitrate to nitrite, referred to as Nar and Nap, which differ in their localization: Nar is a membrane-bound complex while Nap is localized in the periplasm (64). Environmental surveys of the occurrence of these *nar*- and *nap*-type genes proved a nearly equal representation of both groups in nature (65). Besides as nitrate reductase, Nap was also

proposed to play a role in redox homeostasis of the cell adapting to the change from aerobic to anaerobic growth or for the aerobic denitrification (64, 66-69). The subsequent reduction of nitrite to NO can be catalyzed by two isofunctional periplasmic proteins, which are evolutionary unrelated: a homotrimeric copper-containing nitrite reductase, NirK, and a homodimeric cytochrome *cd*₁ nitrite reductase, NirS (70). So far, NirS is the only protein known to contain the heme *d*₁ as an essential cofactor, which is assumed to be the catalytic site for nitrite reduction (71). The biogenesis of heme *d*₁ is thought to be mediated by a set of proteins encoded within the *nir* operon (72-74). The reduction of NO to N₂O is carried out by NO reductase (Nor) members of the heme-copper oxidoreductase (HCO) superfamily (56), which also includes oxygen terminal oxidases. However, different from other HCO members, Nor does not exhibit any proton translocation activity and its highly conserved catalytic center contains an iron ion instead of a copper ion (75, 76). Nos, the last enzyme required for complete denitrification, is a periplasmic multicopper enzyme. Apart from denitrifiers, other nondenitrifying microorganisms are also capable of using N₂O as electron acceptor and reduce it to N₂ via atypical NosZ proteins that possess distinctive regulatory and functional components. These atypical NosZ proteins are shown to be abundant and thus might function as potential contributors to N₂O reduction in sediments and soils, as well as in other habitats where N₂O sources are present (77).

A potential relationship between denitrification and magnetite biomineralization was first realized in *M. magnetotacticum* based on an observation that more cells contained magnetosomes with nitrate than without nitrate in the media (61). In addition, it was also found that *M. magnetotacticum* is capable of microaerobic dissimilatory nitrate reduction and produces N₂O or N₂ as the final products (61). Later, *M. magneticum* was shown to grow by denitrification pathway in the absence of oxygen and nitrate is used to support magnetosome formation (6, 10, 78). In an attempt to understand the link between denitrification and magnetite biomineralization, the enzymology of denitrification has been studied in some detail in *M. magnetotacticum*. A soluble periplasmic nitrate reductase Nap purified from *M. magnetotacticum* contained two subunits of 17 and 86 kDa (79). Deprivation of molybdenum from cells abolished nitrate reductase activity, whereas the magnetosome fraction still had half iron content in the same fraction compared to in the presence of molybdenum. Therefore, Taoka and colleagues hypothesized that nitrate reduction is not required for Fe₃O₄ synthesis (79). In addition to catalyzing the reduction of nitrite to NO, the protein NirS purified from *M. magnetotacticum* accelerated the oxidization of ferrous iron in the presence of nitrite under

anaerobic conditions. This indicated that NirS of magnetotactic bacteria possesses a novel Fe(II):nitrite oxidoreductase activity that may participate in magnetosomal Fe₃O₄ synthesis *in vivo* (80). Wang et al. interrupted a gene (*norB*) for nitric oxide reductase in AMB-1 by transposon insertion and found that shorter magnetosome chains were produced under anaerobic conditions (81). ***However, except for this single study, so far no genetic evidence has been provided for a complete pathway of nitrate reduction in magnetotactic bacteria. The speculated functions of denitrification enzymes in vivo and the exact interrelation between denitrification and magnetite biomineralization have largely remained unknown.***

1.4 Regulation of respiration from aerobic to anaerobic conditions

As mentioned above, the biosynthesis of magnetite crystals only occurred under suboxic conditions, while aerobic conditions completely inhibited the formation of magnetite (47, 48). However, the expression of proteins encoded in the genomic magnetosome island is not likely affected by the concentrations of oxygen, which was concluded based on the following observations: (i) magnetosome genes were transcribed under different oxygen conditions (82), (ii) all tested magnetosome-associated proteins, including MamK, MamA, MamC, MamB, and MamM were still present within the cell under high O₂ conditions, and the amount of these proteins quantified by immunodetection, was indistinguishable at different oxygen concentrations (Y. Li, unpublished data), and (iii) aerobically grown nonmagnetic MSR-1 which did not synthesize any electron-dense particles, but still formed empty vesicles within the cell detected by electron cryotomography (Y. Li and O. Raschdorf, unpublished data). Therefore, the question arose as to whether the aerobic repression for magnetite biomineralization is controlled by biological regulation. In addition, it is also possible that this aerobic repressed process is directly caused by abiogenic chemical oxidation of iron ions within the cells.

In many bacteria, changes in oxygen tension serve as an important environmental signal to trigger adaptive changes between anaerobic and aerobic respiration. This has been well studied in *Escherichia coli* where oxygen deprivation induces the synthesis of a number of enzymes, particularly those carrying out anaerobic respiration (83-87). The alteration of gene expression between aerobic and anaerobic conditions to facilitate such changes in energy metabolism is achieved by a global regulator Fnr (fumarate and nitrate reductase regulation).

Fnr proteins belong to a superfamily of transcriptional regulators which show sequence homology with the cyclic-AMP receptor class of proteins (88). Like all members of this family, Fnr protein comprises an N-terminal sensory domain and a C-terminal DNA-binding domain, which is involved in site-specific DNA recognition (84). In *E. coli*, the sensor domain contains five cysteines and four of them (Cys-20, 23, 29, and 122) are essential to bind either a $[4\text{Fe-4S}]^{2+}$ or a $[2\text{Fe-2S}]^{2+}$ cluster that functions in the O_2 -sensing mechanism (89-91). Under anaerobic conditions, Fnr protein is a homodimer harboring one $[4\text{Fe-4S}]^{2+}$ cluster per monomer as a direct sensor of oxygen. Exposure of the $[4\text{Fe-4S}]^{2+}$ cluster to oxygen results in the conversion of the oxidized cluster to a $[2\text{Fe-2S}]^{2+}$ form, which in turn triggers conformational changes and further induces monomerization to prevent DNA binding (92-98).

1.5 Aims of this work

Although previous observations have implicated oxygen regulation and respiration in redox control of magnetite biomineralization, no genetic evidence was available to elucidate the relationship between respiration and magnetosome formation. Since no oxygen regulators have been identified in metabolically versatile magnetotactic bacteria, it was unclear how growth metabolism and magnetite biomineralization are regulated in response to different oxygen concentrations, and that this aerobic repression of magnetite synthesis is caused by biological regulation process, or alternatively, by directly abiogenic perturbation of the redox balance of iron ions required for magnetite synthesis (Fig. 1-4).

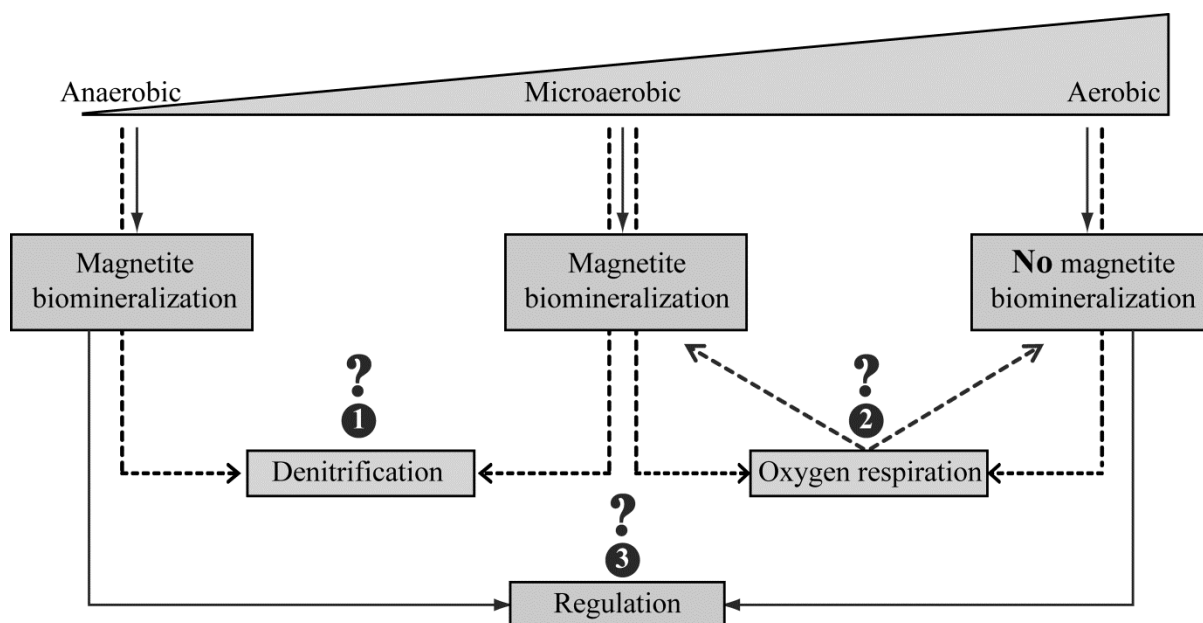


Fig. 1-4 Aims of this work. The interrelation between respiration (denitrification (1) and aerobic respiration (2)) and magnetite biomineralization, as well as regulation (3) for magnetite biomineralization which occurs only under microaerobic and anaerobic conditions is still largely unknown in magnetotactic bacteria.

To explore the role of denitrification in magnetite synthesis, in the **Chapter 2** and **Chapter 3** of this thesis, genes encoding enzymes for denitrification were identified and analyzed with respect to their functions on growth and magnetosome formation in MSR-1. In the **Chapter 2**, we specifically set out to investigate functions of the periplasmic nitrate reductase Nap on magnetite biomineralization by comparing the roles of downstream denitrification enzymes Nor and Nos.

Earlier work suggested that the reduction of nitrite to NO might be linked to magnetite biomineralization in magnetospirilla (80). However, due to the lack of genetic evidence, the exact role of NirS in magnetosome formation has remained unknown. Therefore, in the **Chapter 3**, functional analyses of NirS in nitrite reduction and magnetite biosynthesis were performed.

Magnetite biomineralization was shown to be induced by low oxygen tensions but inhibited by O₂-rich conditions. In other bacteria, the anaerobic regulator Fnr has been shown to be a global oxygen sensor, which is capable of controlling the switch between microaerobic and aerobic metabolism. Therefore, in the **Chapter 4** we attempted to investigate whether the putative oxygen sensor Fnr protein encoded in the genome assembly of MSR-1, is capable of sensing oxygen and further functions on the regulation of growth and magnetite biomineralization in response to different oxygen conditions.

Although O₂ is suggested to act as a major factor controlling the redox state for magnetosome formation, its role in metabolism and magnetite biomineralization has not been well studied in magnetotactic bacteria. In the **Chapter 5**, comprehensive genetic and biochemical analyses were performed to reveal the relationship between oxygen respiration and magnetite biosynthesis.

1.6 REFERENCES

1. **Bellini S.** 2009. On a unique behavior of freshwater bacteria. *Chin. J. Oceanol. Limnol.* **27**:3-5.
2. **Blakemore RP.** 1975. Magnetotactic bacteria. *Science* **190**:377-379.
3. **Jogler C, Schüler D.** 2009. Genomics, genetics, and cell biology of magnetosome formation. *Annu. Rev. Microbiol.* **63**:501-521.
4. **Lower BH, Bazylinski DA.** 2013. The bacterial magnetosome: a unique prokaryotic organelle. *J. Mol. Microbiol. Biotechnol.* **23**:63-80.
5. **Blakemore R, Maratea D, Wolfe R.** 1979. Isolation and pure culture of freshwater magnetic spirillum in chemically defined medium. *J. Bacteriol.* **140**:720-729.
6. **Matsunaga T, Sakaguchi T, Tadokoro F.** 1991. Magnetite formation by a magnetic bacterium capable of growing aerobically. *Appl. Microbiol. Biotechnol.* **35**:651-655.
7. **Schleifer KH, Schüler D, Spring S, Weizenegger M, Amann R, Ludwig W, Köhler M.** 1991. The genus *Magnetospirillum* gen. nov., description of *Magnetospirillum gryphiswaldense* sp. nov. and transfer of *Aquaspirillum magnetotacticum* to *Magnetospirillum magnetotacticum* comb. nov. *Syst. Appl. Microbiol.* **14**:379-385.
8. **Schüler D, Köhler M.** 1992. The isolation of a new magnetic spirillum. *Zentralbl. Mikrobiol.* **147**:150-151.
9. **Schüler D.** 1994. Isolierung und Charakterisierung magnetischer Bakterien - Untersuchungen zur Magnetitbiomineralisation in *Magnetospirillum gryphiswaldense*, Doctoral Thesis.
10. **Yang CD, Takeyama H, Tanaka T, Matsunaga T.** 2001. Effects of growth medium composition, iron sources and atmospheric oxygen concentrations on production of luciferase-bacterial magnetic particle complex by a recombinant *Magnetospirillum magneticum* AMB-1. *Enzyme Microb. Technol.* **29**:13-19.
11. **Murat D, Quinlan A, Vali H, Komeili A.** 2010. Comprehensive genetic dissection of the magnetosome gene island reveals the step-wise assembly of a prokaryotic organelle. *Proc. Natl. Acad. Sci. U. S. A.* **107**:5593-5598.

12. **Lohsse A, Ullrich S, Katzmann E, Borg S, Wanner G, Richter M, Voigt B, Schweder T, Schüler D.** 2011. Functional analysis of the magnetosome island in *Magnetospirillum gryphiswaldense*: the *mamAB* operon is sufficient for magnetite biomineralization. *PLoS One* **6**:e25561.
13. **Ullrich S, Kube M, Schübbe S, Reinhardt R, Schüler D.** 2005. A hypervariable 130-kilobase genomic region of *Magnetospirillum gryphiswaldense* comprises a magnetosome island which undergoes frequent rearrangements during stationary growth. *J. Bacteriol.* **187**:7176-7184.
14. **Grünberg K, Wawer C, Tebo BM, Schüler D.** 2001. A large gene cluster encoding several magnetosome proteins is conserved in different species of magnetotactic bacteria. *Appl. Environ. Microbiol.* **67**:4573-4582.
15. **Grünberg K, Müller EC, Otto A, Reszka R, Linder D, Kube M, Reinhardt R, Schüler D.** 2004. Biochemical and proteomic analysis of the magnetosome membrane in *Magnetospirillum gryphiswaldense*. *Appl. Environ. Microbiol.* **70**:1040-1050.
16. **Tanaka M, Okamura Y, Arakaki A, Tanaka T, Takeyama H, Matsunaga T.** 2006. Origin of magnetosome membrane: Proteomic analysis of magnetosome membrane and comparison with cytoplasmic membrane. *Proteomics* **6**:5234-5247.
17. **Komeili A, Li Z, Newman DK, Jensen GJ.** 2006. Magnetosomes are cell membrane invaginations organized by the actin-like protein MamK. *Science* **311**:242-245.
18. **Katzmann E, Scheffel A, Gruska M, Plitzko JM, Schüler D.** 2010. Loss of the actin-like protein MamK has pleiotropic effects on magnetosome formation and chain assembly in *Magnetospirillum gryphiswaldense*. *Mol. Microbiol.* **77**:208-224.
19. **Uebe R, Junge K, Henn V, Poxleitner G, Katzmann E, Plitzko JM, Zarivach R, Kasama T, Wanner G, Posfai M, Bottger L, Matzanke B, Schüler D.** 2011. The cation diffusion facilitator proteins MamB and MamM of *Magnetospirillum gryphiswaldense* have distinct and complex functions, and are involved in magnetite biomineralization and magnetosome membrane assembly. *Mol. Microbiol.* **82**:818-835.
20. **Komeili A.** 2012. Molecular mechanisms of compartmentalization and biomineralization in magnetotactic bacteria. *FEMS Microbiol. Rev.* **36**:232-255.
21. **D'Orazio SEF, Velasquez M, Roan NR, Naveiras-Torres O, Starnbach MN.** 2003. The *Listeria monocytogenes lemA* gene product is not required for intracellular infection or to activate fMIGWII-specific T cells. *Infect. Immun.* **71**:6721-6727.
22. **Grass G, Otto M, Fricke B, Haney CJ, Rensing C, Nies DH, Munkelt D.** 2005. FieF (YiiP) from *Escherichia coli* mediates decreased cellular accumulation of iron and relieves iron stress. *Arch. Microbiol.* **183**:9-18.
23. **Schüler D, Baeuerlein E.** 1996. Iron-limited growth and kinetics of iron uptake in *Magnetospirillum gryphiswaldense*. *Arch. Microbiol.* **166**:301-307.

24. **Rodionov DA, Gelfand MS, Todd JD, Curson ARJ, Johnston AWB.** 2006. Computational reconstruction of iron- and manganese-responsive transcriptional networks in alpha-proteobacteria. *PLoS Comput. Biol.* **2**:1568-1585.
25. **Uebe R, Voigt B, Schweder T, Albrecht D, Katzmann E, Lang C, Bottger L, Matzanke B, Schüler D.** 2010. Deletion of a *fur-like* gene affects iron homeostasis and magnetosome formation in *Magnetospirillum gryphiswaldense*. *J. Bacteriol.* **192**:4192-4204.
26. **Qi L, Li J, Zhang WJ, Liu JN, Rong CB, Li Y, Wu LF.** 2012. Fur in *Magnetospirillum gryphiswaldense* influences magnetosomes formation and directly regulates the genes Involved in iron and oxygen metabolism. *PLoS One* **7** (1):e29572.
27. **Rong C, Huang Y, Zhang W, Jiang W, Li Y, Li J.** 2008. Ferrous iron transport protein B gene (*feoB1*) plays an accessory role in magnetosome formation in *Magnetospirillum gryphiswaldense* strain MSR-1. *Res. Microbiol.* **159**:530-536.
28. **Rong C, Zhang C, Zhang Y, Qi L, Yang J, Guan G, Li Y, Li J.** 2012. FeoB2 Functions in magnetosome formation and oxidative stress protection in *Magnetospirillum gryphiswaldense* strain MSR-1. *J. Bacteriol.* **194**:3972-3976.
29. **Faivre D, Schüler D.** 2008. Magnetotactic bacteria and magnetosomes. *Chem. Rev. (Washington, DC, U. S.)* **108**:4875-4898.
30. **Faivre D, Agrinier P, Menguy N, Zuddas P, Pachana K, Gloter A, Laval J, Guyot F.** 2004. Mineralogical and isotopic properties of inorganic nanocrystalline magnetites. *Geochim. Cosmochim. Acta* **68**:4395-4403.
31. **Frankel R, Papaefthymiou GC, Blakemore RP, O'Brian W.** 1983. Fe₃O₄ precipitation in magnetotactic bacteria. *Biochim. Biophys. Acta* **763**:147-159.
32. **Faivre D, Böttger LH, Matzanke BF, Schüler D.** 2007. Intracellular magnetite biomineralization in bacteria proceeds by a distinct pathway involving membrane-bound ferritin and an iron(II) species. *Angew. Chem. Int. Ed. Engl.* **46**:8495-8499.
33. **Staniland S, Ward B, Harrison A, Van der Laan G, Telling N.** 2007. Rapid magnetosome formation shown by real-time x-ray magnetic circular dichroism. *Proc. Natl. Acad. Sci. U. S. A.* **104**:19524-19528.
34. **Baumgartner J, Morin G, Menguy N, Gonzalez TP, Widdrat M, Cosmidis J, Faivre D.** 2013. Magnetotactic bacteria form magnetite from a phosphate-rich ferric hydroxide via nanometric ferric (oxyhydr)oxide intermediates. *Proc. Natl. Acad. Sci. U. S. A.* **110**:14883-14888.
35. **Quinlan A, Murat D, Vali H, Komeili A.** 2011. The HtrA/DegP family protease MamE is a bifunctional protein with roles in magnetosome protein localization and magnetite biomineralization. *Mol. Microbiol.* **80**:1075-1087.
36. **Yang W, Li R, Peng T, Zhang Y, Jiang W, Li Y, Li J.** 2010. *mamO* and *mamE* genes are essential for magnetosome crystal biomineralization in *Magnetospirillum gryphiswaldense* MSR-1. *Res. Microbiol.* **161**:701-705.

37. **Murat D, Falahati V, Bertinetti L, Csencsits R, Kornig A, Downing K, Faivre D, Komeili A.** 2012. The magnetosome membrane protein, MmsF, is a major regulator of magnetite biomineralization in *Magnetospirillum magneticum* AMB-1. *Mol. Microbiol.* **85**:684-699.
38. **Raschdorf O, Müller FD, Posfai M, Plitzko JM, Schüler D.** 2013. The magnetosome proteins MamX, MamZ and MamH are involved in redox control of magnetite biomineralization in *Magnetospirillum gryphiswaldense*. *Mol. Microbiol.* **89**:872-886.
39. **Müller FD, Raschdorf O, Nudelman H, Messerer M, Katzmann E, Plitzko JM, Zarivach R, Schüler D.** 2014. The FtsZ-Like protein FtsZm of *Magnetospirillum gryphiswaldense* likely interacts with its generic homolog and is required for biomineralization under nitrate deprivation. *J. Bacteriol.* **196**:650-659.
40. **Siponen MI, Legrand P, Widdrat M, Jones SR, Zhang WJ, Chang MCY, Faivre D, Arnoux P, Pignol D.** 2013. Structural insight into magnetochrome-mediated magnetite biomineralization. *Nature* **502**:681-684.
41. **Siponen MI, Adryanczyk G, Ginet N, Arnoux P, Pignol D.** 2012. Magnetochrome: a c-type cytochrome domain specific to magnetotactic bacteria. *Biochem. Soc. Trans.* **40**:1319-1323.
42. **Scheffel A, Gaerdes A, Gruenberg K, Wanner G, Schüler D.** 2008. The major magnetosome proteins MamGFDC are not essential for magnetite biomineralization in *Magnetospirillum gryphiswaldense* but regulate the size of magnetosome crystals. *J. Bacteriol.* **190**: 377-386
43. **Tanaka M, Mazuyama E, Arakaki A, Matsunaga T.** 2011. MMS6 protein regulates crystal morphology during nano-sized magnetite biomineralization *in vivo*. *J. Biol. Chem.* **286**:6386-6392.
44. **Scheffel A, Gruska M, Faivre D, Linaroudis A, Graumann PL, Plitzko J, Schüler D.** 2006. An acidic protein aligns magnetosomes along a filamentous structure in magnetotactic bacteria. *Nature* **440**:110-114.
45. **Mann S, Sparks NHC, Board RG.** 1990. Magnetotactic bacteria: microbiology, biomineralization, palaeomagnetism and biotechnology. *Adv. Microbiol. Physiol.* **31**:125-181.
46. **Abe M.** 2000. Ferrite plating: a chemical method preparing oxide magnetic films at 24-100 °C, and its applications. *Electrochim. Acta* **45**:3337-3343.
47. **Heyen U, Schüler D.** 2003. Growth and magnetosome formation by microaerophilic *Magnetospirillum* strains in an oxygen-controlled fermentor. *Appl. Microbiol. Biotechnol.* **61**:536-544.
48. **Li Y, Katzmann E, Borg S, Schüler D.** 2012. The periplasmic nitrate reductase Nap is required for anaerobic growth and involved in redox control of magnetite biomineralization in *Magnetospirillum gryphiswaldense*. *J. Bacteriol.* **194**:4847-4856.
49. **Blakemore R.** 1982. Magnetotactic bacteria. *Annu. Rev. Microbiol.* **36**:217-238.

50. **Mandernack KW, Bazylinski D, Shanks WC, Bullen TD.** 1999. Oxygen and iron isotope studies of magnetite produced by magnetotactic bacteria. *Science* **285**:1892-1896.
51. **O'Brien W, Paoletti L, Blakemore R.** 1987. Spectral analysis of cytochromes in *Aquaspirillum magnetotacticum*. *Curr. Microbiol.* **15**:121-127.
52. **Tamegai H, Yamanaka T, Fukumori Y.** 1993. Purification and properties of a 'cytochrom a_1 '-like hemoprotein from a magnetotactic bacterium, *Aquaspirillum magnetotacticum*. *Biochim. Biophys. Acta* **1158**:137-243.
53. **Tamegai H, Fukumori Y.** 1994. Purification and some molecular and enzymatic features of a novel *ccb*-type cytochrome *c* oxidase from a microaerobic denitrifier, *Magnetospirillum magnetotacticum*. *FEBS Lett.* **347**:22-26.
54. **Thöny-Meyr L.** 1997. Biogenesis of respiratory cytochromes in bacteria. *Microbiol. Mol. Biol. Rev.* **61**:337-376.
55. **Saraste M.** 1990. Structural features of cytochrome oxidase. *Q. Rev. Biophys.* **23**:331-366.
56. **Garcia-Horsman JA, Barquera B, Rumbley J, Ma J, Gennis RB.** 1994. The superfamily of heme-copper respiratory oxidases. *J. Bacteriol.* **176**:5587-5600.
57. **Trumpower BL, Gennis RB.** 1994. Energy transduction by cytochrome complexes in mitochondrial and bacterial respiration: the enzymology of coupling electron transfer reactions to transmembrane proton translocation. *Annu. Rev. Biochem.* **63**:675-716.
58. **Pitcher RS, Watmough NJ.** 2004. The bacterial cytochrome *ccb₃* oxidases. *Bba-Bioenergetics* **1655**:388-399.
59. **VanOrsdel CE, Bhatt S, Allen RJ, Brenner EP, Hobson JJ, Jamil A, Haynes BM, Genson AM, Hemm MR.** 2013. The *Escherichia coli* CydX protein is a member of the CydAB cytochrome *bd* oxidase complex and is required for cytochrome *bd* oxidase activity. *J. Bacteriol.* **195**:3640-3650.
60. **Poole RK, Cook GM.** 2000. Redundancy of aerobic respiratory chains in bacteria? Routes, reasons and regulation. *Adv. Microb. Physiol.* **43**:165-224.
61. **Bazylinski D, Blakemore RP.** 1983. Denitrification and assimilatory nitrate reduction in *Aquaspirillum magnetotacticum*. *Appl. Environ. Microbiol.* **46**:1118-1124.
62. **Bazylinski DA, Williams T.** 2006. Ecophysiology of magnetotactic bacteria. *In* D. Schüler (ed.), *Magnetoreception and magnetosomes in bacteria*. SpringerVerlag, Heidelberg.
63. **Zumft WG.** 1997. Cell biology and molecular basis of denitrification. *Microbiol. Mol. Biol. Rev.* **61**:533-616.

64. **Richardson DJ, Berks BC, Russell DA, Spiro S, Taylor CJ.** 2001. Functional, biochemical and genetic diversity of prokaryotic nitrate reductases. *Cell. Mol. Life Sci.* **58**:165-178.
65. **Bru D, Sarr A, Philippot L.** 2007. Relative abundances of proteobacterial membrane-bound and periplasmic nitrate reductases in selected environments. *Appl. Environ. Microbiol.* **73**:5971-5974.
66. **Ellington MJ, Bhakoo KK, Sawers G, Richardson DJ, Ferguson SJ.** 2002. Hierarchy of carbon source selection in *Paracoccus pantotrophus*: strict correlation between reduction state of the carbon substrate and aerobic expression of the *nap* operon. *J. Bacteriol.* **184**:4767-4774.
67. **Sears HJ, Spiro S, Richardi J.** 1997. Effect of carbon substrate and aeration on nitrate reduction and expression of the periplasmic and membrane-bound nitrate reductases in carbon-limited continuous cultures of *Paracoccus denitrificans* Pd1222. *Microbiology* **143**:3767-3774.
68. **Gavira M, Roldan MD, Castillo F, Moreno-Vivian C.** 2002. Regulation of *nap* gene expression and periplasmic nitrate reductase activity in the phototrophic bacterium *Rhodobacter sphaeroides* DSM158. *J. Bacteriol.* **184**:1693-1702.
69. **Tabata A, Yamamoto I, Matsuzaki M, Satoh T.** 2005. Differential regulation of periplasmic nitrate reductase gene (*napKEFDABC*) expression between aerobiosis and anaerobiosis with nitrate in a denitrifying phototroph *Rhodobacter sphaeroides* f. *sp. denitrificans*. *Arch. Microbiol.* **184**:108-116.
70. **Kraft B, Strous M, Tegetmeyer HE.** 2011. Microbial nitrate respiration - genes, enzymes and environmental distribution. *J. Biotechnol.* **155**:104-117.
71. **Rinaldo S, Sam KA, Castiglione N, Stelitano V, Arcovito A, Brunori M, Allen JWA, Ferguson SJ, Cutruzzolà F.** 2011. Observation of fast release of NO from ferrous *d*₁ haem allows formulation of a unified reaction mechanism for cytochrome *cd*₁ nitrite reductases. *Biochem. J.* **435**:217-225.
72. **Kawasaki S, Arai H, Kodama T, Igarashi Y.** 1997. Gene cluster for dissimilatory nitrite reductase (*nir*) from *Pseudomonas aeruginosa*: sequencing and identification of a locus for heme *d*₁ biosynthesis. *J. Bacteriol.* **179**:235-242.
73. **Bali S, Lawrence AD, Lobo SA, Saraiva LM, Golding BT, Palmer DJ, Howard MJ, Ferguson SJ, Warren MJ.** 2011. Molecular hijacking of siroheme for the synthesis of heme and *d*₁ heme. *Proc. Natl. Acad. Sci. U. S. A.* **108**:18260-18265.
74. **Palmedo G, Seither P, Korner H, Matthews JC, Burkhalter RS, Timkovich R, Zumft WG.** 1995. Resolution of the *nirD* locus for heme *d*₁ synthesis of cytochrome *cd*₁ (respiratory nitrite reductase) from *Pseudomonas stutzeri*. *Eur. J. Biochem.* **232**:737-746.
75. **Vanderoost J, Deboer APN, Degier JWL, Zumft WG, Stouthamer AH, Vanspanning RJM.** 1994. The heme-copper oxidase family consists of 3 distinct types of terminal oxidases and is related to nitric-oxide reductase. *FEMS Microbiol. Lett.* **121**:1-9.

76. **Wasser IM, de Vries S, Moenne-Loccoz P, Schroder I, Karlin KD.** 2002. Nitric oxide in biological denitrification: Fe/Cu metalloenzyme and metal complex NOx redox chemistry. *Chem. Rev. (Washington, DC, U. S.)* **102**:1201-1234.
77. **Sanford RA, Wagner DD, Wu Q, Chee-Sanford JC, Thomas SH, Cruz-Garcia C, Rodriguez G, Massol-Deya A, Krishnani KK, Ritalahti KM, Nissen S, Konstantinidis KT, Löffler FE.** 2012. Unexpected nondenitrifier nitrous oxide reductase gene diversity and abundance in soils. *Proc. Natl. Acad. Sci. U. S. A.* **109**:19709-19714.
78. **Matsunaga T, Tsujimura N.** 1993. Respiratory inhibitors of a magnetic bacterium *Magnetospirillum sp.* AMB-1 capable of growing anaerobically. *Appl. Microbiol. Biotechnol.* **39**:368-371.
79. **Taoka A, Yoshimatsu K, Kanemori M, Fukumori Y.** 2003. Nitrate reductase from the magnetotactic bacterium *Magnetospirillum magnetotacticum* MS-1: purification and sequence analyses. *Can. J. Microbiol.* **49**:197-206.
80. **Yamazaki T, Oyanagi H, Fujiwara T, Fukumori Y.** 1995. Nitrite reductase from the magnetotactic bacterium *Magnetospirillum magnetotacticum* - a novel cytochrome *cd₁* with Fe(II)-nitrite oxidoreductase activity. *Eur. J. Biochem.* **233**:665-671.
81. **Wang K, Ge X, Bo T, Chen Q, Chen G, Liu W.** 2011. Interruption of the denitrification pathway influences cell growth and magnetosome formation in *Magnetospirillum magneticum* AMB-1. *Let. Appl. Microbiol.* **53**:55-62.
82. **Schübbe S, Wurdemann C, Peplies J, Heyen U, Wawer C, Glockner FO, Schüler D.** 2006. Transcriptional organization and regulation of magnetosome operons in *Magnetospirillum gryphiswaldense*. *Appl. Environ. Microbiol.* **72**:5757-5765.
83. **Lambden PR, Guest JR.** 1976. Mutants of *Escherichia coli* K12 unable to use fumarate as an anaerobic electron acceptor. *J. Gen. Microbiol.* **97**:145-160.
84. **Spiro S, Guest JR.** 1990. FNR and its role in oxygen-regulated gene expression in *Escherichia coli*. *FEMS Microbiol. Rev.* **6**:399-428.
85. **Tolla DA, Savageau MA.** 2011. Phenotypic repertoire of the FNR regulatory network in *Escherichia coli*. *Mol. Microbiol.* **79**:149-165.
86. **Tseng CP, Albrecht J, Gunsalus RP.** 1996. Effect of microaerophilic cell growth conditions on expression of the aerobic (*cyoABCDE* and *cydAB*) and anaerobic (*narGHJI*, *frdABCD*, and *dmsABC*) respiratory pathway genes in *Escherichia coli*. *J. Bacteriol.* **178**:1094-1098.
87. **Stewart V, Bledsoe PJ, Chen LL, Cai A.** 2009. Catabolite repression control of *napF* (periplasmic nitrate reductase) operon expression in *Escherichia coli* K-12. *J. Bacteriol.* **191**:996-1005.
88. **Shaw DJ, Rice DW, Guest JR.** 1983. Homology between Cap and Fnr, a regulator of anaerobic respiration in *Escherichia coli*. *J. Mol. Biol.* **166**:241-247.

89. **Green J, Sharrocks AD, Green B, Geisow M, Guest JR.** 1993. Properties of FNR proteins substituted at each of the five cysteine residues. *Mol. Microbiol.* **8**:61-68.
90. **Khoroshilova N, Popescu C, Munck E, Beinert H, Kiley PJ.** 1997. Iron-sulfur cluster disassembly in the FNR protein of *Escherichia coli* by O₂: [4Fe-4S] to [2Fe-2S] conversion with loss of biological activity. *Proc. Natl. Acad. Sci. U. S. A.* **94**:6087-6092.
91. **Kiley PJ, Beinert H.** 1998. Oxygen sensing by the global regulator, FNR: the role of the iron-sulfur cluster. *FEMS Microbiol. Rev.* **22**:341-352.
92. **Lazazzera BA, Beinert H, Khoroshilova N, Kennedy MC, Kiley PJ.** 1996. DNA binding and dimerization of the Fe-S-containing FNR protein from *Escherichia coli* are regulated by oxygen. *J. Biol. Chem.* **271**:2762-2768.
93. **Crack J, Green J, Thomson AJ.** 2004. Mechanism of oxygen sensing by the bacterial transcription factor fumarate-nitrate reduction (FNR). *J. Biol. Chem.* **279**:9278-9286.
94. **Khoroshilova N, Beinert H, Kiley PJ.** 1995. Association of a polynuclear iron-sulfur center with a mutant FNR protein enhances DNA binding. *Proc. Natl. Acad. Sci. U. S. A.* **92**:2499-2503.
95. **Lazazzera BA, Bates DM, Kiley PJ.** 1993. The activity of the *Escherichia coli* transcription factor FNR is regulated by a change in oligomeric state. *Genes Dev.* **7**:1993-2005.
96. **Popescu CV, Bates DM, Beinert H, Munck E, Kiley PJ.** 1998. Mössbauer spectroscopy as a tool for the study of activation/inactivation of the transcription regulator FNR in whole cells of *Escherichia coli*. *Proc. Natl. Acad. Sci. U. S. A.* **95**:13431-13435.
97. **Jordan PA, Thomson AJ, Ralph ET, Guest JR, Green J.** 1997. FNR is a direct oxygen sensor having a biphasic response curve. *FEBS Lett.* **416**:349-352.
98. **Sutton VR, Mettert EL, Beinert H, Kiley PJ.** 2004. Kinetic analysis of the oxidative conversion of the [4Fe-4S]²⁺ cluster of FNR to a [2Fe-2S]²⁺ Cluster. *J. Bacteriol.* **186**:8018-8025.

CHAPTER 2

The periplasmic nitrate reductase Nap is required for anaerobic growth and involved in redox control of magnetite biomineralization in *Magnetospirillum gryphiswaldense*

The Periplasmic Nitrate Reductase Nap Is Required for Anaerobic Growth and Involved in Redox Control of Magnetite Biomineralization in *Magnetospirillum gryphiswaldense*

Yingjie Li, Emanuel Katzmann, Sarah Borg, and Dirk Schüler

Ludwig-Maximilians-Universität München, Department Biologie I, Mikrobiologie, Planegg-Martinsried, Germany

The magnetosomes of many magnetotactic bacteria consist of membrane-enveloped magnetite crystals, whose synthesis is favored by a low redox potential. However, the cellular redox processes governing the biomineralization of the mixed-valence iron oxide have remained unknown. Here, we show that in the alphaproteobacterium *Magnetospirillum gryphiswaldense*, magnetite biomineralization is linked to dissimilatory nitrate reduction. A complete denitrification pathway, including gene functions for nitrate (*nap*), nitrite (*nir*), nitric oxide (*nor*), and nitrous oxide reduction (*nos*), was identified. Transcriptional *gusA* fusions as reporters revealed that except for *nap*, the highest expression of the denitrification genes coincided with conditions permitting maximum magnetite synthesis. Whereas microaerobic denitrification overlapped with oxygen respiration, nitrate was the only electron acceptor supporting growth in the entire absence of oxygen, and only the deletion of *nap* genes, encoding a periplasmic nitrate reductase, and not deletion of *nor* or *nos* genes, abolished anaerobic growth and also delayed aerobic growth in both nitrate and ammonium media. While loss of *nosZ* or *norCB* had no or relatively weak effects on magnetosome synthesis, deletion of *nap* severely impaired magnetite biomineralization and resulted in fewer, smaller, and irregular crystals during denitrification and also microaerobic respiration, probably by disturbing the proper redox balance required for magnetite synthesis. In contrast to the case for the wild type, biomineralization in Δnap cells was independent of the oxidation state of carbon substrates. Altogether, our data demonstrate that in addition to its essential role in anaerobic respiration, the periplasmic nitrate reductase Nap has a further key function by participating in redox reactions required for magnetite biomineralization.

Magnetosomes are bacterial organelles synthesized by magnetotactic bacteria (MTB) for orientation in the Earth's magnetic field to facilitate the search for growth-favoring suboxic zones of stratified aquatic habitats (22). In the alphaproteobacterium *Magnetospirillum gryphiswaldense* MSR-1 (in the following referred to as MSR-1) and many other MTB, magnetosomes are membrane-enveloped magnetic crystals of magnetite (Fe_3O_4) which are aligned in chains along cytoskeletal structures (23, 24, 48). The intracellular biomineralization of magnetite is of substantial interdisciplinary interest not only for microbiology and cell biology but also for geobiology, biotechnology, and even astrobiology (22, 28, 48, 63).

Recent studies have shown that the biomineralization of magnetite crystals is under the control of a number of essential and accessory genes which have been speculated to all be encoded within a single genomic magnetosome island (31, 37, 45, 59). The synthesis of magnetosome crystals proceeds in several steps, which include the invagination of magnetosome membrane vesicles (24, 27) and the uptake of iron and its crystallization as magnetite within these vesicles (12, 44). Although the mechanism of biomineralization has not been fully elucidated, it has been suggested that the synthesis of the mixed-valence iron oxide magnetite (Fe_3O_4) occurs by coprecipitation from ferrous and ferric iron in supersaturating concentrations, which is favored by a low redox potential (11, 12, 33). It was observed early that *Magnetospirillum* ("Aquispirillum") *magnetotacticum* MS-1 (MS-1) is capable of microaerobic dissimilatory nitrate reduction and produces N_2O or N_2 as the final products (2), and in *Magnetospirillum magnetitum* strain AMB-1 (AMB-1) nitrate also supported magnetosome formation at low oxygen concentrations (35, 36, 66). Oxystat experiments further demonstrated that magnetite synthesis was in-

duced only when the oxygen concentration was below a threshold value of 2,000 Pa in MSR-1 and other magnetospirilla (19). Although molecular oxygen was initially assumed to be required for Fe_3O_4 biomineralization (6), it was later shown by isotope experiments that the oxygen bound in bacterially synthesized Fe_3O_4 is derived from water (32). In fact, in the marine vibrio strain MV-1 ("*Magnetovibrio blakemorii*") magnetosomes can be biomineralized in the entire absence of oxygen during anaerobic respiration with N_2O as an electron acceptor (3), and in *Desulfovibrio magneticus* RS-1 this can occur using either sulfate or fumarate as an electron acceptor (42). Although previous studies failed to demonstrate oxygen-independent growth and magnetosome synthesis in microaerophilic magnetospirilla MS-1 and MSR-1, earlier observations that magnetite synthesis is stimulated by nitrate suggested a potential link to denitrification also in these organisms (6, 19).

Bacterial denitrification is a respiratory process to reduce nitrate stepwise to nitrogen gas ($NO_3^- \rightarrow NO_2^- \rightarrow NO \rightarrow N_2O \rightarrow N_2$) (67). In many Gram-negative bacteria reduction of nitrate is catalyzed by a membrane-bound nitrate reductase (Nar), whereas in several other bacteria this reaction is instead performed by a periplasmic nitrate reductase (Nap) (30). Two isofunctional

Received 23 May 2012 Accepted 18 June 2012

Published ahead of print 22 June 2012

Address correspondence to Dirk Schüler, dirk.schueler@lmu.de.

Supplemental material for this article may be found at <http://jb.asm.org/>.

Copyright © 2012, American Society for Microbiology. All Rights Reserved.

doi:10.1128/JB.00903-12

periplasmic enzymes may catalyze the subsequent reduction of nitrite to nitric oxide: a homodimeric cytochrome *cd*₁ nitrite reductase, NirS, and a monotrimeric copper-containing enzyme, NirK (30). The further reduction of nitrite to nitric oxide is then catalyzed by an integral membrane protein complex (67). Its catalytic subunit NorB is structurally homologous to oxygen-reducing heme-copper oxidases, whereas NorC is a membrane-anchored protein with a heme domain in the periplasmic face (62). The last step of the denitrification pathway is the reduction of nitrous oxide to dinitrogen gas, which is catalyzed by the periplasmic multicopper enzyme nitrous oxide reductase (Nos) (30).

Despite their potential importance for magnetite biomineralization, the genetics and biochemistry of denitrification processes have not been well studied in MTB. A cytochrome *cd*₁-type nitrite reductase (NirS) was purified from MSR-1 and shown to accelerate the oxidation of ferrous iron in the presence of nitrite under anaerobic conditions *in vitro* (65). Later, a soluble periplasmic nitrate reductase implicated in magnetite synthesis was purified from MSR-1 (56). Wang et al. recently interrupted a gene (*norB*) for nitric oxide reductase in AMB-1 by transposon insertion and found that shorter magnetosome chains were produced under anaerobic conditions (61). However, except for this single study, no genetic evidence has been available for these possible functions *in vivo* so far, and the exact interrelation of these two pathways as well as the redox process governing magnetite biomineralization has largely remained unclear.

Here we started to explore the function of dissimilatory nitrate reduction in MSR-1 by expression analysis and mutagenesis of the periplasmic nitrate reductase Nap and comparison to the roles of downstream denitrification enzymes Nor and Nos. We found that Nap is important for biomineralization of fully functional magnetosomes in MSR-1 during both denitrification and microaerobic respiration. We demonstrate that in addition to its role in anaerobic respiration, Nap has a further key function by participating in redox reactions required for magnetite biomineralization.

MATERIALS AND METHODS

Bacterial strains and growth conditions. The bacterial strains and plasmids used in this study are shown in Tables S1 and S2 in the supplemental material. *Escherichia coli* strains were grown in lysogeny broth (LB) at 37°C. MSR-1 strains were grown at 30°C in modified flask standard medium (FSM) (19), which here was defined as nitrate medium if not specified otherwise. In ammonium medium, nitrate was replaced by 4 mM ammonium chloride. When necessary, antibiotics were added to the medium as follows: for *E. coli*, tetracycline (Tc) at 12 µg/ml, kanamycin (Km) at 25 µg/ml, ampicillin (Amp) at 50 µg/ml, and gentamicin (Gm) at 15 µg/ml, and for MSR-1, Tc at 5 µg/ml, Km at 5 µg/ml, and Gm at 30 µg/ml. When *E. coli* strain BW29427 was used as the donor in conjugation, 300 µM diaminopimelic acid (DAP) was added.

Growth experiments were carried out under microaerobic and anaerobic conditions in Hungate tubes containing 10 ml medium. For microaerobic conditions, Hungate tubes were sealed with butyl rubber stoppers under a microoxic gas mixture containing 2% O₂ and 98% N₂ before autoclaving. Anaerobic conditions were achieved by omitting O₂ from the gas mixture, where some trace oxygen initially being potentially present did not support any detectable growth in the absence of nitrate. For aerobic conditions, cells were incubated in free gas exchange with air in 300-ml flasks containing 20 ml medium agitated at 200 rpm. Optical density (OD) and magnetic response (C_{mag}) were measured photometrically at 565 nm as previously described (47). For gas production assay, cells were inoculated and mixed with FSM medium with 0.3% agar in

oxygen gradient tubes and incubated for 48 h exposed to the air. If not specified otherwise, inocula were prepared under aerobic conditions with a C_{mag} value of zero.

Genetic and molecular biology techniques. Standard molecular biological techniques were performed for DNA isolation, digestion, ligation, and transformation (43). DNA products were sequenced using BigDye Terminator version 3.1 chemistry on an ABI 3700 capillary sequencer (Applied Biosystems, Darmstadt, Germany). Sequence data were analyzed with the software Vector NTI Advance 11.5.1 (Invitrogen, Darmstadt, Germany). All oligonucleotide sequences used in this work are available if required.

Construction of mutant strains. All PCRs were performed using Phusion polymerase (NEB). Enzymes, including restriction enzymes and T4 DNA ligase, were purchased from Fermentas. For the interruption of *napA*, an internal fragment of *napA* was digested with ApaI and SacI and then ligated into pCM184 to yield pLYJ27. pLYJ27 was then inserted into MSR-1 by conjugation as described previously (49) to obtain a *napA::kanR* mutant strain. To generate the unmarked deletion mutant of the entire *nap* operon, a modified *cre-lox* method for large deletions was used (60). A 2-kb upstream PCR fragment of the *nap* operon was generated and cloned into EcoRI/NotI-digested pAL01 to obtain pLYJ85, the plasmid pLYJ85 was conjugationally integrated into the chromosome of MSR-1, and colonies screened positive by PCR for the presence of the kanamycin marker were designated Δnap -up. Subsequently, the plasmid pLYJ92 containing a 2-kb downstream fragment of the *nap* operon was integrated into the chromosome of Δnap -up by conjugation. After the presence of kanamycin and gentamicin markers was verified by screening PCR, the strain was designated Δnap -up-down. The *lox*-mediated excision of the *nap* operon was initiated by conjugational transformation of pCM157 (34). Precise excision was further confirmed by PCR amplification and sequencing. The plasmid pCM157 was lost by passaging cells several times in fresh nitrate medium. Finally, this strain was designated the Δnap mutant.

A two-step, *cre-lox*-based method (58) was used to generate unmarked deletions of *norCB* and *nosZ*. For *norCB* deletion, the 2-kb upstream PCR product was cloned into pCM184 between Acc65I and NotI sites, generating pLYJ31. A 2-kb downstream fragment of *norCB* was then ligated into MluI/SacI-digested pLYJ31 to obtain pLYJ34. For the deletion of *nosZ*, the upstream PCR product of the *nosZ* gene was cloned into NdeI/NotI-digested pCM184 to yield pLYJ32. The 2-kb downstream fragment of *nosZ* was digested with MluI and SacI and then ligated into pLYJ32 to obtain pLYJ35. Allelic exchange vectors pLYJ34 and pLYJ35 were then transformed into MSR-1 by conjugation. Deletion mutants were first screened on replica plates with kanamycin and tetracycline. Screening PCR was further performed for colonies which did not grow on tetracycline plates. To generate unmarked deletion mutants, pCM157 was conjugated into each mutant and subsequently cured from each mutant by several transfers in nitrate medium. Finally, the unmarked mutants were designated the $\Delta norCB$ and $\Delta nosZ$ mutants, respectively.

Complementation experiments. For genetic complementation of Δnap , $\Delta norCB$, and $\Delta nosZ$, a series of pBBR1MCS-2-based plasmids were generated. Plasmid pLYJ80, which contains the *nap* cluster, including its own promoter region, was constructed in three steps as illustrated in Fig. S1 in the supplemental material. For complementation of *norCB* and *nosZ*, pLYJ75 and pLYJ76, respectively, were used, in which the *norCB* and *nosZ* gene sequences with their own promoter regions were ligated into ApaI/SacI-digested pBBR1MCS-2.

Construction and analysis of transcriptional *gusA* fusions. To generate the transcriptional *nap-gusA*, *nirS-gusA*, *nor-gusA*, and *nosZ-gusA* fusion plasmids, the *gusA* gene from pK19mobGII was amplified and cloned between the HindIII and SmaI sites of pBBR1MCS-2 to obtain pLYJ97. Then *nap*, *nirS*, *norCBQD*, and *nosZ* promoter regions were cloned into Acc65I/HindIII-digested pLYJ97, designated pLYJ98, pLYJ94, pLYJ99, and pLYJ100, respectively. Plasmids were then introduced into wild-type (WT) MSR-1 by conjugation.

Cells in post-exponential phase were centrifuged, broken, and suspended in phosphate-buffered saline (PBS) for enzyme assay at 4°C. The protein concentration was determined by the method of Bradford (7). β -Glucuronidase activity was determined at 37°C as described by Wilson et al. (64). Units were expressed as nanomoles product formed per minute per milligram protein. Triplicate assays were performed, and the values reported were averaged by using at least two independent cultures.

Chemical analysis. For nitrate and nitrite analysis, MSR-1 cells were grown under anaerobic conditions for 20 h. Nitrate was detected using Szechrome reagents (Polysciences, Inc.). Diluted 20-fold samples of cultures were prepared, and Szechrome reagents were then added. After half an hour, the absorbance at 570 nm was recorded. When nitrate was no longer detectable, cultures without dilution were used to confirm the absence of nitrate. A nitrate standard curve (0 to 350 μ M) was obtained to convert absorbance values to concentrations.

Nitrite was measured with the modified Griess reagent (Sigma). One hundred microliters of 20-fold-diluted samples of cultures were mixed with equal modified Griess reagent and the absorbance recorded at 540 nm after 15 min. When no nitrite was detected, cultures without dilution were used to confirm the absence of nitrite. A nitrite standard curve (0 to 70 μ M) was generated to calculate final nitrite concentration.

Transmission electron microscopy (TEM). WT MSR-1 and mutants were grown at 25°C under anaerobic or microaerobic conditions up to an OD at 565 nm (OD_{565}) of 0.1 and then were concentrated and adsorbed onto carbon-coated copper grids. Samples were viewed and recorded with a TECNAI FEI20 microscope (FEI, Eindhoven, Netherlands) at 200 kV or with a Morgagni 268 microscope (FEI, Eindhoven, Netherlands) at 80 kV as previously described (25). For magnetosome analysis, more than 200 crystals and 100 cells were detected for each strain.

Bioinformatic analysis. Denitrification genes were identified by BLASTP (<http://blast.ncbi.nlm.nih.gov/Blast.cgi>) homology searches in the genomes of MSR-1 (GenBank accession no. CU459003.1), AMB-1 (GenBank accession no. AP007255.1), MS-1 (NCBI reference sequence NZ_AAAP000000000.1), and *Magnetococcus marinus* MC-1 (MC-1) (GenBank accession no. CP000471.1) with an expectation value E of $<1e-06$ and an amino acid similarity of $>50\%$.

RESULTS

MSR-1 is capable of anaerobic growth by a complete denitrification pathway. Various nitrogen sources were tested for their ability to support anaerobic growth and magnetite synthesis in MSR-1. As expected, no growth was observed in the presence of only NH_4^+ (see Table S3 in the supplemental material). Only very poor growth (OD of 0.01 or less) was observed with the denitrification intermediate nitrite at concentrations of ≤ 1 mM (Table 1), as well as with N_2O (see Table S3 in the supplemental material). However, significant anaerobic growth and magnetite formation was found in the presence of nitrate. Growth was concentration dependent up to 8 mM, and approximately 6 mM nitrate was utilized after 20 hours of incubation (Table 1). Excess nitrate (>10 mM) gradually decreased growth yields to zero at 20 mM. Growth at 4 mM nitrate led to transient accumulation of 0.1 mM nitrite, which was consumed as growth proceeded (see Fig. S2 in the supplemental material). Compared to anaerobic growth, MSR-1 incubated under microaerobic conditions and in the presence of 4 mM nitrate reached higher densities (see Table S3 in the supplemental material) while larger amounts of nitrite (about 1 mM) accumulated, likely due to repression of nitrite reduction by oxygen (described below). If nitrate was replaced by an equal amount of ammonium (4 mM), under microaerobic conditions the final cell yield was slightly reduced (see Table S3 in the supplemental material), whereas highest yields were reached under fully aerobic conditions in both nitrate and ammonium media. This suggested

TABLE 1 Effects of different nitrate and nitrite concentrations on growth and magnetic response after a 20-hour anaerobic incubation^a

Added nitrogen source and concn (mM)	Growth (ΔOD_{565}) ^b	C_{mag}	Nitrate left (mM)	Nitrite left (mM)
Nitrate				
0	0.00	1.7 \pm 0.1	0	0
1	0.06 \pm 0.00	1.8 \pm 0.1	0	0
2	0.12 \pm 0.00	1.9 \pm 0.0	0	0
4	0.20 \pm 0.00	1.8 \pm 0.1	0	0
6	0.25 \pm 0.01	1.7 \pm 0.1	0.36 \pm 0.07	0
8	0.32 \pm 0.02	1.8 \pm 0.0	2.23 \pm 0.25	0
10	0.29 \pm 0.01	1.8 \pm 0.1	3.89 \pm 0.66	0
11	0.14 \pm 0.02	1.9 \pm 0.0	5.42 \pm 0.44	0
12	0.09 \pm 0.04	1.8 \pm 0.1	6.53 \pm 0.12	0
15	0.08 \pm 0.00	1.8 \pm 0.1	7.83 \pm 0.62	0
20	-0.03 \pm 0.01	1.3 \pm 0.1	19.88 \pm 0.52	0
Nitrite				
0	0.00	1.7 \pm 0.1	0	0
0.5	0.01 \pm 0.00	1.7 \pm 0.0	0	0
1.0	0.01 \pm 0.00	1.7 \pm 0.1	0	0
1.5	-0.01 \pm 0.00	0.4 \pm 0.0	0	1.3 \pm 0.1
2.0	-0.02 \pm 0.00	0	0	1.9 \pm 0.0
2.5	-0.02 \pm 0.00	0	0	2.4 \pm 0.0

^a Values are means and standard deviations for experiments with triplicate cultures and repeated three times.

^b Negative values represent a decrease in cell density compared to the initial value on inoculation of 0.04.

that denitrification and aerobic respiration cooccurred simultaneously under microaerobic conditions.

Anaerobic magnetosome formation was independent of nitrate concentrations up to 15 mM (Table 1). However, although the C_{mag} value was slightly lower in anaerobically grown cells than in microaerobically grown cells (see Table S3 in the supplemental material), probably due to subtle effects on cell length (anaerobic, 4.4 ± 0.2 μ m; microaerobic, 4.2 ± 0.2 μ m) that are known to affect C_{mag} readings (26), anaerobically grown cells had higher magnetosome numbers (29, versus 25 in microaerobically grown cells), larger crystals (49.9 ± 5.0 nm, versus 41.1 ± 2.5 nm for microaerobically grown cells), and more regular crystal morphologies and chain alignment (Fig. 1). In microaerobic ammonium medium, cells biomineralized similar amounts of magnetite (23 crystals, 41.9 ± 2.0 nm) (Fig. 1; see Table S3 in the supplemental material), confirming that nitrate reduction is not essential for magnetosome formation under microaerobic conditions. Under aerobic conditions, cells were nonmagnetic ($C_{mag} = 0$) in both nitrate and ammonium media, similar to earlier findings (19).

Identification of denitrification genes in MSR-1 and other MTB. Using the respective protein sequences from *Pseudomonas stutzeri* as queries in BLASTP analysis, we reconstructed a complete pathway of denitrification from the genome of MSR-1. A putative *nap* operon containing *napFDAGHBC* genes for a periplasmic nitrate reductase was identified (Fig. 2; see Table S4 in the supplemental material), whereas we failed to detect *nar* genes encoding a membrane-bound nitrate reductase complex. *nap* operons but no *nar* genes are also present in other MTB, including the magnetospirilla AMB-1 and MS-1 as well as MC-1 (see Table S4 in the supplemental material). The organization of the *napFDAGHBC* operon resembles those of *nap* genes from *E. coli*

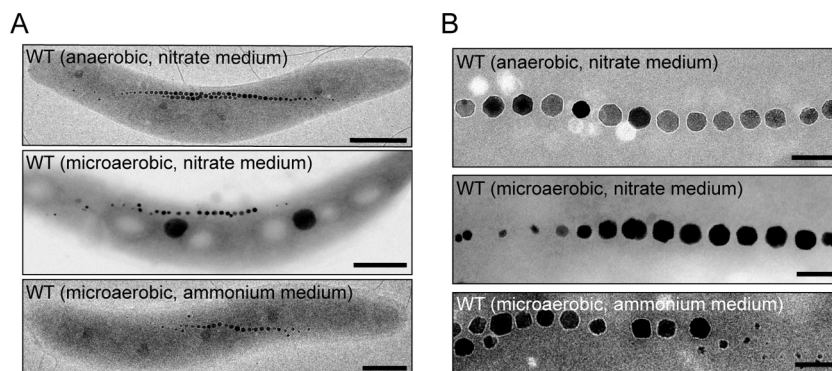


FIG 1 Effect of oxygen and nitrogen sources on magnetosome formation. (A) TEM micrographs of whole cells of the WT under the indicated conditions. Scale bars, 500 nm. (B) Close-up views of the magnetosome crystals shown in panel A. Scale bars, 100 nm.

(21), *Haemophilus influenzae* (17), and *Rhodobacter sphaeroides* 2.4.3 (18), in which this type of clusters has been designated *nap*- β (53). In many bacteria, this Nap cluster is used for anaerobic growth via nitrate respiration (17).

A *nirS* gene, encoding a homodimeric cytochrome *cd*₁ nitrite reductase, was found in MSR-1 next to several other *nir* genes of partially unknown functions located on a short contig of the incomplete genome assembly of MSR-1 (data not shown). *norC* and *norB*, encoding nitric oxide reductase subunits, are part of an operon also comprising *norQ* and *norD* in MSR-1, AMB-1, and MC-1, whereas we failed to detect *nor* genes in strain MS-1, possibly due to the incompleteness of its genome assembly. A singular *nosZ* gene was identified in MSR-1 and AMB-1 but not in MC-1, whereas no other *nos* genes that are usually collocated with *nosZ* in the same operon (5, 8, 20) were found in magnetospirilla. In MS-1 two complementary *nosZ* fragments were detected on two different contigs of the incomplete genome assembly.

Expression of *nir*, *nor*, and *nos* but not *nap* is upregulated by nitrate and downregulated by oxygen. Since maximum magnetite synthesis in MSR-1 occurs at low oxygen tensions and in the presence of nitrate (Table 1; see Table S3 in the supplemental material), we tested whether the expression of denitrification genes is correlated with magnetosome formation. To this end, transcriptional gene fusions of *napFDAGHBC*, *nirS*, *norCBQD*, and *nosZ* with *gusA*, encoding β -glucuronidase, were constructed and transferred into WT MSR-1 by conjugation. As shown in Table 2, cells containing the transcriptional *nap-gusA* reporter

gene fusion exhibited an approximately 2-fold increase of β -glucuronidase activity under aerobic compared to microaerobic conditions, whereas nitrate had no obvious effect on *nap-gusA* expression. In contrast, about a 6-fold-higher level of β -glucuronidase activity was observed under microaerobic conditions with nitrate than without nitrate, whereas increased oxygen concentrations resulted in decreased β -glucuronidase activity. WT MSR-1 carrying *nor-gusA* showed the same pattern as for *nirS-gusA*, i.e., a higher level of *norCBQD* expression under microaerobic conditions in the presence of nitrate (762.7 ± 37.0 U) than in the absence of nitrate (221.5 ± 52.4 U), whereas β -glucuronidase activity was lowered by increasing oxygen concentrations. *nosZ-gusA* also exhibited an approximately 5-fold-higher β -glucuronidase activity under microaerobic conditions in the presence of nitrate than in its absence, and it was downregulated by oxygen.

Notably, the finding that the expression of *nap* was different from that of other denitrification genes suggested that Nap might have a distinct function. In addition, whereas *nirS* and *nosZ* are absent from the genome of nondenitrifying strain MC-1 (46), *nap* and *nor* genes are more widely conserved within alphaproteobacterial MTB. Therefore, further genetic analysis was focused mostly on these genes.

NosZ and NorCB are required for complete denitrification but have only minor roles in magnetite synthesis. A *norCB* deletion strain was constructed as described in Materials and Methods. When Δ *norCB* cells were incubated microaerobically in ammonium medium or aerobically in either nitrate or ammonium

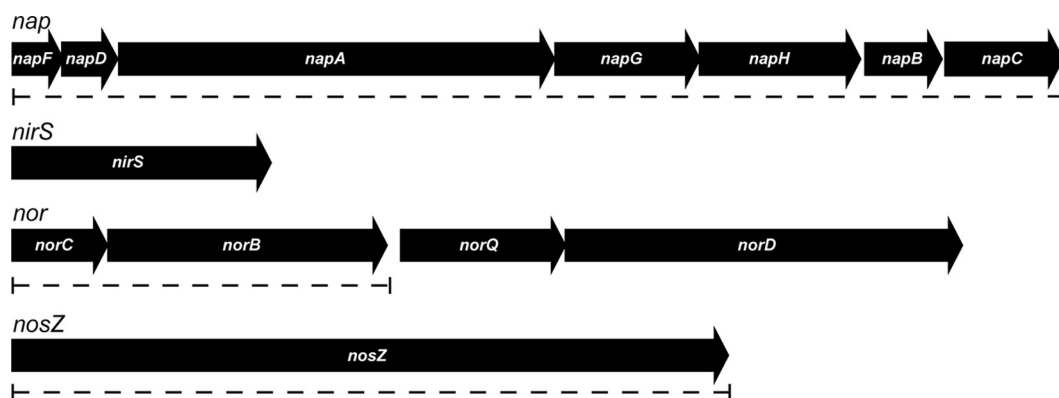


FIG 2 Molecular organization of identified denitrification genes in MSR-1. Dashed lines indicate the extent of deletions in mutant strains.

TABLE 2 Effects of oxygen and nitrate on transcriptional expression of denitrification genes *nap*, *nirS*, *nor*, and *nos* fused with *gusA*

Promoter	β -Glucuronidase activity (U) ^a			
	Microaerobic conditions		Aerobic conditions	
	With NO ₃ ⁻	Without NO ₃ ⁻	With NO ₃ ⁻	Without NO ₃ ⁻
<i>nap</i>	16.2 ± 1.4	15.9 ± 0.8	30.8 ± 2.6	28.6 ± 2.8
<i>nirS</i>	124.0 ± 5.5	21.2 ± 9.6	14.2 ± 7.9	18.3 ± 7.8
<i>norCBQD</i>	762.8 ± 37.0	221.5 ± 52.4	204.4 ± 41.1	151.1 ± 10.5
<i>nosZ</i>	519.0 ± 43.4	118.3 ± 33.3	146.6 ± 34.7	152.5 ± 21.9

^a Values are averages and standard deviations for at least replicate cultures.

medium, no significant effect on growth was observed (Fig. 3A, B, and C). However, no growth occurred in the presence of nitrate under anaerobic and microaerobic conditions, probably due to the toxicity of accumulated nitric oxide, as demonstrated for AMB-1 (61). In the presence of ammonium under microaerobic conditions, the average C_{mag} of the Δ *norCB* mutant was slightly lower than that of the WT (Fig. 3C). Δ *norCB* cells were slightly shorter ($3.7 \pm 0.2 \mu\text{m}$, versus $4.1 \pm 0.3 \mu\text{m}$ for the WT) and contained fewer magnetosomes (14 crystals per cell, versus 23 in the WT) (Fig. 4A and B), whereas crystal size and morphology were unaffected. Complementation of Δ *norCB* mutants with plasmid pLYJ75 harboring a WT *norCB* allele restored growth and magnetosome formation back to the WT levels (Fig. 4C; see Fig. S3A in the supplemental material). For comparison, a *nosZ* deletion mutant was constructed. As shown in Fig. S3B in the supplemental material, in the Δ *nosZ* mutant no bubble was detected in semisolid agar due to the high solubility of N₂O, and Δ *nosZ* was complemented with plasmid pLYJ76, which restored the activity of nitrous oxide reduction to dinitrogen gas. The deletion of *nosZ* did not affect magnetosome formation under any tested condition (Fig. 3A, B, C, D, and E), and cells contained magnetosomes virtually identical to those of the WT with respect to crystal morphology, size, and number (Fig. 4A and B). However, loss of *nosZ* resulted in a slightly reduced growth under anaerobic conditions compared to that of the WT, which may result from reduced energy yields obtained by incomplete denitrification (Fig. 3E).

Nap functions as a nitrate reductase during anaerobic growth. To abolish its function, we first attempted to interrupt the *nap* operon by insertion of a *kanR* cassette into *napA* (*napA::kanR*) in MSR-1 (details are shown in Fig. S4 in the supplemental material). However, this *napA::kanR* mutant still showed a WT-like phenotype for nitrate reduction and magnetite formation, probably due to some residual activity (data not shown). Therefore, a further deletion mutant (Δ *nap*) was constructed by unmarked excision of the entire *nap* operon. Compared to the WT, the Δ *nap* mutant displayed a markedly delayed growth (it took more than 50 h to reach stationary phase, compared to about 24 h for the WT) when cells were cultured aerobically in either nitrate or ammonium medium (Fig. 3A and B). Hardly any difference in growth was found in ammonium medium between the WT and the Δ *nap* mutant under microaerobic conditions (Fig. 3C). However, in microaerobic nitrate medium Δ *nap* cells did not consume and reduce nitrate and reached lower cell densities than the WT, probably due to reduced energy yields (Fig. 3D). No growth or nitrate utilization was observed for the Δ *nap* mutant in nitrate medium under anaerobic conditions, confirming that Nap func-

tions as the primary nitrate reductase for anaerobic respiration in MSR-1.

Deletion of *nap* severely affects microaerobic magnetite biom mineralization. Under microaerobic conditions, the loss of *nap* genes resulted in significantly decreased C_{mag} values (<1.0) (Fig. 3C and D) not only in ammonium medium but also nitrate medium, in which mutant cells grew only by aerobic respiration due to the absence of Nap. As shown in Fig. 4A and B, compared to Δ *nosZ* and Δ *norCB*, deletion of *nap* had a much stronger effect on magnetosomes, which were significantly smaller ($24.8 \pm 4.5 \text{ nm}$, versus $41.1 \pm 2.5 \text{ nm}$ for WT crystals under microaerobic conditions in nitrate medium), present in lower numbers (9 crystals per cell, versus 25 crystals per cell in the WT), and appearing as irregularly shaped, misaligned particles. To ensure that the observed phenotypes in fact were caused by the introduced mutation, the Δ *nap* mutant was complemented with plasmid pLYJ80, which restored the activity of nitrate reduction (data not shown), as well as WT-like growth and magnetosome formation (Fig. 4D; see Fig. S3A in the supplemental material).

Nap functions in maintaining proper redox balance for magnetosome formation. Although nitrate was no longer utilized in Δ *nap* cells, redundant nitrate at levels as high as 8 mM did not affect magnetite synthesis (Table 1). Furthermore, Δ *nap* cells growing microaerobically in ammonium medium (in the absence of nitrate) also produced fewer and irregular magnetosomes, resembling those in the presence of nitrate. This indicated that besides being required for nitrate reduction, Nap might have an additional function for magnetosome formation.

On the other hand, it had been hypothesized previously by Taoka and colleagues that nitrate reduction was not essential for Fe₃O₄ synthesis (56), whereas reduction of nitrite was implicated in the oxidation of ferrous iron to produce the mixed-valence Fe₃O₄ (65). Therefore, we asked whether the observed effect of *nap* deletion on magnetosomes might result indirectly from a regulatory effect on nitrite reduction, which might be suppressed in the Δ *nap* mutant. To test this possibility, aerobically grown non-magnetic Δ *nap* and WT cells were precultured as described in Materials and Methods. Growth experiments were then performed under microaerobic and anaerobic conditions, in which 500 μM nitrite, the product of nitrate reduction catalyzed by Nap in the WT, was added to ammonium medium. As shown in Fig. 5, under microaerobic conditions in the absence of *nap*, nitrite was still utilized. However, again the C_{mag} value was much lower than that of the WT. When Δ *nap* cells were incubated anaerobically in the absence of nitrate but in the presence of 500 μM nitrite, nitrite was completely consumed after 20 h, although neither the WT nor the Δ *nap* mutant obviously grew under these conditions. The C_{mag} was only about 0.6 in the Δ *nap* mutant, while a C_{mag} value of 1.6 was found in the WT. Taken together, these results precluded effects of deregulated nitrite reduction in the Δ *nap* mutant.

Alternatively, it has been shown previously that in other denitrifying bacteria, such as *Paracoccus pantotrophus* and *R. sphaeroides*, the periplasmic Nap enzyme is regulated by the oxidation state of carbon substrates, and it is thought to play a role in maintaining redox homeostasis by dissipating excess reductant during aerobic growth (10, 16, 50, 55). Furthermore, it was observed by us that there was a significant growth lag in the Δ *nap* mutant of MSR-1 under aerobic conditions (Fig. 3A and B), which would be consistent with the suggestion by Richardson et al. (41) that excess reductant causes lower growth rates because NADH has to be

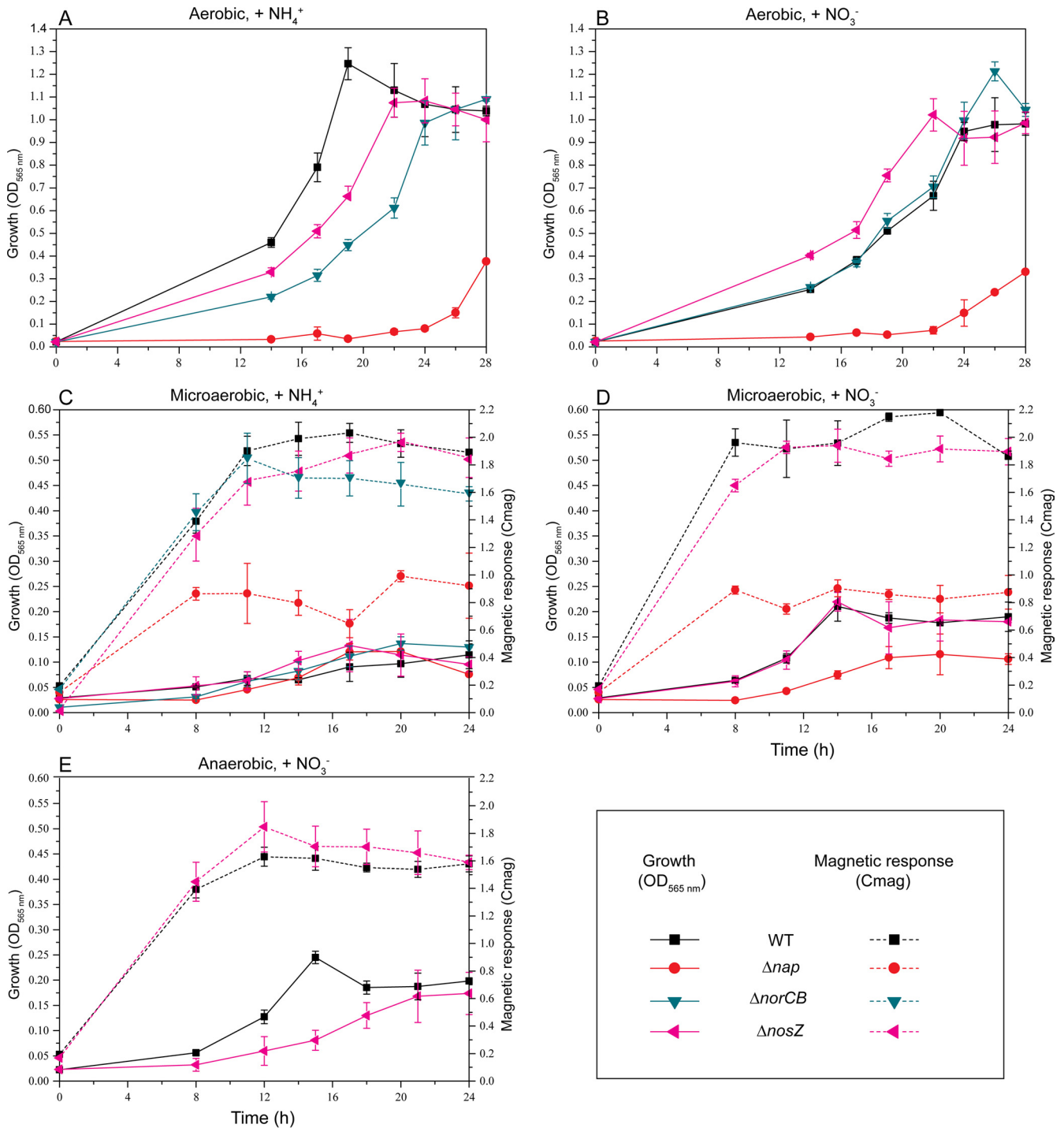


FIG 3 Growth (OD₅₆₅) and magnetic response (C_{mag}) of WT MSR-1 and the Δnap , $\Delta norCB$, and $\Delta nosZ$ mutants under different conditions. Under aerobic conditions, the C_{mag} values were always zero and not shown. (A) Aerobic, ammonium medium; (B) aerobic, nitrate medium; (C) microaerobic, ammonium medium; (D) microaerobic, nitrate medium; (E) anaerobic, nitrate medium. Results from representative experiments were measured in triplicate, and values are given as means and standard deviations.

reoxidized by cell maintenance reactions, as also observed in *P. pantotrophus* and *Rhodobacter capsulatus* growing on carbon sources which are more reduced than the biomass (10, 40). Therefore, we hypothesized that in MSR-1 the Nap system also might be involved in the maintenance of the intracellular redox balance,

which consequently may affect the species of iron within the periplasm and magnetosome vesicles. Transcription from the *nap* promoter was tested in both the WT and the Δnap mutant in the presence of carbon substrates with different oxidation states (Table 3). No difference in the β -glucuronidase activity with different

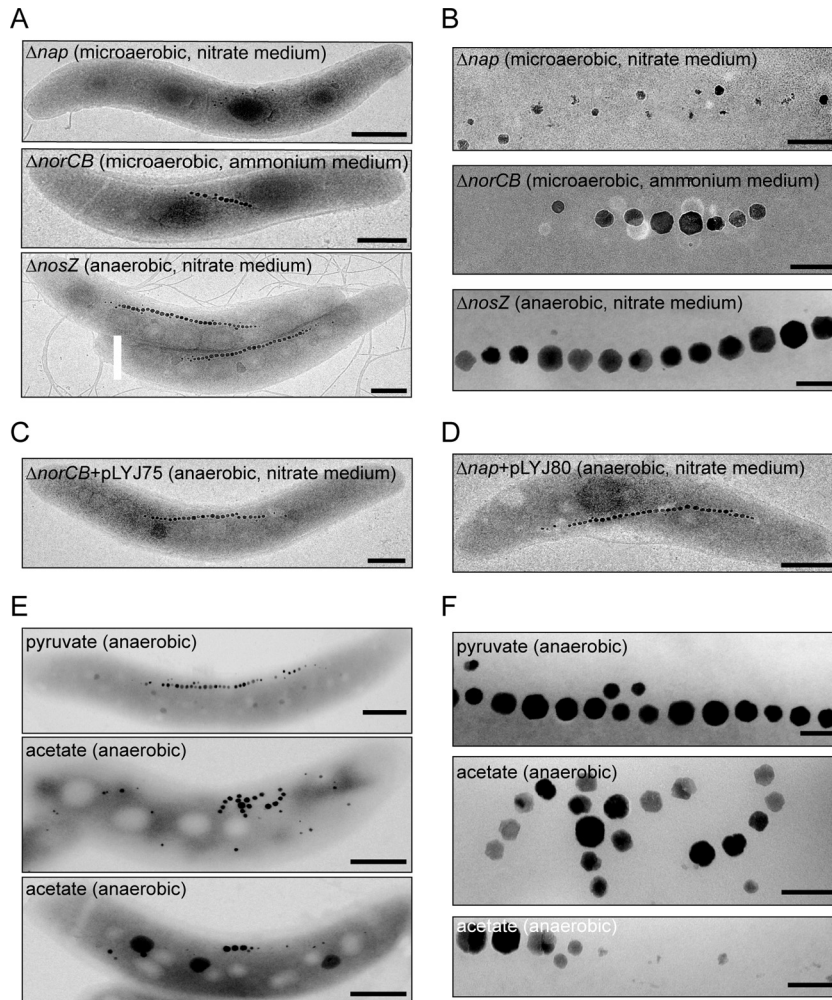


FIG 4 (A) TEM micrographs of Δnap , $\Delta norCB$, and $\Delta nosZ$ whole cells under the indicated conditions. Scale bars, 500 nm. (B) Close-up views of the magnetosome crystals shown in panel A. Scale bars, 100 nm. (C and D) TEM micrographs of anaerobically grown $\Delta norCB$ (C) and Δnap (D) cells complemented with plasmids pLYJ75 and pLYJ80, respectively, harboring their WT alleles. Scale bars, 500 nm. (E) TEM micrographs of WT cells grown anaerobically on pyruvate and acetate. Scale bars, 500 nm. (F) Close-up views of the magnetosome crystals shown in panel E. Scale bars, 100 nm.

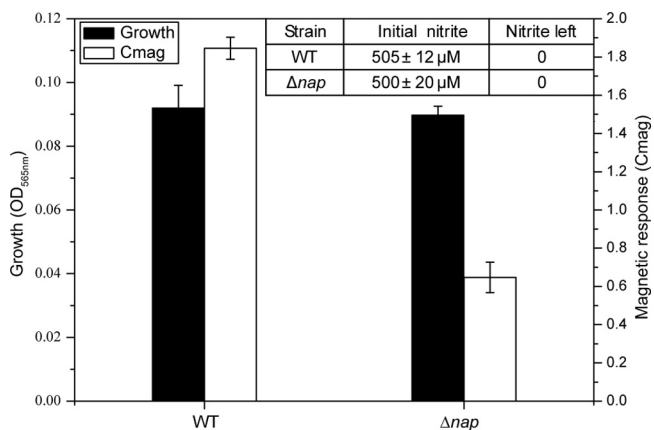


FIG 5 Growth (OD_{565nm}) and magnetic response (C_{mag}) of WT MSR-1 and the Δnap mutant under microaerobic conditions with 500 μM nitrite added to ammonium medium.

carbon substrates under microaerobic conditions and under aerobic conditions was found for the WT (Table 3). Only a slight increase in *nap-gusA* expression was observed in the WT under aerobic conditions compared to that under microaerobic conditions, which is in agreement with the observed upregulation of *nap* expression by oxygen (Table 2). In the Δnap mutant, no effect on expression on different carbon sources was found under microaerobic conditions, and a similar level of β -glucuronidase activity was detectable under aerobic conditions. However, when we shifted nonmagnetic cells from 21% to 0% oxygen, WT cells developed much lower C_{mag} values on the more reduced carbon substrate acetate than on the more oxidized substrates pyruvate and succinate (Table 3). TEM showed that magnetite biomineralization in acetate-grown cells was affected: in addition to cells with regular magnetosome chains, a variable proportion (>50%) of cells with irregular and shorter chains and with fewer (Fig. 4E and F) and smaller crystals (36.2 ± 1.3 nm, versus 42.7 ± 1.2 nm with pyruvate), as well as cells entirely devoid of magnetite crystals, was present. In contrast, C_{mag} values in the Δnap mutant were equally

TABLE 3 Effects of different carbon sources on magnetic response and transcriptional expression of *nap-gusA*

Carbon substrate (concn, mM)	Avg oxidation no. of carbons	C_{mag}		β -Glucuronidase activity (U) ^a			
		Δnap mutant,		WT		Δnap mutant	
		WT, anaerobic	anaerobic	Microaerobic	Aerobic	Microaerobic	Aerobic
Pyruvate (27)	+0.66	1.7 ± 0.1	0.6 ± 0.1	31.7 ± 1.0	49.9 ± 4.4	72.3 ± 7.9	77.3 ± 0.1
Succinate (27)	+0.50	1.6 ± 0.1	0.5 ± 0.0	33.4 ± 1.0	54.2 ± 2.2	77.5 ± 4.0	83.7 ± 6.3
Acetate (27)	+0.00	0.8 ± 0.0	0.5 ± 0.0	31.2 ± 7.7	42.7 ± 1.0	75.3 ± 6.8	78.5 ± 0.2

^a Values are averages and standard deviations for at least replicate cultures.

low with different carbon substrates (Table 3). Therefore, in acetate-grown cells of the WT, impaired magnetosome formation could be due to regulation of Nap activity rather than *nap* expression by the oxidation state of carbon sources, similar to what has been described for Nap of *R. sphaeroides* DSM158, in which expression of a *napA-lacZ* gene fusion was similar in cells grown with carbon substrates of different oxidation states, whereas Nap activity was higher on reduced carbon sources (16).

DISCUSSION

Except for *nap*, the maximum expression of all identified denitrification genes (*nir*, *nor*, and *nos*) coincided with conditions of highest magnetite synthesis, i.e., the presence of nitrate and low concentrations or absence of oxygen. This pattern is similar to that for other nonmagnetic bacteria, such as *P. stutzeri* (29), *R. sphaeroides* 2.4.3 (1, 57), and *Bradyrhizobium japonicum* (5). However, under microaerobic conditions in the absence of nitrate, where expression of denitrification genes *nirS*, *nor*, and *nosZ* was reduced, magnetite biomineralization of WT cells was independent of the presence of nitrate, suggesting that denitrification and oxygen respiration may have overlapping functions under microaerobic conditions. Whereas deletion of *nosZ* only had a weak effect on anaerobic growth and biomineralization, we were unable to detect any growth in our $\Delta norCB$ mutant of MSR-1 under anaerobic and microaerobic conditions in the presence of nitrate, probably due to the toxicity of the accumulated intermediate nitric oxide, since growth could be rescued by additional deletion of *nirS* in the $\Delta norCB$ background (Y. Li and D. Schüler, unpublished data). In contrast, in a previous study Wang and colleagues reported some growth for an AMB-1 $\Delta norB$ mutant under anaerobic conditions (61). The discrepancy between *nor* mutants of MSR-1 (no growth) and AMB-1 (poor growth) might be due to different genotypes, since in the AMB-1 mutant only *norB* (located downstream of *norC*) was interrupted by transposon insertion, thereby possibly retaining some residual activity of the nitric oxide reductase enzyme. The slightly reduced magnetosome number of the MSR-1 $\Delta norCB$ mutant is unlikely to result from limited energy yields during denitrification as speculated by Wang et al. (61), since oxygen respiration in ammonium medium is unlikely to be affected by loss of denitrification proteins. On the other hand, the comparatively high expression levels of our *norCB-gusA* fusion suggest that in the absence of nitrate under microaerobic and aerobic conditions, NorCB may be involved in further, yet-unknown functions directly or indirectly linked to magnetosome formation. For example, it has been shown that Nor from *Paracoccus denitrificans* is capable of reducing oxygen to water *in vitro* (13, 15), which also might be a possible function for Nor in MSR-1 during microaerobic respiration and magnetite biomineralization.

Since only the loss of *nap* genes and not that of other denitri-

fication genes directly abolished growth and since intermediates such as nitrite supported only very weak anaerobic growth of the WT and Δnap strains, the reduction of nitrate to nitrite catalyzed by the periplasmic Nap enzyme, and not the subsequent reduction steps, is the primary energy-generating process of denitrification. Deletion of the entire *nap* cluster not only abolished anaerobic growth but also severely impaired magnetite synthesis under microaerobic conditions in the presence of either nitrate or ammonium, resulting in fewer, smaller, and misshapen magnetosome crystals. This is in agreement with the finding that the abolishment of nitrate reductase activity by deprivation of molybdenum, an essential cofactor of the periplasmic nitrate reductase, resulted in an approximately 60% decrease of iron content of cells from strain MS-1 (56). Unlike growth, magnetite synthesis in the WT showed no dependency on the electron acceptor (i.e., nitrate) concentration, suggesting that this effect was not primarily due to energy limitation of cells. The Nap enzymes of other nonmagnetic bacteria were implicated in redox balancing using nitrate as an ancillary oxidant to dissipate excess reductant (40). Consistent with the suggestion that lower growth rates may be caused by excess reductant (41), we observed a significant lag of growth in Δnap cells under aerobic conditions. In addition, although the oxidation state of carbon sources did not affect transcription of *nap*, WT cells contained shorter and irregular crystal chains on the more reduced substrate acetate than on more oxidized substrate pyruvate, while in the Δnap mutant magnetite synthesis was equally low on different carbon sources. Similar to the case for Nap in other bacteria, such as *P. pantotrophus* Pd1222 (50) and various strains of *R. sphaeroides* (16, 18, 55), our data are consistent with a role of Nap of MSR-1 in the maintenance of the intracellular redox balance, thus posing an optimum redox potential for magnetite synthesis. The lower C_{mag} in acetate-grown cells of even the WT might indicate that Nap activity is still insufficient to dispel all excess reductant originating from reduced carbon substrates. Moreover, the lack of a difference in magnetosome biomineralization in Δnap cells grown on different carbon sources might be explained by excess reductant *in vivo* even in medium with the oxidized substrate pyruvate.

Unlike that of other denitrification genes, transcription of the *nap* operon was induced by oxygen but unaffected by nitrate. This regulation pattern is different from that in *E. coli*, in which *nap* gene expression is induced by anaerobiosis and nitrate limitation (9, 54), and in *P. pantotrophus*, where *nap* genes are expressed only during aerobiosis (51). However, *nap* regulation in MSR-1 resembles that in *Ralstonia eutropha* and *R. sphaeroides* DSM158, in which *nap* systems show a higher expression level under aerobic conditions and are not induced by nitrate (16, 52). Furthermore, a consensus Fnr (fumarate and nitrate reduction regulatory pro-

tein) box (TTGAN₆TCAA) (39) is located about 80 bp upstream of the putative translation start of *napF* of MSR-1, which is also consistent with *nap* regulation by oxygen. Taken together, these data indicate that *Nap* likely functions also during aerobic respiration, which is in agreement with its speculated role in dissipation of intracellular reductant.

Overall, we demonstrated that magnetite biomineralization in MSR-1 in fact is closely linked to nitrate reduction catalyzed by periplasmic nitrate reductase *Nap*, which participates in redox reactions required for magnetite biomineralization in addition to its role in anaerobic respiration. While the absence of *nir* and *nosZ* genes in other MTB such as MC-1 is consistent with their reported inability to grow and respire by denitrification (14, 46), this indicates that a complete denitrification pathway is not absolutely required for magnetosome formation. Interestingly, the presence of a *nap* cluster and *nor* genes even in the MC-1 genome (46) agrees with our observation that these genes are important for magnetosome formation also during aerobic respiration, suggesting that they may have functions in magnetite biomineralization which are distinct from their roles as merely respiratory enzymes. Denitrification genes absent in other MTB might be replaced by genes for other redox enzymes. For example, in the magnetotactic marine vibrio strain MV-1, which can respire anaerobically with N₂O as an electron acceptor, the N-terminal sequence determined from a purified periplasmic, copper-containing Fe(II) oxidase displays homology to the putative N₂O reductase from MS-1 (4), which indicates that magnetosome formation may be linked to respiration by other, unknown functions. Recently, Nishida and Silver have shown that synthesis of magnetic mineral particles is also possible in nonmagnetotactic yeast *Saccharomyces cerevisiae*, which confirms that intracellular redox control through carbon metabolism and iron supply is an important factor for magnetite biomineralization (38). Finally, our study provides evidence that in MSR-1 genes located outside the genomic magnetosome island are also required for synthesis of magnetosomes that are fully functional with respect to their numbers, sizes, and shapes to serve properly as navigational devices.

ACKNOWLEDGMENT

We thank the China Scholarship Council (CSC) for financial support.

REFERENCES

- Bartnikas TB, Tosques IE, Laratta WP, Shi J, Shapleigh JP. 1997. Characterization of the nitric oxide reductase-encoding region in *Rhodobacter sphaeroides* 2.4.3. *J. Bacteriol.* 179:3534–3540.
- Bazylinski DA, Blakemore RP. 1983. Denitrification and assimilatory nitrate reduction in *Aquaspirillum magnetotacticum*. *Appl. Environ. Microbiol.* 46:1118–1124.
- Bazylinski DA, Frankel R, Jannasch HW. 1988. Anaerobic magnetite production by a marine magnetotactic bacterium. *Nature* 334:518–519.
- Bazylinski DA, Williams T. 2006. Ecophysiology of magnetotactic bacteria, p 64. In Schüler D (ed), *Magnetoreception and magnetosomes in bacteria*. Springer Verlag, Heidelberg, Germany.
- Bedmar EJ, Robles EF, Delgado MJ. 2005. The complete denitrification pathway of the symbiotic, nitrogen-fixing bacterium *Bradyrhizobium japonicum*. *Biochem. Soc. Trans.* 33:141–144.
- Blakemore RP, Short KA, Bazylinski DA, Rosenblatt C, Frankel R. 1985. Microaerobic conditions are required for magnetite formation within *Aquaspirillum magnetotacticum*. *Geomicrobiol. J.* 4:53–71.
- Bradford MM. 1976. A rapid and sensitive method for the quantitation of microgram quantities of protein utilizing the principle of protein-dye binding. *Anal. Biochem.* 72:248–254.
- Cuyppers H, Berghofer J, Zumft WG. 1995. Multiple *nosZ* promoters and anaerobic expression of *nos* genes necessary for *Pseudomonas stutzeri* nitrous oxide reductase and assembly of its copper centers. *Biochim. Biophys. Acta* 1264:183–190.
- Darwin AJ, Ziegelhoffer EC, Kiley PJ, Stewart V. 1998. *Fnr*, *NarP*, and *NarL* regulation of *Escherichia coli* K-12 *napF* (periplasmic nitrate reductase) operon transcription *in vitro*. *J. Bacteriol.* 180:4192–4198.
- Ellington MJ, Bhakoo KK, Sawers G, Richardson DJ, Ferguson SJ. 2002. Hierarchy of carbon source selection in *Paracoccus pantotrophus*: strict correlation between reduction state of the carbon substrate and aerobic expression of the *nap* operon. *J. Bacteriol.* 184:4767–4774.
- Faivre D, et al. 2004. Mineralogical and isotopic properties of inorganic nanocrystalline magnetites. *Geochim. Cosmochim. Acta* 68:4395–4403.
- Faivre D, Böttger LH, Matzanke BF, Schüler D. 2007. Intracellular magnetite biomineralization in bacteria proceeds by a distinct pathway involving membrane-bound ferritin and an iron(II) species. *Angew. Chem. Int. Ed. Engl.* 46:8495–8499.
- Flock U, Watmough NJ, Adelroth P. 2005. Electron/proton coupling in bacterial nitric oxide reductase during reduction of oxygen. *Biochemistry* 44:10711–10719.
- Frankel RB, Bazylinski DA, Johnson MS, Taylor BL. 1997. Magnetoaerotaxis in marine coccoid bacteria. *Biophys. J.* 73:994–1000.
- Fujiwara T, Fukumori Y. 1996. Cytochrome *cb*-type nitric oxide reductase with cytochrome *c* oxidase activity from *Paracoccus denitrificans* ATCC 35512. *J. Bacteriol.* 178:1866–1871.
- Gavira M, Roldan MD, Castillo F, Moreno-Vivian C. 2002. Regulation of *nap* gene expression and periplasmic nitrate reductase activity in the phototrophic bacterium *Rhodobacter sphaeroides* DSM158. *J. Bacteriol.* 184:1693–1702.
- Gonzalez PJ, Correia C, Moura I, Brondino CD, Moura JJ. 2006. Bacterial nitrate reductases: molecular and biological aspects of nitrate reduction. *J. Inorg. Biochem.* 100:1015–1023.
- Hartsock A, Shapleigh JP. 2011. Physiological roles for two periplasmic nitrate reductases in *Rhodobacter sphaeroides* 2.4.3 (ATCC 17025). *J. Bacteriol.* 193:6483–6489.
- Heyen U, Schüler D. 2003. Growth and magnetosome formation by microaerophilic *Magnetospirillum* strains in an oxygen-controlled fermentor. *Appl. Microbiol. Biotechnol.* 61:536–544.
- Holloway P, McCormick W, Watson RJ, Chan YK. 1996. Identification and analysis of the dissimilatory nitrous oxide reduction genes, *nosRZDFY*, of *Rhizobium meliloti*. *J. Bacteriol.* 178:1505–1514.
- Jepson BJ, et al. 2006. Evolution of the soluble nitrate reductase: defining the monomeric periplasmic nitrate reductase subgroup. *Biochem. Soc. Trans.* 34:122–126.
- Jogler C, Schüler D. 2009. Genomics, genetics, and cell biology of magnetosome formation. *Annu. Rev. Microbiol.* 63:501–521.
- Jogler C, et al. 2011. Conservation of proteobacterial magnetosome genes and structures in an uncultivated member of the deep-branching *Nitrospira* phylum. *Proc. Natl. Acad. Sci. U. S. A.* 108:1134–1139.
- Katzmann E, Scheffel A, Gruska M, Plitzko JM, Schüler D. 2010. Loss of the actin-like protein MamK has pleiotropic effects on magnetosome formation and chain assembly in *Magnetospirillum gryphiswaldense*. *Mol. Microbiol.* 77:208–224.
- Katzmann E, et al. 2011. Magnetosome chains are recruited to cellular division sites and split by asymmetric septation. *Mol. Microbiol.* 82:1316–1329.
- Kolinko I, Jogler C, Katzmann E, Schüler D. 2011. Frequent mutations within the genomic magnetosome island of *Magnetospirillum gryphiswaldense* are mediated by RecA. *J. Bacteriol.* 193:5328–5334.
- Komeili A, Li Z, Newman DK, Jensen GJ. 2006. Magnetosomes are cell membrane invaginations organized by the actin-like protein MamK. *Science* 311:242–245.
- Komeili A. 2007. Molecular mechanisms of magnetosome formation. *Annu. Rev. Biochem.* 76:351–366.
- Korner H, Zumft WG. 1989. Expression of denitrification enzymes in response to the dissolved oxygen level and respiratory substrate in continuous culture of *Pseudomonas stutzeri*. *Appl. Environ. Microbiol.* 55:1670–1676.
- Kraft B, Strous M, Tegetmeyer HE. 2011. Microbial nitrate respiration—genes, enzymes and environmental distribution. *J. Biotechnol.* 155:104–117.
- Lohsse A, et al. 2011. Functional analysis of the magnetosome island in *Magnetospirillum gryphiswaldense*: the *mamAB* operon is sufficient for magnetite biomineralization. *PLoS One* 6:e25561. doi:10.1371/journal.pone.0025561.

32. Mandernack KW, Bazylinski DA, Shanks WC, Bullen TD. 1999. Oxygen and iron isotope studies of magnetite produced by magnetotactic bacteria. *Science* 285:1892–1896.
33. Mann S, Sparks NHC, Board RG. 1990. Magnetotactic bacteria: microbiology, biomineralization, palaeomagnetism and biotechnology. *Adv. Microb. Physiol.* 31:125–181.
34. Marx C, Lidstrom M. 2002. Broad-host-range *cre-lox* system for antibiotic marker recycling in Gram-negative bacteria. *Biotechniques* 33:1062–1067.
35. Matsunaga T, Sakaguchi T, Tadokoro F. 1991. Magnetite formation by a magnetic bacterium capable of growing aerobically. *Appl. Microbiol. Biotechnol.* 35:651–655.
36. Matsunaga T, Tsujimura N. 1993. Respiratory inhibitors of a magnetic bacterium *Magnetospirillum* sp. AMB-1 capable of growing anaerobically. *Appl. Microbiol. Biotechnol.* 39:368–371.
37. Murat D, Quinlan A, Vali H, Komeli A. 2010. Comprehensive genetic dissection of the magnetosome gene island reveals the step-wise assembly of a prokaryotic organelle. *Proc. Natl. Acad. Sci. U. S. A.* 107:5593–5598.
38. Nishida K, Silver PA. 2012. Induction of biogenic magnetization and redox control by a component of the target of rapamycin complex 1 signaling pathway. *PLoS Biol.* 10:1–10. doi:10.1371/journal.pbio.1001269.
39. Ouchane S, Picaud M, Therizols P, Reiss-Husson F, Astier C. 2007. Global regulation of photosynthesis and respiration by FnrL: the first two targets in the tetrapyrrole pathway. *J. Biol. Chem.* 282:7690–7699.
40. Richardson DJ, et al. 1988. The role of auxiliary oxidants in maintaining redox balance during phototrophic growth of *Rhodobacter capsulatus* on propionate or butyrate. *Arch. Microbiol.* 150:131–137.
41. Richardson DJ, Berks BC, Russell DA, Spiro S, Taylor CJ. 2001. Functional, biochemical and genetic diversity of prokaryotic nitrate reductases. *Cell. Mol. Life Sci.* 58:165–178.
42. Sakaguchi T, Arakaki A, Matsunaga T. 2002. *Desulfovibrio magneticus* sp. nov., a novel sulfate-reducing bacterium that produces intracellular single-domain-sized magnetite particles. *Int. J. Syst. Evol. Microbiol.* 52:215–221.
43. Sambrook J, Russel D. 2001. Molecular cloning: a laboratory manual, 3rd ed. Cold Spring Harbor Laboratory Press, Cold Spring Harbor, NY.
44. Scheffel A, et al. 2006. An acidic protein aligns magnetosomes along a filamentous structure in magnetotactic bacteria. *Nature* 440:110–114.
45. Schübbe S, et al. 2003. Characterization of a spontaneous nonmagnetic mutant of *Magnetospirillum gryphiswaldense* reveals a large deletion comprising a putative magnetosome island. *J. Bacteriol.* 185:5779–5790.
46. Schübbe S, et al. 2009. Complete genome sequence of the chemolithoautotrophic marine *Magnetotactic coccus* strain MC-1. *Appl. Environ. Microbiol.* 75:4835–4852.
47. Schüler D, Baeuerlein E. 1998. Dynamics of iron uptake and Fe₃O₄ biomineralization during aerobic and microaerobic growth of *Magnetospirillum gryphiswaldense*. *J. Bacteriol.* 180:159–162.
48. Schüler D. 2008. Genetics and cell biology of magnetosome formation in magnetotactic bacteria. *FEMS Microbiol. Rev.* 32:654–672.
49. Schultheiss D, Schüler D. 2003. Development of a genetic system for *Magnetospirillum gryphiswaldense*. *Arch. Microbiol.* 179:89–94.
50. Sears HJ, Spiro S, Richardi J. 1997. Effect of carbon substrate and aeration on nitrate reduction and expression of the periplasmic and membrane-bound nitrate reductases in carbon-limited continuous cultures of *Paracoccus denitrificans* Pd1222. *Microbiology* 143:3767–3774.
51. Sears HJ, Sawers G, Berks BC, Ferguson SJ, Richardson DJ. 2000. Control of periplasmic nitrate reductase gene expression (*napEDABC*) from *Paracoccus pantotrophus* in response to oxygen and carbon substrates. *Microbiology* 146:2977–2985.
52. Siddiqui RA, et al. 1993. Structure and function of a periplasmic nitrate reductase in *Alcaligenes eutrophus* H16. *J. Bacteriol.* 175:5867–5876.
53. Simpson PJ, Richardson DJ, Codd R. 2010. The periplasmic nitrate reductase in *Shewanella*: the resolution, distribution and functional implications of two NAP isoforms, NapEDABC and NapDAGHB. *Microbiology* 156:302–312.
54. Stewart V, Bledsoe PJ, Chen LL, Cai A. 2009. Catabolite repression control of *napF* (periplasmic nitrate reductase) operon expression in *Escherichia coli* K-12. *J. Bacteriol.* 191:996–1005.
55. Tabata A, Yamamoto I, Matsuzaki M, Satoh T. 2005. Differential regulation of periplasmic nitrate reductase gene (*napKEFDABC*) expression between aerobiosis and anaerobiosis with nitrate in a denitrifying phototroph *Rhodobacter sphaeroides* f. sp. *denitrificans*. *Arch. Microbiol.* 184:108–116.
56. Taoka A, Yoshimatsu K, Kanemori M, Fukumori Y. 2003. Nitrate reductase from the magnetotactic bacterium *Magnetospirillum magnetotacticum* MS-1: purification and sequence analyses. *Can. J. Microbiol.* 49:197–206.
57. Tosques IE, Kwiatkowski AV, Shi J, Shapleigh JP. 1997. Characterization and regulation of the gene encoding nitrite reductase in *Rhodobacter sphaeroides* 2.4.3. *J. Bacteriol.* 179:1090–1095.
58. Uebe R, et al. 2010. Deletion of a *fur*-like gene affects iron homeostasis and magnetosome formation in *Magnetospirillum gryphiswaldense*. *J. Bacteriol.* 192:4192–4204.
59. Ullrich S, Kube M, Schübbe S, Reinhardt R, Schüler D. 2005. A hyper-variable 130-kilobase genomic region of *Magnetospirillum gryphiswaldense* comprises a magnetosome island which undergoes frequent rearrangements during stationary growth. *J. Bacteriol.* 187:7176–7184.
60. Ullrich S, Schüler D. 2010. *Cre-lox*-based method for generation of large deletions within the genomic magnetosome island of *Magnetospirillum gryphiswaldense*. *Appl. Environ. Microbiol.* 76:2349–2444.
61. Wang K, et al. 2011. Interruption of the denitrification pathway influences cell growth and magnetosome formation in *Magnetospirillum magneticum* AMB-1. *Lett. Appl. Microbiol.* 53:55–62.
62. Watmough NJ, Field SJ, Hughes RJ, Richardson DJ. 2009. The bacterial respiratory nitric oxide reductase. *Biochem. Soc. Trans.* 37:392–399.
63. Weiss BP, et al. 2004. Magnetic tests for magnetosome chains in Martian meteorite ALH84001. *Proc. Natl. Acad. Sci. U. S. A.* 101:8281–8284.
64. Wilson KJ, Hughes SG, Jefferson RA. 1992. The *Escherichia coli* *gus* operon: induction and expression of the *gus* operon in *E. coli* and the occurrence and use of *GUS* in other bacteria, p 7–22. In Gallagher SR (ed), *GUS* protocols. Using the *GUS* gene as reporter of gene expression. Academic Press Inc., San Diego, CA.
65. Yamazaki T, Oyanagi H, Fujiwara T, Fukumori Y. 1995. Nitrite reductase from the magnetotactic bacterium *Magnetospirillum magnetotacticum*—a novel cytochrome *cd*₁ with Fe(II)-nitrite oxidoreductase activity. *Eur. J. Biochem.* 233:665–671.
66. Yang CD, Takeyama H, Tanaka T, Matsunaga T. 2001. Effects of growth medium composition, iron sources and atmospheric oxygen concentrations on production of luciferase-bacterial magnetic particle complex by a recombinant *Magnetospirillum magneticum* AMB-1. *Enzyme Microb. Technol.* 29:13–19.
67. Zumft W. 1997. Cell biology and molecular basis of denitrification. *Microbiol. Mol. Biol. Rev.* 61:533–616.

SUPPLEMENTAL MATERIALS

Table S1 Bacterial strains used in this work

Strain	Important feature (s)	Source or reference
<i>E. coli</i> strain DH5 α	F' Φ 80dlacZ Δ M15 Δ (lacZYA-argF)U169 deoR recA1 endA1 hsdR17 (r _k ⁻ , m _k ⁺) phoA supE44 λ -thi-1 gyrA96 relA1	Invitrogen
<i>E. coli</i> strain BW29427	dap auxotroph derivative of <i>E. coli</i> strain B2155	K. Datsenko and B. L. Wanner, unpublished
MSR-1 WT	Wild type R3/S1, but Rif ^r , Sm ^r	(1)
Δ nirS Δ norCB	R3/S1 Δ nirS Δ norCB	Y. Li and D. Schüler, unpublished data
napA:: <i>kanR</i>	R3/S1 nap:: <i>pLYJ27</i>	This study
Δ nap-up	R3/S1 nap:: <i>pLYJ85</i>	This study
Δ nap-up-down	R3/S1 nap:: <i>pLYJ85::pLYJ92</i>	This study
Δ nap	R3/S1 Δ nap	This study
Δ norCB	R3/S1 Δ norCB	This study
Δ nosZ	R3/S1 Δ nosZ	This study

Table S2 Plasmids used in this work

Plasmid	Important feature(s)	Source or reference
pJTE1.2/blunt	Amp ^r , <i>eco47IR</i> (lethal restriction enzyme gene), <i>rep</i> (pMB-1)	Fermentas
pCM184	Broad-host-range allelic exchange vector, Amp ^r , Km ^r , Tc ^r	(2)
pBBR1MCS-2	Km ^r , mobilizable broad-host-range vector	(3)
pK19mobGII	-	(4)
pAL01	Km ^r , pK19mobGII vector (Km ^r , pMB-1 replicon, <i>gusA</i> , <i>lacZ</i>) containing a 2 kb fragment upstream of <i>mgr4019</i>	(5)
pAL02/2	Gm ^r , pT18mob2 vector containing a 2 kb fragment downstream of <i>mgr4019</i>	(5)
pCM157	Tc ^r , Cre recombinase expression vector	(2)
pLYJ27	pCM184 plus <i>napA</i> 2-kb internal region	This study
pLYJ31	pCM184 plus <i>norCB</i> 2-kb upstream region	This study
pLYJ32	pCM184 plus <i>nosZ</i> 2-kb downstream region	This study
pLYJ34	pLYJ31 plus <i>norCB</i> 2-kb downstream region	This study
pLYJ35	pLYJ32 plus <i>nosZ</i> 2-kb upstream region	This study
pLYJ71	pBBR1MCS-2 plus <i>nap1</i> with its own promoter	This study
pLYJ75	pBBR1MCS-2 plus <i>norCB</i> with its own promoter	This study
pLYJ76	pBBR1MCS-2 plus <i>nosZ</i> with its own promoter	This study
pLYJ78	pJET1.2/blunt plus <i>nap2</i>	This study
pLYJ79	pLYJ71 plus <i>nap2</i> from pLYJ78	This study
pLYJ80	pLYJ78 plus <i>nap3</i>	This study
pLYJ85	pAL01 plus <i>nap</i> 2-kb upstream region	This study
pLYJ92	pAL02/2 plus <i>nap</i> 2-kb downstream region	This study
pLYJ97	pBBR1MCS-2 plus <i>gusA</i> from pK19mobGII	This study
pLYJ94	pLYJ97 plus <i>nirS</i> promoter region	This study
pLYJ98	pLYJ97 plus <i>nap</i> promoter region	This study
pLYJ99	pLYJ97 plus <i>norCB</i> promoter region	This study
pLYJ100	pLYJ97 plus <i>nosZ</i> promoter region	This study

Table S3 Effect of different electron acceptors and oxygen on growth and magnetic response

Culture condition	Nitrogen source	Growth ($\Delta OD_{565 \text{ nm}}^a$)	Magnetic response (Cmag)
Anaerobic	4 mM NO_3^-	0.18 ± 0.02	1.8 ± 0.2
	1 mM NO_2^-	0.01 ± 0.00	1.7 ± 0.0
	10 mM N_2O	0.01 ± 0.000	1.7 ± 0.0
	4 mM NH_4^+	0	ND ^b
Microaerobic	4 mM NO_3^-	0.23 ± 0.01	2.1 ± 0.2
	4 mM NH_4^+	0.17 ± 0.06	2.0 ± 0.2
Aerobic	4 mM NO_3^-	1.21 ± 0.04	0
	4 mM NH_4^+	1.25 ± 0.07	0

^a Values represent means and standard deviations were obtained with triplicate cultures and repeated three times.

^b Cmag value was not tested.

Table S4 BlastP analysis results of denitrification genes in MTB and non-MTB using MSR-1 as a query

Gene in MSR-1	Encoded gene product (aa, kDa, pI)	AMB-1 (e-value, similarity)	MS-1 (e-value, similarity)	MC-1 (e-value, similarity)	Best hit in non-MTB (e-value, similarity)
<i>mgr_4000*</i>	NapF, small transmembrane protein of unknown function (6) (102, 10.17, 8.67)	<i>amb2692</i> (1e-18, 64%) ^b	<i>BAB59020.1</i> (4e-13, 67%)	<i>mmc1_1591</i> (2e-10, 62%)	<i>Serratia odorifera</i> 4Rx13 (1e-18, 64%)
<i>mgr_4001*</i>	NapD, cytoplasmic protein (6) (102, 11.21, 4.91)	<i>amb2691</i> (5e-43, 76%)	<i>magn03008202</i> (2e-41, 77%)	<i>mmc1_1592</i> (8e-07, 54%)	<i>Beggiatoa</i> sp. PS (9e-17, 62%)
<i>mgr_4002*</i>	NapA, nitrate reductase (NR) catalytic subunit containing molybdenum cofactor and a [4Fe-4S] cluster (7) (835, 93.60, 8.70)	<i>amb2690</i> (0, 91%)	<i>magn03008203</i> (0, 91%)	<i>mmc1_1591</i> (0, 83%)	<i>Azoarcus</i> sp. BH72 (0, 85%)
<i>mgr_4003*</i>	NapG, soluble protein (8) (272, 28.92, 7.44)	<i>amb2689</i> (2e-125, 78%)	<i>magn03008204</i> (4e-124, 79%)	<i>mmc1_1590</i> (4e-93, 71%)	<i>Laribacter hongkongensis</i> HLHK9 (3e-111, 78%)
<i>mgr_4004*</i>	NapH, membrane protein (8) (304, 32.72, 9.42)	<i>amb2688</i> (9e-132, 77%)	<i>magn03008205</i> (3e-125, 77%)	<i>mmc1_1589</i> (4e-85, 65%)	<i>Dechloromonas aromatica</i> RCB (3e-112, 70%)
<i>mgr_4005*</i>	NapB, NR subunit, a c-type cytochrome (7) (148, 16.44, 8.66)	<i>amb2687</i> (1e-63, 79%)	<i>magn03008206</i> (1e-66, 79%)	<i>mmc1_1588</i> (8e-31, 56%)	<i>Pseudovibrio</i> sp. JE062 (5e-38, 65%)
<i>mgr_4006*</i>	NapC, a membrane-bound tetraheme (7) (222, 25.53, 8.91)	<i>amb2686</i> (3e-115, 87%)	<i>magn03008207</i> (4e-114, 87%)	<i>mmc1_1587</i> (4e-77, 72%)	<i>Pseudovibrio</i> sp. JE062 (4e-90, 71%)
<i>mgr_1052</i>	Nitrite reductase, NirS (540, 59.26, 8.81)	<i>amb1395</i> (0, 91%) <i>amb4165</i> (0, 78%)	<i>magn03008451</i> (0, 91%)	–	<i>Dechlorosoma suillum</i> PS (0, 90%)
<i>mgr_3484*</i>	Nitric-oxide reductase subunit C, NorC (149, 16.23, 6.90)	<i>amb2945</i> (5e-84, 88%)	–	<i>mmc_0121</i> (4e-57, 72%)	<i>Nitrosococcus halophilus</i> Nc4 (1e-74, 81%)
<i>mgr_3485*</i>	Nitric-oxide reductase subunit B, NorB (445, 50.35, 8.82)	<i>amb2944</i> (0, 93%)	–	<i>mmc_0120</i> (1e-179, 73%)	<i>Azospirillum</i> sp. B510 (0, 87%)
<i>mgr_3486</i>	NorQ (262, 28.95, 5.40)	<i>amb2943</i> (1e-151, 90%)	–	<i>mmc_0119</i> (1e-108, 77%)	<i>Halomonas halodenitrificans</i> (1e-144, 86%)

<i>mgr_3487</i>	NorD (632, 70.80, 7.75)	<i>amb2942</i> (0, 78%)	–	<i>mmc_0117</i> (2e-64, 51%)	<i>Nitrosococcus halophilus</i> Nc4 (0, 70%)
<i>mgr_2761</i> *	Nitrous-oxide reductase, NosZ (760, 83.78, 6.06)	<i>amb3086</i> (0, 90%)	<i>magn03008954</i> (9e-145, 92%) <i>magn03007281</i> (0, 88%)	–	<i>Dechlorosoma suillum</i> PS (0, 86%)

*indicate genes deleted.

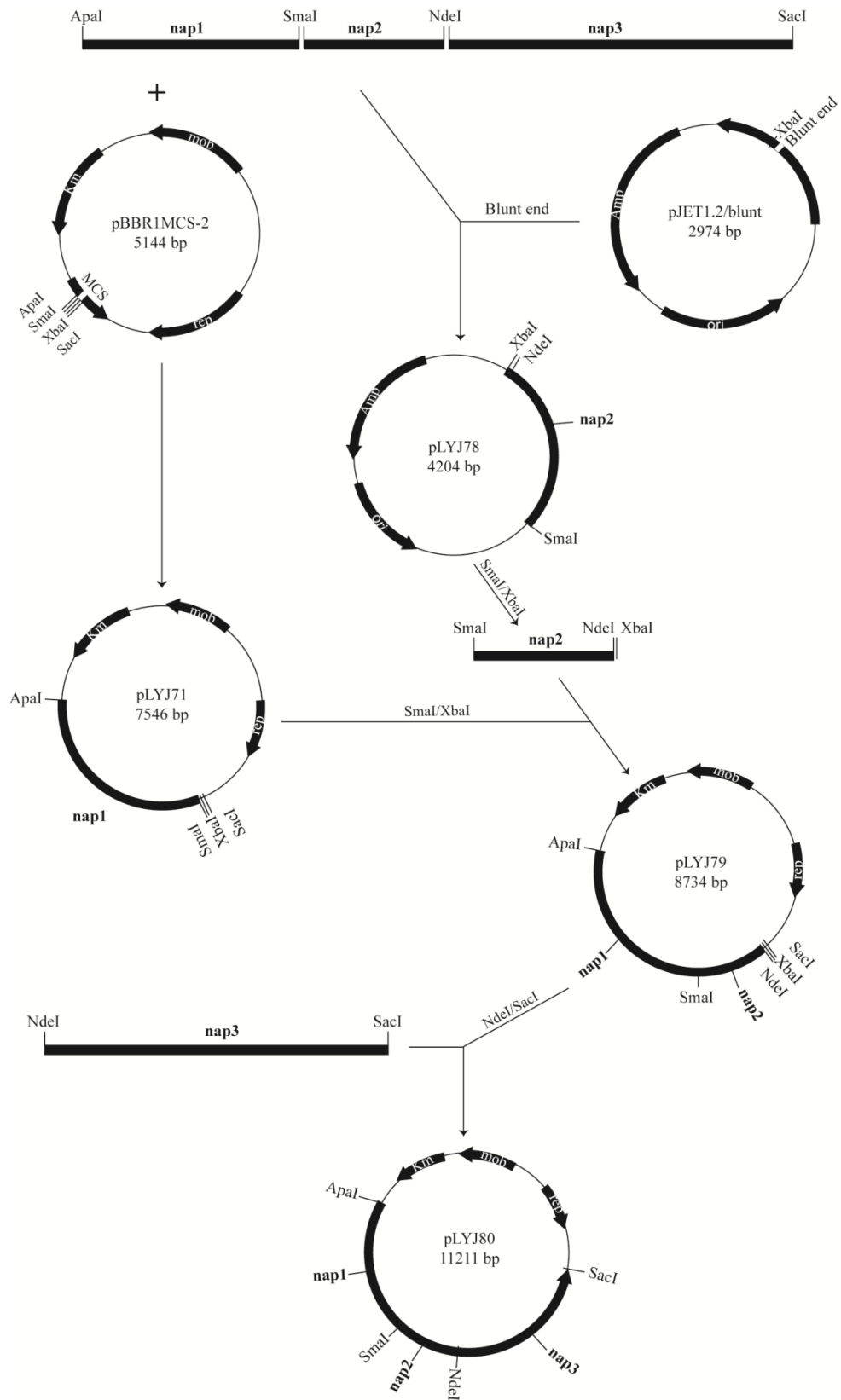


Fig. S1 Scheme for the construction of the large complementation plasmid pLYJ80 (about 11 kb) for Δnap .

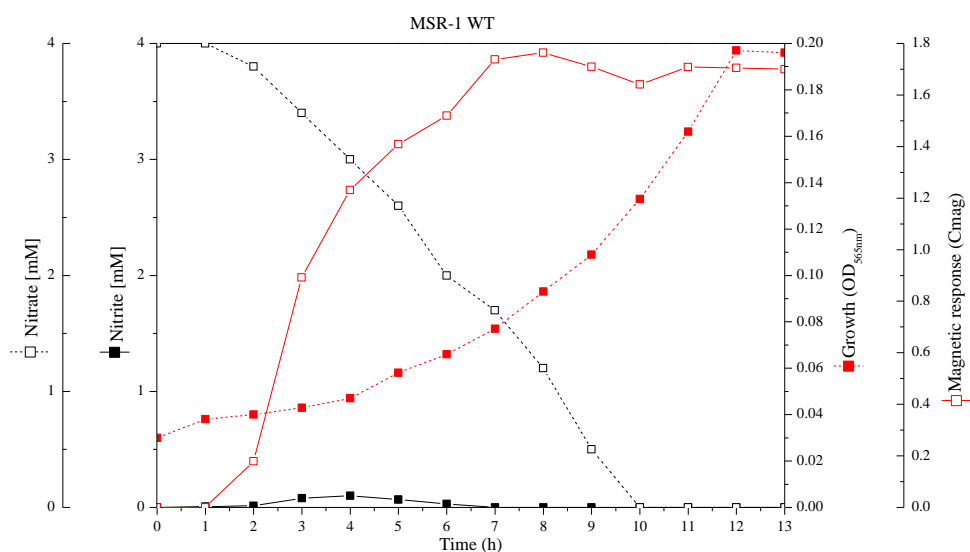


Fig. S2 Nitrate utilization in WT with an initial nitrate concentration of 4 mM (nitrate medium).

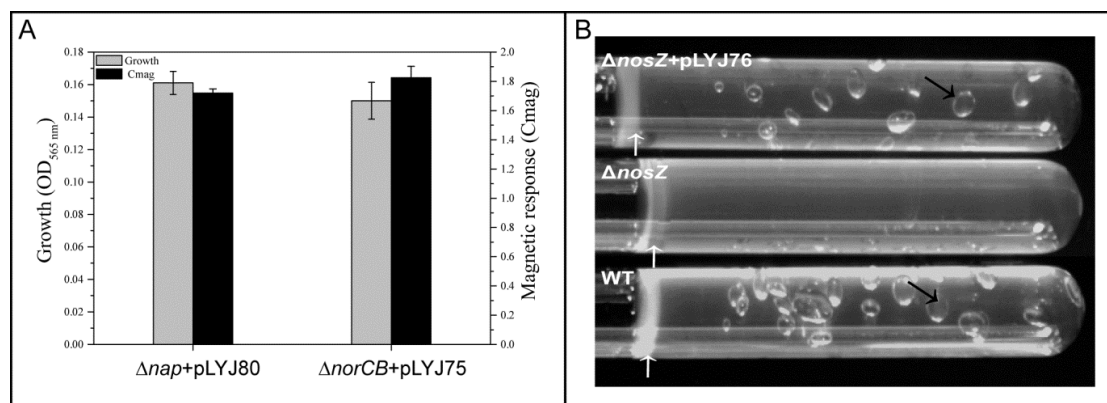


Fig. S3 (A) Growth (OD_{565 nm}) and magnetic response (Cmag) of $\Delta nap+pLYJ80$ and $\Delta norCB+pLYJ75$ under anaerobic conditions. $\Delta nap+pLYJ80$ and $\Delta norCB+pLYJ75$ represented mutant cells harboring their respective WT alleles. (B) Gas production assay in WT, $\Delta nosZ$ and $\Delta nosZ+pLYJ76$ in semisolid agar. $\Delta nosZ+pLYJ76$ represented *nosZ* mutant cell harboring a WT *nosZ* allele. Cells grew as bands (white arrows), and bubbles (black arrows) were detected in WT and complemented *nosZ* strain cultures but not in $\Delta nosZ$ mutant.

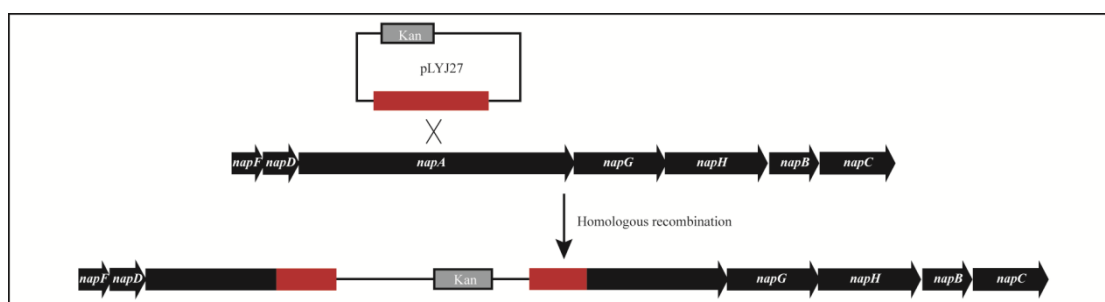


Fig. S4 Schematic representation of steps employed for the interruption of *napA* (*napA::kanR*) in MSR-1. The insertion mutant showed WT-like growth and C_{mag} values. Under microaerobic and anaerobic conditions, it still consumed nitrate like the WT (data not shown).

REFERENCES

1. **Schultheiss D, Kube M, Schüler D.** 2004. Inactivation of the flagellin gene *flaA* in *Magnetospirillum gryphiswaldense* results in nonmagnetotactic mutants lacking flagellar filaments. *Appl. Environ. Microbiol.* **70**:3624-3631.
2. **Marx C, Lidstrom M.** 2002. Broad-host-range *cre-lox* system for antibiotic marker recycling in Gram-negative bacteria. *BioTechniques* **33**:1062-1067.
3. **Kovach ME, Elzer PH, Hill DS, Robertson GT, Farris MA, Roop RM, Peterson KM.** 1995. Four new derivatives of the broad-host-range cloning vector pBBR1MCS, carrying different antibiotic-resistance cassettes. *Gene* **166**:175-176.
4. **Katzen F, Becker A, Ielmini MV, Oddo CG, Ielpi L.** 1999. New mobilizable vectors suitable for gene replacement in gram-negative bacteria and their use in mapping of the 3' end of the *Xanthomonas campestris* pv. *campestris* *gum* operon. *Appl. Environ. Microbiol.* **65**:278-282.
5. **Lohse A, Ullrich S, Katzmann E, Borg S, Wanner G, Richter M, Voigt B, Schweder T, Schüler D.** 2011. Functional analysis of the magnetosome island in *Magnetospirillum gryphiswaldense*: the *mamAB* operon is sufficient for magnetite biomineralization. *PLoS One* **6**:e25561.
6. **Reyes F, Gavira M, Castillo F, Moreno-Vivian C.** 1998. Periplasmic nitrate-reducing system of the phototrophic bacterium *Rhodobacter sphaeroides* DSM 158: transcriptional and mutational analysis of the *napKEFDABC* gene cluster. *Biochem. J.* **331** (Pt 3):897-904.
7. **Moreno-Vivian C, Cabello P, Martinez-Luque M, Blasco R, Castillo F.** 1999. Prokaryotic nitrate reduction: molecular properties and functional distinction among bacterial nitrate reductases. *J. Bacteriol.* **181**:6573-6584.
8. **Berks BC, Ferguson SJ, Moir JW, Richardson DJ.** 1995. Enzymes and associated electron transport systems that catalyse the respiratory reduction of nitrogen oxides and oxyanions. *Biochim. Biophys. Acta* **1232**:97-173.

CHAPTER 3

Cytochrome cd_1 nitrite reductase NirS is involved in anaerobic magnetite biomineralization in *Magnetospirillum gryphiswaldense* and requires NirN for proper d_1 heme assembly

Cytochrome *cd*₁ Nitrite Reductase NirS Is Involved in Anaerobic Magnetite Biomineralization in *Magnetospirillum gryphiswaldense* and Requires NirN for Proper *d*₁ Heme Assembly

Yingjie Li,^a Shilpa Bali,^b Sarah Borg,^a Emanuel Katzmann,^a Stuart J. Ferguson,^b Dirk Schüler^a

Ludwig-Maximilians-Universität München, Department Biologie I, Mikrobiologie, Planegg-Martinsried, Germany^a; Department of Biochemistry, University of Oxford, Oxford, United Kingdom^b

The alphaproteobacterium *Magnetospirillum gryphiswaldense* synthesizes magnetosomes, which are membrane-enveloped crystals of magnetite. Here we show that nitrite reduction is involved in redox control during anaerobic biomineralization of the mixed-valence iron oxide magnetite. The cytochrome *cd*₁-type nitrite reductase NirS shares conspicuous sequence similarity with NirN, which is also encoded within a larger *nir* cluster. Deletion of any one of these two *nir* genes resulted in impaired growth and smaller, fewer, and aberrantly shaped magnetite crystals during nitrate reduction. However, whereas nitrite reduction was completely abolished in the Δ *nirS* mutant, attenuated but significant nitrite reduction occurred in the Δ *nirN* mutant, indicating that only NirS is a nitrite reductase in *M. gryphiswaldense*. However, the Δ *nirN* mutant produced a different form of periplasmic *d*₁ heme that was not noncovalently bound to NirS, indicating that NirN is required for full reductase activity by maintaining a proper form of *d*₁ heme for *holo*-cytochrome *cd*₁ assembly. In conclusion, we assign for the first time a physiological function to NirN and demonstrate that effective nitrite reduction is required for biomineralization of wild-type crystals, probably by contributing to oxidation of ferrous iron under oxygen-limited conditions.

Magnetosomes are bacterial organelles used by magnetotactic bacteria (MTB) for orientation in the Earth's magnetic field to search for growth-favoring suboxic zones of stratified aquatic sediments (1). In the freshwater alphaproteobacterium *Magnetospirillum gryphiswaldense* MSR-1 (here referred to as MSR-1) and related MTB, the magnetosomes are membrane-enveloped crystals of magnetite (Fe₃O₄) (1). Magnetosome synthesis and assembly is controlled by a number of specific proteins, which are mostly encoded within a genomic magnetosome island (2–4). It has been proposed that biomineralization of the mixed-valence iron oxide magnetite (Fe₃O₄) takes place within the magnetosomal membrane vesicles by coprecipitation of ferrous and ferric iron, via supersaturating concentrations, which are favored by a low redox potential (5–7). Magnetite synthesis occurs only under suboxic conditions (8, 9), and previous observations indicated that magnetosome synthesis might be linked to denitrification (10, 11). Bacterial denitrification is a respiratory process in which nitrate is stepwise reduced to nitrogen gas (NO₃[−] → NO₂[−] → NO → N₂O → N₂) (12). Recently, we showed that MSR-1 is capable of anaerobic growth by a complete pathway of denitrification, including gene functions for nitrate (*nap*), nitrite (*nirS*), nitric oxide (*nor*), and nitrous oxide reduction (*nos*) (13). Except for *nap*, which was upregulated by oxygen, the highest expression of other denitrification genes coincided with conditions permitting maximum magnetite synthesis (low oxygen tensions and the presence of nitrate), whereas microaerobic denitrification overlapped with oxygen respiration (13). The deletion of *nap* genes encoding a periplasmic nitrate reductase, but not *nor* or *nos*, abolished anaerobic growth and also delayed aerobic growth in both nitrate and ammonium medium. Inactivation of *nap* also severely impaired magnetite biomineralization and resulted in fewer, smaller, and irregular crystals during denitrification and also microaerobic respiration, demonstrating that the periplasmic nitrate reductase

nap is involved in redox control of magnetite biomineralization (13).

Earlier work suggested that also the second step of denitrification, the reduction of nitrite to nitric oxide (NO₂[−] → NO), might be involved in magnetite biomineralization in magnetospirilla. This was based on the observation that the cytochrome *cd*₁-type nitrite reductase NirS purified from *Magnetospirillum magnetotacticum* accelerated the oxidization of ferrous iron in the presence of nitrite under anaerobic conditions *in vitro* (14), indicating that this enzyme possesses a novel Fe(II):nitrite oxidoreductase activity that may participate in magnetosomal Fe₃O₄ synthesis *in vivo*. However, due to the lack of genetic evidence, the exact functions of NirS in denitrifying growth and magnetite biomineralization have remained unexplored. NirS, the cytochrome *cd*₁-type nitrite reductase, occurs in many denitrifying bacteria, while in others, reduction of nitrite to nitric oxide can also be catalyzed by another type of enzyme, the trimeric copper-containing protein NirK (12). NirS functions as periplasmic homodimeric hemoprotein, in which each subunit contains a covalent *c*-type and a unique noncovalent *d*₁-type heme. NirS is the only protein known to contain the *d*₁ heme as an essential cofactor, which is assumed to be the catalytic site for nitrite reduction (15). Heme *d*₁ biogenesis is

Received 11 June 2013 Accepted 18 July 2013

Published ahead of print 26 July 2013

Address correspondence to Stuart J. Ferguson, stuart.ferguson@bioch.ox.ac.uk, or Dirk Schüler, dirk.schueler@lrz.uni-muenchen.de.

Supplemental material for this article may be found at <http://dx.doi.org/10.1128/JB.00686-13>.

Copyright © 2013, American Society for Microbiology. All Rights Reserved.
doi:10.1128/JB.00686-13

thought to be mediated by a set of further proteins encoded within the *nir* operon (16–18).

Here, we set out to investigate the role of NirS in nitrite reduction and in magnetite biosynthesis in the magnetic bacterium MSR-1. The conspicuous high sequence similarity of NirS to one (NirN) of the proteins encoded in the identified *nir* gene cluster prompted us to investigate the functions of both of these proteins in denitrifying growth as well as magnetite biosynthesis. Genetic and biochemical analyses revealed that only NirS is a nitrite reductase, but NirN is required for its full activity by either maintaining a correct form of d_1 heme for NirS or by acting during assembly of d_1 heme in *holo*-cytochrome cd_1 nitrite reductase; this for the first time assigns a physiological function to NirN. Moreover, deletions of *nirS* and *nirN* also impaired magnetite biomineralization, and functional NirS participates in redox control, probably by contributing to oxidation of ferrous iron under oxygen-limited conditions.

MATERIALS AND METHODS

Bacterial strains and growth conditions. Bacteria strains and plasmids used in this work are shown in Tables S1 and S2 in the supplemental material. *Escherichia coli* strains were cultured in lysogeny broth (LB) broth at 37°C. MSR-1 strains were grown at 30°C in nitrate medium if not specified otherwise (13). Nitrate was replaced with 4 mM ammonium chloride in the ammonium medium. In low-iron medium (LIM), ferric citrate was omitted from the nitrate medium (19). When necessary, antibiotics were added at the following concentration: for *E. coli*, tetracycline (Tc) at 12 µg/ml, kanamycin (Km) at 25 µg/ml; for MSR-1, Tc at 5 µg/ml, Km at 5 µg/ml. Diaminopimelic acid (DAP) at 300 µM was added to the medium when *E. coli* strain BW29427 was used as the donor for conjugation.

Experiments for growth and measurement of the magnetic response (C_{mag} , the ratio of scattering intensities at different angles of the magnetic field relative to the light beam [20]) were carried out under microaerobic and anaerobic conditions in 250-ml flasks containing 100 ml medium. For microaerobic conditions, prior to autoclaving, flasks were sealed with butyl rubber stoppers under a microoxic gas mixture containing 2% O₂ and 98% N₂. When oxygen was omitted from the gas mixture, anaerobic conditions were achieved. For aerobic conditions, cells were cultured in an environment with free gas exchange with air in 300-ml flasks containing 20 ml medium agitated at 200 rpm. The optical density (OD) and the magnetic response (C_{mag}) were monitored photometrically at 565 nm as previously described (21). For the gas production assay, cells were inoculated to a final OD₅₆₅ of about 0.02 and mixed with nitrate medium with 0.3% agar in oxygen gradient tubes and exposed to air. If not specified, inocula were prepared aerobically by repeated passaging in fresh nitrate medium to a final C_{mag} value of 0.

Genetic and molecular biology techniques. Standard molecular and genetic techniques were performed for DNA isolation, digestion, ligation, and transformation (22). All DNA products were sequenced using BigDye Terminator version 3.1 chemistry on an ABI 3700 capillary sequencer (Applied Biosystems, Darmstadt, Germany). Sequence data were analyzed with the software Vector NTI Advance 11.5.1 (Invitrogen, Darmstadt, Germany). All oligonucleotide sequences used in this study are available if required.

Identification of a *nir* cluster. Because *nir* genes were located on two different contigs of the incomplete genome assembly of MSR-1, a PCR amplicon, obtained with primers *nirB*-down-F and *nirC*-up-R, comprising the missing *nirE* gene was used to bridge the gap between a 6,541-bp contig (containing nucleotide sequence from 286116 to 292656) and a 50,562-bp contig (nucleotide sequence from 2411316 to 2461877). The *nirE* sequence was submitted to GenBank (see below).

Construction of mutant strains. All PCRs were performed by using Phusion polymerase (NEB). Enzymes in this work, including restriction

enzymes and T4 DNA ligase, were purchased from Fermentas. A two-step, *cre-lox*-based method was used to generate unmarked deletions of *nirS* and *nirN*, respectively (13). The plasmid used to delete the *nirS* gene was constructed in two steps. First, a 2-kb downstream PCR fragment of *nirS* was digested with NdeI and KpnI and cloned into pCM184 to yield pLYJ06. Second, the 2-kb upstream PCR product of *nirS* was ligated into SacI/AgeI-digested pLYJ06 to yield *nirS* deletion plasmid pLYJ08. For *nirN* deletion, the 2-kb upstream PCR product was cloned into pCM184 between Acc65I and NotI sites, generating pLYJ20. An approximately 2-kb downstream fragment of *nirN* was then ligated into MluI/SacI-digested pLYJ20 to obtain pLYJ23. After that, allelic exchange vectors pLYJ08 and pLYJ23 were transformed into MSR-1 by conjugation. First, deletion mutants were screened on replica plates with kanamycin and tetracycline. Then, screening PCR was performed for colonies that did not grow on tetracycline plates. To generate unmarked deletion mutants, pLYJ86 was constructed by ligating *cre* genes from pCM157 into SmaI/XbaI-digested pLYJ36. After that, the *nirS* promoter region and *cre* fusion from pLYJ86 was digested with Acc65I and XbaI and cloned into pBBR1MCS-3 to generate pLYJ87. The plasmid pLYJ87 was then transformed into each mutant and subsequently cured from each mutant by several transfers in nitrate medium without any antibiotics. Unmarked mutants were finally designated Δ *nirS* and Δ *nirN* mutants, respectively.

Complementation experiments. For genetic complementation of the Δ *nirS* and Δ *nirN* mutants, two plasmids based on pBBR1MCS-2 were generated. For complementation of *nirS*, pLYJ51 was used, in which the *nirS* gene sequence with its own promoter region was ligated into Acc65I-digested pBBR1MCS-2. Other *nirS* genes from *Magnetospirillum magneticum* (*amb1395* and *amb4165*) and *Pseudomonas stutzeri* (*PST_3532*) were also hetero-complemented into the Δ *nirS* strain. The *nirS* promoter region from MSR-1 was ligated into Acc65I/HindIII-digested pBBR1MCS-2 to generate pLYJ36. Subsequently, *amb1395* and *amb4165* were cloned into HindIII/SmaI-digested pLYJ36 to obtain pLYJ88 and pLYJ89, respectively. The PCR fragment of *PST_3532* was digested with HindIII and XbaI and ligated into pLYJ36 to yield pLYJ95. The *nirN* gene sequence was digested with ApaI and SacI and cloned into pRU1 to yield pLYJ74. *nirN* gene from *M. magneticum* (*amb1408*) was ligated into ApaI/SacI-digested pRU1 to obtain pLYJ113. *nirN* from *P. stutzeri* (*PST_3538*) was cloned into pLYJ36 between HindIII and XbaI sites, yielding pLYJ124.

Chemical analysis. For nitrate and nitrite analyses, MSR-1 cells were grown under anaerobic conditions at 20°C, at which nitrate and nitrite was reduced more slowly. The nitrate concentration was measured using Szechrome reagents (Polysciences, Inc.). Diluted 20-fold samples of cultures were prepared, and Szechrome reagents were subsequently added. The absorbance was recorded at 570 nm after 0.5 hour. When nitrate was no longer detectable, samples without dilution were used to confirm the absence of nitrate. A nitrate standard curve (0 to 350 µM) was generated to convert absorbance values to concentrations.

Nitrite was detected by using the modified Griess reagent (Sigma). Samples of 100 µl of cultures diluted 20-fold were reacted with an equal amount of modified Griess reagent, and after 15 min the absorbance at 540 nm was recorded. When no nitrite was found, cultures without dilution were used to confirm the absence of nitrite. A nitrite standard curve (0 to 70 µM) was obtained to calculate the final nitrite concentration.

Preparation of the periplasmic fraction and purification of cytochrome cd_1 . For the preparation of the periplasmic fraction and NirS purification, large quantities (100 liters for each strain) of anaerobic cultivated cells were obtained at 20°C in a fermentor (Sartorius, Göttingen, Germany), in which 1 g/liter peptone was added while HEPES and a trace element mixture were omitted from the nitrate medium. The pH of the culture was maintained by the addition of either H₂SO₄ (1 M) or NaOH (1 M) via peristaltic pumps. After harvesting at 4°C, 3-g (wet weight) cell pellets were resuspended in 15 ml of SET buffer (0.5 M sucrose, 200 mM Tris-HCl [pH 7.5], 1 mM EDTA). Culture with lysozyme (15 mg/liter) was added, immediately followed by 15 ml of ice-cold water to administer a mild osmotic shock. This mixture was incubated at 37°C for 30 min and

then centrifuged at $9,000 \times g$ for 15 min. The supernatant was retained as the periplasmic fraction. Purification of cytochrome cd_1 was carried out as described in reference 14 with slight modifications. Briefly, purification was done at room temperature, and the periplasmic extracts were diluted 4 times before loading onto a DEAE-Sepharose column equilibrated with 50 mM Tris-HCl (pH 8.0). NirS in the flowthrough was dialyzed against 10 mM sodium phosphate (pH 6.5) for 12 h, and the desalted solution was further applied to a carboxymethyl (CM)-Toyopearl column. NirS was eluted with a linear gradient of 0 to 0.5 M NaCl. For the cytochrome cd_1 (NirS) fraction, solid ammonium sulfate was added to 40% saturation. After slow stirring for 1 h at 4°C, the solution was centrifuged at $10,000 \times g$ for 20 min. Solid ammonium sulfate was further added to the supernatant up to 80% saturation. The suspension was again stirred for 1 h at 4°C and centrifuged at $8,000 \times g$ for 20 min. The supernatant was applied to a CM-32 column equilibrated with 10 mM sodium phosphate, pH 6.5, containing 80% saturated ammonium sulfate solution. The cytochrome cd_1 , adsorbed on the column, was washed with the same buffer used for equilibration. The enzyme was subsequently eluted with 10 mM sodium phosphate, pH 6.5, containing 0.2 M NaCl, and buffer was exchanged into 50 mM Tris-HCl, pH 7.5.

Heme staining. Activity staining of SDS-polyacrylamide gels for the covalently bound heme was conducted using the method described in reference 23. Briefly, the gel was soaked in 70 ml of 0.5 M sodium acetate (pH 5.0) for 20 min, followed by addition of 30 ml methanol containing 3 mg of *N,N,N',N'*-tetramethylbenzidine (TMBZ). After shaking the gel for 5 min, 100 μ l of H_2O_2 was added to develop the bands for detection of hemoproteins.

Absorbance spectra detection. UV-visible spectra were acquired on a PerkinElmer 3 UV-visible scanning spectrophotometer at room temperature, using fused quartz cuvettes with a 1-cm path length (Merck) and samples that were in 50 mM Tris-HCl buffer at pH 7.5. Pyridine heme-chrome spectra were obtained according to the method of Bartsch (24) using 5 μ M protein in 19% (vol/vol) pyridine and 0.15 M NaOH.

Analysis of transcriptional *gusA* fusions. To generate the transcriptional *nirTBECFDLGHJN-gusA* fusion plasmids, the *nirTBECFDLGHJN* promoter region was cloned into Acc65I/HindIII-digested pLYJ97, designated pLYJ104. To investigate the expression of *nirS* under different conditions, pLYJ94 containing the *nirS* promoter fused with *gusA* was used. Then pLYJ104 and pLYJ94 were introduced into MSR-1 wild-type (WT) and Δ *nirS* strains, respectively, by conjugation. β -Glucuronidase activity was determined at 37°C as described before (13). Units were recorded as nanomoles of product formed per minute. Triplicate assays were conducted, and the values reported are averages from at least two independent experiments.

Growth experiments with different iron sources. To determine effects of different iron sources on MSR-1 WT and Δ *nirS* strains, exponential-phase iron-deprived nonmagnetic precultures (200 ml) of MSR-1 WT and Δ *nirS* strains were obtained by culturing cells in LIM under microaerobic conditions. Concentrated cells were washed twice by using nitrate-free LIM and subsequently suspended in LIM in the presence (LIM) or absence (nitrate-free LIM) of nitrate to a final OD_{565} of 0.1. Prior to inoculation, either an anoxic ferrous chloride or ferric chloride stock was added to a final concentration of 100 μ M for the anaerobic growth medium. Reduced iron was maintained by adding 0.2 mM sodium ascorbate. A preliminary experiment has shown that 0.2 mM sodium ascorbate alone has no effect on growth and magnetite biomineralization (data not shown). As revealed by the ferrozine assay, all iron in the medium was in the ferrous form in the presence of ascorbate, whereas in the absence of the reductant all added iron remained in the ferric form. Then, iron-deprived nonmagnetic cells were inoculated to a final OD_{565} of 0.1. After a 6-hour iron induction, the C_{mag} was measured, and extracellular iron concentrations were quantified at 562 nm in a ferrozine assay (25). For the analysis of Fe(II), 100 μ l of sample was added into 900 μ l 1 M HCl in an anaerobic chamber and determined directly by a ferrozine assay. Total iron [Fe(II) and Fe(III)] was measured by reducing 100 μ l of sample with hydroxyl-

amine hydrochloride before addition of the ferrozine reagent. The amount of Fe(III) was calculated by subtracting the amount of Fe(II) from the total Fe.

Construction of the NirS-mCherry fusion protein and fluorescence microscopy. For construction of the NirS-mCherry fusion protein, first the *nirS* sequence without the putative promoter region or candidate signal peptides was amplified using a forward primer, that included a 12-amino-acid linker sequence at the 5' end, and cloned between SmaI and XbaI sites of pBBR1MCS-2 to give plasmid pLYJ52. Subsequently, the putative *nirS* promoter region together with the candidate signal peptide was cloned into Acc65I/HindIII-digested pLYJ52 to obtain pLYJ59. To generate an N-terminal *mcherry* fusion, *mcherry* was amplified from pFM208 and inserted into HindIII/SmaI-digested pLYJ59 to generate plasmid pLYJ64. Then, MSR-1 WT and Δ *nirS* strains containing plasmid pLYJ64 were cultured in Hungate tubes under microaerobic conditions for 16 h and immobilized on agarose pads (flask standard medium salts in water, supplemented with 1% agarose) as described previously (26).

The localization of mCherry-tagged proteins was then determined using an Olympus IX81 fluorescence microscope equipped with a Hamamatsu Orca-ER camera. The excitation wavelength for mCherry was 587 nm and emission was recorded at 610 nm.

Transmission electron microscopy (TEM) and crystal analysis. If not specified, MSR-1 WT and mutants were grown at 25°C under anaerobic conditions for 24 h, concentrated, and adsorbed onto carbon-coated copper grids. Samples were viewed and recorded with a TECNAI F20 microscope (FEI, Eindhoven, Netherlands) at 200 kV or a Morgagni 268 microscope (FEI, Eindhoven, Netherlands) at 80 kV as previously described (27). For magnetosome analysis, more than 300 crystals and 100 cells were detected for each strain.

Bioinformatic analysis. Using respective protein sequences from *Pseudomonas aeruginosa* as a query in a BLASTP analysis, *nirS* and *nirN* genes were identified by BLASTP (<http://blast.ncbi.nlm.nih.gov/Blast.cgi>) homology searching in the genomes of MSR-1 (GenBank accession number CU459003.1), *M. magnetotacticum* strain (GenBank accession number AP007255.1), *M. magnetotacticum* (NCBI reference sequence NZ_AAAP0000000.1), and *Magnetococcus marinus* (GenBank accession number CP000471.1), with an expectation value (E) of $<1e-06$ and amino acid similarity of $>50\%$. ClustalW was used for sequence alignment. Signal sequences and peptides were predicted by using SignalP (<http://www.cbs.dtu.dk/services/SignalP/>) (28).

Nucleotide sequence accession number. The *nirE* sequence has been submitted to the GenBank database under accession number JN634764.

RESULTS

Identification of a *nir* cluster in MSR-1. Several *nir* genes were identified on two different contigs of the incomplete genome assembly of MSR-1. After gap closure by PCR, we found that *nirS*, encoding the nitrite reductase (cytochrome cd_1), along with all other *nir* genes (*nirTBECFDLGHJN*), is localized within a single cluster (Fig. 1A), which with some notable differences is mostly conserved in other magnetospirilla (see Fig. S1 and Table S3 in the supplemental material). *nirEFDLGHJ* are known to be necessary for d_1 heme synthesis (16–18), whereas a multiheme *c*-type cytochrome encoded by *nirT* is necessary for nitrite reduction as an endogenous electron donor in *P. stutzeri* (29), and *nirC* encodes a *c*-type cytochrome which in *P. aeruginosa* is suggested to be an electron donor for the nitrite reductase NirS (30). These genes are followed downstream by *nirN*, which encodes a *c*-type cytochrome in *Paracoccus pantotrophus*, although its function *in vivo* is not clear (31).

Deletions of *nirS* and *nirN* impair denitrification growth and magnetite synthesis. Interestingly, NirN showed conspicuous sequence similarity to NirS (43% similarity, 26% identity) (see Fig. S1C in the supplemental material), which prompted us to discern

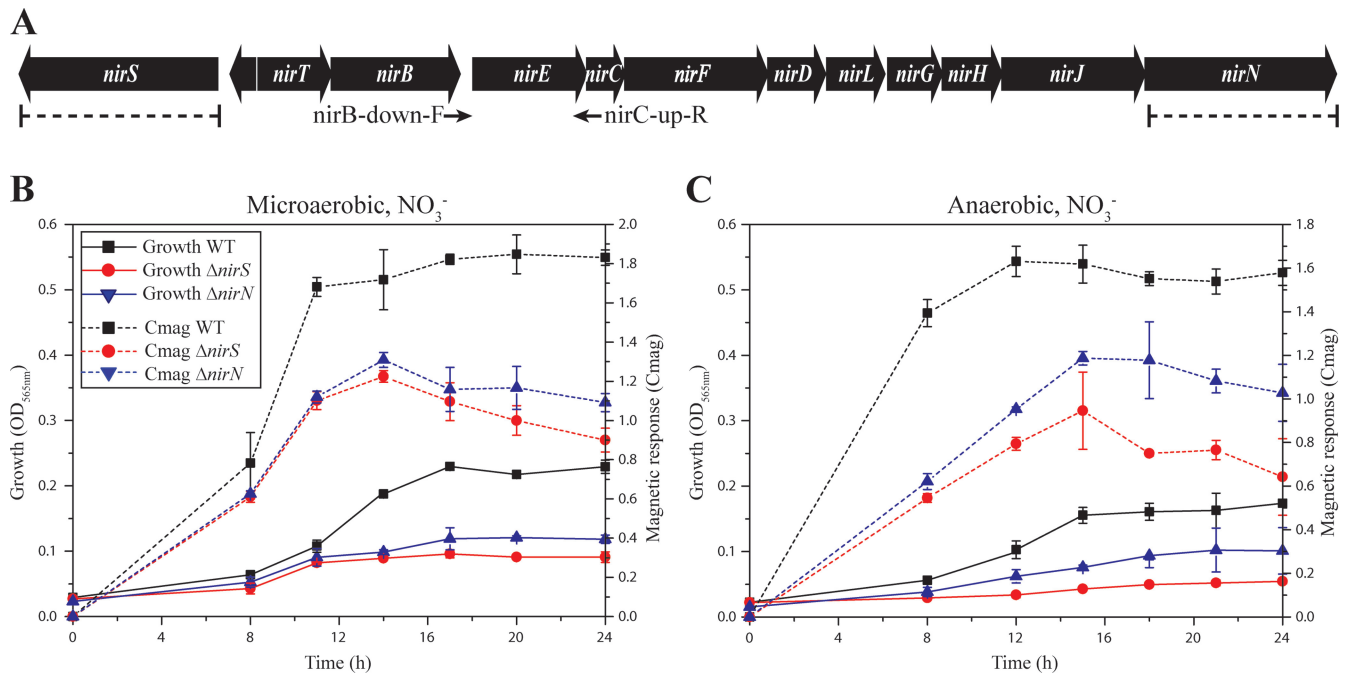


FIG 1 (A) Molecular organization of identified *nir* genes in MSR-1. Arrows indicate the PCR primers *nirB*-down-F and *nirC*-up-R, which were used for gap closure between *nirB* and *nirC* (see Materials and Methods). Dashed lines indicate the extent of deletions in Δ *nirS* and Δ *nirN* mutants. (B and C) Growth (based on the $\text{OD}_{565\text{nm}}$) and magnetic response (C_{mag}) of MSR-1 WT, Δ *nirS*, and Δ *nirN* cells under different conditions at 30°C. (B) Microaerobic, nitrate medium; (C) anaerobic, nitrate medium. Results from representative experiments were measured in triplicate, and values are given as means and standard deviations.

their individual roles in growth, magnetosome formation, and nitrite reduction by the construction of unmarked deletion mutants of both genes. The Δ *nirS* mutant displayed no difference from the WT in growth and C_{mag} under aerobic conditions in either nitrate or ammonium medium (see Fig. S2A and B). Under microaerobic conditions in ammonium medium (in the absence of nitrate), the WT and Δ *nirS* strains also reached comparable growth yields and C_{mag} values (see Fig. S2C). However, when cells were grown microaerobically in nitrate medium, both yields and C_{mag} values were significantly lower in the Δ *nirS* mutant than in the WT (Fig. 1B). Under anaerobic conditions, the Δ *nirS* mutant still grew poorly for 2 to 3 generations before growth ceased entirely. However, C_{mag} values were substantially decreased below 1.0 (Fig. 1C). TEM images revealed severe defects in magnetosome organization and crystal morphology: the anaerobic Δ *nirS* mutant produced much smaller (27.4 ± 0.7 nm, versus 49.9 ± 5.0 nm for WT crystals [means \pm standard deviations]), fewer (average of 12 crystals per cell versus 35 in the WT), and irregularly shaped crystals, which were arranged in loose chains (Fig. 2A and B).

Deletion of *nirN* did not affect aerobic growth in the presence of nitrate or ammonium (see Fig. S2A and B in the supplemental material), and hardly any difference in growth or magnetite biomineralization was observed in microaerobic ammonium medium between the WT and Δ *nirN* mutant (see Fig. S2C). However, in microaerobic nitrate medium, loss of *nirN* resulted in weaker growth and lower C_{mag} values, which were only slightly higher than those in the Δ *nirS* mutant (Fig. 1B). The anaerobically grown Δ *nirN* mutant reached higher cell densities than the Δ *nirS* mutant, but the densities were still much lower than for the WT, and the C_{mag} was also much lower than in the WT, but higher than in the Δ *nirS* mutant (Fig. 1C). As shown in Fig. 2A and B, Δ *nirN*

cells produced much shorter magnetosome chains (average of 7 crystals per cell, versus 35 crystals per cell in WT), whereas crystals were only slightly smaller (40.4 ± 2.0 nm, versus 49.9 ± 5.0 nm for WT). Magnetosome morphology was variable, including regular crystals in the middle of chains in addition to irregular and loosely aligned particles at the ends of chains (Fig. 2A and B). Transcomplementation of Δ *nirS* and Δ *nirN* mutants with their respective WT alleles (pLYJ51 and pLYJ74) restored denitrifying growth (data not shown) and magnetosome formation (Fig. 2C) back to the WT levels. Altogether, these results indicate that both NirS and NirN are required for WT-like denitrifying growth and magnetite biomineralization.

NirS is the only nitrite reductase, while NirN is essential for fully active nitrite reduction. Since deletion of either *nirS* or *nirN* seemed to impair denitrifying growth and magnetite biomineralization in a similar manner, we wanted to dissect their functions in nitrite reduction. First, we inoculated WT and mutant strains into deep slush agar (0.3%) tubes containing nitrate medium, in which entrapped gas bubbles are indicative for N_2 evolution. At 30°C, WT cells produced bubbles after 24 h, while in the Δ *nirS* mutant no bubbles were observed at any length of incubation, indicating a block of denitrification due to the complete absence of nitrite reduction (Fig. 3A). In contrast, Δ *nirN* cultures generated only a few bubbles after the first 24 h (data not shown) but as many as the WT after 40 h (Fig. 3A), which indicated that only NirS, and not NirN, is a genuine nitrite reductase and is sufficient for nitrite reduction in the absence of NirN.

In agreement with those results, we found WT cells growing at 30°C consumed 4 mM nitrate within 10 h, during which period only about 100 μM nitrite was transiently accumulated. However, both Δ *nirS* and Δ *nirN* cultures incubated at 30°C accumulated

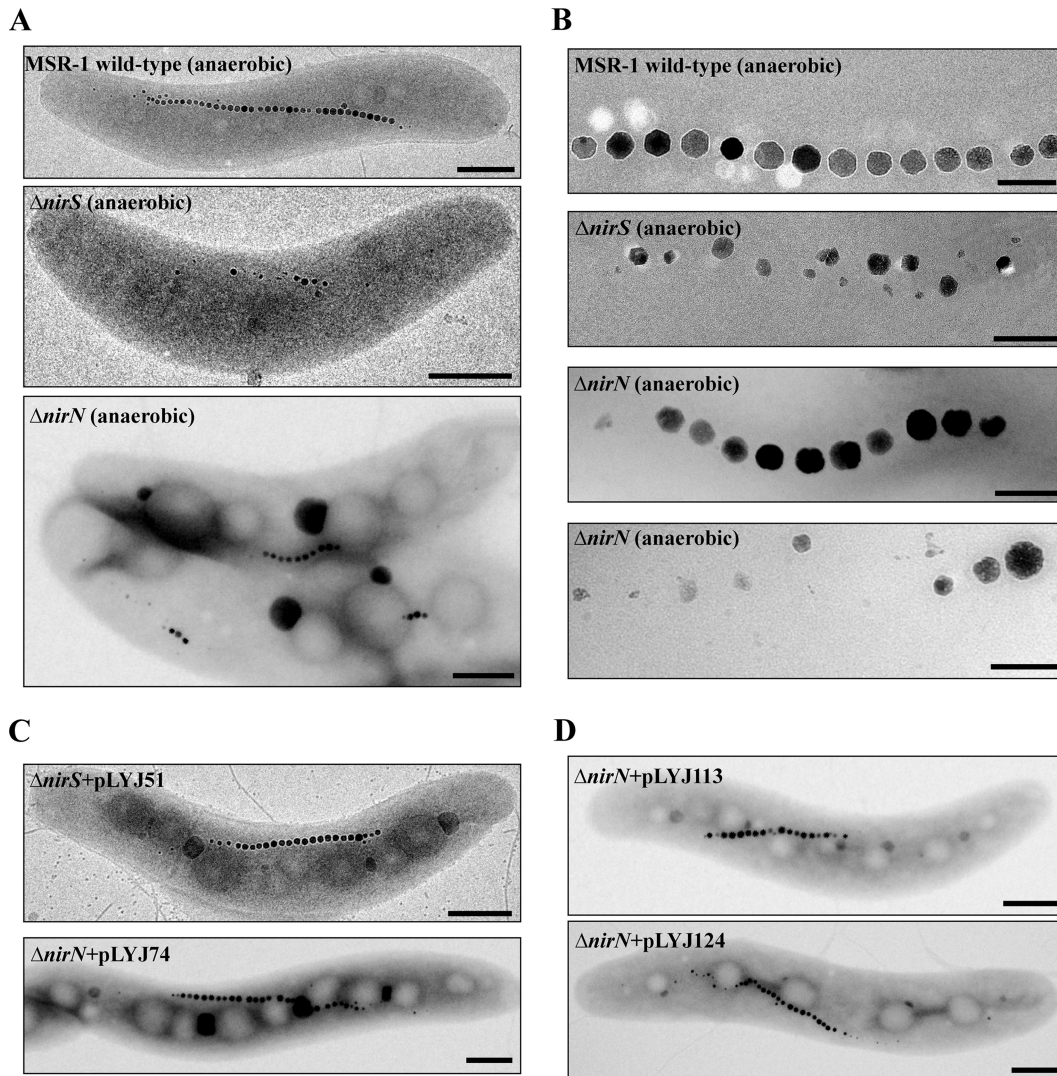


FIG 2 Effects of deletions of *nirS* and *nirN* on magnetosome formation. (A) TEM images of whole cells of (from top to bottom) WT (anaerobic, nitrate medium), $\Delta nirS$ mutant (anaerobic, nitrate medium), and $\Delta nirN$ mutant (anaerobic, nitrate medium). Bar, 500 nm. (B) Closeup views of magnetosome crystals shown in panel A. Bar, 100 nm. (C) TEM images of anaerobically grown $\Delta nirS$ and $\Delta nirN$ cells complemented with plasmids pLYJ51 and pLYJ74, respectively, harboring their WT alleles. Bars, 500 nm. (D) TEM images of anaerobically grown the $\Delta nirN$ strain carrying *nirN* (from top to bottom) from *M. magneticum* (*amb1408*) and *P. stutzeri* (*PST_3538*), respectively. Bar, 500 nm.

approximately 2.0 to 2.5 mM nitrite after the first 16 h in the medium, while no nitrite was detected in $\Delta nirN$ cultures after 48 h (data not shown). When grown at 20°C, at which temperature the WT displayed slower growth but slightly increased magnetite formation, nitrite became entirely consumed by $\Delta nirN$ cultures after about 7 days, again indicating that nitrite reduction still occurred in the $\Delta nirN$ mutant although much slower than in the WT. The roles of NirS and NirN were further assessed by following nitrate consumption and nitrite accumulation, as well as growth and magnetite formation, during anaerobic incubation at 20°C. In this experiment, nonmagnetic, aerobically grown cells were inoculated as described before (13). After a lag of 30 to 33 h, cell densities increased in WT cultures for around 15 h, after which growth ceased due to depletion of nitrate, the only added electron acceptor (Fig. 4A, panel i). During the entire growth period, C_{mag} values continuously increased, which coincided with the alignment of

maturing magnetite crystals in typical chains (Fig. 4A). During the first 30 to 33 h, WT cultures consumed only a little nitrate, and then nitrate was rapidly depleted within the following approximately 30 h. Yet, nitrite accumulation was hardly detectable during the entire growth period (Fig. 4A, panel i).

$\Delta nirS$ cells grew slowly, to a final OD of only 0.08 after about 75 h (Fig. 4B, panel i), after which cells entirely ceased growth but continued to consume trace amounts of nitrate. Although C_{mag} values increased rapidly during the first 30 to 33 h and slightly beyond that time period, to a final value of 0.65 to 0.70, $\Delta nirS$ cells only produced a few irregularly shaped crystals (Fig. 4B, panels ii to v). During incubation, nitrate was gradually consumed, but approximately 0.8 to 1.0 mM remained in the culture after 90 h, while the cell densities did not increase after 75 h (Fig. 4B, panel i); the implication is that besides acting as an electron acceptor, nitrate is also assimilated and thus is a nitrogen source. Meanwhile,

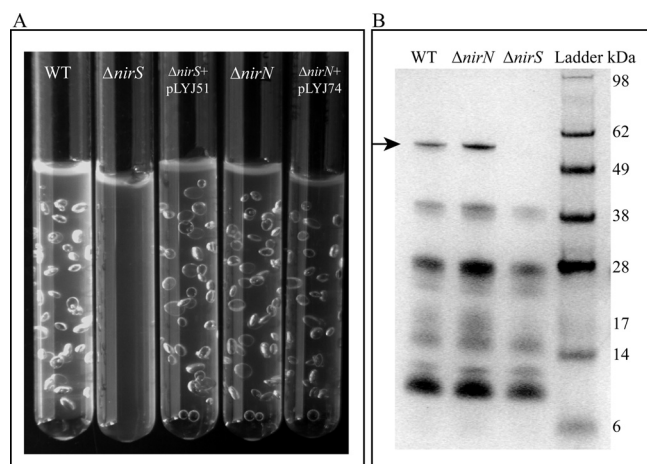


FIG 3 (A) Gas production in WT, $\Delta nirS$, $\Delta nirS$ plus pLYJ51, $\Delta nirN$, and $\Delta nirN$ plus pLYJ74 cultures in oxygen gradient tubes with 0.3% agar at 30°C. $\Delta nirS$ with pLYJ51 and $\Delta nirN$ with pLYJ74 cells harbored their respective WT alleles. Except for the $\Delta nirN$ mutant, which was incubated for 40 h, all others were cultured for 24 h. (B) Detection of heme-containing proteins. Fifty micrograms of periplasmic protein was loaded per lane. Compared to the WT and $\Delta nirN$ strains, the periplasmic fraction from the $\Delta nirS$ mutant lacked a characteristic band of cytochrome cd_1 at around 60 kDa (black arrow).

as cell densities increased slowly, nitrite gradually built up in the medium to about 2.3 to 2.5 mM after 75 h and then was not consumed further (Fig. 4B, panel i), which again demonstrated that NirS but not NirN catalyzes nitrite reduction in the absence of the other. In $\Delta nirS$ cultures, inorganic nitrogen (0.8 to 1.0 mM nitrate plus 2.3 to 2.5 mM nitrite) together amounted to about 3.0 to 3.5 mM at the end of growth, once again suggesting that about 0.5 to 1.0 mM nitrate was assimilated by cells from the 4 mM initially present in the medium.

When the same experiments were carried out with the $\Delta nirN$ mutant, during first 75 h cell densities slowly increased, as with the $\Delta nirS$ mutant (Fig. 4C, panel i). Then, growth transiently ceased for about 40 h, before it resumed (Fig. 4C, panel i). During first 75 h, compared to the WT, $\Delta nirN$ cells produced much shorter magnetosome chains with irregular and misaligned particles at chain ends resembling those shown in Fig. 2A and B (Fig. 4C, panels ii and iii), whereas during the second growth phase we frequently observed parallel chain fragments in the $\Delta nirN$ mutant that contained both regular and irregular magnetosome particles (Fig. 4C, TEM images b in panels iv and v) and which were never present in the $\Delta nirN$ mutant cultivated at 30°C. Nitrate gradually disappeared from the medium after 200 h of incubation (Fig. 4C, panel i). Coincident with this finding, nitrite transiently accumulated up to 1.8 to 2.0 mM during the first 100 h but was eventually entirely consumed as cells resumed growth (Fig. 4C, panel i). These data demonstrated that NirN *per se* is neither a nitrite reductase nor absolutely essential for nitrite reduction, but the absence of NirN lowers the activity of nitrite reduction and indirectly impairs growth and magnetite biomineralization under denitrifying conditions, in an unknown fashion.

NirN is required to synthesize the proper form of d_1 heme. Previously, NirN of *P. pantotrophus* was found to be able to bind d_1 heme *in vitro* and subsequently transfer it to the semi-*apo* cytochrome cd_1 , which lacks d_1 heme, suggesting that NirN may play a role in the assembly or maturation of *holo*-NirS (31). To clarify

the function of NirN in MSR-1, we analyzed the form of cytochrome cd_1 present in WT, $\Delta nirS$, and $\Delta nirN$ cells by visible absorption spectroscopy of periplasmic extracts and by reduced alkaline pyridine ferroheme analysis on the purified NirS.

NirS from MSR-1 WT displayed absorption maxima characteristic for *c* heme (409 nm for the oxidized form and 551, 522, and 418 nm for the reduced form) and d_1 heme (643 nm in the oxidized form and 663 and 620 nm in the reduced form) (Fig. 5A). However, compared to NirS homologs from nonmagnetic denitrifiers (such as *P. pantotrophus*), MSR-1 cytochrome cd_1 showed some different spectral features: the peak at 550 nm (for *c* heme) was not split, and NirS protein did not display a prominent 460-nm shoulder in the reduced form (Fig. 5A). However, this shoulder, as well as absorption peaks at 620 (attributable to d_1 heme) and 550 and 522 nm (attributable to *c* heme), were observed in a reduced alkaline pyridine ferroheme spectrum of the purified cytochrome cd_1 of MSR-1 (Fig. 5B). The spectroscopic properties of *holo*- cd_1 nitrite reductase from MSR-1 were similar to those reported for the nitrite reductase from the related *M. magnetotacticum* (14). In addition, d_1 heme was also extracted from cytochrome cd_1 with acidified acetone protocol (32), with a final yield of 4.2 μ M per gram (wet weight) of WT cells.

In the $\Delta nirS$ mutant, although we observed absorption peaks for *c* heme, neither the UV-Vis spectrum nor the reduced alkaline pyridine ferroheme spectrum of periplasmic fraction showed an absorption peak for the d_1 heme (in the region of 600 to 700 nm) (Fig. 5C and D), indicating that expression of functional NirS, and thus production of NO, is required for d_1 heme biosynthesis, a conclusion which has been drawn for *P. stutzeri* and *P. pantotrophus* (33, 34). To further test whether genes for d_1 heme biogenesis are expressed in the MSR-1 $\Delta nirS$ mutant, we constructed a transcriptional gene fusion of *nirTBCEFDLGHJN* with *gusA* (*nir-gusA*), which encoded β -glucuronidase, and transferred it into MSR-1 WT and $\Delta nirS$ strains by conjugation of a replicative plasmid. As shown in Table 1, WT cells containing the *nir-gusA* fusion exhibited a higher-than-3-fold level of β -glucuronidase activity under microaerobic conditions with nitrate compared to that without nitrate, whereas an increased oxygen concentration resulted in decreased β -glucuronidase activity. However, in the $\Delta nirS$ mutant, the expression of *nir* was neither upregulated by nitrate nor downregulated by oxygen; it only reached a similar but low level of β -glucuronidase activity (about 20 U/mg) under different tested conditions, which suggested that functional NirS protein is necessary for significant expression of *nir* genes for d_1 heme biogenesis. In addition, periplasmic fractions from the different strains ($\Delta nirS$, $\Delta nirN$, and WT strains) were resolved by gel electrophoresis and stained for heme-containing proteins. As expected, the WT displayed a characteristic band at around 60 kDa, which was not found in the $\Delta nirS$ mutant (Fig. 3B), indicating that NirS is located in the periplasm with covalently bound heme in both WT and $\Delta nirN$ strains, but is absent from the $\Delta nirS$ mutant.

In the $\Delta nirN$ mutant, similar to the WT, the reduced periplasmic fraction displayed absorption maxima characteristic of *c*-type cytochromes (551, 522, and 418 nm), while the oxidized form showed an absorption peak at 409 nm (Fig. 5E). However, the UV-Vis spectrum of putative d_1 heme from the periplasmic fraction was distinct from that in the WT: although the characteristic peak at 643 nm in the oxidized form for d_1 heme was present, the absorption peaks at 620 nm and 663 nm in the reduced form were missing. Instead, a new 650-nm shoulder was observed, indicating

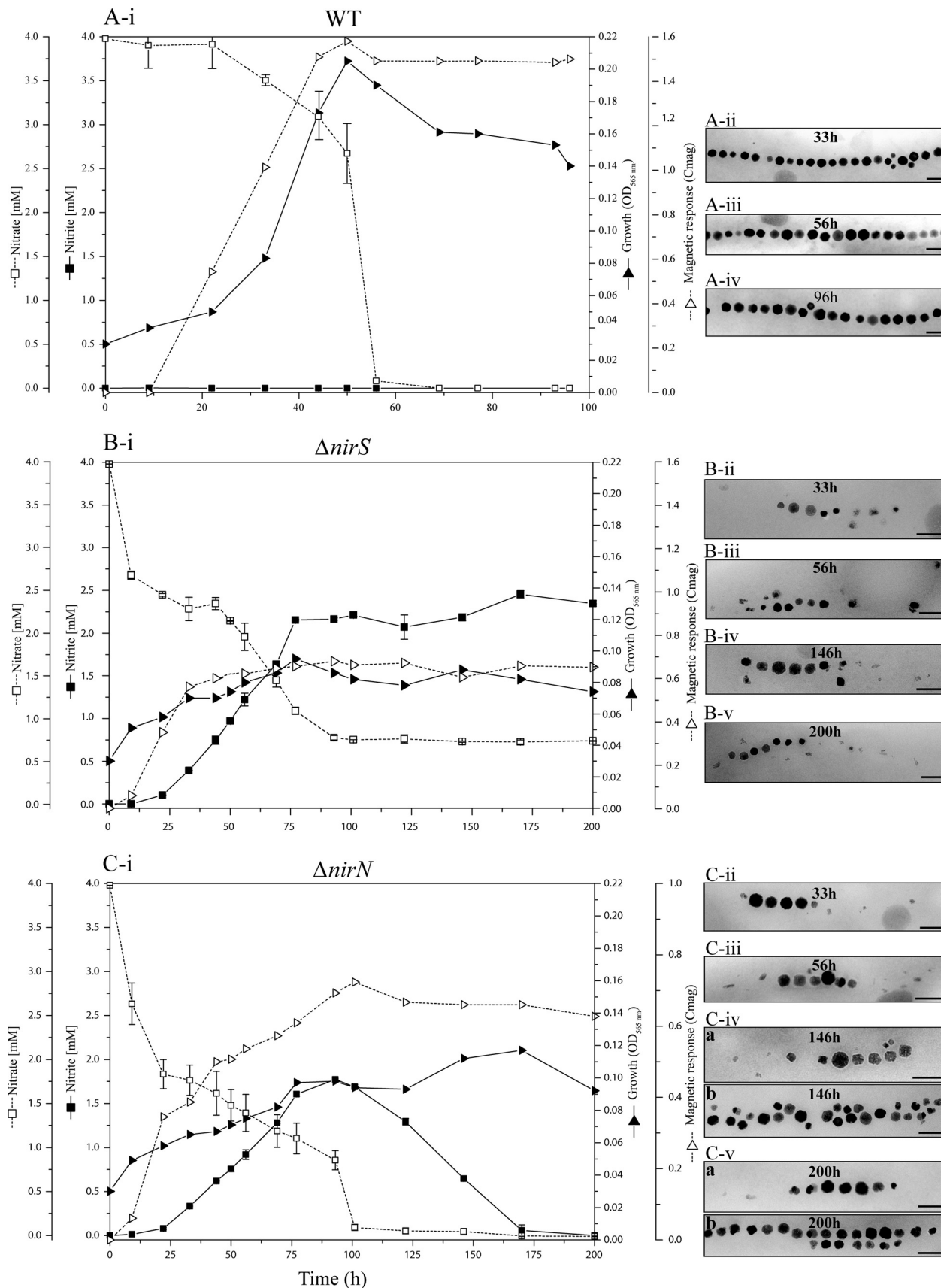


FIG 4 Left: Time courses of nitrate and nitrite utilization and magnetite biomineralization during anaerobic denitrifying growth of WT, $\Delta nirS$, and $\Delta nirN$ strains at 20°C. The initial nitrate concentration was 4 mM, and the concentrations of nitrate and nitrite were measured over time. (Right) TEM images of WT, $\Delta nirS$, and $\Delta nirN$ cells from aliquots taken at different time points are shown. Bars, 100 nm. The results shown come from one data set representative of two independent experiments.

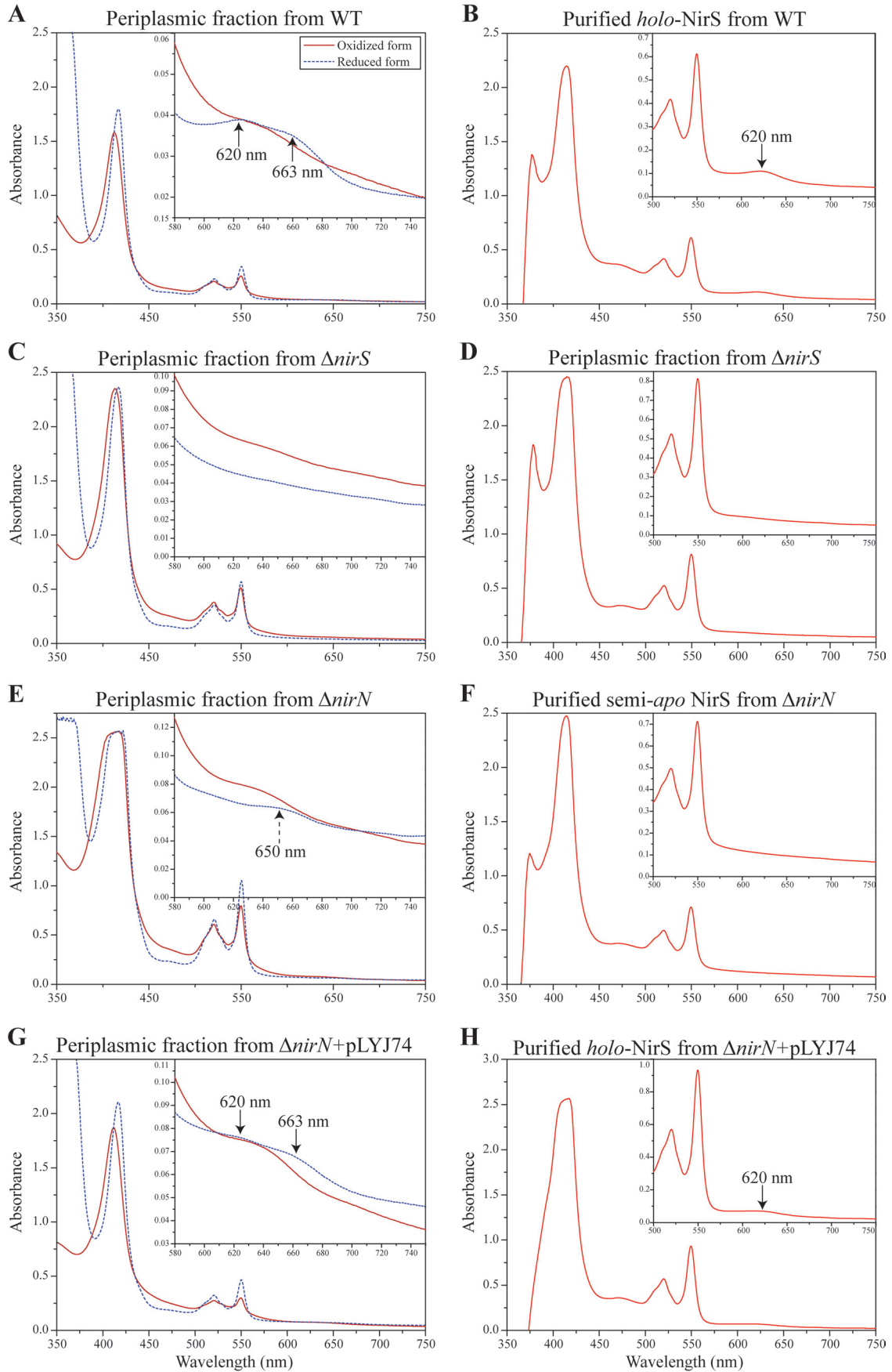


TABLE 1 Expression of transcriptional *nirTBECFDLGHJN-gusA* gene fusion in WT and Δ *nirS* strains under different conditions

Cultivation conditions	β -Glucuronidase activity (U/mg) ^a	
	WT	Δ <i>nirS</i> mutant
Microaerobic, with nitrate	99.8 \pm 3.8	24.5 \pm 4.5
Microaerobic, without nitrate	26.1 \pm 6.9	24.2 \pm 5.9
Aerobic, with nitrate	27.5 \pm 3.2	21.1 \pm 4.2
Aerobic, without nitrate	19.1 \pm 3.4	16.4 \pm 3.6

^a The values of β -glucuronidase activity were averages of at least replicate cultures. Means and standard deviations are shown.

that a variant form of d_1 heme was present in the Δ *nirN* mutant compared to the WT spectra (Fig. 5E). These spectral differences in WT and Δ *nirN* strains are suggestive of a different form of d_1 heme. Unexpectedly, the reduced alkaline pyridine ferrohemo-chrome spectrum of purified cytochrome cd_1 in the Δ *nirN* mutant lacked the characteristic d_1 heme peak at 620 nm (Fig. 5F), which suggested that no d_1 heme was present in purified NirS, or that the different form of d_1 heme might be more susceptible to dissociation from the enzyme or degradation under the aerobic conditions that were used during the purification of NirS. We also failed to detect any d_1 heme by acidified acetone extraction on the purified nitrite reductase protein from the Δ *nirN* strain, again implying that the purified nitrite reductase lacked d_1 heme. Notably, heme-stained gels of periplasmic fractions of both the control strain *P. pantotrophus* (data not shown), in which NirN is known to localize in the periplasm (31), and Δ *nirN* mutants of MSR-1 (Fig. 3B) were indistinguishable from their WT, probably due to low expression of NirN.

As shown in Fig. 5G, peaks characteristic for c and d_1 heme (643 and 409 nm in oxidized form and 663, 620, 551, 522, and 418 nm in reduced form) were restored in the Δ *nirN* mutant complemented with pLYJ74. Likewise, the reduced alkaline pyridine ferrohemo-chrome spectrum of purified cytochrome cd_1 from the Δ *nirN* mutant with pLYJ74 also displayed the WT-like shoulder at 460 nm and absorption peaks at 620, 522, and 550 nm (Fig. 5H). In agreement with this finding, we also harvested about 0.9 μ M d_1 heme per gram (wet weight) from the purified cytochrome cd_1 of the Δ *nirN* complementation strain.

Because the observed phenotypic effects were different from those reported for *nirN* deletions in other, nonmagnetic denitrifiers, we wondered whether the function of NirN of MSR-1 might be somehow distinct. This idea was further supported by the presence of an additional stretch of 20 amino acids located between the d_1 heme and c heme binding domains that is shared by all NirN

TABLE 2 Expression of transcriptional *nirS-gusA* gene fusion in WT and Δ *nirS* strains under anaerobic and microaerobic conditions with different nitrogen sources

Addition	β -Glucuronidase activity (U/mg) ^a			
	Anaerobic cultures		Microaerobic cultures	
	WT	Δ <i>nirS</i> mutant	WT	Δ <i>nirS</i> mutant
None ^b	ND ^c	ND	6.4 \pm 1.4	10.8 \pm 1.7
NaNO ₂ (0.5 mM)	ND	ND	51.1 \pm 3.3	11.9 \pm 2.0
NaNO ₃ (1 mM)	49.0 \pm 4.9	16.1 \pm 4.1	ND	ND
NaNO ₃ (4 mM)	104.2 \pm 14.7	25.2 \pm 1.9	171.7 \pm 10.3	18.6 \pm 3.0
NaNO ₃ (10 mM)	147.7 \pm 25.5	20.9 \pm 5.9	187.8 \pm 10.4	35.2 \pm 2.9

^a Values are averages of at least replicate cultures \pm standard deviations.

^b There was no nitrate or nitrite added to the medium.

^c ND, not determined; the β -glucuronidase activity was not measured.

homologs from MTB but absent from their non-MTB counterparts (see Fig. S3 in the supplemental material). To test this hypothesis, we carried out transcomplementational analysis of the MSR-1 Δ *nirN* strain with *nirN* genes from *M. magneticum* and the nonmagnetic bacterium *P. stutzeri*. However, *nirN* genes from both *M. magneticum* and *P. stutzeri* were capable of fully rescuing both magnetosome formation (Fig. 2D) and nitrite reduction (data not shown) to a WT-like level without any difference, indicating that NirN homologs from magnetotactic and nonmagnetotactic bacteria have equivalent functions.

NirS is involved in nitrite-dependent iron oxidation during anaerobic biomineralization. Because all previous observations pointed toward a key role of NirS in magnetite biomineralization, we reasoned that there were two possible explanations for the observed magnetosome defects in the Δ *nirS* mutant: (i) nitrate or nitrite accumulation in Δ *nirS* mutant but not WT cultures may inhibit magnetite biomineralization via toxic effects, or (ii) the NirS protein may participate directly in magnetosome formation by oxidizing ferrous iron to produce magnetite, as hypothesized for *M. magnetotacticum* (14). To distinguish between these two possibilities, first the effects of nitrite and nitrate on *nirS-gusA* expression were investigated in WT and Δ *nirS* cultures. Expression from the *nirS* promoter increased in the WT and the Δ *nirS* mutant from 0 to 10 mM nitrate under microaerobic conditions (Table 2). Under anaerobic conditions, in the WT the same increase in expression was observed when the nitrate concentration was raised from 1 to 10 mM. However, in the Δ *nirS* mutant, 10 mM nitrate inhibited *nirS-gusA* expression. On the other hand, under microaerobic conditions, 500 μ M nitrite moderately increased *nirS* expression in the WT but had no effect on *nirS* ex-

FIG 5 Spectral analysis of cytochrome cd_1 from WT, Δ *nirS* mutant, Δ *nirN* mutant, and Δ *nirN* mutant plus pLYJ74. (A) UV-visible absorption spectra of oxidized and sodium dithionite reduced periplasmic fraction from WT cells showing characteristic spectra (black arrow) for cytochrome cd_1 . (B) Pyridine ferrohemo-chrome spectrum of purified *holo*-cytochrome cd_1 (in 50 mM Tris-HCl [pH 7.5]) from WT cells. A characteristic peak for d_1 heme at 620 nm was present (black arrow). (C) UV-visible absorption spectra of oxidized and sodium dithionite-reduced periplasmic fractions from the Δ *nirS* mutant for cytochrome cd_1 . No peak for d_1 heme was found due to the deletion of *nirS*. (D) Pyridine ferrohemo-chrome spectrum of the periplasmic fraction (in 50 mM Tris-HCl [pH 7.5]) from the Δ *nirS* mutant. To avoid the effects from other heme-containing proteins, the periplasmic fraction was purified by DEAE chromatography before analysis. It lacked the characteristic d_1 heme absorption peak at 620 nm. (E) UV-visible absorption spectra of oxidized and sodium dithionite-reduced periplasmic fraction from the Δ *nirN* mutant for cytochrome cd_1 . The absorption peaks for d_1 heme at 620 nm and 663 nm in a reduced form were missing, and instead a new 650-nm shoulder was observed (black dashed arrow). (F) Pyridine ferrohemo-chrome spectrum of purified semi-*apo* cytochrome cd_1 (in 50 mM Tris-HCl, pH 7.5) from the Δ *nirN* mutant. No characteristic peak for d_1 heme was found. (G) UV-visible absorption spectra of the oxidized and sodium dithionite-reduced periplasmic fractions from the Δ *nirN* mutant with pLYJ74, which carries *nirN*. The peaks characteristic for d_1 heme (643 nm in oxidized form and 663 and 620 nm in reduced form) were restored (black arrow). (H) Pyridine ferrohemo-chrome spectrum of purified *holo*-cytochrome cd_1 (in 50 mM Tris-HCl [pH 7.5]) from the Δ *nirN* mutant with pLYJ74 with plasmid-borne *nirN*. A characteristic peak for d_1 heme was observed (black arrow). The results shown come from one data set representative of two independent experiments.

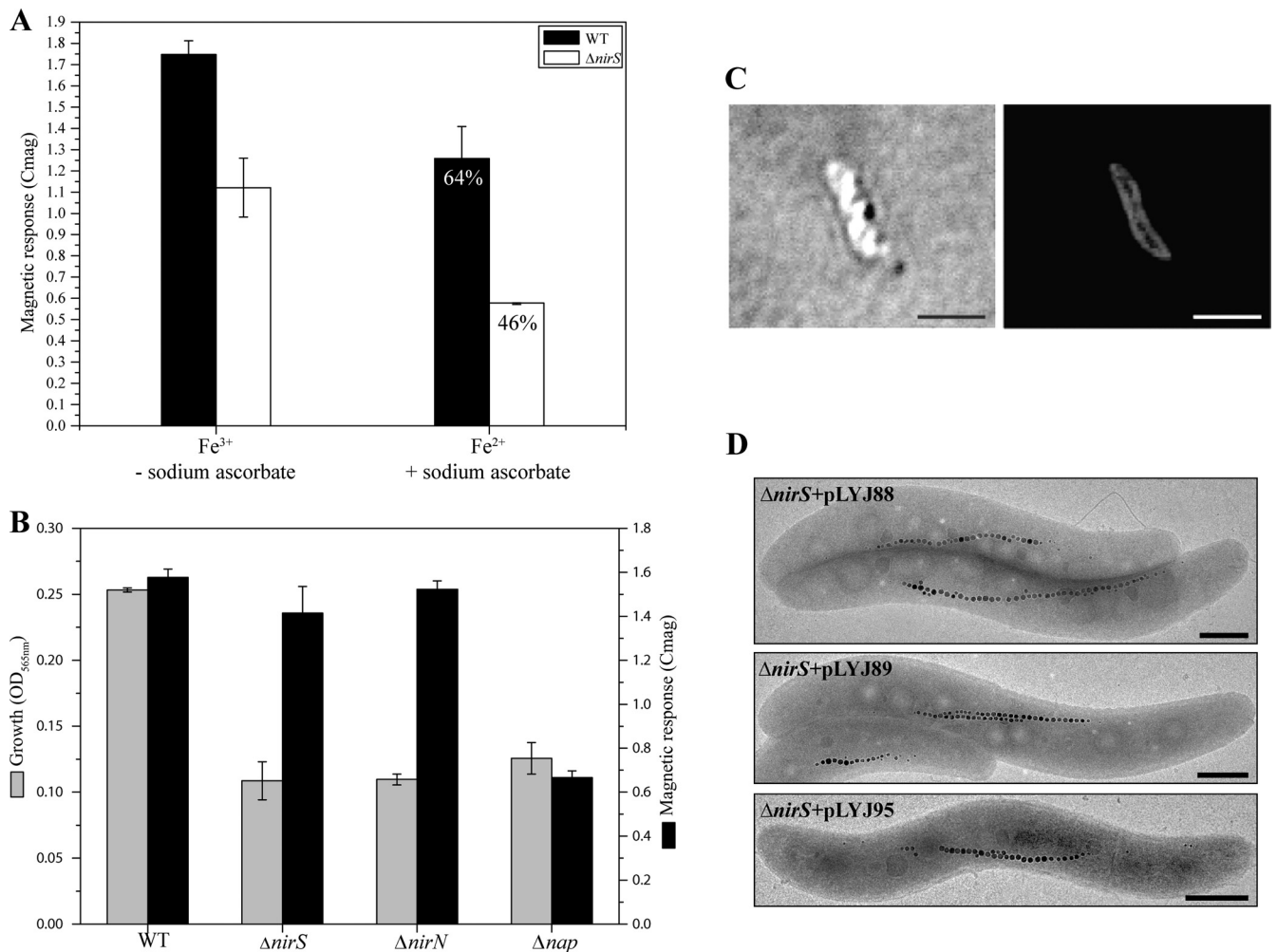


FIG 6 (A) Magnetic response (C_{mag}) of WT and $\Delta nirS$ mutant after three serial transfers under microaerobic conditions in iron-depleted medium. Nonmagnetic WT and the $\Delta nirS$ mutant were induced anaerobically for 6 h in the presence of reduced (100 μ M ferrous chloride plus 0.2 mM ascorbate) and oxidized (100 μ M ferric chloride) iron sources. (B) Growth (based on the OD_{565}) and magnetic response (C_{mag}) of WT, $\Delta nirS$, $\Delta nirN$, and Δnap strains in an incubator hood with a constant atmosphere of 2% O_2 and 98% N_2 . (C) Intracellular localization of the MSR-1 NirS protein N-terminally tagged with mCherry in the $\Delta nirS$ mutant. Differential interference contrast microscopy (left) and fluorescence microscopy (right) were used. Bar, 2 μ m. (D) TEM images of the anaerobically grown $\Delta nirS$ mutant carrying *nirS* (top to bottom) from *M. magneticum* (*amb1395*, *amb4165*) and *P. stutzeri* (*PST_3532*), respectively. Bar, 500 nm.

pression in the $\Delta nirS$ mutant (Table 2). This suggests that the product of nitrite reduction, NO, rather than nitrite itself causes increased *nirS* expression, consistent with the observation that in *P. stutzeri*, *nirSTB* transcription was activated by NO but not nitrite (33). On the other hand, the $\Delta nirS$ mutant still showed some expression of *nirS* in the presence of nitrate, although the reaction of NO_2^- reduction to NO was blocked, indicating that NO_3^- *per se* is capable of increasing the expression of *nirS*. In line with this, the *nirS* expression level in the Δnap mutant, in which denitrification is completely blocked (13), was nearly as high as that in the $\Delta nirS$ strain (data not shown), which further demonstrated that the product of nitrate reduction nitrite is not an inducer for *nirS* expression, whereas nitrate is able to induce the expression of *nirS*. In addition, different concentrations of nitrate and nitrite were added to microaerobically and anaerobically growing cells. Likewise, as shown for the WT before (13), neither nitrate nor nitrite had effects on growth or magnetite synthesis in the $\Delta nirS$ mutant (data not shown). On the other hand, the $\Delta nirN$ mutant also

produced fewer magnetosomes, even though it consumed all transiently accumulated nitrite (Fig. 4C, TEM images in subpanels a of panels iv and v), which also demonstrated that nitrate or nitrite did not affect magnetite biomineralization.

To test whether NirS plays a role in oxidation of ferrous iron for the biomineralization of the mixed-valence oxide magnetite [$FeII(FeIII)_2O_4$], growth experiments in the presence of fully reduced (100 μ M ferrous chloride plus 0.2 mM ascorbate) and fully oxidized (100 μ M ferric chloride) iron sources were performed under anaerobic conditions. Iron-depleted nonmagnetic cells were inoculated to a final OD_{565} of 0.1. More than 6 h after inoculation, if only ferrous iron was available, the C_{mag} of the WT was about 64% of that in the presence of ferric iron (Fig. 6A). A decrease was also observed for the $\Delta nirS$ mutant; however, the difference in the C_{mag} between reducing and oxidizing conditions was markedly larger (about 46% of that under oxidizing conditions) than in the WT. Consistent with previous reports that ferrous iron can be chemically oxidized

by nitrite or nitrous oxide (35), the ferrozine assay showed that ferrous iron was completely oxidized to ferric iron in the $\Delta nirS$ culture by the accumulated nitrite. In contrast, in the WT no detectable oxidation of ferrous iron was found, as in the noninoculated control, implying that in the $\Delta nirS$ mutant ferrous iron becomes oxidized anaerobically by accumulated nitrite. Thus, the reduced C_{mag} of the $\Delta nirS$ mutant in ferrous iron medium may result from the combined effects of only ferrous iron being present initially and its subsequent rapid and complete oxidation to ferric iron. Therefore, to maintain a permanent supply of ferrous iron and to prevent complete chemical oxidation of all ferrous iron by nitrite in the $\Delta nirS$ mutant, washed nonmagnetic cells were suspended in nitrate-free LIM to a final OD_{565} of 0.1 and incubated under anaerobic conditions in the presence of either ferrous or ferric iron. However, no magnetic response was found in either MSR-1 WT or $\Delta nirS$ mutant cultures after incubation for 6 h (data not shown). This demonstrated that the presence of nitrate is essential for supplying energy for growth and magnetite biomineralization under strictly anaerobic conditions. Furthermore, when the $\Delta nirS$ or $\Delta nirN$ mutant was incubated at a constant oxygen concentration of 2% in the presence of nitrate, for both of them magnetosome formation was rescued to the WT level, indicating that in the absence of nitrite reduction, ferrous iron is oxidized by oxygen to ferric iron (Fig. 6B). However, in the Δnap mutant, in which microaerobic magnetite biosynthesis is also impaired in the absence of nitrate (13), no obvious difference was detected between oxygen-limited cultures (grown in 20-ml sealed Hungate tubes with 10 ml of medium under 2% O_2) and those exposed to the same oxygen concentration in the nonlimiting atmosphere of an incubator hood (Fig. 6B). This again indicated that NirS is capable of oxidizing ferrous to ferric iron for anaerobic magnetosome formation during reduction of nitrite to nitric oxide, and the decreased C_{mag} under sealed microaerobic conditions was caused by oxidant limitation.

It was suggested previously that iron oxidation activity might be a specific property of NirS proteins from MTB species, as only NirS from *M. magnetotacticum* showed Fe(II):nitrite oxidoreductase activity *in vitro*, whereas NirS from *P. aeruginosa* lacked this activity (14). On the other hand, most of NirS of *M. magnetotacticum* was detected in the periplasmic fraction, and a putative spatial connection with the magnetosome membrane was inferred (14). As predicted by using the SignalP program (28), our functional MSR-1 NirS-mCherry fusion (as shown by its ability to complement the $\Delta nirS$ mutant) displayed an evenly distributed periplasmic fluorescence in the $\Delta nirS$ mutant, much like that reported for NirS proteins from nonmagnetic denitrifying bacteria (Fig. 6C), but it lacked the characteristic filamentous signal of magnetosome proteins (26, 36), indicating that magnetosomal localization is not required for its function in biomineralization. As shown in Fig. 6D, all tested plasmids carrying different *nirS* genes from either the magnetic *M. magneticum* (*amb1395* and *amb4165*) or the nonmagnetic bacterium *P. stutzeri* (*PST_3532*) rescued both growth and magnetite synthesis in the $\Delta nirS$ mutant to levels comparable to the WT. These data indicate that nitrite reductases of magnetic and nonmagnetic denitrifying bacteria are functionally equivalent with respect to both denitrification and magnetite biomineralization.

DISCUSSION

The conspicuous sequence similarity to NirS of NirN suggested a similar or related function and raised the question of whether NirN itself may catalyze nitrite reduction. However, despite the superficially similar phenotypes in denitrifying growth and biomineralization, closer inspection revealed that, whereas deletion of *nirS* abolished nitrite reduction completely, the $\Delta nirN$ mutant was still capable of nitrite reduction upon prolonged incubation at different temperatures (20°C or 30°C), although utilization of nitrate and nitrite was substantially attenuated compared to WT. This demonstrated that NirN alone is not able to support nitrite reduction in the absence of NirS, and NirN plays an indirect role in nitrite reduction. Based on *in vitro* data for NirN from *P. pantotrophus*, NirN was suggested to possibly function as a d_1 donor in the assembly of d_1 heme into NirS (31). Our biochemical and *in vivo* data are consistent with this assumption, because the form of periplasmic d_1 heme from the $\Delta nirN$ mutant was different from the WT. Likewise, cytochrome cd_1 (NirS) purified from the $\Delta nirN$ mutant only displayed absorption maxima of *c*-type but no d_1 -type heme, possibly due to an aberrant form of d_1 heme. Thus, besides maintaining a correct form of d_1 heme, NirN might be further required for capture and subsequent transfer of a functional d_1 heme to semi-*apo* NirS, as speculated before (31). As a consequence, in the $\Delta nirN$ strain, d_1 heme cannot be properly assembled in NirS, resulting in poor nitrite-reducing activity. This different form of d_1 heme from the $\Delta nirN$ strain might be more sensitive to oxygen and therefore be degraded under our conditions of preparation. Intriguingly, the effect of *nirN* deletion on magnetite biomineralization was partly compensated by growing the cells at 20°C. The lower temperature is favorable for magnetite biomineralization in the WT, although it causes slower growth, which might facilitate the assembly of heme d_1 into NirS in the absence of NirN. Alternatively, NirN might ensure the proper assembly of heme d_1 at elevated temperatures by a chaperone-like function, required in particular under growth conditions atypical for a moderately psychrophilic bacterium from a freshwater environment. However, the suggested NirN function does not seem to be a peculiarity of MSR-1, since in our cross-complementation experiments, all tested *nirN* homologs from various magnetic and nonmagnetic denitrifiers restored denitrifying growth, nitrite reduction, and magnetosome formation of the $\Delta nirN$ mutant back to WT-like levels. Although NirN proteins are conserved in all bacterial *nir* clusters, their physiological function is unknown, as no phenotypic effects could be assigned to any *nirN* deletion in various analyzed denitrifiers (16, 30, 31). Thus, our study provides the first evidence for a physiological function of NirN *in vivo*. The different phenotypes in MSR-1 and nonmagnetic denitrifiers may be also explained by the unusually high susceptibility of MSR-1 to nitrate (<20 mM) and nitrite (<1.5 mM) (13), while nonmagnetic nitrate reducers are capable of growth in the presence of much higher concentrations (16, 31), making MSR-1 less tolerant to any impairment in the detoxifying reduction of nitrite.

While NirN is likely linked to biomineralization only indirectly through a functional interaction with NirS, our data argue for a more direct role of the nitrite reductase NirS. In contrast to Nap, NirS is not absolutely required for anaerobic respiration, which substantiates the previous finding that nitrate reduction catalyzed by Nap is the primary energy-generating process in denitrification of MSR-1 (13). In *M. magneticum*, a similar phenotype (poor an-

aerobic growth, impaired magnetite synthesis) was observed upon concomitant interruption of *norB* and *nirS* (*amb1395*) (37). Since an additional *nirS* homolog (*amb4165*) is present in the *M. magneticum* genome, the results of Wang et al. (37) imply that Amb1395 might be the main nitrite reductase, while Amb4165 has no significant function in denitrification and magnetite synthesis. However, in our experiments, both *amb1395* and *amb4165* from *M. magneticum* when placed under the control of the *nirS* promoter region from MSR-1 were able to fully restore WT-like growth and magnetosome formation in the MSR-1 Δ *nirS* mutant, indicating that the speculated lack of *amb4165* function might be due to transcriptional inactivity under the test conditions.

Taken together, the observed defects in magnetite biomineralization in the Δ *nirS* mutant are not directly caused by the accumulation of nitrite, as we concluded from the following observations: (i) although nitrite accumulated up to 1 to 2 mM when cells of the WT (13) and Δ *nirS* mutant were incubated under a constant microaerobic atmosphere, no effect was found on magnetite biomineralization; (ii) as shown for the WT before (13), concentrations of added nitrate (20 mM) and nitrite (2.5 mM) had no effect on biomineralization in the Δ *nirS* mutant (data not shown); (iii) a Δ *nirN* culture still displayed defects in magnetite biomineralization, even though all nitrite was depleted from the medium at the end of incubation. Another possible explanation for impaired biomineralization in the Δ *nirS* mutant might be the energy limitation in poorly growing cells. However, we never observed similar severe defects in magnetite synthesis upon deletions of other terminal oxidases, such as *cbb₃*, for aerobic respiration, which also caused very poor growth but had no obvious effect on magnetosome morphology under microaerobic conditions in the absence of nitrate (Y. Li and D. Schüler, unpublished data). Taken together, these data suggest that the observed effects on magnetite biosynthesis in the Δ *nirS* mutant are directly associated with its enzymatic activity, which is consistent with the proposed Fe(II): nitrite oxidoreductase function of NirS in magnetospirilla (14) and might be explained by an unbalanced ferrous-to-ferric iron ratio required for the formation of the mixed-valence iron oxide magnetite [FeII(FeIII)₂O₄] in the Δ *nirS* mutant when ferrous iron oxidation is limited (i.e., in the absence of oxygen). In contrast to earlier speculations that iron-oxidizing activity is a function specific to nitrite reductases of MTB (14), we demonstrated that the suspected iron-oxidizing activity is not confined to NirS of magnetospirilla but might be a property common to other cytochrome *cd₁* nitrite reductases. Taken together, these findings suggest that the impaired magnetite synthesis in the Δ *nirS* mutant is likely a consequence of decreased oxidation of ferrous iron, which in the WT takes place in the periplasm with nitrite as electron acceptor catalyzed by NirS. On the other hand, ferrous iron can also be chemically oxidized with nitrite (35, 38), and nitrite and oxygen are potent oxidants for ferrous iron also in ferrite plating, a chemical method for the preparation of magnetite films (39). Therefore, magnetite biomineralization might be favored by combined abiotic oxidation and bioenzymatic catalysis.

In conclusion, our genetic and biochemical analyses revealed that the reduction of nitrite to nitric oxide requires the activity of NirS and that proper assembly of *d₁* heme in *holo*-NirS depends on the functional interaction with NirN, a protein with previously unknown function. Although in some other magnetosome-biomineralizing bacteria, such as *Magnetococcus marinus*, *nir* genes are absent, consistent with the reported inability to grow by

denitrification (40, 41), our data demonstrated that enzymatic nitrite reduction, besides its key respiratory function, also participates in redox homeostasis required for magnetite biomineralization under oxidant-limited conditions (i.e., anaerobic growth) in magnetospirilla. This presents further evidence that, in addition to specific and essential functions provided by proteins encoded within the genomic magnetosome island, the biosynthesis of magnetosomes also relies on a number of auxiliary functions contributed by general metabolism.

ACKNOWLEDGMENTS

We thank Heinrich Jung, Ludwig-Maximilians-Universität München, for strain *P. stutzeri*.

The China Scholarship Council is greatly acknowledged for financial support (Y. Li).

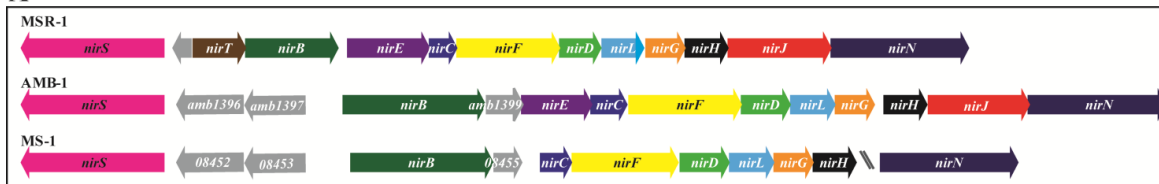
REFERENCES

- Jogler C, Schüler D. 2009. Genomics, genetics, and cell biology of magnetosome formation. *Annu. Rev. Microbiol.* 63:501–521.
- Ullrich S, Kube M, Schübbe S, Reinhardt R, Schüler D. 2005. A hyper-variable 130-kilobase genomic region of *Magnetospirillum gryphiswaldense* comprises a magnetosome island which undergoes frequent rearrangements during stationary growth. *J. Bacteriol.* 187:7176–7184.
- Murat D, Quinlan A, Vali H, Komeili A. 2010. Comprehensive genetic dissection of the magnetosome gene island reveals the step-wise assembly of a prokaryotic organelle. *Proc. Natl. Acad. Sci. U. S. A.* 107:5593–5598.
- Lohsse A, Ullrich S, Katzmann E, Borg S, Wanner G, Richter M, Voigt B, Schweder T, Schüler D. 2011. Functional analysis of the magnetosome island in *Magnetospirillum gryphiswaldense*: the *mamAB* operon is sufficient for magnetite biomineralization. *PLoS One* 6(10):e25561. doi:10.1371/journal.pone.0025561.
- Mann S, Sparks NHC, Board RG. 1990. Magnetotactic bacteria: microbiology, biomineralization, palaeomagnetism and biotechnology. *Adv. Microb. Physiol.* 31:125–181.
- Faivre D, Agrinier P, Menguy N, Zuddas P, Pachana K, Gloter A, Laval J, Guyot F. 2004. Mineralogical and isotopic properties of inorganic nanocrystalline magnetites. *Geochim. Cosmochim. Acta* 68:4395–4403.
- Faivre D, Böttger LH, Matzanke BF, Schüler D. 2007. Intracellular magnetite biomineralization in bacteria proceeds by a distinct pathway involving membrane-bound ferritin and an iron(II) species. *Angew. Chem. Int. Ed. Engl.* 46:8495–8499.
- Yang CD, Takeyama H, Tanaka T, Matsunaga T. 2001. Effects of growth medium composition, iron sources and atmospheric oxygen concentrations on production of luciferase-bacterial magnetic particle complex by a recombinant *Magnetospirillum magneticum* AMB-1. *Enzyme Microb. Technol.* 29:13–19.
- Heyen U, Schüler D. 2003. Growth and magnetosome formation by microaerophilic *Magnetospirillum* strains in an oxygen-controlled fermentor. *Appl. Microbiol. Biotechnol.* 61:536–544.
- Blakemore RP, Short KA, Bazylinski D, Rosenblatt C, Frankel R. 1985. Microaerobic conditions are required for magnetite formation within *Aquaspirillum magnetotacticum*. *Geomicrobiol. J.* 4:53–71.
- Bazylinski D, Blakemore RP. 1983. Denitrification and assimilatory nitrate reduction in *Aquaspirillum magnetotacticum*. *Appl. Environ. Microbiol.* 46:1118–1124.
- Zumft WG. 1997. Cell biology and molecular basis of denitrification. *Microbiol. Mol. Biol. Rev.* 61:533–616.
- Li Y, Katzmann E, Borg S, Schüler D. 2012. The periplasmic nitrate reductase Nap is required for anaerobic growth and involved in redox control of magnetite biomineralization in *Magnetospirillum gryphiswaldense*. *J. Bacteriol.* 194:4847–4856.
- Yamazaki T, Oyanagi H, Fujiwara T, Fukumori Y. 1995. Nitrite reductase from the magnetotactic bacterium *Magnetospirillum magnetotacticum*: a novel cytochrome *cd₁* with Fe(II)-nitrite oxidoreductase activity. *Eur. J. Biochem.* 233:665–671.
- Rinaldo S, Sam KA, Castiglione N, Stelitano V, Arcovito A, Brunori M, Allen JWA, Ferguson SJ, Cutruzzolà F. 2011. Observation of fast release of NO from ferrous *d₁* haem allows formulation of a unified reaction mechanism for cytochrome *cd₁* nitrite reductases. *Biochem. J.* 435:217–225.

16. Kawasaki S, Arai H, Kodama T, Igarashi Y. 1997. Gene cluster for dissimilatory nitrite reductase (*nir*) from *Pseudomonas aeruginosa*: sequencing and identification of a locus for heme *d*₁ biosynthesis. *J. Bacteriol.* 179:235–242.
17. Bali S, Lawrence AD, Lobo SA, Saraiva LM, Golding BT, Palmer DJ, Howard MJ, Ferguson SJ, Warren MJ. 2011. Molecular hijacking of siroheme for the synthesis of heme and *d*₁ heme. *Proc. Natl. Acad. Sci. U. S. A.* 108:18260–18265.
18. Palmedo G, Seither P, Korner H, Matthews JC, Burkhalter RS, Timkovich R, Zumft WG. 1995. Resolution of the *nirD* locus for heme *d*₁ synthesis of cytochrome *cd*₁ (respiratory nitrite reductase) from *Pseudomonas stutzeri*. *Eur. J. Biochem.* 232:737–746.
19. Faivre D, Menguy N, Posfai M, Schüler D. 2008. Environmental parameters affect the physical properties of fast-growing magnetosomes. *Am. Mineral.* 93:463–469.
20. Schüler D, Uhl R, Bäuerlein E. 1995. A simple light scattering method to assay magnetism in *Magnetospirillum gryphiswaldense*. *FEMS Microbiol. Lett.* 132:139–145.
21. Schüler D, Bäuerlein E. 1998. Dynamics of iron uptake and Fe₃O₄ biomineralization during aerobic and microaerobic growth of *Magnetospirillum gryphiswaldense*. *J. Bacteriol.* 180:159–162.
22. Sambrook J, Russel D. 2001. Molecular cloning: a laboratory manual, 3rd ed. Cold Spring Harbor Laboratory Press, Cold Spring Harbor, NY.
23. Goodhew CF, Brown KR, Pettigrew GW. 1986. Heme staining in gels, a useful tool in the study of bacterial *c*-type cytochromes. *Biochim. Biophys. Acta* 852:288–294.
24. Bartsch RG, Kakuno T, Horio T, Kamen MD. 1971. Preparation and properties of *Rhodospirillum rubrum* cytochromes *c*₂, *cc'*, and *b*_{557.5}, and flavin mononucleotide protein. *J. Biol. Chem.* 246:4489–4496.
25. Viollier E, Inglett PW, Hunter K, Roychoudhury AN, Van Cappellen P. 2000. The ferrozine method revisited: Fe(II)/Fe(III) determination in natural waters. *Appl. Geochem.* 15:785–790.
26. Katzmann E, Scheffel A, Gruska M, Plitzko JM, Schüler D. 2010. Loss of the actin-like protein MamK has pleiotropic effects on magnetosome formation and chain assembly in *Magnetospirillum gryphiswaldense*. *Mol. Microbiol.* 77:208–224.
27. Katzmann E, Müller FD, Lang C, Messerer M, Winkhofer M, Plitzko JM, Schüler D. 2011. Magnetosome chains are recruited to cellular division sites and split by asymmetric septation. *Mol. Microbiol.* 82:1316–1329.
28. Petersen TN, Brunak S, von Heijne G, Nielsen H. 2011. SignalP 4.0: discriminating signal peptides from transmembrane regions. *Nat. Methods* 8:785–786.
29. Jüngst A, Wakabayashi Matsubara S, Zumft H, WG. 1991. The *nirSTBM* region coding for cytochrome *cd*₁-dependent nitrite respiration of *Pseudomonas stutzeri* consists of a cluster of mono-, di-, and tetraheme proteins. *FEBS Lett.* 279:205–209.
30. Hasegawa N, Arai H, Igarashi Y. 2001. Two *c*-type cytochromes, NirM and NirC, encoded in the *nir* gene cluster of *Pseudomonas aeruginosa* act as electron donors for nitrite reductase. *Biochem. Biophys. Res. Commun.* 288:1223–1230.
31. Zajicek RS, Bali S, Arnold S, Brindley AA, Warren MJ, Ferguson SJ. 2009. *d*₁ haem biogenesis: assessing the roles of three *nir* gene products. *FEBS J.* 276:6399–6411.
32. Hill KE, Wharton DC. 1978. Reconstitution of apoenzyme of cytochrome oxidase from *Pseudomonas aeruginosa* with heme *d*₁ and other heme groups. *J. Biol. Chem.* 253:489–495.
33. Vollack KU, Zumft WG. 2001. Nitric oxide signaling and transcriptional control of denitrification genes in *Pseudomonas stutzeri*. *J. Bacteriol.* 183:2516–2526.
34. Zajicek RS, Cartron ML, Ferguson SJ. 2006. Probing the unusual oxidation/reduction behavior of *Paracoccus pantotrophus* cytochrome *cd*₁ nitrite reductase by replacing a switchable methionine heme iron ligand with histidine. *Biochemistry* 45:11208–11216.
35. Moraghan JT, Buresh RJ. 1977. Chemical reduction of nitrite and nitrous oxide by ferrous iron. *Soil Sci. Soc. Am. J.* 41:47–50.
36. Lang C, Schüler D. 2008. Expression of green fluorescent protein fused to magnetosome proteins in microaerophilic magnetotactic bacteria. *Appl. Environ. Microbiol.* 74:4944–4953.
37. Wang K, Ge X, Bo T, Chen Q, Chen G, Liu W. 2011. Interruption of the denitrification pathway influences cell growth and magnetosome formation in *Magnetospirillum magneticum* AMB-1. *Let. Appl. Microbiol.* 53:55–62.
38. Vancleemput O, Baert L. 1983. Nitrite stability influenced by iron compounds. *Soil Biol. Biochem.* 15:137–140.
39. Abe M. 2000. Ferrite plating: a chemical method preparing oxide magnetic films at 24–100 degrees C, and its applications. *Electrochim. Acta* 45:3337–3343.
40. Frankel RB, Bazylinski DA, Johnson MS, Taylor BL. 1997. Magnetoaerotaxis in marine coccoid bacteria. *Biophys. J.* 73:994–1000.
41. Schütte S, Williams T, Xie G, Kiss H, Brettin T, Martinez D, Ross C, Schüler D, Cox B, Neelson K, Bazylinski D. 2009. Complete genome sequence of the chemolithoautotrophic marine magnetotactic coccus strain MC-1. *Appl. Environ. Microbiol.* 75:4835–4852.

SUPPLEMENTAL MATERIALS

A



B

Mgr_1052	MLKGLRNALL	LSVMP -MAMA	TGAFANEAA -	-----	-----	-----	-----	L	TGATKDAAAK	IYFERCAGCH	49
Amb1395	MWKGVRNALL	LTALP -FAMS	GAFAQEAT -	-----	-----	-----	-----	L	SKEAKEASAK	IYFERCAGCH	49
Magn03008451	-----	-----	GAFAQEAT -	-----	-----	-----	-----	L	SKDAKEASAK	IYFERCAGCH	32
PST_3532	-MSNVGKPI L	AGVIAGLSLL	GLAVAQAAAP	E-----	-----	-----	-----	M	TAEKEAAKQ	IYFERCAGCH	51
Amb4165	--MKAAATWMM	AALAV - -AWA	GTAAAEKPA	HGAGEHYETS	GDQLRAAPMS	QPGAQPPQL	SAAEFTRAKQ	IYFERCAGCH	76		
PA14_06750	--MPFGKPLV	GTLLASLTL	GLATAHAKDD	MKAAEQYQGA	ASAVDPAHVV	RTNG - -APDM	SESEFNEAKQ	IYFQR	CAGCH	76	
Mgr_1052	GVLKRGATGK	NLEP - - - - -	-----	AAT	SKLGGQRLEK	I I ANGTGGM	VNFDD - - ILS	KDEIKMMATY	IQMPDPSPE	114	
Amb1395	GVLKRGATGK	NLEP - - - - -	-----	ANT	TKLGGARLEK	ILTNGTGGM	VNFDD - - ILS	KDEIKMMATY	IQMPDPSPE	114	
Magn03008451	GVLKRGATGK	NLEP - - - - -	-----	ANT	TKLGGARLEK	ILTNGTGGM	VNFDD - - ILS	KDEIKMMATY	IQMPDPSPE	97	
PST_3532	GVLKRGATGK	NLEPHWTKTD	ADGKKTEGGT	LNLGTRKLEN	I I AYGTGGM	VNYDD - - ILS	KDEIKMMATY	IQMPDPSPE	129		
Amb4165	GVLKRGATGK	PLTT - - - - -	-----	DIT	RERGFDAKKA	F I TYGSAAGM	PNWGS SGLS	EAEDVLMKY	LLNEPPQPE	143	
PA14_06750	GVLKRGATGK	PLTP - - - - -	-----	DIT	QQRGGYLEA	L I TYGFPLGM	PNWGS SGLS	KEQITLMKY	IQHTPPQPE	143	
Mgr_1052	WGLADMKGWS	K I I VVDKRP	TKMNNVND	NVFSVTRDS	GEVALIDGDT	KKIWNIVKTG	YAVHISRISY	SGRYVYVIGR	194		
Amb1395	WGIKEMTASW	KVTVKPEDRP	KKQMNKVNK	NVFSVTRDS	GEVALIDGDT	KKIWTI IKTG	YAVHISRISA	SGRFVYVIGR	194		
Magn03008451	WGIKEMTASW	KVVVKPEDRP	KKQLNKVNK	NVFSVTRDS	GEVALIDGDT	KKIWTI IKTG	YAVHISRISA	SGRFVYVIGR	177		
PST_3532	FSLQDMKDSW	KL I VVDQRP	KKQMNKINLK	NVFAITLDRD	GKALVLDGDT	HTIWKVLDTG	YAVHISRISA	SGRYVYVIGR	209		
Amb4165	FGMDEIKATW	KVQIPADKRP	ARKMNTLDS	NLFSVTRDS	GEVALIDGAS	KNIVSI IKTG	YAVHISRISA	SGRYLVYIGR	223		
PA14_06750	WGMPEMRESW	KVLVKPEDRP	KKQLNDLDP	NLFSVTRD	GQIALVDGDS	KKIVKVIDTG	YAVHISRISA	SGRYLVYIGR	223		
Mgr_1052	DGKLDLIDLW	MEKPQVAT I	KTGLDARSVE	TSKFKGYEDK	YAIAGSYWPP	QYVIMDGLTL	EPLKIVSTRG	NTVDG - EYHP	273		
Amb1395	DGKLDLIDLW	METPAVVAT I	KIGMDARSVE	TSKFKGFEDK	YAVAGSYWPP	QYVIMDGADL	KPLKIVSTRG	ITVDG - EYHP	273		
Magn03008451	DGKLDLIDLW	METPAVVAT I	KIGMDARSVE	TSKFKGFEDK	YAVAGSYWPP	QYVIMDGADL	KPLKIVSTRG	ITVDG - EYHP	256		
PST_3532	DGLTTI I DMW	YEEPTTAVT V	RLGSDARSVD	TSKFKGYEDK	YLIAGSYWPP	QYSIMDGETL	EPKIVSTRG	QTVDG - EYHP	288		
Amb4165	DAKINLIDLW	MEKPEVVAE V	KIGMEARSVE	TSKFKGFEDK	YAIAGAYWPP	QFVIMDGNL	EPKIVSTRG	MTSDKQYHP	303		
PA14_06750	DARIDMIDLW	AKEPTKVAE I	KIGIEARSVE	SSKFKGYEDR	YTIAGAYWPP	QFAIMDGETL	EPKIVSTRG	MTVDTQTYHP	303		
Mgr_1052	EPRVASIVAS	QIKPEFVVNV	KETGLIKLVD	YTDIKNLKEY	TIESAKFLHD	GGWDASKRYF	LVAANASNKV	AVVDTKDGKL	353		
Amb1395	EPRVASIVAS	MIKPEWVNI	KETGLIKLVD	YSDIKNLKET	TIESAKFLHD	GGWDASKRYF	LVAANASNKV	AVVDTKDGKL	353		
Magn03008451	EPRVASIVAS	MIKPEWVNI	KETGLIKLVD	YSDIKNLKET	TIESAKFLHD	GGWDASKRYF	LVAANASNKV	AVVDTKDGKL	336		
PST_3532	EPRVASIVAS	HIKPEWVVNV	KETGQI I LVD	YTDLKNLKT	TIESAKFLHD	GGWDASKRYF	LVAANASNKV	AVVDTKDGKL	368		
Amb4165	EPRVASIVAS	HFKPEFVVNV	KETGLI I LVD	YSDIKNLKVT	SIEAERFLHD	GGFDASKRYF	LVAANARNKI	AVVDTKEDKL	383		
PA14_06750	EPRVAIIAS	HEHPEFIVNV	KETGKVLVNV	YKDINLTVT	SIGAAPFLHD	GGWDSHRYF	MTAANNSNKV	AVIDSKDRRL	383		
Mgr_1052	AALVDTKSKP	HPGRGANFVH	PKFGPVWATS	HLGADVITLI	GTDP - - - - E	KHPEFAWKV	EELKNHGSGS	LFVKTHPKSS	428		
Amb1395	AGLVDTKSKP	HPGRGANFNH	PKFGPVWATS	HLGADVITLI	GTDP - - - - A	KHKDQAWKV	AELKNHGAGS	LFVKTHPKSS	428		
Magn03008451	AGLVDTKSKP	HPGRGANFVH	PKFGPVWATS	HLGADVITLI	GTDP - - - - A	KHKDQAWKV	AELKNHGAGS	LFVKTHPKSS	411		
PST_3532	AALVDTAKIP	HPGRGANFIH	PQFGPVWTTG	HLGDDVVS LI	STASDDPKYA	KYKEHNWKV	QELKMPGAGN	LFVKTHPKSS	448		
Amb4165	VGMVEVGATP	HPGRGTNFVH	PKFGPVWATG	HLGDDSVALI	GTDP - - - - K	GHPKQAWTKV	ASLTGGGGS	LFVKTHPKSS	458		
PA14_06750	SALVDVGKTP	HPGRGANFVH	PKYGPVWSTS	HLGDGSI S LI	GTDP - - - - K	NHPQYAWKKV	AELQGGGGS	LFVKTHPKSS	458		
Mgr_1052	NLWADAPLMP	EREAEESVTV	YDINNLA KGP	EVINVA KMAG	LPESKAVKRT	VHA EYNEAGD	EWVFSWAGK	TEPSA I V I LD	508		
Amb1395	NLWADAPLFP	EKDMAESVTV	YDIKNLDKGP	EVINI AKLAD	LPETKAVKRA	VQAEYNEKGD	EWVFSWAGK	TEPSA I V V MD	508		
Magn03008451	NLWADAPLFP	EKDMAESVTV	YDIKNLDKGP	EVINI AKLAD	LPETKAVKRA	VQAEYNEKGD	EWVFSWAGK	TEPSA I V V MD	491		
PST_3532	NLWADAPMNP	EREVAESVTV	YDLADLSKAP	KRLDVA KDSG	LPESKAIRRA	THPEYNEAGD	EWVFSWAGK	TEPSA I V I Y D	528		
Amb4165	NLWVDTTINP	DADVAASI AV	FDINNLDKPA	EVLP I AKWAG	ISDG - - APRV	VQPEYNKAGD	EWVFSWAGK	TEPSA I V V V D	536		
PA14_06750	HLVYDTTFNP	DARISQSVAV	FDLKNLDAKY	QVLP I AEWAD	LGEG - - AKRV	VQPEYNKRGD	EWVFSWAGK	TEPSA I V V V D	536		
Mgr_1052	DKTRKMKAVI	KDPKLITPTG	KFNVKNTQHD	IY	540						
Amb1395	DKTRKMKAVI	KDPKLITPTG	KFNVKNTQHD	IY	540						
Magn03008451	DKTRKMKAVI	KDPKLITPTG	KFNVKNTQHD	IY	523						
PST_3532	DKTLKLVKVI	TDPAVITPTG	KFNVTNTMHD	VY	560						
Amb4165	DKTRKLVKVI	KDPRLITPTG	KFNVTNTLHD	VY	568						
PA14_06750	DKTLKLVKVI	KDPRLITPTG	KFNVKNTQHD	VY	568						

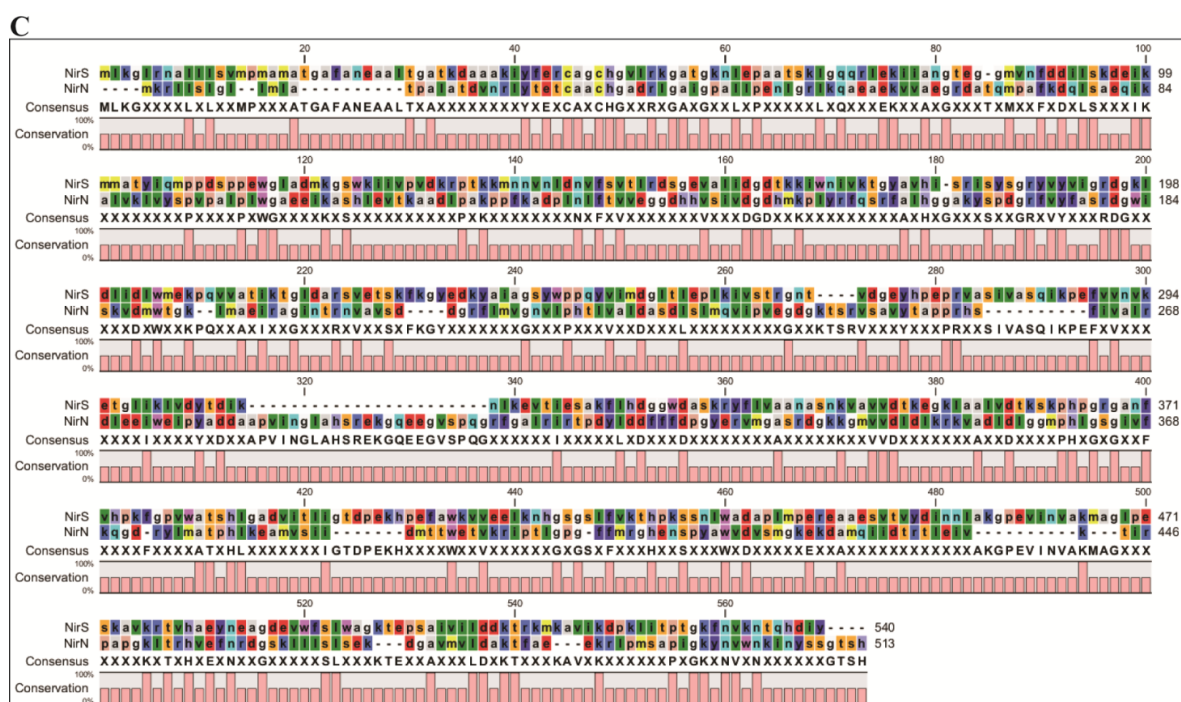


Fig. S1 (A) Molecular organization of identified *nir* genes in *Magnetospirillum magneticum* and *Magnetospirillum magnetotacticum*. Double backslash represents *nirN* and other *nir* genes are found in different contigs from the incomplete genome assembly in *M. magnetotacticum*. (B) Sequence alignment of NirS with selected homologs from MTB and non-MTB. PST_3532 and PA14_06750 refer to NirS from *Pseudomonas stutzeri* A1501 and *Pseudomonas aeruginosa* UCBPP-PA14, respectively. Conserved, homologous, and nonconserved residues among the various species are shown in red, blue, and black, respectively. Residues involved in d_1 heme binding site are indicated by green stars. Heme *c* binding site is shown in a black box. (C) Sequence alignment of NirS and NirN from MSR-1. The level of conserved amino acid residues among the various species are shown below the sequences. The residues of the alignment are color-coded according to the Rasmol colour scheme (<http://life.nthu.edu.tw/~fmhsu/rasframe/COLORS.HTM#aminocolors>).

Compared to MSR-1, a similar *nir* cluster was observed in both *M. magneticum* and *M. magnetotacticum* (Fig. S1A). While neither *nirS* nor other *nir* genes are present in *Magnetococcus marinus* MC-1 (1), two homologs of *nirS* (*amb1395* and *amb4165*) are present in *M. magneticum* (Table S1), thus being the only known bacterium having more than one *nirS* gene. As in MSR-1, *amb1395* is part of a larger *nir* cluster and shares high amino acid similarity (91%) with NirS of both MSR-1 (Mgr_1052) and *M. magnetotacticum* (Magn03008451), respectively (Table S1), whereas *amb4165* is more divergent (78% similarity to NirS of MSR-1) and not adjacent to other *nir* genes. Also, the N-terminus of Amb4165 containing the heme *c*-binding region differs from that of other magnetobacterial

NirS homologs, but rather resembles NirS from *Ps. aeruginosa*, whereas in NirS from *Ps. stutzeri* this region is absent (Fig. S1B) (2).

In *M. magneticum* and *M. magnetotacticum*, *nirCFDLGH* genes also show synteny. However, compared to MSR-1 their *nir* clusters also display some differences (Fig. S1A): First, in *M. magnetotacticum* and *M. magneticum* *nirT* and *nirB* genes are fused into a single gene designated as *nirB*. Second, in *M. magneticum* and *M. magnetotacticum* an additional gene (*amb1399* and *magn03008455*) encoding a copper-binding protein of plastocyanin/azurin family is present between *nirB* and *nirE*. Third, *nirJ* is missing in *M. magnetotacticum*, probably due to the incompleteness of its genome assembly. Fourth, *nirE* encoding an S-adenosylmethionine (SAM)-dependent uroporphyrinogen methyltransferase is absent from *M. magnetotacticum*. The monocistronic organization of *nirS* encoding a cytochrome *cd*₁ nitrite reductase in MSR-1 and other magnetospirilla is unique compared to all other non-magnetic denitrifiers in which *nirS* is part of a single operon along with other *nir* genes. In magnetospirilla we found all other *nir* genes (*nirTBECFDLGHJN*) within a closely adjacent, but distinct cluster, which encodes a set of proteins likely required for synthesis of *d*₁ heme. This different organization might reflect a somewhat distinct regulation or function of magnetobacterial nitrite reduction proteins.

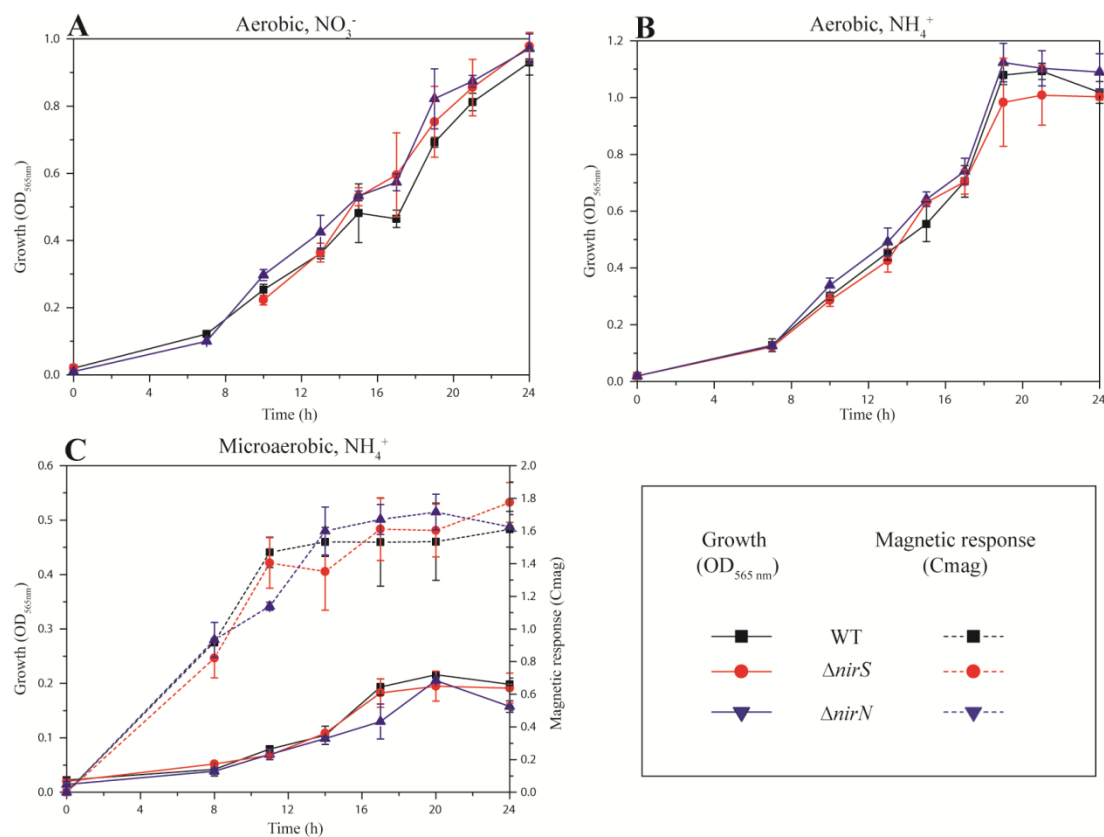


Fig. S2 Growth ($\text{OD}_{565\text{ nm}}$) and magnetic response (C_{mag}) of MSR-1 WT, $\Delta nirS$, and $\Delta nirN$ under different conditions at 30°C . Under aerobic conditions, the C_{mag} values were always zero and not shown. (A) Aerobic, nitrate medium; (B) Aerobic, ammonium medium; (C) Microaerobic, ammonium medium. Results from representative experiments were measured in triplicate, and values are given as means and standard deviations.

Mgr_0419	-----	-----	-----mk	r-llslgll	mlatpal-at	dvnrlytetc	aachgadrfg	aigpallpen	49	
Amb_1408	msifdlssra	lrgisarsav	rvllrrarmg	slplmvvgmt	ilatptlaae	daprlyaehc	aachggdrfg	aigpallpen	80	
Magn03008348	-----	-----	-----	---mvvgmt	ilatpaqave	daprlyaehc	aachggdrfg	aigpallpen	46	
BAA12683	-----	-----	-----m	rliglalgl	lgalaqagea	pgealyrqhc	qachgvrfg	gsgptllpes	51	
AAZ43116	-----	mqli---	pa	lvlaaalpa	tfvaldlalp	-raaaatqpt	dsqalyeqhc	qschgvrfg	gagpallpes	65
Pden_2495	-----	-----	-----mir--	---ptaafsl	llalplitaha	dpaadyaehc	aachgedrfg	gtgpallipet	50	
Mgr_0419	Igrlkqaee	kvvaegrdat	qmpafkdqls	aeqikalvkl	vysvpvalpl	wgaaekash	levtkaadlp	akppfkadpl	129	
Amb_1408	Igrlrkaeae	kvlaqgrpat	qmpahgdkln	aeqikalae	vytplaavpa	wgmaekasr	vinvdpaslp	akpqwntdpl	160	
Magn03008348	Igrlrkaeae	tviargraat	qmpahgdklt	peqikalae	vftplaavpv	wgmeerasr	vvnvdpdqlp	srpqwadapl	126	
BAA12683	Isrlkpaqar	evilhgrpat	qmagfagql	daaadalvay	lyqapprepq	wsaedirasq	vqphplatlp	srprfeadpl	131	
AAZ43116	Isrlkpaeah	svirdgrpas	qmaayshvln	daqitglvdy	lyqpaavppt	wsdadirash	riikdvatlp	tapqhgadpr	145	
Pden_2495	Igrvrgi--d	tviaqgrvst	qmegfadrln	pesitalvdy	vtaplthrpd	wsaeqiassr	empdy-qpa	ekpvfaadpl	127	
Mgr_0419	nlfvtvveggd	hhvsvldgdh	mkplyrfqsr	fahlggakys	pdgrfvyfas	rdgwiskvdm	wtgklmaeir	agintrnvav	209	
Amb_1408	nlfvtvvegd	hhvtildges	fkpltrfqsr	fahlggakys	pdgrfvyfas	rdgwitkydl	ytliqivaeir	agvntnrnvav	240	
Magn03008348	nlfvtvvegd	hhvtildgds	fkplarfqs	fahlggakys	pdgrfvyfas	rdgwitkydl	ysliqivaeir	agvntnrnvav	206	
BAA12683	nlfvvesgd	hhvtildgdr	fepiarfpr	yahlggpkfs	pdgrlvyfas	rdgwvtlydl	ynlkvvaevr	aglntrnlav	211	
AAZ43116	nlfvveagn	hhvrvldgdr	feelfarfqs	fahlggpkfs	pdgrfvyfas	rdgwisyvdl	hnlcmiaevr	aglntrnlav	225	
Pden_2495	niltvvetgd	hhvsvldgdt	fevlarfatp	fahlggpkfs	pdgrfvyims	rdgwvqkydi	wslaevgrir	aalnsrniai	207	
Mgr_0419	sddgrflmvg	nylphltlval	dasdlslmqv	lpvegd-gkt	srvsavytap	prhsfvialr	dleeiweipy	addaapving	288	
Amb_1408	shdgrflmvg	nmlphltlval	dardltplqv	lpvvgdagat	srvsavytap	prasfvvalk	dlepveipy	addagpvmng	320	
Magn03008348	shdgrflmvg	nmlphltlval	dardltplqv	lpvvgdagat	srvsavytap	prasfvvalk	dlepveipy	addagpvmng	286	
BAA12683	sdhgrwlvlg	nylpgnlvll	dardlslvqv	ipaadaqqga	srvsavytap	prhsfvvalk	dvhelweipy	angk-----	285	
AAZ43116	sndgrwlvlg	nylpgnlvll	dardlslk	lptvqdgtp	srvsavytap	prdsfvvalk	dvqeaewlsy	agep-----	299	
Pden_2495	spdgqriava	nylpsltil	ds-dlnplr	latq-vdgt	srvsavyqap	qrhsfvialk	dapeiwevat	td-----	277	
Mgr_0419	lahsrekqge	egvspqgrfg	alrirtpdyl	ddfffdpgye	rvmgasrdgk	kgmvvdldik	rkvadldlgg	mphilgsgivf	368	
Amb_1408	fvhsyekghe	egispqgrfq	airiripdf	ddffdrtye	ramgasrdgt	kglvvdldik	rkvaeidlpg	mphilgsgiif	400	
Magn03008348	fvhsyekghe	egispqgrfq	airiripdf	ddffdrtye	rvmgasrdgt	kglvvdldik	rkvaeidlpg	mphilgsgiif	366	
BAA12683	-----	-----pva	pkrlavadyl	ddfsfspdyr	yllgssrqar	ggevieldsg	arvasipisg	mphilgsgiyw	348	
AAZ43116	-----	-----tfe	prrikaadyl	ddfsftpdyr	yllatsrkah	ggqvildtg	kavtdlipg	mphilgsgiyw	362	
Pden_2495	-----	-----ls	irripidepl	ddfsfspdyr	qliganrdgd	kgvaiddgd	hkvaelpipg	mphilgsgitw	339	
Mgr_0419	kqgdrylmat	phlkeamvsi	idmttwetvk	riptlpggff	mrghenspya	wdvsmgkek	damqiidtrt	leivktirpa	448	
Amb_1408	akdghdymat	phlkeavvsi	idmqwktvk	riptlpggff	mrshentgya	widvsmgkek	daiqiidlsa	meivrtlrpa	480	
Magn03008348	kkdgrdfmat	phlkeavvsi	idmstwktyk	riptlpggff	mrshentgya	widvsmgkek	daiqiidlda	meivrtlrpa	446	
BAA12683	krdgrwvfat	pnisrgvisv	idlqnwplk	eivtdggpff	mrshadspya	wtdtflgkhh	deillidkqt	leiahrlrps	428	
AAZ43116	krdgkvwfat	pnvskglisv	ldletwklk	eiptegpff	mrsganspya	wtdvffgpnn	davhlikqt	levahtrrpm	442	
Pden_2495	erdgrvrmat	phlgegvisv	idmqdwslvk	qiktsggpff	lrghatspyv	wadvffgphk	demhvldkqt	leivktlapf	419	
Mgr_0419	pgkltrhvef	nrdgskllls	lsekdgavmv	ldaktfaeek	rlpmsapigk	ynvwnkinys	sgtsh	513		
Amb_1408	pgrttahae	drsgkhvlis	vmeaegeliv	fdaesfevvt	rmpmkrpvkg	ynvfnkinys	sgtsh	545		
Magn03008348	agrttahae	drsgrhvlis	vmeaegeliv	fdaqsfvvt	rmpmkrpvkg	ynvfnkinys	sgtsh	511		
BAA12683	pgkvaghvef	trdgryalis	vwdrdgalv	ydahsleevk	rlpmnkpsgk	ynvgnkigya	egtsh	493		
AAZ43116	pgknaahvef	tndgryalis	vwdtdgalv	ydantleevk	rlpmnkpsgk	ynvgnkief	egtsh	507		
Pden_2495	pgqtfahsef	trdgrshvls	lwedegavvi	yaktldevk	rlpmrkpsgk	ynvwnkitfe	dgtsh	484		

Fig. S3 Sequence alignment of NirN with selected homologs from MTB and non-MTB. PST_3538, PA14_06650, and Pden_2495 refer to NirN from *Pseudomonas stutzeri* A1501, *Pseudomonas aeruginosa* UCBPP-PA14, and *Paracoccus denitrificans* PD1222, respectively. Conserved, homologous, and nonconserved residues among the various species are shown in red, blue, and black, respectively.

Table S1 Bacterial strains used in this work

Strain	Important feature (s)	Source or reference
<i>E. coli</i> strain DH5 α	F' Φ 80 <i>lacZ</i> Δ M15 Δ (<i>lacZYA-argF</i>)U169 <i>deoR recA1 endA1 hsdR17</i> (<i>r_k</i> ⁻ , <i>m_k</i> ⁺) <i>phoA supE44 λ-thi-1 gyrA96 relA1</i>	Invitrogen
<i>E. coli</i> strain BW29427	<i>dap</i> auxotroph derivative of <i>E. coli</i> strain B2155	K. Datsenko and B. L. Wanner, unpublished
<i>Ps. stutzeri</i>	Wild type	H. Jung
MSR-1 WT	Wild type R3/S1, but Rif ^r , Sm ^r	(3)
Δ <i>nirS</i>	R3/S1 Δ <i>nirS</i>	This study
Δ <i>nirN</i>	R3/S1 Δ <i>nirN</i>	This study

Table S2 Plasmids used in this work

Plasmid	Important feature (s)	Source or reference
pCM184	Broad-host-range allelic exchange vector, Amp ^r , Km ^r , Tc ^r	(4)
pBBR1MCS-2	Km ^r , mobilizable broad-host-range vector	(5)
pBBR1MCS-3	Tc ^r , mobilizable broad-host-range vector	(5)
pK19mobGII	-	(6)
pFM208	Km ^r	F. D. Müller, unpublished data
pRU1	Km ^r	R. Uebe, unpublished data
pCM157	Tc ^r , Cre recombinase expression vector	(4)
pLYJ06	pCM184 plus <i>nirS</i> 2-kb downstream region	This study
pLYJ08	pLYJ06 plus <i>nirS</i> 2-kb upstream region	This study
pLYJ20	pCM184 plus <i>nirN</i> 2-kb upstream region	This study
pLYJ23	pLYJ06 plus <i>nirN</i> 2-kb downstream region	This study
pLYJ36	pBBR1MCS-2 plus <i>nirS</i> promoter region	This study
pLYJ51	pBBR1MCS-2 plus <i>nirS</i> with its own promoter	This study
pLYJ52	pBBR1MCS-2 plus <i>nirS</i> without its candidate signal peptide sequence	This study
pLYJ59	pLYJ52 with <i>nirS</i> promoter and signal peptide sequence	This study
pLYJ64	pLYJ59 plus <i>mcherry</i>	This study
pLYJ74	pRU1 plus <i>nirN</i>	This study
pLYJ86	pCM157 plus <i>nirS</i> promoter region from pLYJ36	This study
pLYJ87	pBBR1MCS-2 plus <i>nirS</i> promoter and <i>cre</i> fusion from pLYJ86	This study
pLYJ88	pLYJ36 plus <i>amb1395</i> from <i>M. magneticum</i>	This study
pLYJ89	pLYJ36 plus <i>amb4165</i> from <i>M. magneticum</i>	This study
pLYJ94	pLYJ97 plus <i>nirS</i> promoter region	(7)
pLYJ95	pLYJ36 plus <i>nirS</i> from <i>P. stutzeri</i>	This study
pLYJ97	pBBR1MCS-2 plus <i>gusA</i> from pK19mobGII	(7)
pLYJ104	pLYJ97 plus <i>nirTBECFDLGHJN</i> promoter region	This study
pLYJ113	pRU1 plus <i>nirN</i> from <i>M. magneticum</i>	This study
pLYJ124	pRU1 plus <i>nirN</i> from <i>P. stutzeri</i>	This study

Table S3 BlastP analysis results of denitrification genes in MTB and non-MTB using MSR-1 as a query.

Gene in MSR-1	Encoded gene product (aa, kDa, pI)	<i>M. magneticum</i> (e-value, similarity)	<i>M. magnetotacticum</i> (e-value, similarity)	Best hit in non-MTB (e-value, similarity)
<i>mgr_1052*</i>	Nitrite reductase, NirS (540, 59.26, 8.81)	<i>ambI395</i> (0, 91%) <i>amb4165</i> (0, 78%)	<i>magn03008451</i> (0, 91%)	<i>Dechlorosoma suillum</i> PS (0, 90%)
<i>mgr_1053</i>	NirT (199, 22.62, 8.38)	<i>ambI398</i> (6e-110, 89%)	<i>magn03008454</i> (2e-108, 91%)	<i>Endoriffia Persephone</i> (2e-93, 79%)
<i>mgr_1055</i>	NirB (341, 36.22, 8.41)	<i>ambI398</i> (3e-161, 81%)	<i>magn03008454</i> (1e-149, 77%)	<i>Endosymbiont of Riftia pachyptila</i> (2e-99, 67%)
<i>jn634764</i>	NirE (304, 32.12, 6.86)	<i>ambI400</i> (1e-91, 77%)	–	<i>Pectobacterium wasabiae</i> WPP163 (3e-85, 69%)
<i>mgr_0426</i>	NirC (104, 11.05, 7.83)	<i>ambI401</i> (4e-29, 73%)	<i>magn03008456</i> (2e-31, 76%)	<i>Dechloromonas aromatica</i> RCB (2e-30, 70%)
<i>mgr_0425</i>	NirF (387, 42.85, 6.27)	<i>ambI402</i> (0, 82%)	<i>magn03008457</i> (0, 82%)	<i>Thiobacillus denitrificans</i> (7e-179, 79%)
<i>mgr_0424</i>	NirD (149, 16.39, 5.22)	<i>ambI403</i> (2e-56, 74%)	<i>magn03008458</i> (6e-59, 77%)	<i>Pseudomonas aeruginosa</i> PAO1 (4e-47, 68%)
<i>mgr_0423</i>	NirL (165, 18.51, 8.97)	<i>ambI404</i> (2e-69, 77%)	<i>magn03008459</i> (5e-66, 75%)	<i>Dechloromonas aromatica</i> RCB (3e-54, 71%)
<i>mgr_0422</i>	NirG (148, 16.33, 5.41)	<i>ambI405</i> (7e-59, 73%)	<i>magn03008460</i> (3e-56, 72%)	<i>Beggiatoa</i> sp. PS (3e-61, 74%)
<i>mgr_0421</i>	NirH (161, 17.60, 9.29)	<i>ambI407</i> (2e-70, 80%)	<i>magn03008461</i> (3e-71, 78%)	<i>Rubrivivax gelatinosus</i> IL144 (5e-63, 71%)
<i>mgr_0420</i>	NirJ (375, 41.28, 7.16)	<i>I530431-1531552 bp</i> (2e-155, 72%)	–	<i>Dechloromonas aromatica</i> RCB (1e-75, 76%)
<i>mgr_0419*</i>	NirN (513, 56.40, 6.72)	<i>ambI408</i> (0, 83%)	<i>magn03008348</i> (0, 84%)	<i>Dechloromonas aromatica</i> RCB (0, 73%)

*indicate genes deleted.

REFERENCES

1. **Schübbe S, Williams T, Xie G, Kiss H, Brettin T, Martinez D, Ross C, Schüler D, Cox B, Nealson K, Bazylinski D. 2009.** Complete genome sequence of the chemolithoautotrophic marine *magnetotactic coccus* strain MC-1. *Appl. Environ. Microbiol.* **75**:4835-4852.
2. **Jüngst A, Wakabayashi S, Matsubara H, Zumft WG. 1991.** The *nirSTBM* region coding for cytochrome *cd₁*-dependent nitrite respiration of *Pseudomonas stutzeri* consists of a cluster of mono-, di-, and tetraheme proteins. *FEBS Lett.* **279**:205-209.
3. **Schultheiss D, Kube M, Schüler D. 2004.** Inactivation of the flagellin gene *flaA* in *Magnetospirillum gryphiswaldense* results in nonmagnetotactic mutants lacking flagellar filaments. *Appl. Environ. Microbiol.* **70**:3624-3631.
4. **Marx C, Lidstrom M. 2002.** Broad-host-range *cre-lox* system for antibiotic marker recycling in Gram-negative bacteria. *BioTechniques* **33**:1062-1067.
5. **Kovach ME, Elzer PH, Hill DS, Robertson GT, Farris MA, Roop RM, Peterson KM. 1995.** Four new derivatives of the broad-host-range cloning vector pBBR1MCS, carrying different antibiotic-resistance cassettes. *Gene* **166**:175-176.
6. **Katzen F, Becker A, Ielmini MV, Oddo CG, Ielpi L. 1999.** New mobilizable vectors suitable for gene replacement in gram-negative bacteria and their use in mapping of the 3' end of the *Xanthomonas campestris* pv. *campestris* *gum* operon. *Appl. Environ. Microbiol.* **65**:278-282.
7. **Li Y, Katzmann E, Borg S, Schüler D. 2012.** The periplasmic nitrate reductase Nap is required for anaerobic growth and involved in redox control of magnetite biomineralization in *Magnetospirillum gryphiswaldense*. *J. Bacteriol.* **194**:4847-4856.

CHAPTER 4

The oxygen sensor MgFnr controls magnetite biomineralization by regulation of denitrification in *Magnetospirillum gryphiswaldense*

4.1 ABSTRACT

The alphaproteobacterium *Magnetospirillum gryphiswaldense* and other magnetotactic bacteria (MTB) are capable of synthesizing magnetosomes only in suboxic conditions. However, the mechanism of the oxygen-dependent magnetite biomineralization has remained unknown. In *Escherichia coli* and other bacteria, Fnr (fumarate and nitrate reductase regulation) proteins are involved in controlling the switch between microaerobic and aerobic metabolism. Here we identified a magnetobacterial Fnr-like protein (MgFnr), which plays a role in regulating the transcription of denitrification genes in response to different oxygen concentrations. Deletion of *Mgfnr* not only resulted in decreased N₂ production due to reduced N₂O reductase activity, but also impaired magnetite biomineralization under microaerobic conditions in the presence of nitrate. Overexpression of MgFnr in the WT also caused the synthesis of smaller magnetite particles under anaerobic and microaerobic conditions in the presence of nitrate. These data suggest that proper expression of MgFnr is required for WT-like magnetosome synthesis, which is regulated by MgFnr itself and oxygen. Analyses of transcriptional *gusA* reporter fusions revealed that besides showing similar properties to Fnr proteins reported in other bacteria, MgFnr is involved in the repression of the transcription of denitrification genes *nor* and *nosZ* under aerobic conditions, possibly owing to several unique amino acid residues specific to MTB-Fnr. Overall, we show that the global oxygen regulator MgFnr is a genuine O₂ sensor involved in controlling expression of denitrification genes and thereby plays an indirect role in maintaining proper redox conditions required for magnetite biomineralization.

4.2 INTRODUCTION

Magnetotactic bacteria (MTB) use magnetosomes for orientation in the Earth's magnetic field to search for growth-favoring suboxic zones of stratified aquatic habitats (1). In the freshwater alphaproteobacterium *Magnetospirillum gryphiswaldense* (in the following referred to as MSR-1) and other MTB, magnetosomes are membrane-enveloped magnetic crystals of magnetite (Fe_3O_4) that are aligned in chains (1). Magnetite biomineralization is not only controlled by more than 30 specific genes encoded within a genomic magnetosome island (MAI) (2-4), but also genes located outside MAI are required for synthesis of WT-like magnetosomes (5, 6). Although the mechanism of biomineralization is not completely understood, it has been proposed that the biosynthesis of mixed-valence iron oxide magnetite [$\text{FeII(FeIII)}_2\text{O}_4$] occurs by coprecipitation of ferrous and ferric iron in supersaturating concentrations, which requires a balanced ratio of ferrous and ferric iron (7-9). In magnetospirilla, magnetosome formation is only induced at low oxygen tension, and maximum magnetosome yield was found under microaerobic conditions in the presence of nitrate, whereas aerobic conditions completely inhibit magnetite biomineralization (5, 10). However, it is unknown whether this aerobic repression is controlled by biological regulation, or alternatively, directly caused by chemical oxidation of iron ions within the cells. In addition, our recent work indicated that magnetite biomineralization in MSR-1 is linked to denitrification (5, 6). Deletion of *nap* genes encoding a periplasmic nitrate reductase not only abolished anaerobic growth and delayed aerobic growth in both nitrate and ammonium medium, but also severely impaired magnetite biomineralization and resulted in biosynthesis of fewer, smaller and irregular crystals during denitrification and microaerobic respiration (5). In addition, loss of the nitrite reductase gene *nirS* led to defective growth of cells, which synthesized fewer, smaller and irregular crystals during nitrate reduction (6). Transcriptional *gusA* fusions revealed that expression of *nap* is upregulated by oxygen, whereas other denitrification genes including *nirS*, *nor*, and *nosZ* display the highest expression under microaerobic conditions in the presence of nitrate.

In *Escherichia coli*, transcription of these nitrate and nitrite reductase genes is positively regulated by Fnr (fumarate and nitrate reductase regulation), a global anaerobic regulator under anaerobic or microaerobic conditions (11, 12). Fnr is a member of a superfamily of transcriptional sensors sharing sequence homology with the cyclic-AMP receptor class of

proteins (13). Like all members of this family, Fnr protein comprises a C-terminal DNA-binding domain involved in site-specific DNA recognition of target promoters, and an N-terminal sensory domain (14). In *E. coli*, the sensor domain contains five cysteines, four of them (Cys-20, 23, 29, and 122) are essential and bind either a $[4\text{Fe-4S}]^{2+}$ or a $[2\text{Fe-2S}]^{2+}$ cluster (15-17). Under anaerobic conditions, the Fnr protein is folded as a homodimer that contains one $[4\text{Fe-4S}]^{2+}$ cluster per monomer. The Fnr dimers are able to bind target promoters and regulate transcription. Exposure of the $[4\text{Fe-4S}]^{2+}$ clusters to oxygen results in its conversion to a $[2\text{Fe-2S}]^{2+}$ oxidized form, which triggers conformational changes and further induces the protein monomerization and prevents its binding to DNA (18-24).

In the metabolically versatile MTB so far no oxygen regulators have been identified, and it is unknown how growth metabolism and magnetite biomineralization are regulated in response to different oxygen concentrations. Here, we for the first time identified a putative oxygen sensor MgFnr protein and analyzed its role in magnetite biomineralization. We showed that the MgFnr protein is involved in regulating expression of all denitrification genes in response to different oxygen concentrations, and thus plays an indirect role in magnetosome formation during denitrification. Although sharing similar characteristics with Fnr of other bacteria, MgFnr is able to repress the transcription of denitrification genes (*nor* and *nosZ*) under aerobic conditions, possibly owing to several unique amino acid residues specific to MTB-Fnr.

4.3 MATERIALS AND METHODS

4.3.1 Bacterial strains and growth conditions

Bacteria strains and plasmids used in this study are shown in Table 4-S1. If not specified otherwise, *E. coli* strains were grown in lysogeny broth (LB) at 37°C, and MSR-1 strains were cultivated at 30°C in nitrate medium as described before (5). In ammonium medium, nitrate was substituted by 4 mM ammonium chloride. When necessary, antibiotics were used at the following concentrations: *E. coli*: tetracycline (Tc), 12 µg/ml, kanamycin (Km), 25 µg/ml, and gentamicin (Gm), 15 µg/ml; MSR-1: Tc, 5 µg/ml, Km, 5 µg/ml, and Gm, 30 µg/ml. When *E. coli* strain BW29427 was used as donor in conjugation, 300 µM diaminopimelic acid (DAP) was added.

Experiments for growth and magnetic response (C_{mag}) were monitored under microaerobic and anaerobic conditions in 250 ml flasks containing 100 ml media. For microaerobic conditions, flasks were sealed with butyl-rubber stoppers under a microaerobic gas mixture containing 2% O₂ and 98% N₂ before autoclaving. Anaerobic conditions were achieved by omitting oxygen from gas mixture. For aerobic conditions, strains were cultured in free gas exchange with air in 300 ml flasks containing 20 ml medium agitated at 200 rpm. Optical density (OD) and magnetic response (C_{mag}) were measured photometrically at 565 nm as previously described (25). For gas production assay, cells were inoculated and mixed with nitrate medium with 0.3% agar in oxygen gradient tubes and exposed to the air. The concentration of intracellular iron was measured by a modified ferrozine assay as described before (26).

4.3.2 Genetic and molecular biology techniques

Standard molecular and genetic techniques were carried out for DNA isolation, digestion, ligation, and transformation (27). All DNA products were sequenced using BigDye Terminator version 3.1 chemistry on an ABI 3700 capillary sequencer (Applied Biosystems, Darmstadt, Germany), and sequence data were analyzed with the software Vector NTI Advance[®] 11.5.1 (Invitrogen, Darmstadt, Germany). All oligonucleotide sequences used in this work are available if required.

4.3.3 Construction of a MSR-1 $\Delta Mgfnr$ deletion mutant

All PCRs were performed using Phusion polymerase (NEB). Enzymes, including restriction enzymes and T4 DNA ligase, were purchased from Fermentas. To generate the unmarked $\Delta Mgfnr$ deletion mutant, a modified *cre-lox* method was used as previously described (28). An about 2-kb downstream PCR fragment of *Mgfnr* was generated and cloned into NotI/EcoRI-digested pAL01 to obtain pLYJ106. The plasmid pLYJ106 was conjugationally integrated into the chromosome of MSR-1 and colonies screened positively by PCR for the presence of the kanamycin marker were designated as $\Delta Mgfnr$ -down strain. Subsequently, the plasmid pLYJ105 containing a 2-kb upstream fragment of *Mgfnr* was integrated into the chromosome of $\Delta Mgfnr$ -down strain by conjugation. After verified by screening PCR for the presence of kanamycin and gentamicin markers, the strain was designated $\Delta Mgfnr$ -up-down strain. The *lox*-mediated excision of *Mgfnr* was initiated by conjugational transformation of

pLYJ87 (6). Precise excision was further confirmed by PCR amplification and sequencing. The plasmid pLYJ87 was lost by successive cultures in fresh nitrate medium. Finally, this strain was designated $\Delta Mgfnr$ mutant.

For genetic complementation of $\Delta Mgfnr$ mutant, the *Mgfnr* gene with its own promoter region was ligated into Acc65I/SacII-digested pBBR1MCS-2, yielding pLYJ110. Subsequently, pLYJ110 was transformed into MSR-1 WT and $\Delta Mgfnr$ mutant by conjugation. The *Ecfnr* gene from *E. coli* K-12 was also hetero-complemented into $\Delta Mgfnr$ mutant and WT. The PCR fragment of *Ecfnr* from *E. coli* was digested with HindIII and XbaI and ligated into pLYJ36 to yield pLYJ153.

4.3.4 Heterologous transcomplementation of an *E. coli* $\Delta Ecfnr$ mutant

First, $\Delta Ecfnr$ mutant with kanamycin marker was excised with the *E. coli* Quick and Easy gene deletion kit (Gene Bridges) and the Bac modification kit (Gene Bridges), as reported in (29). This unmarked mutant was designated $\Delta Ecfnr$ mutant. To express MgFnr protein from MSR-1, *Mgfnr* was ligated into SmaI/XbaI-digested pBBR1MCS-2 to yield pLYJ132. Plasmid pLYJ132 was then transformed into $\Delta Ecfnr$ mutant. For transcomplementation analysis, strains were anaerobically grown in glucose minimal medium and lactate minimal medium (30).

4.3.5 Construction of different *Mgfnr* variants

Substitutions at amino acid positions 27, 34, 98, and 153 were created by site-directed mutagenesis. First, PstI-SpeI digested fragment for each of substitutions was cloned into pOR093 to create pLYJ141 (*Mgfnr*-N27D), pLYJ142 (*Mgfnr*-I34L), pLYJ143 (*Mgfnr*-D153E), and pLYJ144 (*Mgfnr*-L98H), respectively. The different MgFnr mutants were subsequently obtained by a two-step homologous recombination technique in the same manner as described previously (31). The *Mgfnr* variants were confirmed by PCR and sequencing.

4.3.6 Analysis of transcriptional *gusA* fusions

To obtain the transcriptional *Mgfnr-gusA* fusion plasmid, *Mgfnr* promoter region was cloned into Acc65I/HindIII-digested pLYJ97, designated as pLYJ109. To investigate the expression of *Mgfnr* under different conditions, β -glucuronidase activity was determined at 37°C as described before (5). Units were recorded as nanomoles of product formed per minute per mg protein. Triplicate assays were measured and the values reported were averaged by using at least two independent experiments.

4.3.7 Nitrate and nitrite concentration assay

WT and Δ *Mgfnr* strains were grown under microaerobic conditions in the presence of nitrate. 1 ml culture at different time points was taken to detect nitrate and nitrite concentration as described in (5). Duplicate assays were carried out and the values reported were measured in one representative experiment.

4.3.8 Mass spectrometry measurements of O₂ respiration and nitrate reduction

WT and Δ *Mgfnr* strains were grown under microaerobic conditions in the presence or absence of nitrate. The cells were centrifuged and resuspended in fresh ammonium medium. Then the suspension was placed in the measuring chamber (1.5 ml) of a mass spectrometer (model Prima δ B; Thermo Electron). The bottom of the chamber (Hansatech electrode type) was sealed by a Teflon membrane, allowing dissolved gases to be directly introduced through a vacuum line into the ion source of the mass spectrometer. The chamber was thermostated at 28°C, and the cell suspension was stirred continuously by a magnetic stirrer. For O₂ respiration measurement, air was sparged into the suspension before chamber closing. The consumption of oxygen by the cells was followed at m/e=32. For denitrification, the cells were sparged with Argon and nitrate reduction was measured using 2 mM K¹⁵NO₃ (CEA 97.4% ¹⁵N). NO, N₂O and N₂ concentrations were followed as a function of time.

4.3.9 TEM and crystal analysis

If not specified, MSR-1 WT and mutants were grown at 30°C under anaerobic or microaerobic conditions for 20 h, concentrated and adsorbed onto carbon-coated copper grids. Samples were viewed and recorded with a Morgagni 268 microscope (FEI, Eindhoven, Netherlands) at 80 kV. For magnetosome analysis, more than 300 crystals were characterized for each strain.

4.3.10 Sequence analysis

fnr genes were identified by BLASTP (<http://blast.ncbi.nlm.nih.gov/Blast.cgi>) homology searching in the genomes of MSR-1 (GenBank: CU459003.1), *Magnetospirillum magneticum* (GenBank AP007255.1), *Magnetospirillum magnetotacticum* (NCBI reference sequence NZ_AAAP00000000.1), *Magnetococcus marinus* (GenBank accession number CP000471.1), and *Desulfovibrio magneticus* strain RS-1 (GenBank accession number AP010904.1). ClustalW was used for sequence alignment. The identification of Fnr binding sites in the promoter regions of the different operons encoding denitrification enzymes were performed with the virtual footprint software (PRODORIC, <http://prodoric.tu-bs.de/vfp/index2.php>).

4.4 RESULTS

4.4.1 Deletion of *Mgfnr* impairs biomineralization during microaerobic denitrification

Using *E. coli* Fnr (hereafter referred to as EcFnr, GenBank accession no. AAC74416.1) as a query, we identified one putative Fnr protein, named MgFnr (Mgr_2553), encoded in the genome of MSR-1 (Fig. 4-1). MgFnr has a higher similarity to Fnr proteins from other magnetospirilla, including Amb4369 from *M. magneticum* strain and Magn03010404 from *M. magnetotacticum* (76% identity, 97% similarity), than to EcFnr (28% identity, 37% similarity). Nevertheless, the MgFnr contains all signatory features of the Fnr family proteins: a C-terminal helix-turn-helix DNA binding domain and an N-terminal sensory domain containing the four cysteines (C25, C28, C37, and C125) found to be essential in EcFnr (Fig. 4-1) (15).

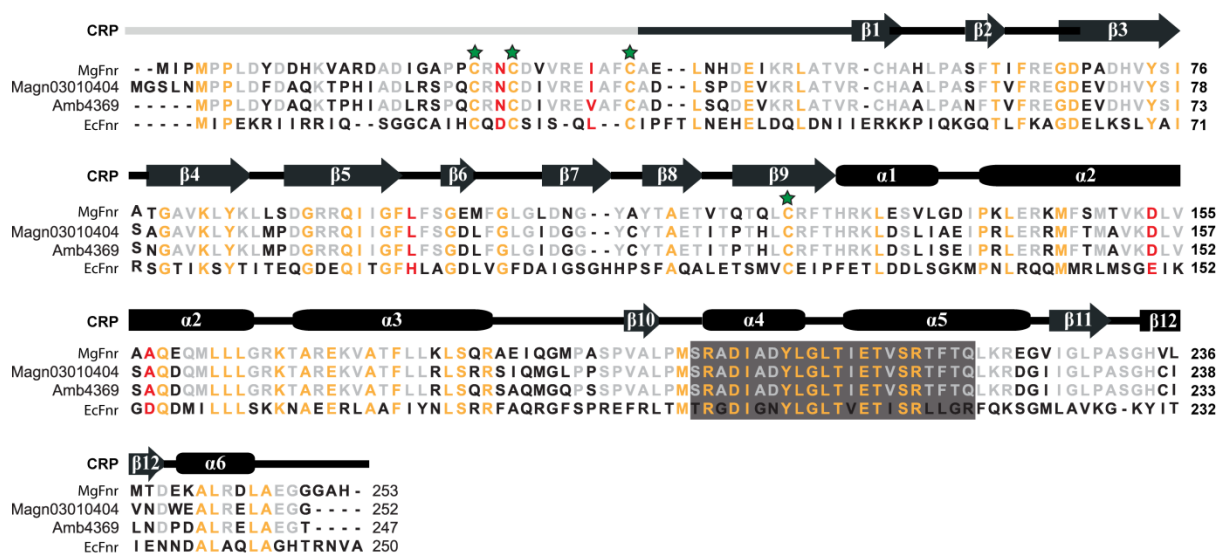


Fig. 4-1 Sequence alignment of Fnr proteins from different bacteria and proposed domain structure of one subunit of Fnr based on the structure of its homolog Crp from *E. coli*. Conserved residues are shown in orange while residues which are only conserved in magnetospirilla are indicated in gray. In MSR-1, the first 37 amino acids that are absent in Crp contain three of the four Cys (Cys25, Cys28, Cys37, and C125 indicated by green stars) which ligate the [4Fe-4S] cluster. Gray boxes indicate DNA-binding motif. Single residue changes which are capable to activate transcription of nitrate reductase genes under aerobic conditions in *E. coli* are shown in red. Amb4369 is from *M. magneticum* strain and Magn03010404 is from *M. magnetotacticum*.

We constructed an unmarked $\Delta Mgfnr$ mutant by a modified *cre-lox* based technique as described previously (28). In both microaerobic ammonium medium and anaerobic nitrate medium, $\Delta Mgfnr$ mutant cells displayed WT-like growth and magnetic response (C_{mag}) (data not shown) and produced WT-like magnetosome crystals (Fig. 4-2A and B) with similar crystal size (40.2 ± 15.3 nm versus 38.0 ± 15.8 nm in WT under anaerobic conditions; 30.0 ± 13.6 nm versus 29.9 ± 14.5 nm in WT in microaerobic ammonium medium). However, although the $\Delta Mgfnr$ mutant grew as the WT in microaerobic nitrate medium, C_{mag} values were slightly lower than those in the WT during the entire growth (Fig. 4-3). In agreement with this, $\Delta Mgfnr$ mutant cells contained smaller and aberrantly shaped particles in addition to particles with a WT-like size and appearance (Table 4-1, Fig. 4-2B). Transcomplementation of $\Delta Mgfnr$ strain with the WT allele ($\Delta Mgfnr$ +pLYJ110) restored magnetosome formation back to the WT level with similar crystal size (Fig. 4-2C, Table 4-1). However, WT overexpressing *Mgfnr* (WT+pLYJ110) produced smaller magnetite particles under anaerobic conditions (30.3 ± 15.1 nm, which was similar to that of WT in microaerobic nitrate medium) (Table 4-1, Fig. 4-S1) and also under microaerobic conditions in the presence of nitrate (23.5 ± 13.8 nm versus 30.5 ± 12.4 in WT). This indicated that MgFnr is involved in magnetosome formation during nitrate reduction, and that the expression level of MgFnr is crucial for proper magnetite biomineralization.

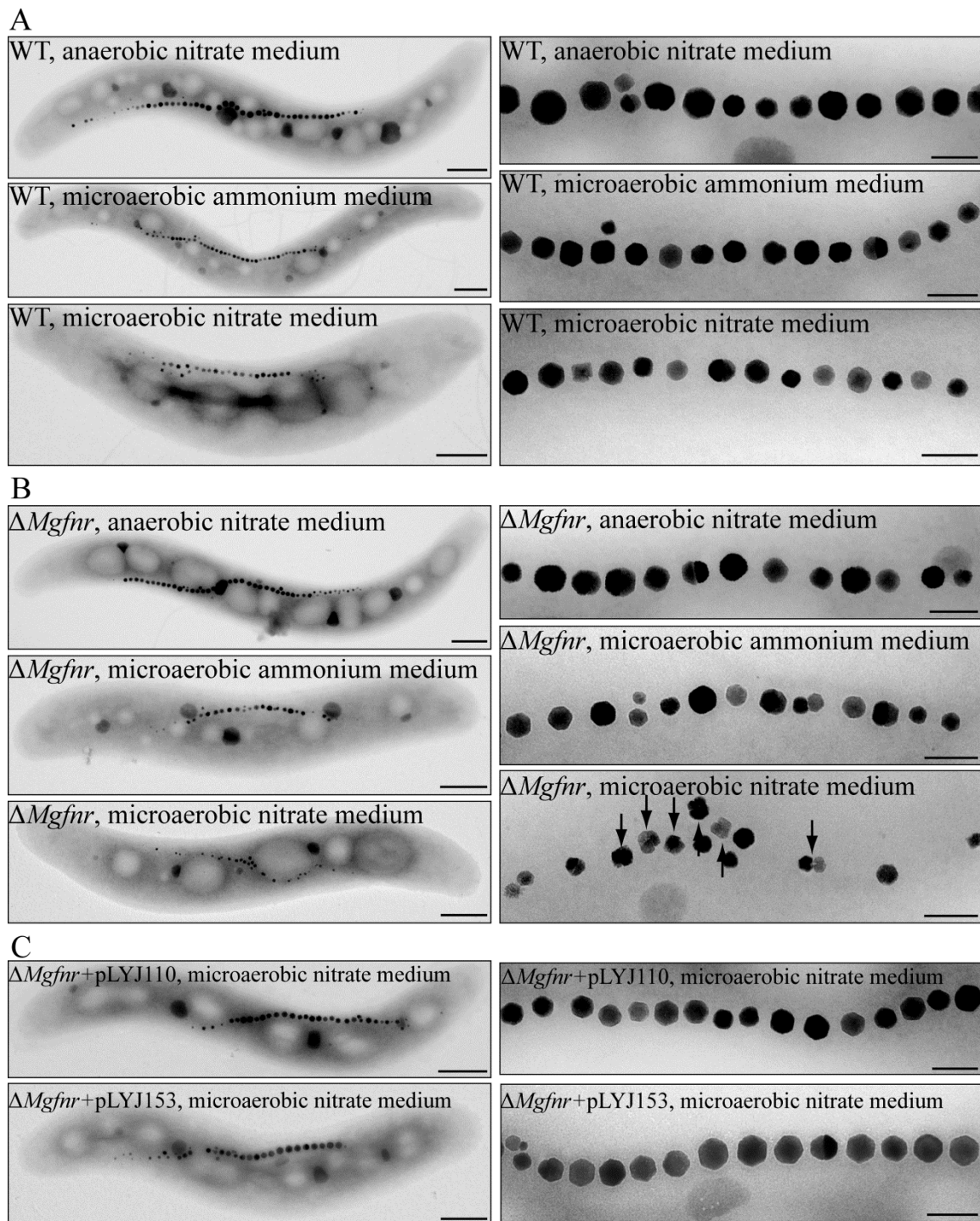


Fig. 4-2 Effects of *Mgfnr* deletions on magnetosome formation. (A) Left: TEM images of whole cells of WT (from top to bottom) in anaerobic nitrate medium, microaerobic ammonium medium, and microaerobic nitrate medium. Bar, 500 nm. Right: Closeup views of magnetosome crystals shown on the left. Bar, 100 nm. (B) Left: TEM images of whole cells of $\Delta Mgfnr$ mutant (from top to bottom) in anaerobic nitrate medium, microaerobic ammonium medium, and microaerobic nitrate medium. Bar, 500 nm. Right: Closeup views of magnetosome crystals shown on the left. Irregular shaped particles are indicated by black arrows. Bar, 100 nm. (C) Left: TEM images of $\Delta Mgfnr$ mutant complemented with plasmids pLYJ110 harboring *Mgfnr* gene and pLYJ153 harboring *Ecfnr* gene in microaerobic nitrate medium. Bar, 500 nm. Right: Closeup views of magnetosome crystals shown on the left. Bar, 100 nm.

Table 4-1 Crystal sizes in various strains under different conditions

Strain	Anaerobic nitrate medium	Microaerobic nitrate medium
WT	38.0 ± 15.8 nm	30.5 ± 12.4 nm
$\Delta Mgfnr$ mutant	40.2 ± 15.3 nm	21.9 ± 7.7 nm
WT+pLYJ110	30.3 ± 15.1 nm	23.5 ± 13.8 nm
$\Delta Mgfnr$ +pLYJ110	42.1 ± 21.9 nm	30.3 ± 22.3 nm
WT+pLYJ153	31.7 ± 18.7 nm	30.0 ± 21.6 nm
$\Delta Mgfnr$ +pLYJ153	40.9 ± 20.2 nm	31.3 ± 20.7 nm

4.4.2 In $\Delta Mgfnr$ expression patterns of denitrification genes are different from those in WT

Deletion of *Mgfnr* resulted in impaired magnetite biomineralization only under microaerobic conditions in the presence of nitrate, suggesting a potential link to nitrate reduction. In addition, in *E. coli* and other bacteria, Fnr was shown to upregulate the expression of denitrification genes under microaerobic or anaerobic conditions (30, 32). Our earlier studies on MSR-1 showed that all denitrification genes in the WT were regulated by oxygen, and except for *nap*, which was upregulated by oxygen, the highest expression of other denitrification genes coincided with conditions permitting maximum magnetosome formation (e.g., low oxygen tensions and the presence of nitrate) (5). Consistent with this, we found Fnr binding sites (TTGAN₆TCAA) in the promoter regions of all operons involved in denitrification (Table 4-S2). To gain insight whether these observed defects in magnetosome formation in $\Delta Mgfnr$ strain are indirectly caused by deregulation of denitrification genes, we analyzed the transcription of all denitrification genes by constructing *gusA* fusions in the $\Delta Mgfnr$ background (Table 4-2). In $\Delta Mgfnr$ strain, expression of *nap* was no longer upregulated by oxygen but displayed similar levels of β -glucuronidase activity under all tested conditions, which was higher than the maximum level in the WT. *nirS-gusA* showed a similar pattern as in WT, that is, it was upregulated by nitrate and downregulated by oxygen. However, an about 5-fold higher β -glucuronidase activity was measured under aerobic conditions compared to the WT. $\Delta Mgfnr$ mutant cells harboring the transcriptional *nor-gusA* reporter gene fusion exhibited a higher β -glucuronidase activity under microaerobic conditions in the presence of nitrate (416 U/mg) than in the absence of nitrate (151 U/mg), while it was lower than in the WT under the same conditions. However, oxygen did not inhibit the expression of *nor-gusA* in the $\Delta Mgfnr$ strain. Similarly, under microaerobic conditions, *nosZ-gusA* in the $\Delta Mgfnr$ strain also showed a higher β -glucuronidase activity in the presence of nitrate than in its absence, but compared to WT, expression of *nosZ-gusA*

under microaerobic conditions in the presence of nitrate was decreased. Again, highest expression of *nosZ* was observed under aerobic conditions in the presence of nitrate. Taken together, these data indicated that deletion of *Mgfnr* resulted in a different oxygen-dependent regulation of denitrification genes, suggesting that MgFnr is involved in controlling the expression of denitrification and the observed defects in magnetosome formation in Δ *Mgfnr* mutant might indirectly result from loss of proper regulation of denitrification genes.

Table 4-2 Effects of oxygen and nitrate on the expression of denitrification genes *nap*, *nirS*, *nor*, and *nosZ* in Δ *Mgfnr* mutant

Promoter	Microaerobic conditions		Aerobic conditions	
	+ NO ₃ ⁻	- NO ₃ ⁻	+ NO ₃ ⁻	- NO ₃ ⁻
<i>nap</i>	79.5 ± 41.8 ^a (16.2 ± 1.4) ^b	67.0 ± 29.4 (15.9 ± 0.8)	79.6 ± 38.5 (30.8 ± 2.6)	85.4 ± 30.9 (28.6 ± 2.8)
<i>nirS</i>	266.3 ± 10.8 (124.0 ± 5.5)	76.5 ± 28.3 (21.2 ± 9.6)	85.4 ± 23.0 (14.2 ± 7.9)	88.4 ± 54.9 (18.3 ± 7.8)
<i>nor</i>	414.7 ± 52.8 (762.8 ± 37.0)	150.9 ± 52.4 (221.5 ± 52.4)	559.7 ± 74.0 (204.4 ± 41.1)	493.4 ± 52.9 (151.1 ± 10.5)
<i>nosZ</i>	327.8 ± 32.9 (519.0 ± 43.4)	153.2 ± 62.5 (118.3 ± 33.3)	751.3 ± 76.1 (146.6 ± 34.7)	525.7 ± 53.6 (152.5 ± 21.9)

^a Values of β -glucuronidase activity are averages and standard deviations for at least two replicate cultures. Units are recorded as nanomoles of product formed per minute per mg protein.

^b Expression in the WT are shown in the “()” for comparison (5).

4.4.3 Decreased N₂ production in Δ *Mgfnr* mutant is due to lower N₂O reductase activity

We next monitored the overall denitrification of MSR-1 WT and Δ *Mgfnr* mutant by growing cells in deep slush agar (0.3%) tubes containing nitrate medium in which entrapped gas bubbles are indicative for N₂ production (5). We found that although deletion of *Mgfnr* did not cause any growth defects under all tested conditions, in WT culture many N₂ bubbles became visible after 24 h, while in Δ *Mgfnr* mutant only few bubbles were observed at any time of incubation, indicating that denitrification was reduced in this strain (Fig. 4-4A). In contrast, the Δ *Mgfnr* complemented strain (Δ *Mgfnr*+pLYJ110) generated bubbles after 24 h as the WT. We therefore wanted to dissect at which step(s) of denitrification N₂ production was affected. First, concentrations of nitrate and nitrite in microaerobic nitrate medium were measured during the entire growth of WT and Δ *Mgfnr* mutant to assess nitrate and nitrite reduction, which are catalyzed by Nap and NirS, respectively. As shown in Fig. 4-3, no significant difference between WT and Δ *Mgfnr* mutant was observed for reduction of nitrate and nitrite. Nitrate disappeared slightly faster in the Δ *Mgfnr* mutant than in the WT, but this

was not accompanied by an increased accumulation of nitrite. This meant that deletion of *Mgfnr* does not affect activities of the nitrate and nitrite reductase. We also measured the overall reduction of NO_3^- to N_2O and N_2O to N_2 by detecting the emission rate of respective reaction products in cell suspension at $\text{OD}_{565 \text{ nm}}$ of 1 with a gas-mass spectrometer (Table 4-3). For cultures grown in microaerobic ammonium medium, neither emission of N_2O nor N_2 was found in WT and the ΔMgfnr mutant, suggesting that the presence of nitrate is essential to activate denitrification. After growth in microaerobic nitrate medium, N_2O emission rates from nitrate were similar in WT and ΔMgfnr mutant (Table 4-3). As estimated by N_2 evolution, we found that N_2O reductase activity was very low in both strains compared to nitrate, nitrite, and NO reductase activities, since the rate for N_2O production from nitrate was 20-fold higher than the rate for N_2 production. Due to the low values and the detection limit of the gas-mass spectrometer, the standard deviation is quite critical for evaluation of significance of the N_2 emission values. However, in 8 independent experiments the N_2 emission rates appeared lower for ΔMgfnr strain than for the WT ($0.4 \mu\text{M}/\text{min}$ versus $0.7 \mu\text{M}/\text{min}$). In addition, we also tested oxygen reduction in both WT and ΔMgfnr mutant grown under microaerobic conditions by determining the consumption rate of oxygen in cell suspension with the gas-mass spectrometer. WT and ΔMgfnr mutant cells consumed oxygen at similar rates (Table 4-3), which indicated that MgFnr is not involved in regulation of O_2 respiration.

Table 4-3 Rates of N_2O and N_2 emission in WT and ΔMgfnr mutant after nitrate addition and rates of O_2 consumption during aerobic respiration

Culture (2% oxygen)	N_2O emission ($\mu\text{M}/\text{min}^{\text{a}}$)	N_2 emission ($\mu\text{M}/\text{min}$)	O_2 consumption ($\mu\text{M}/\text{min}$)
WT without nitrate	ND ^b	ND	50.7 ± 10.0
ΔMgfnr mutant without nitrate	ND	ND	44.0 ± 2.0
WT with nitrate	14.1 ± 2.0	0.7 ± 0.5	41.3 ± 2.0
ΔMgfnr mutant with nitrate	12.0 ± 2.0	0.4 ± 0.2	44.0 ± 4.7

^a The values (in μM per min for a cell suspension of $\text{OD}_{565 \text{ nm}}$ of 1) are the average of eight independent experiments. ^b ND: not detectable.

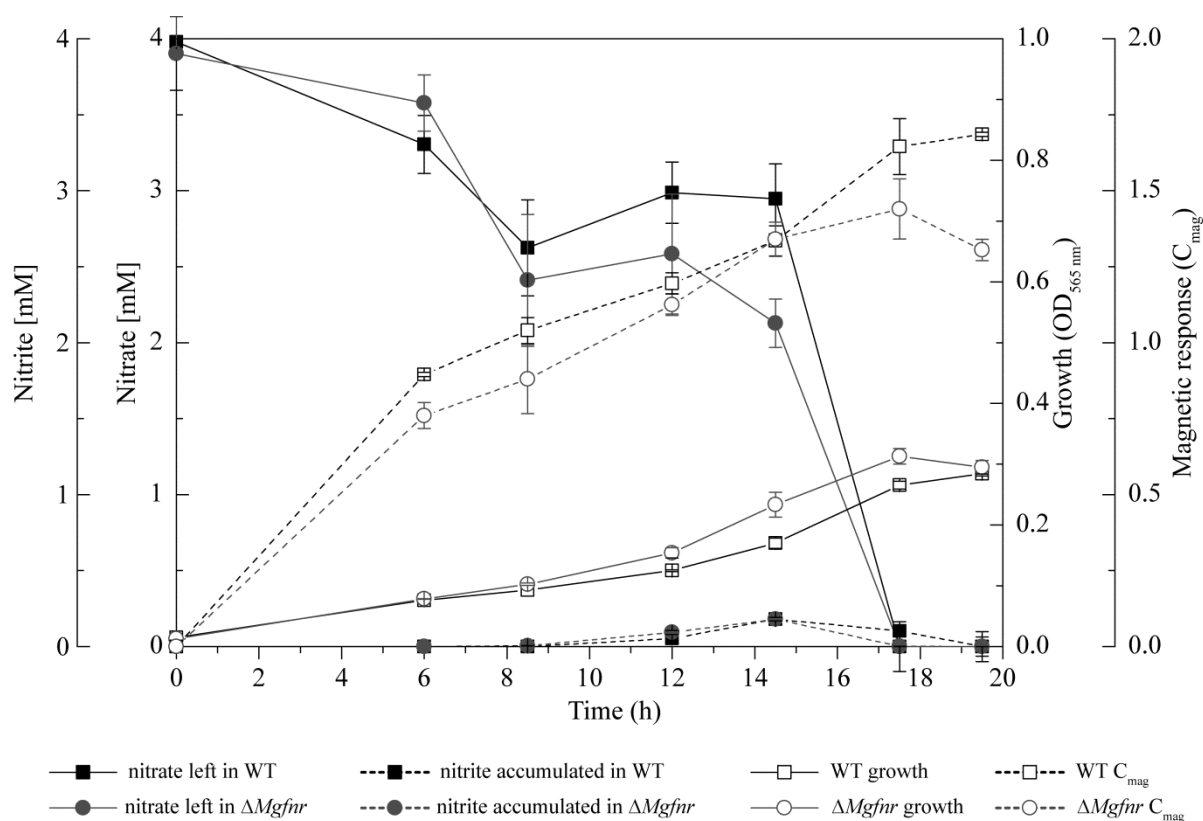


Fig. 4-3 Time courses of nitrate and nitrite utilization during microaerobic growth of WT and Δ Mgfnr mutant in nitrate medium.

4.4.4 Expression of *Mgfnr* is increased by oxygen and upregulated by itself

Under aerobic conditions, the expression of denitrification genes *nor* and *nosZ* was upregulated in the Δ Mgfnr mutant, which suggested that MgFnr might be also active as repressor under aerobic conditions. Therefore, we first asked if transcription of the *Mgfnr* gene itself is under oxygen-dependent regulation. WT cells expressing *Mgfnr-gusA* showed the lowest β -glucuronidase activity under microaerobic conditions in the absence of nitrate, while the presence of nitrate slightly increased microaerobic expression of *Mgfnr* (Fig. 4-4B). The expression of *Mgfnr* was induced approximately 4-fold in the presence of nitrate and more than 2-fold in the absence of nitrate under aerobic conditions relative to microaerobic conditions, which again suggested that MgFnr is likely active and acts as a repressor under aerobic conditions. In the Δ Mgfnr mutant, *Mgfnr-gusA* also exhibited the highest β -glucuronidase activity under aerobic conditions in the presence of nitrate. However, compared to WT under aerobic conditions, expression levels of *Mgfnr* in Δ Mgfnr mutant were significantly decreased, which indicated that expression of *Mgfnr* is upregulated not

only by oxygen, but also by MgFnr itself, as already suggested in *E. coli* (33). However, we failed to observe a putative Fnr binding site in the *Mgfnr* promoter region.

4.4.5 MgFnr can complement *E. coli* $\Delta Ecfnr$ mutant

All previous observations were pointing towards a scenario, in which MgFnr may also repress expression of denitrification genes under aerobic conditions, which however has never been reported for any Fnr protein from other bacteria. Therefore, the question arose as to whether MgFnr is a genuine oxygen-responsive regulator. Consequently, an *Ecfnr* deletion mutant $\Delta Ecfnr$ was transcomplemented with *Mgfnr*. As shown before (34), $\Delta Ecfnr$ cells displayed deficient anaerobic growth when nitrate was used as the sole electron acceptor on lactate minimal medium, whereas they grew to similar yields as the WT anaerobically growing on glucose medium (Fig. 4-4C). However, in the $\Delta Ecfnr$ +pLYJ132 strain which contained the WT-*Mgfnr* gene, anaerobic growth in the presence of nitrate was restored back to *E. coli* WT-like level, which demonstrated that MgFnr is also functional in *E. coli*. Vice versa, the MSR-1 $\Delta Mgfnr$ strain containing *Ecfnr* gene ($\Delta Mgfnr$ +pLYJ153) generated N₂ bubbles after 24 h (Fig. 4-4A), suggesting that EcFnr also functions in MSR-1. As shown in Fig. 4-2C and table 4-1, $\Delta Mgfnr$ +pLYJ153 strain containing *Ecfnr* again synthesized WT-like magnetite crystals. Under anaerobic conditions, overexpression of EcFnr resulted in a decrease in crystals size as overexpression of MgFnr does (Table 4-1, Fig. 4-S1). However, when EcFnr was overexpressed in MSR-1 WT under microaerobic conditions, magnetite crystals with WT size were formed, contrary to what was observed with overexpression of MgFnr. Altogether, our observations suggested that MgFnr is a genuine oxygen sensor and displays an equivalent *in vivo* function as EcFnr in *E. coli*, but some functions of the MgFnr might be slightly distinct from the EcFnr.

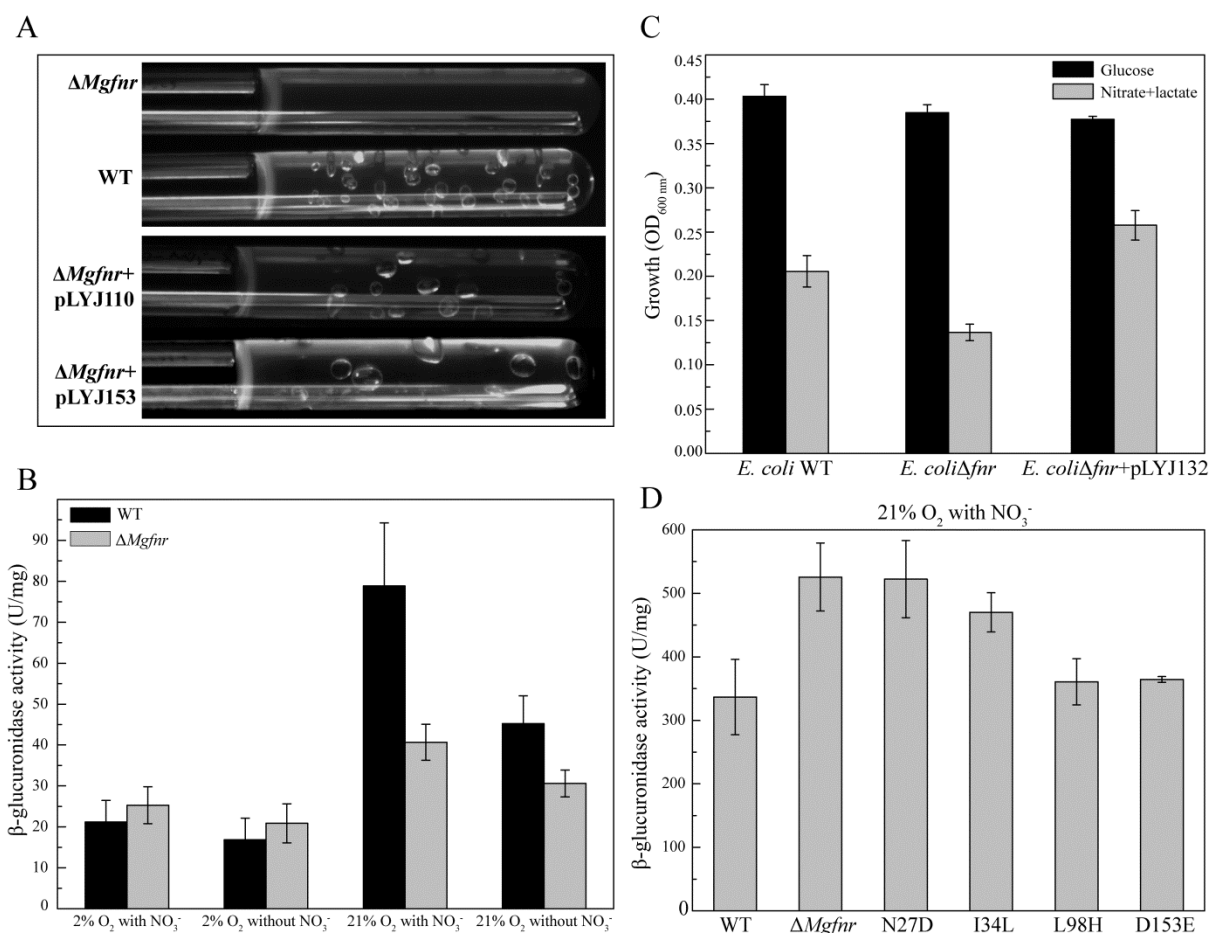


Fig. 4-4 (A) N₂ production in WT, Δ *Mgfnr* mutant, Δ *Mgfnr* mutant plus pLYJ110, and Δ *Mgfnr* mutant plus pLYJ153 cultures in oxygen gradient tubes with 0.3% agar. Δ *Mgfnr* mutant plus pLYJ110, and Δ *Mgfnr* mutant plus pLYJ153 cells contained respective *fnr* gene from MSR-1 and *E. coli*. (B) Transcription of *Mgfnr* promoter fused to *gusA* in both WT and Δ *Mgfnr* mutant under different conditions. Expression was measured by β -glucuronidase activity. Cultures were grown aerobically or microaerobically in nitrate and ammonium medium. (C) Heterologous transcomplementation of Δ *Ecfnr* mutant which contains with plasmid pLYJ132 which contains *Mgfnr*. Cultures were grown anaerobically in glucose minimal medium (black box) and lactate minimal medium (gray box). (D) Transcription of *nosZ* fused to *gusA* in *Mgfnr* variant strains under aerobic conditions in the presence of nitrate. Expression was measured by β -glucuronidase activity.

4.4.6 MgFnr mutations N27D and I34L increase expression of *nosZ* under aerobic conditions

In *E. coli*, it was observed that some single amino acid substitutions at positions not widely conserved among the Fnr family caused an increased stability of Fnr toward oxygen, and consequently, transcription of nitrate reductase genes became activated under aerobic conditions (21, 30, 35). As shown in Fig. 4-1, none of these reported amino acids in EcFnr (Asp-22, Leu-28, His-93, Glu-150, and Asp-154) is conserved in MgFnr (Asn-27, Ile-34, Leu-98, Asp-153, and Ala-157, respectively). However, the residues present in MgFnr are highly conserved among Fnr proteins from magnetospirilla except for MgFnr Ile-34 which is

replaced by Val in *M. magneticum* Fnr. This indicates that some functional difference might occur between Fnr proteins from magnetospirilla and *E. coli*. Therefore, to test whether these sequence differences affect the stability of MgFnr to oxygen, we constructed several *Mgfnr* mutants, in which single amino acids of MgFnr were substituted by those present in EcFnr (N27D, I34L, L98H, and D153E) (Fig. 4-1). With *nosZ* as an example, we measured β -glucuronidase activity of *nosZ-gusA* fusion in *Mgfnr* variant strains under different conditions. All MgFnr mutants exhibited decreased levels of *nosZ-gusA* (70%-90% of WT) expression in microaerobic nitrate medium (Fig. 4-S2). Under aerobic conditions, N27D and I34L strains showed high *nosZ-gusA* expression, similar to that in Δ *Mgfnr* mutant, whereas L98H and D153E displayed the lowest expression which was similar to the WT (Fig. 4-4D). We also investigated denitrification by N₂ bubble formation of *Mgfnr* variant strains in deep slush agar tubes. Hardly any N₂ was produced in all *Mgfnr* mutant strains (data not shown). All *Mgfnr* variant strains produced smaller magnetite particles and showed decreased iron concentrations and magnetic response (C_{mag} value) compared to the WT (Table 4-4, Fig. 4-S3). However, the differences to the WT were more pronounced in the N27D and I34L strains, whose phenotypes were similar to those observed in Δ *Mgfnr* mutant (Table 4-4). This suggested that Asn-27 and Ile-34, which are located near Cys-28 and Cys-37, play an important role in maintaining a functional MgFnr.

Table 4-4 Measurements of magnetic response (C_{mag}), iron content, and crystal size for various *Mgfnr* strains in microaerobic nitrate medium

Strain	Magnetic response (C_{mag})	Iron content (%)	Crystal size (nm)
WT	2.22 \pm 0.01	100	29.3 \pm 18.6
Δ <i>Mgfnr</i> mutant	1.78 \pm 0.03	76.0 \pm 0.06	20.7 \pm 15.9
MgFnrN27D	1.77 \pm 0.02	83.6 \pm 0.03	19.2 \pm 18.9
MgFnrI34L	1.83 \pm 0.02	74.2 \pm 0.07	21.3 \pm 18.2
MgFnrL98H	1.91 \pm 0.02	95.6 \pm 0.16	24.3 \pm 19.9
MgFnrD153E	1.93 \pm 0.03	85.8 \pm 0.14	23.6 \pm 19.4

4.5 DISCUSSION

Our previous findings have implicated denitrification to be involved in redox control of anaerobic and microaerobic magnetite biomineralization (5, 6). In *E. coli* and other bacteria the switch between aerobic and microaerobic respiration such as nitrate reduction is primarily controlled by the Fnr regulator (11, 12). In this study, we have characterized the effect of the

MgFnr protein on growth and magnetite biomineralization in MSR-1. Deletion of *Mgfnr* did not affect the growth yield, but impaired magnetosome formation under microaerobic conditions only in the presence of nitrate (i.e., when denitrification was active) but not in its absence. This implies that MgFnr might be involved in magnetite synthesis by regulation of denitrification genes, whereas expression of terminal oxidases for O₂ respiration is likely not under the control of MgFnr, similar to Fnr from *Shewanella oneidensis* (36). In fact, we found that neither the rates of oxygen consumption nor transcription of terminal oxidase genes (Y. Li and D. Schüler, unpublished data) displayed any difference between the WT and Δ *Mgfnr* mutant. The presence of putative Fnr binding sites in the promoter regions of all operons of denitrification further indicates that MgFnr is involved in controlling the transcription of denitrification genes in response to different oxygen concentrations. Consistent with this, transcription patterns of denitrification genes in Δ *Mgfnr* mutant were different from WT. For example, in the Δ *Mgfnr* strain the expression of *nap* was no longer upregulated by oxygen, expression of *nirS* was much higher under aerobic conditions than WT, and aerobic expression of *nor* and *nosZ* was no longer repressed but upregulated by oxygen. Furthermore, we failed to identify a putative Fnr protein encoded in the genome of the nondenitrifying magnetotactic bacteria *Ms. marinus* or *D. magneticus* strain RS-1, which also suggests that Fnr of MTB is likely only responsible to regulate genes encoding for denitrification, but not required for aerobic respiration. In addition, we also observed significantly decreased N₂ evolution in deep slush agar tubes in Δ *Mgfnr* mutant. This raised the question at which step(s) of denitrification is affected by the loss of MgFnr. We propose that this is not likely caused by the reduction steps from NO₃⁻ to N₂O based on the following observations: (i) The consumption rate of NO₃⁻ and NO₂⁻ did not decrease in Δ *Mgfnr* mutant; (ii) NO is lethal to the cells while no defective growth was found in Δ *Mgfnr* mutant, and no NO emission was observed during mass spectrometry experiments which also implies that the activity of NO reductase is not decreased; (iii) The N₂O emission rate after addition of nitrate was similar for Δ *Mgfnr* mutant and WT. Therefore, we conclude that loss of MgFnr affects the last step of denitrification, the reduction of N₂O to N₂. In agreement, the emission rate of N₂ was lower for Δ *Mgfnr* mutant than for the WT. However, we cannot exclude the possibility that loss of MgFnr has an impact on further pathways involved in biomineralization other than denitrification. For instance, we have previously shown that (i) besides acting as nitrate reductase, Nap also plays a role in redox control for magnetosome formation, (ii) nitrite reductase NirS is capable to oxidize ferrous iron to ferric iron for magnetite synthesis, and (iii) NO reductase Nor also participates in magnetosome formation

by yet unknown functions (5, 6). On the other hand, in the magnetotactic *Magnetovibrio blakemorei* strain MV-1 which is capable of anaerobic respiration with N_2O as electron acceptor, a putative periplasmic Fe(II) oxidase was identified and proposed as N_2O reductase NosZ (37), which suggests that N_2O reductase might be also involved in magnetite biomineralization by unknown functions. In addition, in $\Delta Mgfnr$ mutant the different phenotypes observed under anaerobic and microaerobic conditions in the presence of nitrate indicate that MgFnr plays a more important role in magnetite biomineralization when O_2 respiration and denitrification occur simultaneously. Our recent findings showed that maintaining a balance between aerobic respiration and denitrification is crucial for WT-like magnetite biomineralization (Y. Li and D. Schüler, unpublished data). In this case, MgFnr might provide the main contribution to mediate the expression of denitrification genes and therefore, poise the redox state for magnetosome formation.

Since deletion of *Mgfnr* altered oxygen-dependent regulation of denitrification genes under aerobic conditions, we hypothesized that MgFnr protein is active under aerobic conditions. Consistent with this, the expression of *Mgfnr* was upregulated by oxygen, which, however, was never reported for any Fnr protein from other bacteria. Studies on EcFnr mutants in *E. coli* have established the important role of a $[4Fe-4S]^{2+}$ cluster in regulating EcFnr activity, and some single amino acid substitutions at positions not conserved in the Fnr family led to increased stability of Fnr to oxygen and activated transcription of nitrate reductase genes under aerobic growing conditions (20, 21, 30, 35, 38). None of these reported amino acids of EcFnr are conserved in MgFnr, which might cause a more active MgFnr under aerobic conditions. Among them, Ans-27 and Ile-34 of MgFnr are located very closely to Cys-28 and Cys-37, two of the four cysteine residues that bind the $[4Fe-4S]^{2+}$ cluster (39, 40). An *E. coli* EcFnr mutant protein containing amino acid substitution at either of these two positions showed increased expression of an EcFnr-dependent *lac* promoter under aerobic conditions (30, 35, 38). In agreement with these observations, MgFnr mutants including N27D and I34L showed increased aerobic expression of *nosZ* promoter, suggesting that Ans-27 and Ile-34 of MgFnr are required for a functional MgFnr and likely play a role in maintaining the stability of $[4Fe-4S]^{2+}$ cluster. However, MgFnr was able to complement $\Delta Ecfnr$ mutant back to WT-like growth, which indicates that MgFnr also has the universal properties of EcFnr. Nonetheless, $\Delta Ecfnr$ mutant and $\Delta Mgfnr$ mutant displayed significant different phenotypes during anaerobic growth, such as a largely decreased growth yield in $\Delta Ecfnr$ mutant, but no defective growth in $\Delta Mgfnr$ mutant. These differences might be explained by different media

used for cultivation because in *E. coli* deletion of *Ecfnr* only resulted in growth defect in some minimal media (34) while there is no minimal medium available, which provides reliable growth for MSR-1. In addition, not only deletion of *Mgfnr* but also overexpression of *Mgfnr* in WT affected anaerobic and microaerobic magnetite biomineralization in the presence of nitrate and caused the synthesis of smaller magnetosome particles, which indicates that the balanced expression of MgFnr is crucial for WT-like magnetosome synthesis and the expression level is under precise control, be regulated by itself and oxygen. Therefore, MgFnr might play an important role in maintaining redox balance for magnetite synthesis by controlling the expression of denitrification genes, and thus the expression of MgFnr is required to be strictly regulated. On the other hand, since MgFnr serves as an activator for expression of denitrification genes (*nor* and *nosZ*) under microaerobic conditions while as a repressor on the same genes under aerobic conditions, it is proposed that other oxygen sensors involved in expression of *nor* and *nosZ* are regulated by MgFnr. For example, a NosR protein has been shown to be required to activate the transcription of *nos* gene in *Pseudomonas stutzeri* (41). However, our data cannot rule out the possibility that MgFnr is also regulated by other yet unknown proteins and that other genes involved in magnetosome formation is controlled by MgFnr.

In conclusion, we for the first time in a magnetotactic bacterium demonstrated that MgFnr is a genuine oxygen regulator and mediates anaerobic respiration. The expression of MgFnr is required to be precisely controlled, which is regulated by oxygen and MgFnr itself. In addition, MgFnr is also involved in regulation of magnetite biomineralization during denitrification, likely by controlling proper expression of denitrification genes. This allows the transcription to be adapted to changes in oxygen availability, and thus maintaining proper redox conditions for magnetite synthesis. Despite of general similarities with Fnr proteins from other bacteria, MgFnr is more insensitive to O₂ and further displays additional functions for aerobic conditions, which might result from some non-conserved amino acids.

Although oxygen is known to be a major factor affecting magnetite biomineralization for decades, the mechanism of this effect in MTB is still unknown. The common observation that magnetosomes are only synthesized under suboxic conditions raised the possibility of protein-mediated regulation of the biomineralization process. However, although MgFnr mediates oxygen-dependent regulation, its relatively subtle and indirect effects on magnetite biomineralization cannot account for the observed complete inhibition of magnetite

biosynthesis under aerobic conditions. In addition to a possible effect caused by directly perturbing the redox balance of iron ions required for magnetite synthesis, another level of genetic regulation may exist in MSR-1. Since MgFnr only affects expression of denitrification genes but not genes encoding O₂ respiration enzymes, magnetite biomineralization is also probably regulated by other unknown O₂ sensors. Therefore, further research on respiratory pathways in MTB is likely to gain further insights into the mechanism of oxygen-dependent regulation of biomineralization.

4.6 ACKNOWLEDGEMENTS

We thank Kirsten Jung, Ludwig-Maximilians-Universität München, for courtesy of strain $\Delta Ecfnr$ mutant. The China Scholarship Council (CSC) is greatly acknowledged for the financial support of Y. Li, and the Brazilian CNPq program for the financial support of K. T. Silva. This work was supported by grants DFG Schu1080/11-1 and 15-1, and HFSP RGP0052/2012 to D. Schüler.

4.7 REFERENCES

1. **Jogler C, Schüler D.** 2009. Genomics, genetics, and cell biology of magnetosome formation. *Annu. Rev. Microbiol.* **63**:501-521.
2. **Ullrich S, Kube M, Schübbe S, Reinhardt R, Schüler D.** 2005. A hypervariable 130-kilobase genomic region of *Magnetospirillum gryphiswaldense* comprises a magnetosome island which undergoes frequent rearrangements during stationary growth. *J. Bacteriol.* **187**:7176-7184.
3. **Murat D, Quinlan A, Vali H, Komeili A.** 2010. Comprehensive genetic dissection of the magnetosome gene island reveals the step-wise assembly of a prokaryotic organelle. *Proc. Natl. Acad. Sci. U. S. A.* **107**:5593-5598.
4. **Lohsse A, Ullrich S, Katzmann E, Borg S, Wanner G, Richter M, Voigt B, Schweder T, Schüler D.** 2011. Functional analysis of the magnetosome island in *Magnetospirillum gryphiswaldense*: the *mamAB* operon is sufficient for magnetite biomineralization. *PLoS One* **6**:e25561.
5. **Li YJ, Katzmann E, Borg S, Schüler D.** 2012. The periplasmic nitrate reductase Nap is required for anaerobic growth and involved in redox control of magnetite biomineralization in *Magnetospirillum gryphiswaldense*. *J. Bacteriol.* **194**:4847-4856.

6. **Li YJ, Bali S, Borg S, Katzmann E, Ferguson SJ, Schüler D.** 2013. Cytochrome *cd*₁ nitrite reductase NirS is involved in anaerobic magnetite biomineralization in *Magnetospirillum gryphiswaldense* and requires NirN for proper *d*₁ heme assembly. *J. Bacteriol.* **195**:4297-4309.
7. **Mann S, Sparks NHC, Board RG.** 1990. Magnetotactic bacteria: microbiology, biomineralization, palaeomagnetism and biotechnology. *Adv. Microbiol. Physiol.* **31**:125-181.
8. **Faivre D, Agrinier P, Menguy N, Zuddas P, Pachana K, Gloter A, Laval J, Guyot F.** 2004. Mineralogical and isotopic properties of inorganic nanocrystalline magnetites. *Geochim. Cosmochim. Acta* **68**:4395-4403.
9. **Faivre D, Böttger LH, Matzanke BF, Schüler D.** 2007. Intracellular magnetite biomineralization in bacteria proceeds by a distinct pathway involving membrane-bound ferritin and an iron(II) species. *Angew. Chem. Int. Ed. Engl.* **46**:8495-8499.
10. **Heyen U, Schüler D.** 2003. Growth and magnetosome formation by microaerophilic *Magnetospirillum* strains in an oxygen-controlled fermentor. *Appl. Microbiol. Biotechnol.* **61**:536-544.
11. **Uden G, Becker S, Bongaerts J, Holighaus G, Schirawski J, Six S.** 1995. O₂-sensing and O₂-dependent gene regulation in facultatively anaerobic bacteria. *Arch. Microbiol.* **164**:81-90.
12. **Bueno E, Mesa S, Bedmar EJ, Richardson DJ, Delgado MJ.** 2012. Bacterial adaptation of respiration from oxic to microoxic and anoxic conditions: redox control. *Antioxid. Redox Signal.* **16**:819-852.
13. **Shaw DJ, Rice DW, Guest JR.** 1983. Homology between Cap and Fnr, a regulator of anaerobic respiration in *Escherichia coli*. *J. Mol. Biol.* **166**:241-247.
14. **Spiro S, Guest JR.** 1990. FNR and its role in oxygen-regulated gene expression in *Escherichia coli*. *FEMS Microbiol. Rev.* **6**:399-428.
15. **Green J, Sharrocks AD, Green B, Geisow M, Guest JR.** 1993. Properties of FNR proteins substituted at each of the five cysteine residues. *Mol. Microbiol.* **8**:61-68.
16. **Khoroshilova N, Popescu C, Munck E, Beinert H, Kiley PJ.** 1997. Iron-sulfur cluster disassembly in the FNR protein of *Escherichia coli* by O₂: [4Fe-4S] to [2Fe-2S] conversion with loss of biological activity. *Proc. Natl. Acad. Sci. U. S. A.* **94**:6087-6092.
17. **Kiley PJ, Beinert H.** 1998. Oxygen sensing by the global regulator, FNR: the role of the iron-sulfur cluster. *FEMS Microbiol. Rev.* **22**:341-352.
18. **Lazazzera BA, Beinert H, Khoroshilova N, Kennedy MC, Kiley PJ.** 1996. DNA binding and dimerization of the Fe-S-containing FNR protein from *Escherichia coli* are regulated by oxygen. *J. Biol. Chem.* **271**:2762-2768.

19. **Crack J, Green J, Thomson AJ.** 2004. Mechanism of oxygen sensing by the bacterial transcription factor fumarate-nitrate reduction (FNR). *J. Biol. Chem.* **279**:9278-9286.
20. **Khoroshilova N, Beinert H, Kiley PJ.** 1995. Association of a polynuclear iron-sulfur center with a mutant FNR protein enhances DNA binding. *Proc. Natl. Acad. Sci. U. S. A.* **92**:2499-2503.
21. **Lazazzera BA, Bates DM, Kiley PJ.** 1993. The activity of the *Escherichia coli* transcription factor FNR is regulated by a change in oligomeric state. *Genes Dev.* **7**:1993-2005.
22. **Popescu CV, Bates DM, Beinert H, Munck E, Kiley PJ.** 1998. Mössbauer spectroscopy as a tool for the study of activation/inactivation of the transcription regulator FNR in whole cells of *Escherichia coli*. *Proc. Natl. Acad. Sci. U. S. A.* **95**:13431-13435.
23. **Jordan PA, Thomson AJ, Ralph ET, Guest JR, Green J.** 1997. FNR is a direct oxygen sensor having a biphasic response curve. *FEBS Lett.* **416**:349-352.
24. **Sutton VR, Mettert EL, Beinert H, Kiley PJ.** 2004. Kinetic analysis of the oxidative conversion of the $[4\text{Fe-4S}]^{2+}$ cluster of FNR to a $[2\text{Fe-2S}]^{2+}$ Cluster. *J. Bacteriol.* **186**:8018-8025.
25. **Schüler D, Baeuerlein E.** 1998. Dynamics of iron uptake and Fe_3O_4 biomineralization during aerobic and microaerobic growth of *Magnetospirillum gryphiswaldense*. *J. Bacteriol.* **180**:159-162.
26. **Viollier E, Inglett PW, Hunter K, Roychoudhury AN, Van Cappellen P.** 2000. The ferrozine method revisited: Fe(II)/Fe(III) determination in natural waters. *Appl. Geochem.* **15**:785-790.
27. **Sambrook J, Russel D.** 2001. *Molecular cloning: A laboratory manual*, vol. 3rd ed. Cold Spring Harbor Laboratory Press, Cold Spring Harbor, New York.
28. **Ullrich S, Schüler D.** 2010. Cre-lox-based method for generation of large deletions within the genomic magnetosome island of *Magnetospirillum gryphiswaldense*. *Appl. Environ. Microbiol.* **76**:2349-2444.
29. **Heermann R, Zeppenfeld T, Jung K.** 2008. Simple generation of site-directed point mutations in the *Escherichia coli* chromosome using Red^R/ET^R Recombination. *Microb. Cell Fact.* **7**:14.
30. **Kiley PJ, Reznikoff WS.** 1991. Fnr mutants that activate gene-expression in the presence of oxygen. *J. Bacteriol.* **173**:16-22.
31. **Raschdorf O, Müller FD, Posfai M, Plitzko JM, Schüler D.** 2013. The magnetosome proteins MamX, MamZ and MamH are involved in redox control of magnetite biomineralization in *Magnetospirillum gryphiswaldense*. *Mol. Microbiol.* **89**:872-886.

32. **Cruz-Garcia C, Murray AE, Rodrigues JLM, Gralnick JA, McCue LA, Romine MF, Löffler FE, Tiedje JM.** 2011. Fnr (EtrA) acts as a fine-tuning regulator of anaerobic metabolism in *Shewanella oneidensis* MR-1. *BMC Microbiol.* **11**:64.
33. **Gerasimova AV, Rodionov DA, Mironov AA, Gelfand AS.** 2001. Computer analysis of regulatory signals in bacterial genomes. Fnr binding sites. *Mol. Biol.* **35**:853-861.
34. **Lambden PR, Guest JR.** 1976. Mutants of *Escherichia coli* K12 unable to use fumarate as an anaerobic electron acceptor. *J. Gen. Microbiol.* **97**:145-160.
35. **Bates DM, Popescu CV, Khoroshilova N, Vogt K, Beinert H, Munck E, Kiley PJ.** 2000. Substitution of leucine 28 with histidine in the *Escherichia coli* transcription factor FNR results in increased stability of the [4Fe-4S]²⁺ cluster to oxygen. *J. Biol. Chem.* **275**:6234-6240.
36. **Zhou G, Yin J, Chen H, Hua Y, Sun L, Gao H.** 2013. Combined effect of loss of the *caa3* oxidase and Crp regulation drives *Shewanella* to thrive in redox-stratified environments. *ISME J.* **7**:1752-1763.
37. **Bazylinski DA, Williams T.** 2006. Ecophysiology of magnetotactic bacteria. In D. Schüler (ed.), *Magnetoreception and magnetosomes in bacteria*. SpringerVerlag, Heidelberg.
38. **Bates DM, Lazazzera BA, Kiley PJ.** 1995. Characterization of FNR* mutant proteins indicates two distinct mechanisms for altering oxygen regulation of the *Escherichia coli* transcription factor FNR. *J. Bacteriol.* **177**:3972-3978.
39. **Sharrocks AD, Green J, Guest JR.** 1990. *In vivo* and *in vitro* mutants of FNR the anaerobic transcriptional regulator of *E. coli*. *FEBS Lett.* **270**:119-122.
40. **Melville SB, Gunsalus RP.** 1990. Mutations in *fnr* that alter anaerobic regulation of electron transport-associated genes in *Escherichia coli*. *J. Biol. Chem.* **265**:18733-18736.
41. **Wunsch P, Zumft WG.** 2005. Functional domains of NosR, a novel transmembrane iron-sulfur flavoprotein necessary for nitrous oxide respiration. *J. Bacteriol.* **187**:1992-2001.

4.8 SUPPLEMENTAL MATERIALS

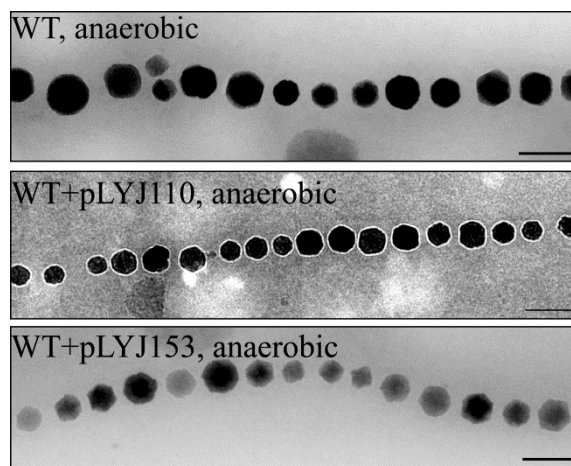


Fig. 4-S1 Magnetosome formation in WT overexpressing MgFnr. Plasmid pLYJ110 and pLYJ153 contains *fmr* gene from MSR-1 and *E. coli*, respectively. Cells were grown in anaerobic nitrate medium. Bar, 100 nm.

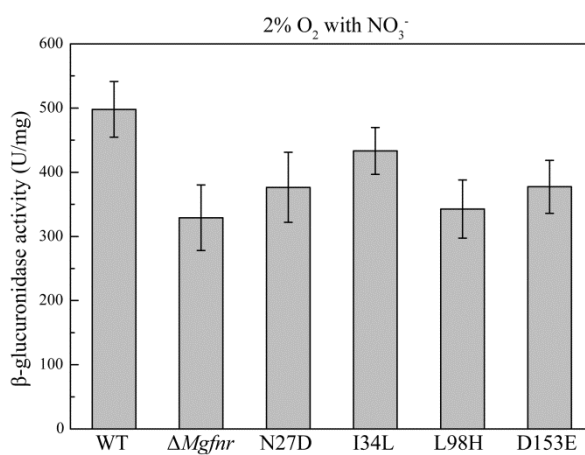


Fig. 4-S2 Transcription of *nosZ* fused to *gusA* in *Mgfnr* variant strains under microaerobic conditions in the presence of nitrate. Expression was measured by β -glucuronidase activity.

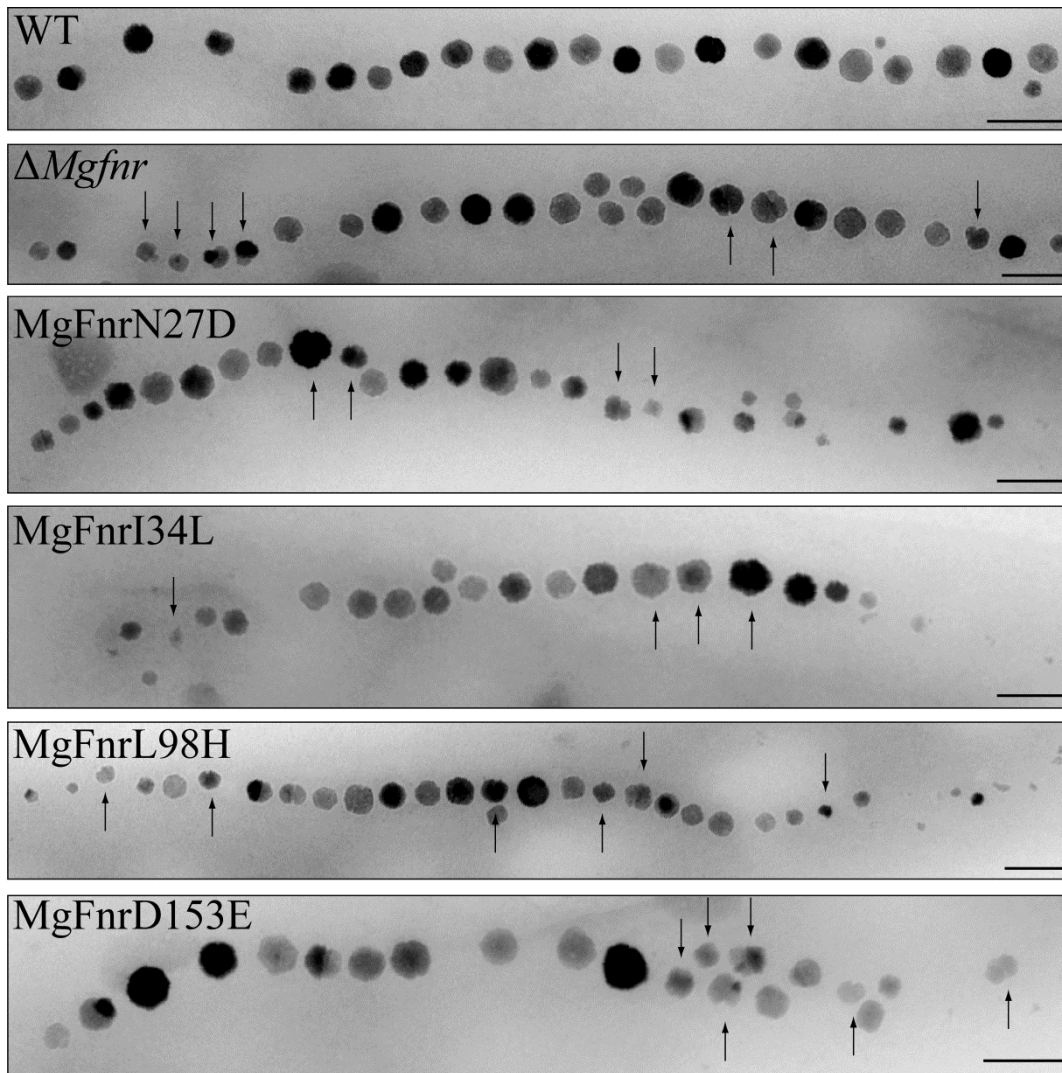


Fig. 4-S3 Magnetosome formation in different *Mgfnr* variant strains. Cells were grown in microaerobic nitrate medium. Bar, 100 nm. Irregular shaped particles are indicated by black arrows.

Table 4-S1 Bacterial strains and plasmids used in this work

Strain or plasmid	Important feature (s)	Source or reference
Strain		
<i>E. coli</i> strain DH5 α	F ['] Φ 80dlacZ Δ M15 Δ (<i>lacZYA-argF</i>)U169 <i>deoR recA1 endA1 hsdR17</i> (r_{k^-} , m_k^+) <i>phoA supE44 λ- thi-1 gyrA96 relA1</i>	Invitrogen
<i>E. coli</i> strain BW29427	<i>dap</i> auxotroph derivative of <i>E. coli</i> strain B2155	K. Datsenko and B. L. Wanner, unpublished
Δ <i>Ecfnr</i> mutant	<i>E. coli</i> K-12 substr. MG1655	K. Jung, unpublished
MSR-1 WT	Wild type R3/S1, but Ri^r , Sm^r	(1)
Δ <i>Mgfnr</i>	R3/S1 Δ <i>Mgfnr</i>	This study
MgFnrN27D	R3/S1 MgFnrN27D mutants	This study
MgFnrI34L	R3/S1 MgFnrI34L mutant	This study
MgFnrL98H	R3/S1 MgFnrL98H mutant	This study
MgFnrD153E	R3/S1 MgFnrD153E mutant	This study
Plasmid		
pBBR1MCS-2	Km^r , mobilizable broad-host-range vector	(2)
pK19mobGII	-	(3)
pAL01	Km^r , pK19mobGII vector (Km^r , pMB-1 replicon, <i>gusA</i> , <i>lacZ</i>) containing a 2 kb fragment upstream of <i>mgr4019</i>	(4)
pAL02/2	Gm^r , pT18mob2 vector containing a 2 kb fragment downstream of <i>mgr4019</i>	(4)
pLYJ87	pBBR1MCS-2 plus <i>nirS</i> promoter and <i>cre</i> fusion	(5)
pLYJ97	pBBR1MCS-2 plus <i>gusA</i> from pK19mobGII	(6)
pOR093	<i>mamX</i> CXXCH (65,104)->AXXAH, pK19mobGII derivative, Km^r	(7)
pLYJ105	pAL02/2 plus <i>Mgfnr</i> 2-kb upstream region	This study
pLYJ106	pAL01 plus <i>Mgfnr</i> 2-kb downstream region	This study
pLYJ109	pLYJ97 plus <i>Mgfnr</i> promoter region	This study
pLYJ110	pBBR1MCS-2 plus <i>Mgfnr</i> with its own promoter region	This study
pLYJ132	pBBR1MCS-2 plus <i>Mgfnr</i>	This study
pLYJ141	pOR093 plus <i>MgfnrN27D</i>	This study
pLYJ142	pOR093 plus <i>MgfnrI34L</i>	This study
pLYJ143	pOR093 plus <i>MgfnrD153E</i>	This study
pLYJ144	pOR093 plus <i>MgfnrL98H</i>	This study
pLYJ153	pLYJ36 plus <i>Ecfnr</i>	This study

Table 4-S2 Detection of Fnr binding sites in the upstream regions of *nap*, *nirS*, *nor*, and *nosZ*. The putative Fnr binding sites in the promoter regions are indicated in yellow.

<p>>MGR_4000_5' <i>nap</i> operon ATGTGGACCACAATCCCAAGACCGCCGAGATCGCCCGCCATCATCGGCCTGAGTCGCGGCCT CAACCTGGAAGTGGTGGCCGAGGGCTGCGAGATCGCCGCCATATCCAGTTCCTCAAGGATAAT GGCTGCGACACTGTGCAGGGTTCTTCTATTCCCGACCGGTTCCGGCAGAGCAATTCCAGGCCA TGCTGGCCGATGGTTTCTGCGCGGCCAAGCCTGAGCGGCTAAATCACCAATCACTGATATTTG AATAACCAAGTAACGGGGTCGAAAAGACCCTGCTTACTGTGTGGTCTTCTTGACCAAAATCAA ATGCGATTCCGACCGATGGGTCCACTCTGGCGGTGCCGGCTCTCCGTTCCGGAAGGCCTGCGA TTACGGGGCCGTTATG</p>
<p>>MGR_1052_5' <i>nirS</i> CCCCGAACAGGGACGCCCCAGTATTTTCATTTTGGACAGCCGGCTGAACAGTGACTGATTGGA AGCCATGGCTTTAACCCCGAGGGTCTCCTTTTATTCCGGCATTATGCGCCTTGTAACACGCC CCCTAGACCTGAACTTGACGTTGGACAAACCGTCACCGCCAATCACGGCCAGTGCCCAGACCCT ATCCCGACCTGCCTGTTGGACTTTGTGACATTTGGTCAATTTGGCTTTGACGCATCAAATGCTGAT GTTCGCTGCCGATGACTTTTCGATCGCCTATTTGACTTTGGTTAAAGTCGCTGGCCGACCAAGC GCCAAGGTGGCCCCACTCGATACCGGTGCTCTCAAAGGGGGGAGCGGAGCGATCATTATCAA GTGGAGGTAAAGG</p>
<p>>MGR_3484_5' <i>nor</i> operon GGGCCGATCTTGGCCGCCAGACTGGCCGGCCCCCAGCCGATCTCATCGGCGAACGCGCCCAATC CCAACACTACCACAGATAGACGATGACCAGCGGCAGCCATCGCATCAGCCCAAAGCCCGCCG GTCCCACCATCAGTGGGATGACGCTGTCGTCCTGACCGGTTCCGGCGGTGCCATGGCTTGCGCAT GGGCGGCATTTTCGCCGGTGACGCCCGCTTTGTCTCGGTCTTTTCGACACCAGCTTGACCAACGTT AAAGCTGACCAATCGTCTGGGTCATAGGGTCATGGTGACGGGGGAGCCCAAGGTTCCC GCGTGTGAGTTCAGGGTGCACACCAGCGGGGGGAGTTTCCGCGGTGGGTTGATCTCAAACCCTTGAA ACCCTTAGGAGCGACC</p>
<p>>MGR_2761_5' <i>nosZ</i> CCCAGCAGATCAAGGGCGGCAGCCATGGTTCGACAATGCGGTTCGGGCAGACGTCGGGGCAGAAG GTGTAGCCGAAGGCCATCATCCGCACCTTGCCTTGAAGCTTTCGTCATTGACCCGCTTGCCGTC GTGGGTTTCCAGCAGGAAACGGCCTGAAAACCTCTGGGCTTGTGCGGGCAGTGCCGTCAAAGCC AGGGCGCCAGCCAGCATCAGGGAACCGAGCTTCATCACGTGCACTCCGCTTGCCGTCATCGTTG AAGGCAGTGAAGCAGATCACCGTTTCACGCGACTTGATCAAGGTCACGGCTGGGTCATTAGCGG GCGCGCATGTTTGTGGCGAAGTGTGGGTAACCTCTGTCCCCTTTTAAACAGAAACAAGGTGGG GAAAATGAATCGTACA</p>

REFERENCES

1. **Schultheiss D, Kube M, Schüler D.** 2004. Inactivation of the flagellin gene *flaA* in *Magnetospirillum gryphiswaldense* results in nonmagnetotactic mutants lacking flagellar filaments. *Appl. Environ. Microbiol.* **70**:3624-3631.
2. **Kovach ME, Elzer PH, Hill DS, Robertson GT, Farris MA, Roop RM, Peterson KM.** 1995. Four new derivatives of the broad-host-range cloning vector pBBR1MCS, carrying different antibiotic-resistance cassettes. *Gene* **166**:175-176.
3. **Katzen F, Becker A, Ielmini MV, Oddo CG, Ielpi L.** 1999. New mobilizable vectors suitable for gene replacement in gram-negative bacteria and their use in mapping of the 3' end of the *Xanthomonas campestris* pv. *campestris* gum operon. *Appl. Environ. Microbiol.* **65**:278-282.

4. **Lohsse A, Ullrich S, Katzmann E, Borg S, Wanner G, Richter M, Voigt B, Schweder T, Schüler D.** 2011. Functional analysis of the magnetosome island in *Magnetospirillum gryphiswaldense*: the *mamAB* operon is sufficient for magnetite biomineralization. *PLoS One* **6**:e25561.
5. **Li YJ, Bali S, Borg S, Katzmann E, Ferguson SJ, Schüler D.** 2013. Cytochrome *cd*₁ nitrite reductase NirS is involved in anaerobic magnetite biomineralization in *Magnetospirillum gryphiswaldense* and requires NirN for proper *d*₁ heme assembly. *J. Bacteriol.* **195**:4297-4309.
6. **Li YJ, Katzmann E, Borg S, Schüler D.** 2012. The periplasmic nitrate reductase Nap is required for anaerobic growth and involved in redox control of magnetite biomineralization in *Magnetospirillum gryphiswaldense*. *J. Bacteriol.* **194**:4847-4856.
7. **Raschdorf O, Müller FD, Posfai M, Plitzko JM, Schüler D.** 2013. The magnetosome proteins MamX, MamZ and MamH are involved in redox control of magnetite biomineralization in *Magnetospirillum gryphiswaldense*. *Mol. Microbiol.* **89**:872-886.

CHAPTER 5

The terminal oxidase *cbb*₃ functions as an O₂ sensor to maintain redox balance for magnetite biomineralization in *Magnetospirillum gryphiswaldense*

5.1 ABSTRACT

Magnetosomes of many magnetotactic bacteria consist of membrane-enveloped magnetite crystals, which are synthesized only under suboxic conditions. However, the mechanism of the oxygen-dependent magnetite biomineralization is still unclear. Here, we set out to investigate the role of oxygen as well as aerobic respiration in metabolism and magnetite biomineralization. Like most bacteria, the alphaproteobacterium *Magnetospirillum gryphiswaldense* possesses multiple terminal oxidases, including two heme-copper oxidases *aa*₃ and *cbb*₃ and a *bd*-type quinol oxidase. In addition to denitrification pathway, *M. gryphiswaldense* also contains two different branches of respiration chains for oxygen reduction. One is achieved by the quinol oxidase *bd*, which accepts electrons directly from quinol, while the other is to transport electrons via cytochrome *bc*₁-*c-cbb*₃. However, the *aa*₃ oxidase has no physiological significance under test conditions. Aerobic respiration is a prerequisite for microaerobic denitrification, and loss of both oxidases *cbb*₃ and *bd* completely abolished microaerobic and aerobic growth even in the presence of nitrate. While loss of *bd* oxidase had no effects on growth and magnetosome synthesis, inactivation of *cbb*₃ oxidase caused pleiotropic effects under microaerobic conditions in the presence of nitrate. In addition to the incapability of co-occurrence of denitrification and aerobic respiration, loss of *cbb*₃ oxidase caused complex biomineralizing phenotypes and aberrant cell morphologies, probably by disturbing the proper redox balance required for metabolism and magnetite biomineralization. Altogether, besides as primary terminal oxidase for aerobic respiration, the *cbb*₃ oxidase may serve as an oxygen sensor and have a further role in poising proper redox potential required for magnetite biomineralization.

5.2 INTRODUCTION

Magnetotactic bacteria (MTB) are capable of orientation in the Earth's magnetic field to search for their preferred low-oxygen environment, which is achieved by unique intracellular organelles, magnetosomes (1). In the alphaproteobacterium *Magnetospirillum gryphiswaldense* (in the following referred to as MSR-1) and related MTB, magnetosomes comprise of membrane-enveloped magnetite crystals and are aligned in chains (1). Previous studies have revealed that the process of magnetite biomineralization is not only under the control of genes encoded within a single genomic magnetosome island (MAI) (2-5), but also genes located outside MAI (6, 7). The synthesis of the mixed-valence iron oxide magnetite [FeII(FeIII)₂O₄] is proposed to proceed by coprecipitation of balanced amounts of ferrous and ferric iron, which thus requires a precise biological regulation of redox conditions (8-10). As one of the major redox pathways in microaerophilic or anaerobic bacteria such as MTB, denitrification is a respiratory process to stepwise reduce nitrate to N₂ (11). Our recent work showed that in MSR-1 denitrification plays an important role in poisoning redox conditions for magnetite biomineralization (6, 7). The deletion of *nap* genes encoding a periplasmic nitrate reductase not only abolished anaerobic growth and delayed aerobic growth, but also severely affected magnetite synthesis and led to the formation of fewer, smaller and irregular magnetosomes during denitrification and microaerobic respiration (6). Inactivation of nitrite reductase NirS resulted in defective growth and biosynthesis of smaller and irregular particles during nitrate reduction (7). Alternatively, aerobic respiration also occurs in MTB by using O₂ as terminal electron acceptor. Although isotope experiments demonstrated that oxygen bound in biologically synthesized Fe₃O₄ is derived from water but not O₂, it has been observed that O₂ concentration is a crucial factor which significantly affects magnetite biomineralization (12). Magnetite particles are synthesized only under microaerobic and anaerobic conditions whereas aerobic environment completely inhibits the formation of magnetosomes (6, 13). However, the role of O₂ and aerobic respiration in magnetite biomineralization is still unclear.

In prokaryotes, there are two major groups of terminal oxidases involved in O₂ reduction: the universal cytochrome *c* oxidases and the quinol oxidases (14). All of cytochrome *c* oxidases, which relay electrons from cytochrome *c* to O₂, are members of heme-copper oxidases (HCOs). Based on the evolutionary relationships, HCOs are classified into three different

types: (i) type A oxidases, grouped as cytochrome oxidases aa_3 , which are homologous to the mitochondrial oxidases (15), (ii) type B oxidases, in which the catalytic subunit and two other subunits are analogous to the subunits of aa_3 -type cytochrome c oxidases (16), and (iii) type C oxidases, the cytochrome oxidases cbb_3 , which are structurally different from the two other types A and B (17). Unlike oxidase aa_3 which functions under aerobic conditions, the cbb_3 oxidase encoded by the *ccoNOQP* operon is expressed primarily under O_2 -limiting conditions reflecting its high affinity for O_2 (18). In *Rhodobacter sphaeroides*, cbb_3 oxidase exhibits multiple roles. In addition to its role in aerobic respiration, cbb_3 oxidase further functions as a redox sensor to control the expression of photosynthesis genes (19, 20). The *bd*-type quinol oxidases provide an alternative route of electrons and accept electrons directly from quinol for O_2 reduction (14). Since the *bd* quinol oxidases do not pump any proton, they are typically less efficient at creating the charge gradient for ATP synthesis compared with HCOs. However, they have been found to have a higher affinity for O_2 than other cytochrome oxidases (21), therefore, it is proposed that *bd* oxidases function for aerobic respiration under low O_2 conditions (22). Nevertheless, the physiological function of *bd* oxidases remains unclear.

Despite its potential importance for magnetosome formation in MTB, only a few studies have been shown to investigate the role of O_2 in magnetite biomineralization. It was found that a higher O_2 tension from 1% saturation to 10% led to an increased activity of a manganese-type superoxide dismutase relative to that of an iron-type superoxide dismutase in *Magnetospirillum magnetotacticum* (23). Sakaguchi et al. showed that the presence of O_2 repressed the synthesis of a 140-kDa membrane protein from *M. magnetotacticum* (24). Therefore, it is assumed that O_2 is involved in poisoning the redox potential for magnetite synthesis (25). Yet, no genetic evidence has been available to elucidate the role of O_2 *in vivo*, and the exact relationship between aerobic respiration and magnetite biomineralization has largely unknown. Here, we set out to explore the role of O_2 and aerobic respiration in metabolism and magnetite biomineralization by mutagenesis of different terminal oxidases in MSR-1. Although three putative terminal oxidases were identified in MSR-1, we for the first time demonstrated that only oxidases cbb_3 and *bd* are required for O_2 reduction while cytochrome c oxidase aa_3 does not have any physiological function for aerobic respiration in the laboratory. Genetic and biochemical analyses revealed that aerobic respiration is essential to microaerobic denitrification, and the cbb_3 oxidase is required for the co-occurrence of denitrification and aerobic respiration in the presence of oxygen. Moreover,

besides as primary terminal oxidase, *cbb₃* oxidase is also involved in magnetite biomineralization and loss of *cbb₃* oxidase caused pleiotropic effects under microaerobic conditions in the presence of nitrate, such as significant delays of growth, severely impaired magnetite synthesis, and various morphologies of cells, probably by disturbing the intracellular redox state required for metabolism and magnetite biomineralization.

5.3 MATERIALS AND METHODS

5.3.1 Bacterial strains and growth conditions

Bacterial strains and plasmids used in these studies are list in Table 5-S1. *Escherichia coli* strains were routinely cultured in lysogeny broth (LB) at 37°C, and MSR-1 strains were grown at 30°C in nitrate medium if not specified otherwise (6). In ammonium medium nitrate was substituted by 4 mM ammonium chloride. When needed, kanamycin was used at the following concentration: *E. coli*, 25 µg/ml; MSR-1, 5 µg/ml. 300 µM diaminopimelic acid (DAP) was added to the medium when *E. coli* strain BW29427 was used as donor in conjugation.

Under anaerobic and microaerobic conditions optical density and magnetic response (C_{mag}) were measured spectrophotometrically at 565 nm in 300 ml bottles containing 50 ml medium as previously described (26). For microaerobic conditions, before autoclaving bottles were sealed with butyl-rubber stoppers under a microoxic gas mixture containing 2% O₂ and 98% N₂. Anaerobic conditions were achieved by omitting oxygen from the gas mixture. For aerobic conditions, cells were grown in free gas exchange with air in 500 ml flasks containing 40 ml medium agitated at 200 rpm. If not specified, inocula were prepared anaerobically.

5.3.2 Genetic and molecular biology techniques

Standard molecular and genetic techniques were used for DNA isolation, digestion, ligation and transformation (27). All DNA products were sequenced using BigDye Terminator version 3.1 chemistry on an ABI 3700 capillary sequencer (Applied Biosystems, Darmstadt, Germany). Sequence data were analyzed with the software Vector NTI Advance[®] 11.5.1

(Invitrogen, Darmstadt, Germany). All oligonucleotide sequences used in this work are available if required.

5.3.3 Construction of mutant strains

First the fused flanking sections of operons encoding *cbb₃*, *aa₃*, and *bd* oxidases were cloned into PstI/SpeI-digested pOR093 to yield pLYJ128, pLYJ129, and pLYJ130, respectively. Unmarked deletion mutagenesis deletion of *cbb₃*, *aa₃*, and *bd* oxidases was performed by a two-step homologous recombination technique in the same manner as described previously (28). After screening PCR, unmarked deletion mutants were generated and finally designated Δcbb_3 mutant, Δaa_3 mutant, and Δbd mutant, respectively. For double deletion mutants, pLYJ128 was transformed into Δaa_3 mutant and Δbd mutant by conjugation and two different double mutants, $\Delta aa_3\Delta cbb_3$ mutant and $\Delta bd\Delta cbb_3$ mutant were obtained, respectively. Plasmid pLYJ129 was transformed into Δbd mutant by conjugation to generate $\Delta bd\Delta aa_3$ double deletion mutant.

For genetic complementation of Δcbb_3 mutant, $\Delta aa_3\Delta cbb_3$ mutant, and $\Delta bd\Delta cbb_3$ mutant, *ccoNOQP* operon encoding *cbb₃* oxidase with its own promoter region was ligated into HindIII/SmaI-digested pBBR1MCS-2 to obtain plasmid pLYJ138. In addition, as controls, operons encoding respective *aa₃* and *bd* oxidases were also complemented into $\Delta aa_3\Delta cbb_3$ mutant and $\Delta bd\Delta cbb_3$ mutant. The PCR product of *coxBAC* operon encoding *aa₃* oxidase with its own promoter region was digested with HindIII and SmaI and further ligated into pBBR1MCS-2 to generate pLYJ139. The PCR fragment of *cydAB* operon encoding *bd* oxidase with its own promoter region was digested with ApaI and SacI and also ligated into pBBR1MCS-2 to generate plasmid pLYJ140.

5.3.4 Analysis of transcriptional *gusA* fusions

To investigate the transcription of different terminal oxidases under different conditions, promoter regions of the *ccoNOQP*, *coxBAC*, and *cydAB* operons were cloned into Acc65I/HindIII-digested pLYJ97, designated pLYJ115, pLYJ135, and pLYJ137, respectively. And β -glucuronidase activity was determined at 37°C as described as before (6). Triplicate assays were performed and the values reported were averaged by using at least two independent experiments.

5.3.5 Nadi assay

The Nadi assay was used for the detection of cytochrome *c* oxidase activity (29). A mixture of 1% α -naphthol (Sigma-Aldrich) in ethanol and 1% *N, N*-dimethyl-*p*-phenylenediamine monohydrochloride (Sigma-Aldrich) was applied to cover colonies. Strains containing an active cytochrome *c* oxidase turn blue within 5 min.

5.3.6 Nitrate and nitrite concentration assay

Different strains were grown under microaerobic conditions in the presence of nitrate. 1 ml culture at different time point was used to detect nitrate and nitrite concentration, which has been described before in (6). Duplicate assays were carried out and the values reported were measured in one representative experiment.

5.3.7 NAD⁺/NADH ratio assay

Different strains were grown in nitrate or ammonium medium under different conditions and harvested at OD_{565 nm} of 0.1-0.2. Each culture containing about 10⁵ cells was suspended in 50 μ l PBS buffer and subjected to extraction and detection using NAD/NADH-GloTM Assay (Promega) following the manufacturer's instruction. Luminescence was recorded by a Synergy 2 multimode microplate reader from BioTek.

5.3.8 TEM

MSR-1 WT and mutants were grown at 30°C under different conditions, and concentrated and adsorbed onto carbon-coated copper grids. Samples were viewed and recorded with a TECNAI FEI20 microscope (FEI, Eindhoven, Netherlands) at 200 kV, or a Morgagni 268 microscope (FEI, Eindhoven, Netherlands) at 80 kV as previously described (30). More than 300 crystals were measured for each strain.

5.3.9 Sequence analysis

Genes encoding different oxygen terminal oxidases were identified by BLASTP (<http://blast.ncbi.nlm.nih.gov/Blast.cgi>) homology searching in the genomes of MSR-1 (GenBank: CU459003.1), *Magnetospirillum magneticum* strain (GenBank accession number AP007255.1), *M. magnetotacticum* (NCBI reference sequence NZ_AAAP00000000.1), *Magnetococcus marinus* (GenBank accession number CP000471.1), and *Desulfovibrio magneticus* strain RS-1 (GenBank accession number AP010904.1).

5.4 RESULTS

5.4.1 Identification of terminal oxidases involved in aerobic respiration

Three operons encoding putative terminal *cbb*₃-type, *aa*₃-type, and *bd*-type oxidases involved in aerobic respiration were identified in the draft genome assembly of MSR-1 (Fig. 5-1A). The *cbb*₃ and *aa*₃ oxidases encoded by their respective operons *ccoNOQP* and *coxBAC*, belong to the family of cytochrome *c* oxidases. In other bacteria, cytochrome *c* oxidase *aa*₃ is the predominant enzyme under O₂-rich growing conditions, whereas *cbb*₃ is expressed only at O₂ limitation (31). In other MTB including *M. magneticum*, *M. magnetotacticum*, and *Ms. marinus*, although *ccoNOQP* operons are present, but several *ccoNOQP* genes are absent (Table 5-S2). A *coxBAC* operon is present in *M. magneticum* and of *M. magnetotacticum*, whereas none of *coxBAC* genes were detected in *Ms. marinus*, which is only capable of microaerobic but not aerobic or anaerobic growth, suggesting that *aa*₃ oxidase is not necessary for microaerobic O₂ reduction. Cytochrome *c* oxidases seem to be absent in the magnetotactic bacterium *D. magneticus* strain RS-1 (Table 5-S2), which utilizes sulfate and fumarate but not nitrate or O₂ as electron acceptor (32). The third oxidase identified in MSR-1, *bd* oxidase encoded by a *cydAB* operon, is a member of the quinol oxidase family, which is able to accept electrons directly from quinol for O₂ reduction. However, we failed to detect any *cydAB* homologs in the genomes of other MTB except for *D. magneticus* strain RS-1. Despite of distinct gene content and organization encoding terminal oxidases, all known magnetospirilla are capable to grow under both microaerobic and aerobic conditions with O₂

as electron acceptor (13), indicating that different pathways for aerobic respiration might occur in different magnetospirilla.

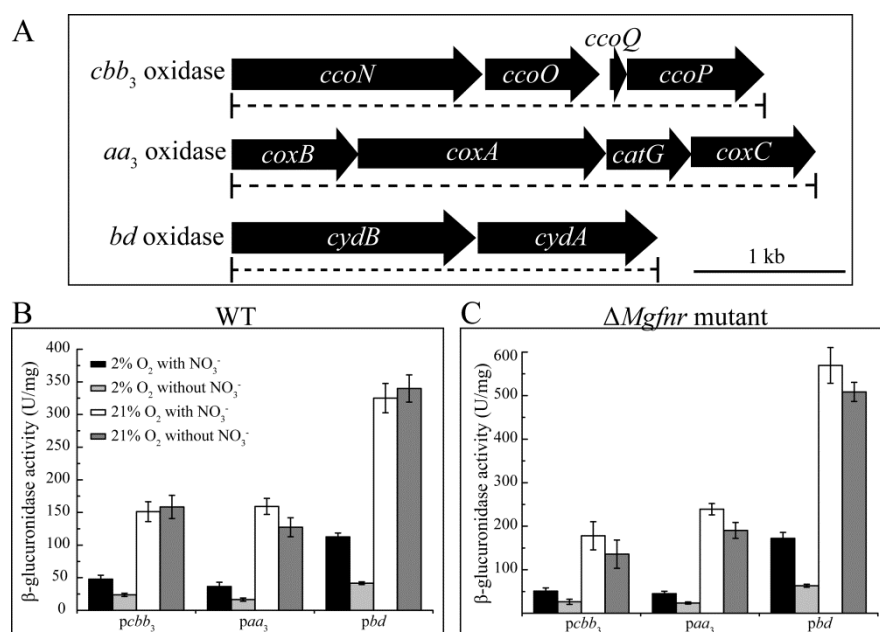


Fig. 5-1 (A) Molecular organization of putative terminal oxidase operons in the genome of MSR-1. Dashed lines indicate the extent of deletions in mutant strains. (B) and (C) Expression of putative terminal oxidase genes fused with *gusA* in WT (B) and Δ Mgfnr mutant (C). Cultures were grown aerobically in nitrate and ammonium medium and microaerobically in nitrate and ammonium medium and expression was measured by β -glucuronidase activities.

5.4.2 Expression of *ccoNOQP*, *coxBAC*, and *cydAB* operons is upregulated by oxygen and MgFnr is not involved in the regulation of aerobic respiration

Since the three putative terminal oxidases in other bacteria were reported to show distinct affinities to oxygen and thus exhibit their maximum expression levels at different oxygen concentrations (31), we tested their expression patterns in MSR-1 under different conditions. By *gusA* fusions we found that the expression of all putative terminal oxidase operons was upregulated by oxygen and highest levels of β -glucuronidase activity were detected under aerobic conditions, whereas nitrate did not affect their aerobic expression. Under microaerobic conditions, an about 2-fold higher level of β -glucuronidase activity was observed in the presence of nitrate than in its absence (Fig. 5-1B). In addition, because Fnr as a global regulator is known to play a role in controlling the transcription of aerobic respiration genes (19, 31), we asked whether Fnr in MSR-1 (named MgFnr) is involved in regulating expression of these terminal oxidase operons in response to variable O₂ concentrations by performing the same experiments in a Δ Mgfnr mutant, in which

deregulated expression of several denitrification genes (*nirS*, *nor*, and *nosZ*) under aerobic conditions was recently shown (Y. Li et al., submitted). As shown in Fig. 5-1C, Δ *Mgfnr* mutant cells carrying *ccoNOQP-gusA*, *coxBAC-gusA*, and *cydAB-gusA* showed the same expression patterns as the WT. For example, oxygen increased β -glucuronidase activity while nitrate did not cause any effect on their aerobic expression, and microaerobically grown Δ *Mgfnr* mutant cells exhibited higher levels of β -glucuronidase activity in the presence of nitrate than in its absence. Altogether, these data suggested that in MSR-1 the transcription of putative terminal oxidases is not under the control of MgFnr and thereby other unknown regulators likely mediate their expression in response to different O₂ concentrations.

5.4.3 The *cbb*₃ and *bd* oxidases but not *aa*₃ are essential to growth in the presence of oxygen and aerobic respiration is a prerequisite for microaerobic denitrification

To determine whether the *cbb*₃, *aa*₃, and *bd* oxidases fulfill similar physiological functions in aerobic respiration, and whether they are involved in magnetite biomineralization, we constructed several different mutants including Δ *cbb*₃, Δ *aa*₃, and Δ *bd* single deletions, and Δ *bd* Δ *aa*₃, Δ *aa*₃ Δ *cbb*₃, and Δ *bd* Δ *cbb*₃ double deletions. Upon repeated attempts, Δ *cbb*₃, Δ *aa*₃ Δ *cbb*₃, and Δ *bd* Δ *cbb*₃ mutants could be obtained only when the entire selection (e.g., plating and culturing of colonies) was performed under strictly anaerobic conditions. Phenotypes of all mutants with respect to growth and magnetite biomineralization are summarized in Table 5-1 and Table 5-S3. Hardly any difference in growth was observed between Δ *aa*₃, Δ *bd*, Δ *bd* Δ *aa*₃ mutants and the WT under all test conditions. Although the Δ *bd* Δ *cbb*₃ double deletion mutant displayed anaerobic growth indistinguishable from the WT, no growth was observed under microaerobic or aerobic conditions (Table 5-1). This demonstrated that only *cbb*₃ and *bd* but not *aa*₃ oxidases act as terminal oxidases for O₂ reduction in the laboratory. The observation that Δ *bd* Δ *cbb*₃ did not grow microaerobically even in the presence of nitrate further indicated that aerobic respiration is a prerequisite to activate the denitrification pathway in the presence of oxygen. Under aerobic conditions WT cells grew to stationary phase within about 24 h in both nitrate and ammonium medium, whereas both Δ *cbb*₃ and Δ *aa*₃ Δ *cbb*₃ mutants required about 120 h and 140 h to achieve WT-like cell densities in nitrate and ammonium medium, respectively (Fig. 5-2A and B). When Δ *cbb*₃ and Δ *aa*₃ Δ *cbb*₃ strains were incubated microaerobically in ammonium medium, final cell yields were reached 3 h later in both mutants than in the WT (Fig. 5-2C). In microaerobic nitrate medium Δ *cbb*₃ and Δ *aa*₃ Δ *cbb*₃ mutants showed even larger lags of about 12 h to reach

the stationary phase (Fig. 5-3A). Taken together, based on observations that Δcbb_3 and $\Delta aa_3\Delta cbb_3$ mutants had similar phenotypes (delayed growth) while Δaa_3 mutant did not show any growth impairment, we concluded that the aa_3 oxidase in MSR-1 has no physiological significance and does not participate in aerobic respiration. Furthermore, loss of bd oxidase did not affect microaerobic or aerobic growth, whereas loss of cbb_3 oxidase led to severely impaired microaerobic and aerobic growth, suggesting that compared to the bd oxidase, cbb_3 oxidase plays a more pronounced role in aerobic respiration under both O_2 -rich and O_2 -limited conditions.

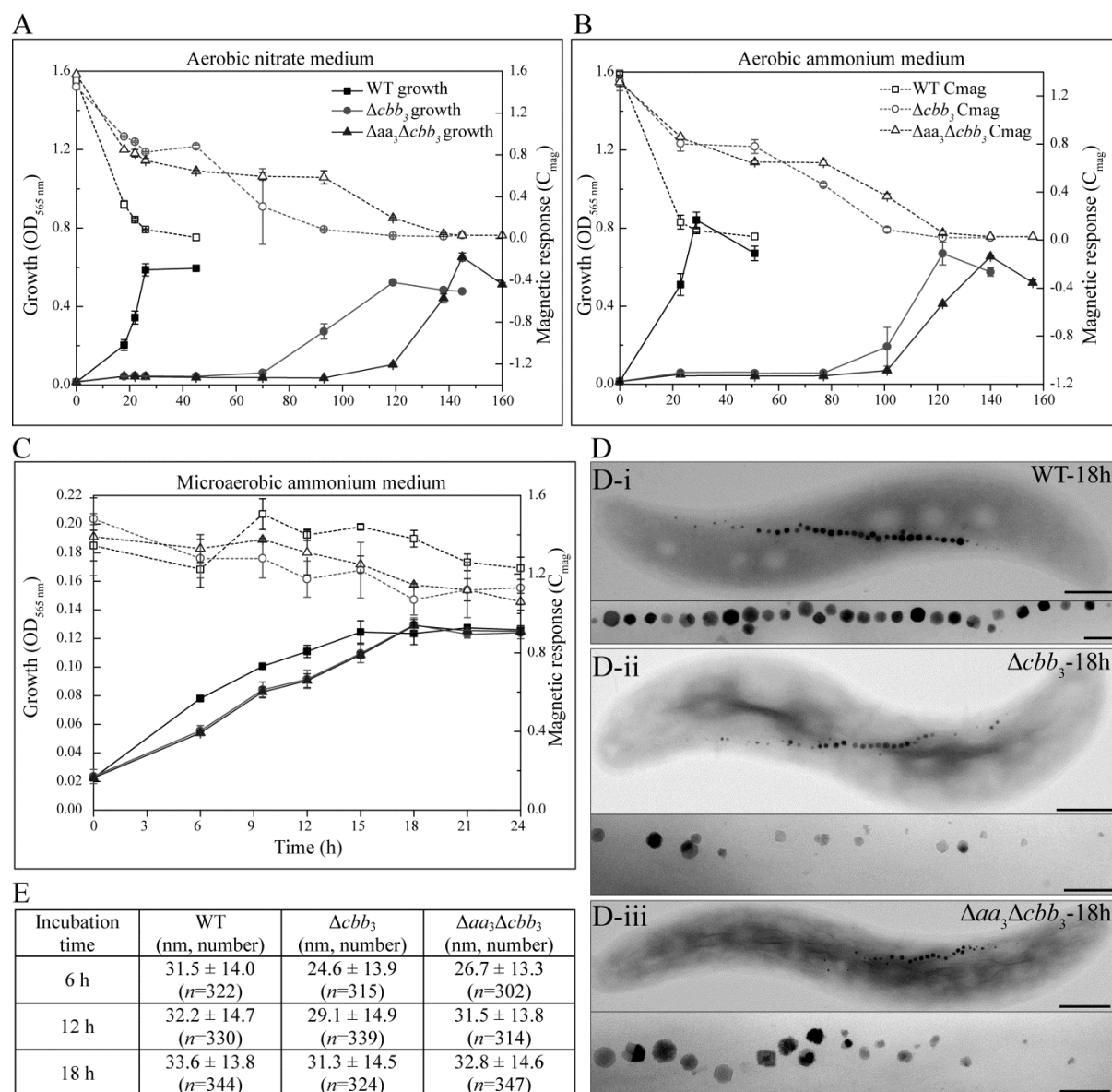


Fig. 5-2 (A), (B), and (C) Growth ($OD_{565\text{ nm}}$) and magnetic response (C_{mag}) of MSR-1 WT, Δcbb_3 , and $\Delta aa_3\Delta cbb_3$ strains under different conditions. (A) Aerobic, nitrate medium, (B) Aerobic, ammonium medium, and (C) Microaerobic, ammonium medium. (D) TEM images of microaerobically grown WT (D-i), Δcbb_3 mutant (D-ii), and $\Delta aa_3\Delta cbb_3$ mutant (D-iii) in ammonium medium. Scale bars: 500 nm (whole cells) and 100 nm (magnetosomes). (E) Measurements of crystal size for MSR-1 WT, Δcbb_3 , and $\Delta aa_3\Delta cbb_3$ strains at

different time points in microaerobic ammonium medium. Results from representative experiments were measured in triplicate, and values are given as means and standard deviations.

Table 5-1 Phenotypic characterization of different terminal oxidase mutants

Strain	0% O ₂	2% O ₂ , +NO ₃ ⁻	2% O ₂ , +NH ₄ ⁺	21% O ₂ , +NO ₃ ⁻	21% O ₂ , +NH ₄ ⁺
Δaa_3	WT-like	WT-like	WT-like	WT-like	WT-like
Δbd	WT-like	WT-like	WT-like	WT-like	WT-like
$\Delta bd\Delta aa_3$	WT-like	WT-like	WT-like	WT-like	WT-like
Δcbb_3	WT-like	Delayed growth	Delayed growth	Delayed growth	Delayed growth
		Severely impaired biomineralization	Weakly impaired biomineralization		
		Aberrant shape of cells			
$\Delta aa_3\Delta cbb_3$	WT-like	Delayed growth	Delayed growth	Delayed growth	Delayed growth
		Severely impaired biomineralization	Weakly impaired biomineralization		
		Aberrant shape of cells			
$\Delta bd\Delta cbb_3$	WT-like	No growth	No growth	No growth	No growth

WT-like, growth and magnetite biomineralization are not visibly different from WT; Delayed growth, cells grow slowly compared to the WT; Phenotypes of mutants different from the WT are indicated in gray boxes.

To further prove that in MSR-1 *cbb*₃ but not *aa*₃ is the only physiologically functional cytochrome *c* oxidase, we performed the Nadi assay which is commonly used to specifically detect cytochrome *c* oxidase activity (29). Using *N, N*-dimethyl-*p*-phenylenediamine monohydrochloride as an exogenous electron donor, cytochrome *c* oxidase is capable to catalyze the rapid formation of indophenol blue from colorless α -naphthol. As shown in Fig. 5-4A, Δaa_3 , Δbd , and $\Delta bd\Delta aa_3$ strains showed similar reaction rates as the WT, forming indophenol blue visibly within < 1 min and developing maximum coloration within 5 min. However, *cbb*₃-deficient mutants including Δcbb_3 , $\Delta aa_3\Delta cbb_3$, and $\Delta bd\Delta cbb_3$ mutants did not exhibit any blue color. Only when Δcbb_3 , $\Delta aa_3\Delta cbb_3$, and $\Delta bd\Delta cbb_3$ mutants were complemented by plasmid pLYJ138 containing a WT *cbb*₃ allele, colonies formed indophenol blue, indicating that oxidase *cbb*₃ itself is sufficient to rescue the cytochrome *c* oxidase activity. However, the formation of indophenol blue was not restored in $\Delta aa_3\Delta cbb_3$ and $\Delta bd\Delta cbb_3$ mutants by complementation with a WT *aa*₃ and *bd* allele, respectively (Fig. 5-4B). These data demonstrated again that only cytochrome *c* oxidase *cbb*₃ but not *aa*₃ is capable of oxygen reduction.

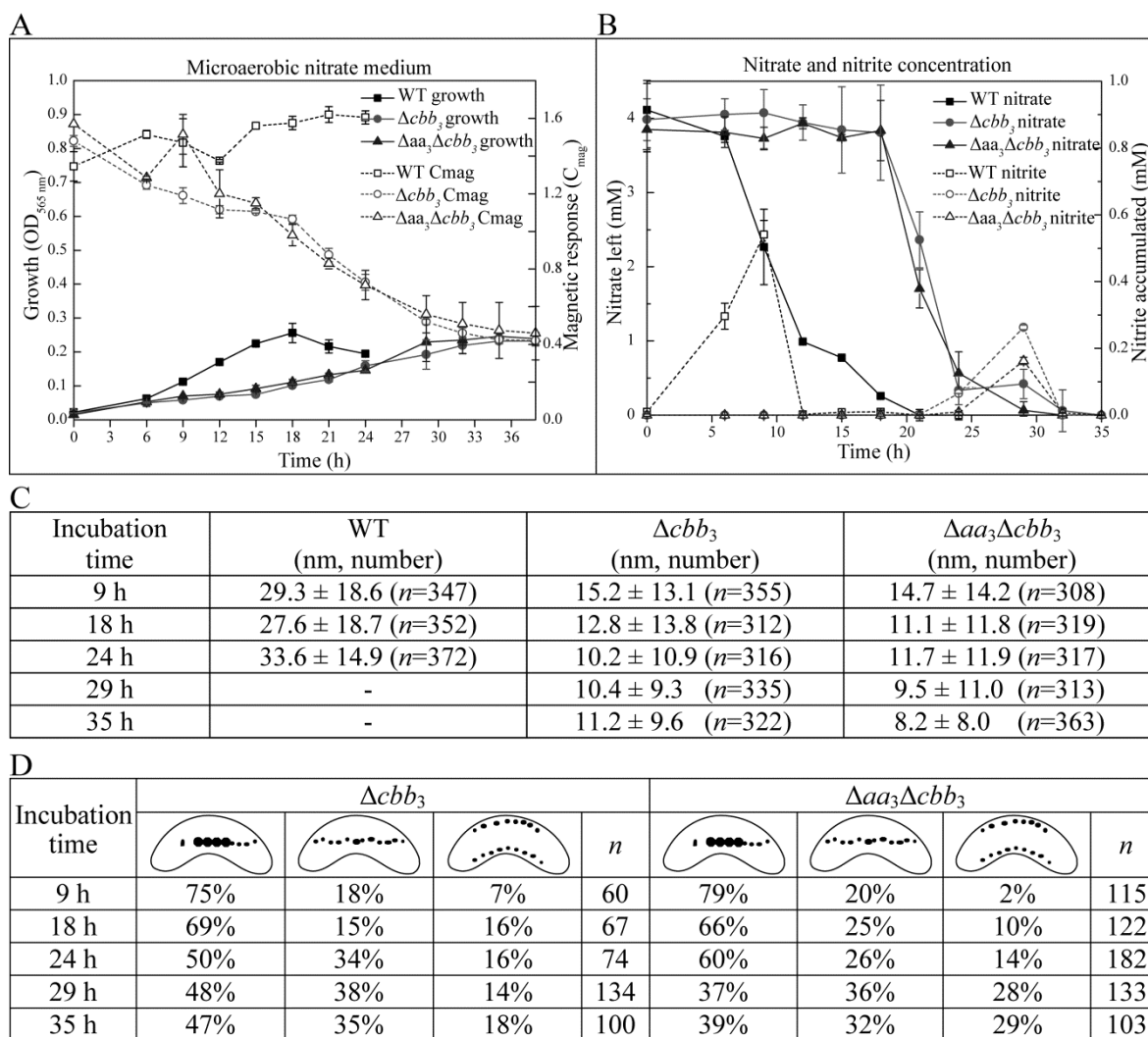


Fig. 5-3 (A) Growth ($OD_{565 \text{ nm}}$) and magnetic response (C_{mag}) of MSR-1 WT, Δcbb_3 , and $\Delta aa_3 \Delta cbb_3$ strains in microaerobic nitrate medium. (B) Time courses of nitrate and nitrite utilization during microaerobic growth in nitrate medium. (C) Measurements of crystal size for MSR-1 WT, Δcbb_3 , and $\Delta aa_3 \Delta cbb_3$ strains at different time points in microaerobic nitrate medium. Number of crystals measured for each strain (n) is present. (D) Magnetosome morphotypes in Δcbb_3 and $\Delta aa_3 \Delta cbb_3$ mutants and the proportion of each morphotype at different time point. Number of cells measured for each strain (n) is presented.

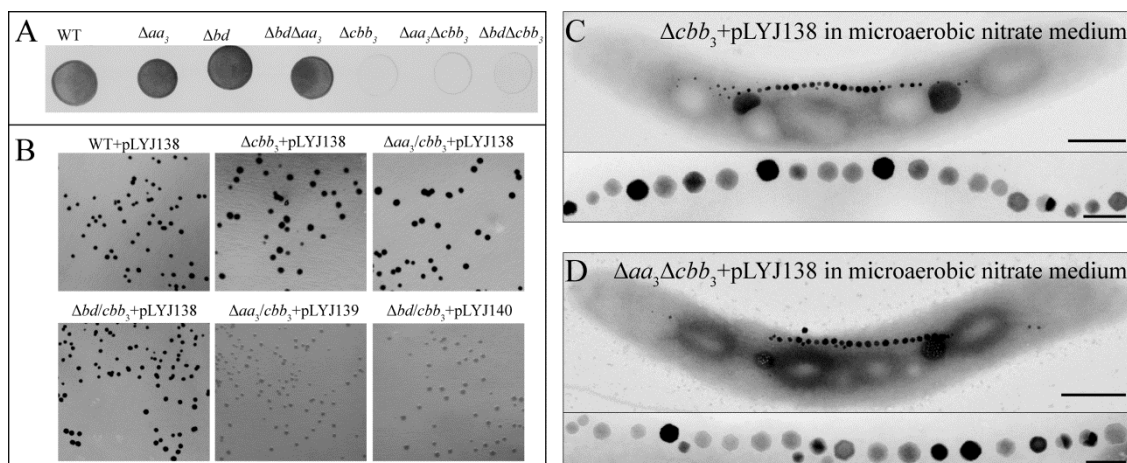


Fig. 5-4 (A) Nadi assay of anaerobic grown WT and various mutant strains. (B) Nadi assay of anaerobic grown complementation strains. Plasmid pLYJ138 contains a WT *cbb*₃ allele while pLYJ139 and pLYJ140 harbor a WT *aa*₃ and *bd* allele, respectively. (C) TEM images of Δcbb_3 and $\Delta aa_3\Delta cbb_3$ stains complemented with plasmid pLY138 harboring the WT *cbb*₃ alleles grown in microaerobic nitrate medium. Scale bars: 500 nm (whole cells) and 100 nm (magnetosomes).

5.4.4 Loss of *cbb*₃ impairs magnetite biomineralization and causes aberrant cell morphologies under microaerobic conditions in the presence of nitrate

Compared to the WT, Δaa_3 , Δbd , and $\Delta bd\Delta aa_3$ mutants showed similar magnetic response (C_{mag}) and size, number and appearance of magnetosomes under anaerobic and microaerobic conditions (Table 5-S3). Likewise, the Δcbb_3 , $\Delta aa_3\Delta cbb_3$, and $\Delta bd\Delta cbb_3$ mutants displayed WT-like magnetic responses (C_{mag}), magnetosome sizes and morphologies under anaerobic conditions (Table 5-S3). Under microaerobic conditions in the absence of nitrate, the average C_{mag} values of Δcbb_3 and $\Delta aa_3\Delta cbb_3$ mutants were slightly lower than those of the WT during entire growth (Fig. 5-2C). TEM revealed that both Δcbb_3 and $\Delta aa_3\Delta cbb_3$ cells synthesized slightly smaller magnetosomes only at the beginning of the growth (6 h), whereas in the following the average particle size in both mutants was not different from that in the WT (Fig. 5-2E). However, during the entire growth magnetosome morphology and organization in these two mutants was variable, including regular particles in the middle of chains in addition to small and irregular crystals at the ends of chains (Fig. 5-2D), which likely caused reduced C_{mag} values. In microaerobic nitrate medium, loss of *cbb*₃ oxidase resulted in significantly lower C_{mag} values, which gradually decreased further during growth (Fig. 5-3A). In agreement with this, magnetosomes in Δcbb_3 and $\Delta aa_3\Delta cbb_3$ mutants were much smaller than in the WT, and this difference became more obvious with the OD increasing (Fig. 5-3C). In addition, the phenotypes were inconsistent and displayed various distinct types of magnetosome formation and assembly (Fig. 5-5, Fig. 5-S1): (i) Type 1: magnetosome chains containing WT-like particles in the middle flanked by small, irregular particles at each end (≥ 3 WT-like particles in the middle) (Fig. 5-5A-i, B-i, C-i, and D-i); (ii) Type 2: magnetosomes appearing as much smaller and irregularly shaped particles, which were arranged in loose chains (≤ 2 WT-like particles) (Fig. 5-5A-ii, B-ii, C-ii, and D-ii); (iii) Type 3: two loose magnetosome chains present at each side of the cell (Fig. 5-5A-iii, B-iii, C-iii, and D-iii). These two chains further exhibited two different appearances: one is containing two chains as type 2, which only had smaller and irregular particles (Fig. 5-5A-iii and B-iii), and the other consists of one chain as the type 1 and the second as the type 2 (Fig. 5-5C-iii and D-iii). Similar phenotypes were observed at different growth points, including 9 h- (Fig.

5-5), 18 h-, 24 h-, 29 h-, and 35 h-cultured Δcbb_3 and $\Delta aa_3\Delta cbb_3$ cells (TEM images of 24 h and 35 h grown cells were shown in Fig. 5-S1). However, the proportion of type 1 magnetosomes was reduced as the OD was increased (Fig. 5-3D), which probably resulted in decreased average size of particles during the growth.

In addition, differential interference contrast microscopy (DIC) (data not shown) and TEM also showed that the cell morphology of Δcbb_3 and $\Delta aa_3\Delta cbb_3$ mutants was affected under microaerobic conditions in the presence of nitrate. Analyses of more than 300 cells for each strain revealed three morphotypes in the two mutants: (i) only < 10% of Δcbb_3 and $\Delta aa_3\Delta cbb_3$ cells showed WT-like spiral shape (Fig. 5-6A-i and A-ii); (ii) about 30% cells were thicker spirals (> 0.7 μM versus 0.5-0.6 μM width in the WT) (Fig. 5-6B-i and B-ii); (iii) > 60% cells were thicker and smaller vibrioid (Fig. 5-6C-i, C-ii, D-i, and D-ii).

Transcomplementation of Δcbb_3 (Δcbb_3 +pLYJ138) and $\Delta aa_3\Delta cbb_3$ ($\Delta aa_3\Delta cbb_3$ +pLYJ138) mutants with WT cbb_3 allele restored magnetosome formation and cell morphology back to the WT-like levels in microaerobic nitrate medium (Fig. 5-4C and D). Taken together, these data indicated that besides for aerobic respiration, cbb_3 oxidase also functions in magnetosome formation under microaerobic conditions. Loss of cbb_3 oxidase caused a pronounced impairment of magnetite biomineralization and disturbed cell morphology in the presence of nitrate than in its absence, which suggested that cytochrome *c* oxidase cbb_3 is more important in controlling magnetosome formation when denitrification and oxygen respiration overlap.

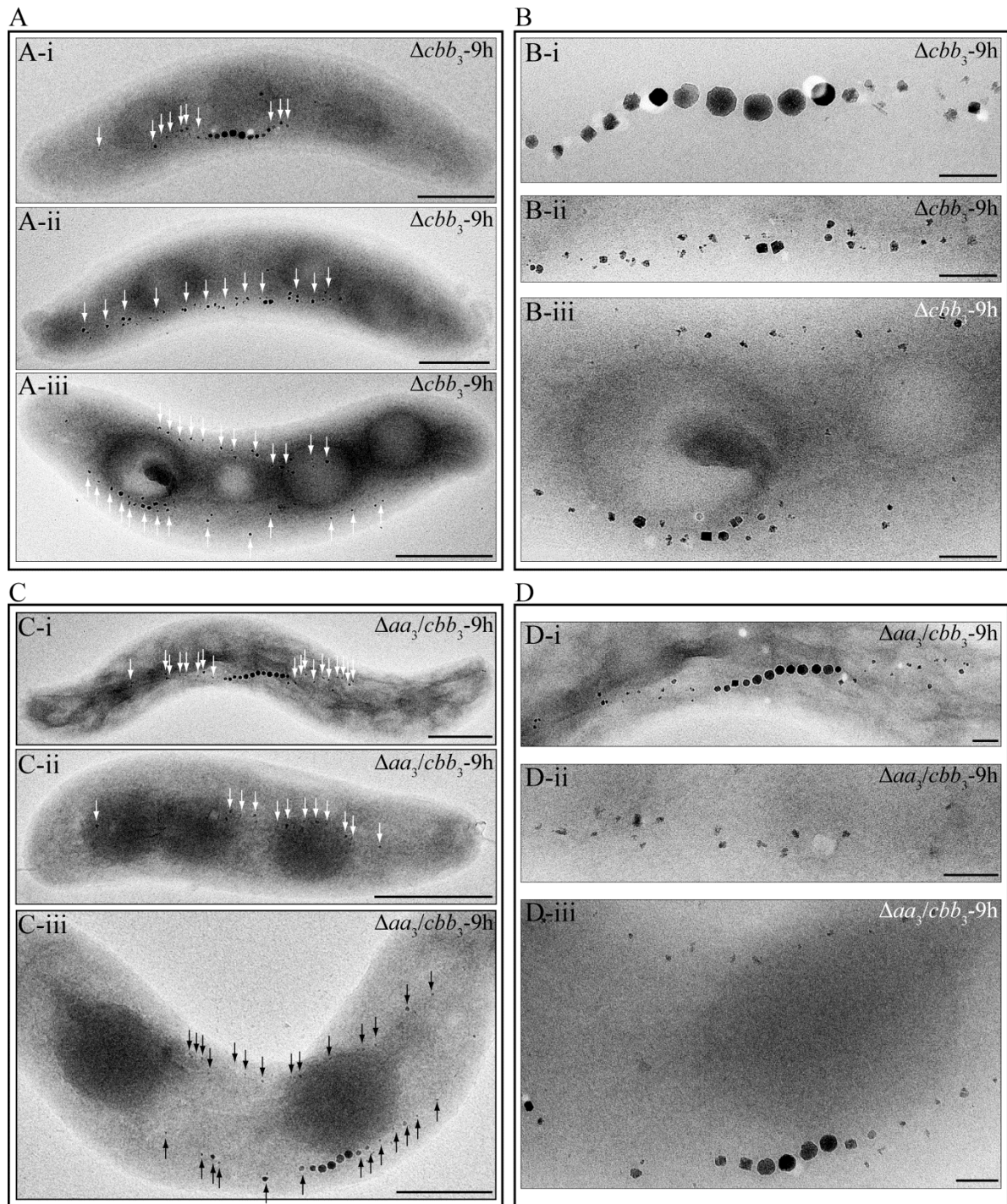


Fig. 5-5 Biom mineralization phenotypes of Δcbb_3 and $\Delta aa_3\Delta cbb_3$ mutants incubated for 9 h in microaerobic nitrate medium. (A) and (C) TEM images of whole cells of Δcbb_3 and $\Delta aa_3\Delta cbb_3$ mutants, respectively. Scale bar, 500 nm. (B) and (D) Closeup views of magnetosome crystals shown in A and C, respectively. Scale bar, 100 nm. Irregular shaped particles are indicated by arrows.

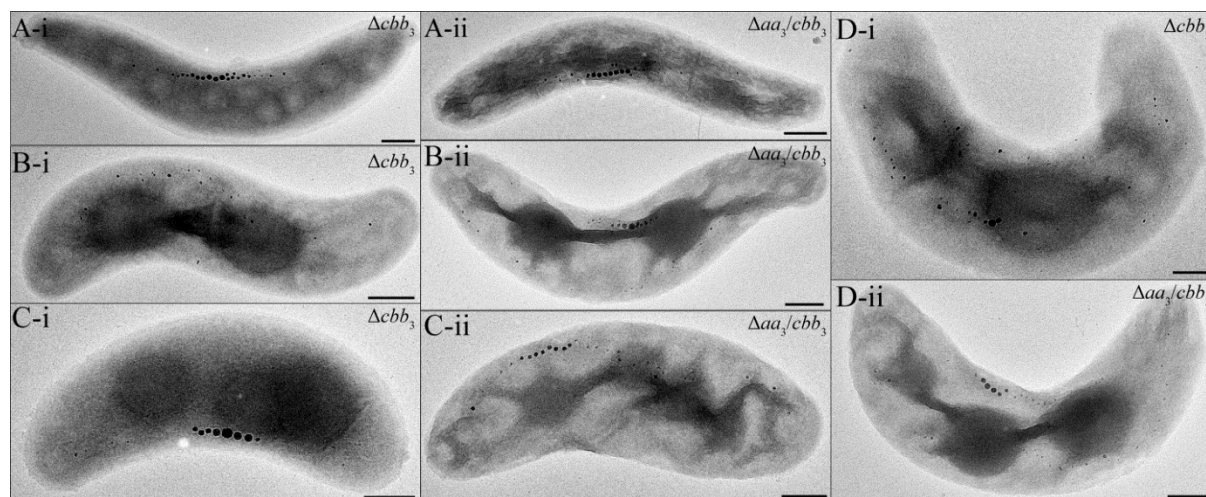


Fig. 5-6 Morphologies found in different cells of Δcbb_3 and $\Delta aa_3\Delta cbb_3$ mutants in microaerobic nitrate medium. (A) WT-like spiral shaped mutant cells; (B) thicker spiral cells; (C) and (D) thicker and smaller vibrioid shaped cells. Scale bar, 500 nm.

5.4.5 Cytochrome *c* oxidase *cbb₃* functions as an O₂ sensor and plays a role in maintaining proper redox conditions by balancing nitrate and oxygen reduction

Since only loss of *cbb₃* oxidase led to delayed microaerobic and aerobic growth and impaired magnetite biomineralization, we wanted to further clarify the function of *cbb₃* oxidase. The observation that both Δcbb_3 and $\Delta aa_3\Delta cbb_3$ mutants displayed a more substantial lag of microaerobic growth in the presence of nitrate than in its absence prompted us first to monitor the denitrification process in these two mutants during growth experiments in sealed bottles under microaerobic conditions (Fig. 5-3B). WT cells started to reduce nitrate after about 6 h and then consumed all nitrate within the following 12-14 h, after which growth ceased, probably due to the depletion of both nitrate and oxygen. This growth combined with the one in microaerobic ammonium medium, that WT cells took about 15 h to reach stationary phase, suggested that denitrification and aerobic respiration occurred simultaneously under microaerobic conditions, thereby confirming our earlier observation (6). During the entire growth of the WT strain, maximum concentration of about 0.5 mM nitrite was built up at the first 12 h. Unexpectedly, Δcbb_3 and $\Delta aa_3\Delta cbb_3$ mutant cells were unable to reduce nitrate during the first 15-18 h, and only O₂-dependent growth occurred with a maximum OD of about 0.11, which was similar to the final OD of about 0.12 in microaerobic ammonium medium after 15 h incubation. This implied that oxygen was nearly completely depleted after about 18 h, when nitrate reduction became detectable. Then, nitrate gradually disappeared within 15-18 h and Δcbb_3 and $\Delta aa_3\Delta cbb_3$ mutants reached a final OD of about 0.25, which was similar to the value of stationary phase of the WT cells. These findings

revealed that *cbb₃* oxidase is required for conditions when denitrification and aerobic respiration occur simultaneously.

On the other hand, in the alphaproteobacterium *R. sphaeroides* it has been shown that besides as terminal oxidase, the *cbb₃* oxidase also functions as an O₂ sensor to control the expression of photosynthesis genes (19, 20, 33, 34). Therefore, we hypothesized that *cbb₃* oxidase of MSR-1 also may act as an O₂ sensor to simultaneously activate and balance denitrification and aerobic respiration, and thus to maintain proper redox conditions for magnetite synthesis under microaerobic conditions. To test this hypothesis, we determined the ratio of NAD⁺ (oxidized)/NADH (reduced) in the WT, Δcbb_3 , and $\Delta aa_3\Delta cbb_3$ strains because nicotinamide adenine dinucleotide (NAD) as a coenzyme is regarded an important redox factor involved in multiple redox reactions. Variable ratios of NAD⁺/NADH corresponding to different oxygen concentrations were observed in the WT (Fig. 5-7). WT cells showed more than 2-fold higher ratios of NAD⁺/NADH under microaerobic conditions than under anaerobic conditions, which indicated that anaerobic conditions caused more reduced redox state as expected. The absence of any difference in the WT cultures with nitrate and without nitrate under microaerobic conditions suggested that oxygen respiration plays a primary role in maintaining a proper ratio of NAD⁺/NADH. Although oxygen reduction catalyzed by *bd* quinol oxidase still occurred in Δcbb_3 mutant, the ratio of NAD⁺/NADH under microaerobic conditions did not significantly increase compared to anaerobic conditions. The $\Delta aa_3\Delta cbb_3$ mutant displayed a similar pattern, with hardly different ratios of NAD⁺/NADH between anaerobic and microaerobic conditions. Compared to the WT, the ratios of NAD⁺/NADH in both Δcbb_3 and $\Delta aa_3\Delta cbb_3$ strains under anaerobic conditions were higher, implying that anaerobic cellular redox state is more oxidized in Δcbb_3 and $\Delta aa_3\Delta cbb_3$ strains. However, under microaerobic conditions the ratios of NAD⁺/NADH in both Δcbb_3 and $\Delta aa_3\Delta cbb_3$ strains were much lower than those of WT, indicating a more reduced state in Δcbb_3 and $\Delta aa_3\Delta cbb_3$ strains. As under microaerobic conditions Δcbb_3 and $\Delta aa_3\Delta cbb_3$ strains did not reduce nitrate until oxygen was completely consumed, we wondered whether the ratio of NAD⁺/NADH depended on the stage of growth. To this end, we examined the ratios of NAD⁺/NADH in Δcbb_3 and $\Delta aa_3\Delta cbb_3$ strains at different time points. However, a similar ratio of about 3-4 of NAD⁺/NADH was obtained at all tested stages of growth. Our data altogether suggested that *cbb₃* oxidase may serve as an O₂ sensor to activate denitrification when O₂ is still available, and loss of *cbb₃* oxidase results in the incapability of regulating the

intracellular redox state in response to different oxygen concentrations and thus further impairs magnetite biomineralization.

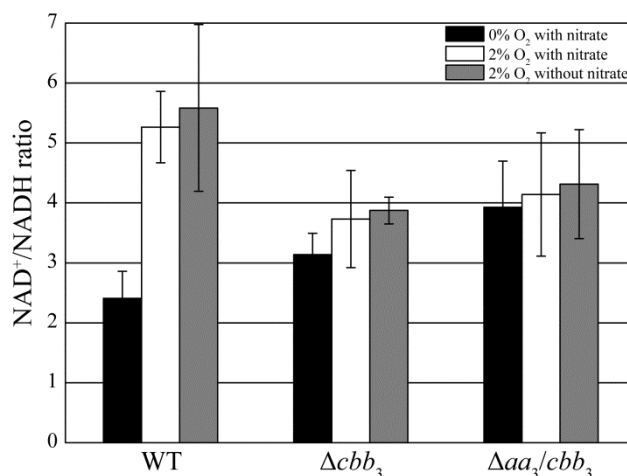


Fig. 5-7 Cellular NAD^+/NADH ratio measurement of WT, Δcbb_3 , and $\Delta aa_3\Delta cbb_3$ strains under different conditions. NAD^+ and NADH were extracted from cells grown in liquid medium, measured, normalized by luminescence signal, and plotted with mean values and standard deviations ($n = 3$).

5.5 DISCUSSION

Consistent with our previous findings that deletion of *Mgfnr* did not affect oxygen consumption and microaerobic magnetite biomineralization in the absence of nitrate (Y. Li et al., submitted), we found that the expression of three putative terminal oxidase operons (encoding *cbb₃*-type, *aa₃*-type, and *bd*-type oxidases) was not regulated by the global oxygen sensor MgFnr but increased by O_2 , similar to that shown in *Shewanella oneidensis* (35). This suggested that some unknown O_2 regulators are probably present and mediate the expression of aerobic terminal oxidase genes in response to different oxygen concentrations. Mutagenesis of different terminal oxidases demonstrated that cytochrome oxidases *cbb₃* and *bd* are the only functional enzymes for aerobic respiration, whereas *aa₃* oxidase has not any physiological significance for O_2 reduction under all test conditions. This could explain why Δcbb_3 and $\Delta aa_3\Delta cbb_3$ mutants had identical phenotypes. In natural habitats, MSR-1 cells adapt to the low- O_2 conditions, under which high-affinity terminal oxidases like *cbb₃* are favorable for O_2 respiration and energy conservation. In contrast, the *aa₃* oxidase which has a low affinity for O_2 (31), therefore, is insufficient to utilize trace amount of O_2 . In this case, it is not surprising that *aa₃* oxidase does not show any activity on O_2 reduction. However, we

cannot exclude that *aa₃* oxidase has some properties in nature, such as for O₂-detoxification in O₂-rich environments.

A $\Delta bd\Delta cbb_3$ double deletion mutant did not grow in the presence of oxygen, indicating that aerobic respiration is a prerequisite for the co-occurrence of denitrification in the presence of oxygen. However, the observation that loss of the *bd* oxidase alone did not affect growth and magnetite biomineralization, implies that when *cbb₃* oxidase is present, the *bd* oxidase might only provide a minor contribution to aerobic respiration. It is also possible that the activity of the *bd* oxidase is only induced to compensate the activity of *cbb₃* when *cbb₃* oxidase is eliminated. Unlike *cbb₃* and *aa₃* oxidases which are present in the related magnetospirilla *M. magneticum* and *M. magnetotacticum*, *bd* oxidase is completely absent in these strains. This implies that *bd* oxidase is likely dispensable in various MTB, and *aa₃* probably acts as an alternative terminal oxidase in these two magnetospirilla, while in *Ms. marinus* which is unable to grow aerobically, neither *bd* nor *aa₃* oxidase is present. Nevertheless, *bd* oxidase might have unknown functions in MSR-1 whereas *cbb₃* oxidase may also be the only functional enzyme used for aerobic respiration in *M. magneticum* and *M. magnetotacticum*.

Δcbb_3 and $\Delta aa_3\Delta cbb_3$ mutants showed delayed growth in microaerobic ammonium medium. This might be caused by the low efficiency of *bd* oxidase, which is not able to pump protons but only accepts electrons directly from quinol for O₂ reduction, while cytochrome *c* oxidase *cbb₃* is more efficient at creating the charge gradient for ATP synthesis via the *bc-c-cbb₃* branch (21). An even larger delay of growth was observed in Δcbb_3 and $\Delta aa_3\Delta cbb_3$ mutants in microaerobic nitrate medium. Unexpectedly, in this condition mutant cells did not start to reduce nitrate until O₂ was completely depleted, which suggested that the *cbb₃* oxidase *per se*, but not aerobic respiration is crucial for O₂ and nitrate reduction to occur simultaneously. This therefore indicates that besides as a terminal oxidase, *cbb₃* oxidase may be capable to sense O₂ and have a further key function to activate denitrification and aerobic respiration simultaneously. In microaerobic nitrate medium during early growth only aerobic respiration occurred (similar to conditions in microaerobic ammonium medium), while during the later growth only denitrification occurred and mutant cells showed similar growth rates as the anaerobically growing WT. However, the biomineralization phenotypes of Δcbb_3 and $\Delta aa_3\Delta cbb_3$ mutants in this condition were much different from those in either microaerobic ammonium medium or anaerobic nitrate medium. Thus, we can rule out that the severe defects in magnetite synthesis in Δcbb_3 and $\Delta aa_3\Delta cbb_3$ mutants were caused by the

incapability of co-occurrence of denitrification and aerobic respiration. Instead, severely impaired magnetosome formation likely results from the loss of *cbb₃* oxidase *per se*, which argues for a more direct role of *cbb₃* oxidase in magnetite biomineralization. In *R. sphaeroides*, besides as a terminal oxidase, *cbb₃* oxidase also functions as a redox sensor to repress the activity of photosynthesis genes under aerobic conditions by controlling the activity of transcriptional regulators of photosynthesis gene expression (19, 20, 33, 34). Furthermore, *cbb₃* oxidase of MSR-1 seems to share some functions with the periplasmic nitrate reductase Nap, one of the enzymes involved in poisoning the redox state for magnetite synthesis (6). This can be concluded from the following observations: (i) a significant growth lag was found in the Δcbb_3 and $\Delta aa_3\Delta cbb_3$ mutants under aerobic conditions, similar as in Δnap mutant (6). The lower growth rates might be due to an excess of the reductant NADH, which needs to be reoxidized by cell maintenance reactions, as also observed in *Rhodobacter capsulatus* and *Paracoccus pantotrophus* grown on carbon sources that are more reduced than the biomass (36, 37). Yet, the lower growth rates might be also directly caused by the lower efficiency of *bd* oxidase. (ii) aberrant cell morphologies of Δcbb_3 and $\Delta aa_3\Delta cbb_3$ mutants in microaerobic nitrate medium, a similar observation in WT cells grown in more reduced carbon source acetate (6). Thus, we assume that a more reduced state of intracellular redox occurs in Δcbb_3 and $\Delta aa_3\Delta cbb_3$ mutants, and *cbb₃* oxidase is required for dissipating excess reductant. In line with this, in Δcbb_3 and $\Delta aa_3\Delta cbb_3$ mutants the NAD⁺/NADH ratio under microaerobic conditions was more reduced than that in the WT. This is not surprising since as a terminal oxidase, *cbb₃* is capable of accepting electrons during O₂ reduction. However, an optimal redox state (i.e., balanced ratio of Fe²⁺/Fe³⁺) seems very important for microaerobic biomineralization of the mixed-valence iron oxide magnetite [Fe(II)Fe(III)₂O₄] especially in the presence of nitrate. Since we have shown previously that neither nitrate nor nitrite impacts magnetite synthesis (6, 7), it is suggested that severely impaired biosynthesis of magnetosomes is directly caused by the loss of *cbb₃*, and some other factors involved in magnetite biosynthesis are also likely affected by the loss of *cbb₃* oxidase. For example, some proteins encoded by genes within magnetosome island, such as MamX, MamZ, and FtsZ-like protein FtsZm, displayed different effects on magnetosome formation between in the presence of nitrate and in the absence of nitrate (28, 38). Also, MTB contain a set of redox active magnetosome-associated proteins, which share a unique configuration of two close CXXCH heme-binding motifs, magnetochrome domain (28, 39, 40). In this case, the change of intracellular redox state may affect the activity or conformation of these proteins and further impair the redox balance of ferrous and ferric iron for magnetite synthesis. More

complex magnetosome phenotypes, such as the presence of two magnetosome chains in the mutants indicated that magnetosome vesicle or chain assembly might be also regulated by the cellular redox state. Besides magnetosome-related proteins, the nitrite reductase NirS which shows a Fe(II): nitrite oxidoreductase activity, plays a role in magnetite biomineralization only under low O₂ conditions in the presence of nitrate (7). However, more reduced conditions in Δcbb_3 and $\Delta aas_3\Delta cbb_3$ mutants likely limit the concentration of ferric iron and further prevent the oxidation of ferrous iron for magnetite synthesis and result in severely defective magnetosome formation in the presence of nitrate. In addition, variable cell morphologies of microaerobically growing Δcbb_3 and $\Delta aas_3\Delta cbb_3$ mutants in the presence of nitrate, which are likely caused by delayed growth as well as reduced intracellular redox conditions, might be used to adapt to survival in a different environment.

In conclusion, although O₂ has been suggested to act as a major factor controlling magnetosome formation for decades, the roles of O₂ as well as O₂ respiration in metabolism and biomineralization had remained unknown. Here, we showed that in addition to denitrification regulated by Fnr, two different branches of the respiration chain occur for O₂ reduction: one is the cytochrome *bc₁-c-cbb₃* branch, while the other is that quinol oxidase *bd* directly accepts the electrons from quinol. Our genetic and biochemical analyses further showed that O₂ respiration is a prerequisite to activate the activities of denitrification in the presence of oxygen. Besides as a dominant terminal oxidase, *cbb₃* is also required to sense O₂ for the co-occurrence of denitrification and aerobic respiration. Furthermore, the *cbb₃* oxidase plays a role in maintaining redox balance for magnetite biomineralization under microaerobic conditions.

5.6 REFERENCES

1. **Jogler C, Schüler D.** 2009. Genomics, genetics, and cell biology of magnetosome formation. *Annu. Rev. Microbiol.* **63**:501-521.
2. **Schübbe S, Kube M, Scheffel A, Wawer C, Heyen U, Meyerdierks A, Madkour MH, Mayer F, Reinhardt R, Schüler D.** 2003. Characterization of a spontaneous nonmagnetic mutant of *Magnetospirillum gryphiswaldense* reveals a large deletion comprising a putative magnetosome island. *J. Bacteriol.* **185**:5779-5790.
3. **Ullrich S, Kube M, Schübbe S, Reinhardt R, Schüler D.** 2005. A hypervariable 130-kilobase genomic region of *Magnetospirillum gryphiswaldense* comprises a

- magnetosome island which undergoes frequent rearrangements during stationary growth. *J. Bacteriol.* **187**:7176-7184.
4. **Murat D, Quinlan A, Vali H, Komeili A.** 2010. Comprehensive genetic dissection of the magnetosome gene island reveals the step-wise assembly of a prokaryotic organelle. *Proc. Natl. Acad. Sci. U. S. A.* **107**:5593-5598.
 5. **Lohsse A, Ullrich S, Katzmann E, Borg S, Wanner G, Richter M, Voigt B, Schweder T, Schüler D.** 2011. Functional analysis of the magnetosome island in *Magnetospirillum gryphiswaldense*: the *mamAB* operon is sufficient for magnetite biomineralization. *PLoS One* **6**:e25561.
 6. **Li Y, Katzmann E, Borg S, Schüler D.** 2012. The periplasmic nitrate reductase Nap is required for anaerobic growth and involved in redox control of magnetite biomineralization in *Magnetospirillum gryphiswaldense*. *J. Bacteriol.* **194**:4847-4856.
 7. **Li YJ, Bali S, Borg S, Katzmann E, Ferguson SJ, Schüler D.** 2013. Cytochrome *cd*₁ nitrite reductase NirS is involved in anaerobic magnetite biomineralization in *Magnetospirillum gryphiswaldense* and requires NirN for proper *d*₁ heme assembly. *J. Bacteriol.* **195**:4297-4309.
 8. **Faivre D, Schüler D.** 2008. Magnetotactic bacteria and magnetosomes. *Chem. Rev. (Washington, DC, U. S.)* **108**:4875-4898.
 9. **Faivre D, Agrinier P, Menguy N, Zuddas P, Pachana K, Gloter A, Laval J, Guyot F.** 2004. Mineralogical and isotopic properties of inorganic nanocrystalline magnetites. *Geochim. Cosmochim. Acta* **68**:4395-4403.
 10. **Faivre D, Böttger LH, Matzanke BF, Schüler D.** 2007. Intracellular magnetite biomineralization in bacteria proceeds by a distinct pathway involving membrane-bound ferritin and an iron(II) species. *Angew. Chem. Int. Ed. Engl.* **46**:8495-8499.
 11. **Zumft WG.** 1997. Cell biology and molecular basis of denitrification. *Microbiol. Mol. Biol. Rev.* **61**:533-616.
 12. **Mandernack KW, Bazylinski D, Shanks WC, Bullen TD.** 1999. Oxygen and iron isotope studies of magnetite produced by magnetotactic bacteria. *Science* **285**:1892-1896.
 13. **Heyen U, Schüler D.** 2003. Growth and magnetosome formation by microaerophilic *Magnetospirillum* strains in an oxygen-controlled fermentor. *Appl. Microbiol. Biotechnol.* **61**:536-544.
 14. **Thöny-Meyr L.** 1997. Biogenesis of respiratory cytochromes in bacteria. *Microbiol. Mol. Biol. Rev.* **61**:337-376.
 15. **Saraste M.** 1990. Structural features of cytochrome oxidase. *Q. Rev. Biophys.* **23**:331-366.
 16. **Garcia-Horsman JA, Barquera B, Rumbley J, Ma J, Gennis RB.** 1994. The superfamily of heme-copper respiratory oxidases. *J. Bacteriol.* **176**:5587-5600.

17. **Buschmann S, Warkentin E, Xie H, Langer JD, Ermler U, Michel H.** 2010. The structure of *cbb₃* cytochrome oxidase provides insights into proton pumping. *Science* **329**:327-330.
18. **Pitcher RS, Watmough NJ.** 2004. The bacterial cytochrome *cbb₃* oxidases. *Bba-Bioenergetics* **1655**:388-399.
19. **Oh JI, Kaplan S.** 2001. Generalized approach to the regulation and integration of gene expression. *Mol. Microbiol.* **39**:1116-1123.
20. **Oh JI, Kaplan S.** 2002. Oxygen adaptation . The role of the CcoQ subunit of the *cbb₃* cytochrome *c* oxidase of *Rhodobacter sphaeroides* 2.4.1. *J. Biol. Chem.* **277**:16220-16228.
21. **VanOrsdel CE, Bhatt S, Allen RJ, Brenner EP, Hobson JJ, Jamil A, Haynes BM, Genson AM, Hemm MR.** 2013. The *Escherichia coli* CydX protein is a member of the CydAB cytochrome *bd* oxidase complex and is required for cytochrome *bd* oxidase activity. *J. Bacteriol.* **195**:3640-3650.
22. **Poole RK, Cook GM.** 2000. Redundancy of aerobic respiratory chains in bacteria? Routes, reasons and regulation. *Adv. Microb. Physiol.* **43**:165-224.
23. **Short K, Blakemore R.** 1989. Periplasmic superoxide dismutase in *Aquaspirillum magnetotacticum*. *Arch. Microbiol.* **152**:342-346.
24. **Sakaguchi H, Hagiwara H, Fukumori Y, Tamaura Y, Funaki M, Hirose S.** 1993. Oxygen concentration-dependent induction of a 140-kDa protein in magnetic bacterium *Magnetospirillum magnetotacticum* MS-1. *FEMS Microbiol. Lett.* **107**:169-174.
25. **Bazylinski DA, Williams T.** 2006. Ecophysiology of magnetotactic bacteria. *In* D. Schüler (ed.), *Magnetoreception and magnetosomes in bacteria*. SpringerVerlag, Heidelberg.
26. **Schüler D, Baeuerlein E.** 1998. Dynamics of iron uptake and Fe₃O₄ biomineralization during aerobic and microaerobic growth of *Magnetospirillum gryphiswaldense*. *J. Bacteriol.* **180**:159-162.
27. **Sambrook J, Russel D.** 2001. *Molecular cloning: A laboratory manual*, vol. 3rd ed. Cold Spring Harbor Laboratory Press, Cold Spring Harbor, New York.
28. **Raschdorf O, Müller FD, Posfai M, Plitzko JM, Schüler D.** 2013. The magnetosome proteins MamX, MamZ and MamH are involved in redox control of magnetite biomineralization in *Magnetospirillum gryphiswaldense*. *Mol. Microbiol.* **89**:872-886.
29. **Marrs B, Gest H.** 1973. Genetic mutations affecting the respiratory electron-transport system of the photosynthetic bacterium *Rhodospseudomonas capsulata*. *J. Bacteriol.* **114**:1045-1051.

30. **Katzmann E, Müller FD, Lang C, Messerer M, Winklhofer M, Plitzko JM, Schüler D.** 2011. Magnetosome chains are recruited to cellular division sites and split by asymmetric septation. *Mol. Microbiol.* **82**:1316-1329.
31. **Bueno E, Mesa S, Bedmar EJ, Richardson DJ, Delgado MJ.** 2012. Bacterial adaptation of respiration from oxic to microoxic and anoxic conditions: redox control. *Antioxid. Redox Signal.* **16**:819-852.
32. **Sakaguchi T, Arakaki A, Matsunaga T.** 2002. *Desulfovibrio magneticus sp. nov.*, a novel sulfate-reducing bacterium that produces intracellular single-domain-sized magnetite particles. *Int. J. Syst. Evol. Microbiol.* **52**:215-221.
33. **O'Gara JP, Kaplan S.** 1997. Evidence for the role of redox carriers in photosynthesis gene expression and carotenoid biosynthesis in *Rhodobacter sphaeroides* 2.4.1. *J. Bacteriol.* **179**:1951-1961.
34. **O'Gara JP, Eraso JM, Kaplan S.** 1998. A redox-responsive pathway for aerobic regulation of photosynthesis gene expression in *Rhodobacter sphaeroides* 2.4.1. *J. Bacteriol.* **180**:4044-4050.
35. **Zhou G, Yin J, Chen H, Hua Y, Sun L, Gao H.** 2013. Combined effect of loss of the *caa₃* oxidase and Crp regulation drives *Shewanella* to thrive in redox-stratified environments. *ISEM J.* **7**:1752-1763.
36. **Richardson DJ, King GF, Kelly DJ, Mcewan AG, Ferguson SJ, Jackson JB.** 1988. The role of auxiliary oxidants in maintaining redox balance during phototrophic growth of *Rhodobacter capsulatus* on propionate or butyrate. *Arch. Microbiol.* **150**:131-137.
37. **Ellington MJ, Bhakoo KK, Sawers G, Richardson DJ, Ferguson SJ.** 2002. Hierarchy of carbon source selection in *Paracoccus pantotrophus*: strict correlation between reduction state of the carbon substrate and aerobic expression of the *nap* operon. *J. Bacteriol.* **184**:4767-4774.
38. **Müller FD, Raschdorf O, Nudelman H, Messerer M, Katzmann E, Plitzko JM, Zarivach R, Schüler D.** 2013. The FtsZ-like protein FtsZm of *M. gryphiswaldense* likely interacts with its generic homolog and is required for biomineralization under nitrate deprivation. *J. Bacteriol.*
39. **Siponen MI, Adryanczyk G, Ginet N, Arnoux P, Pignol D.** 2012. Magnetochrome: a c-type cytochrome domain specific to magnetotactic bacteria. *Biochem. Soc. Trans.* **40**:1319-1323.
40. **Siponen MI, Legrand P, Widdrat M, Jones SR, Zhang WJ, Chang MCY, Faivre D, Arnoux P, Pignol D.** 2013. Structural insight into magnetochrome-mediated magnetite biomineralization. *Nature* **502**:681-684.

5.7 SUPPLEMENTAL MATERIALS

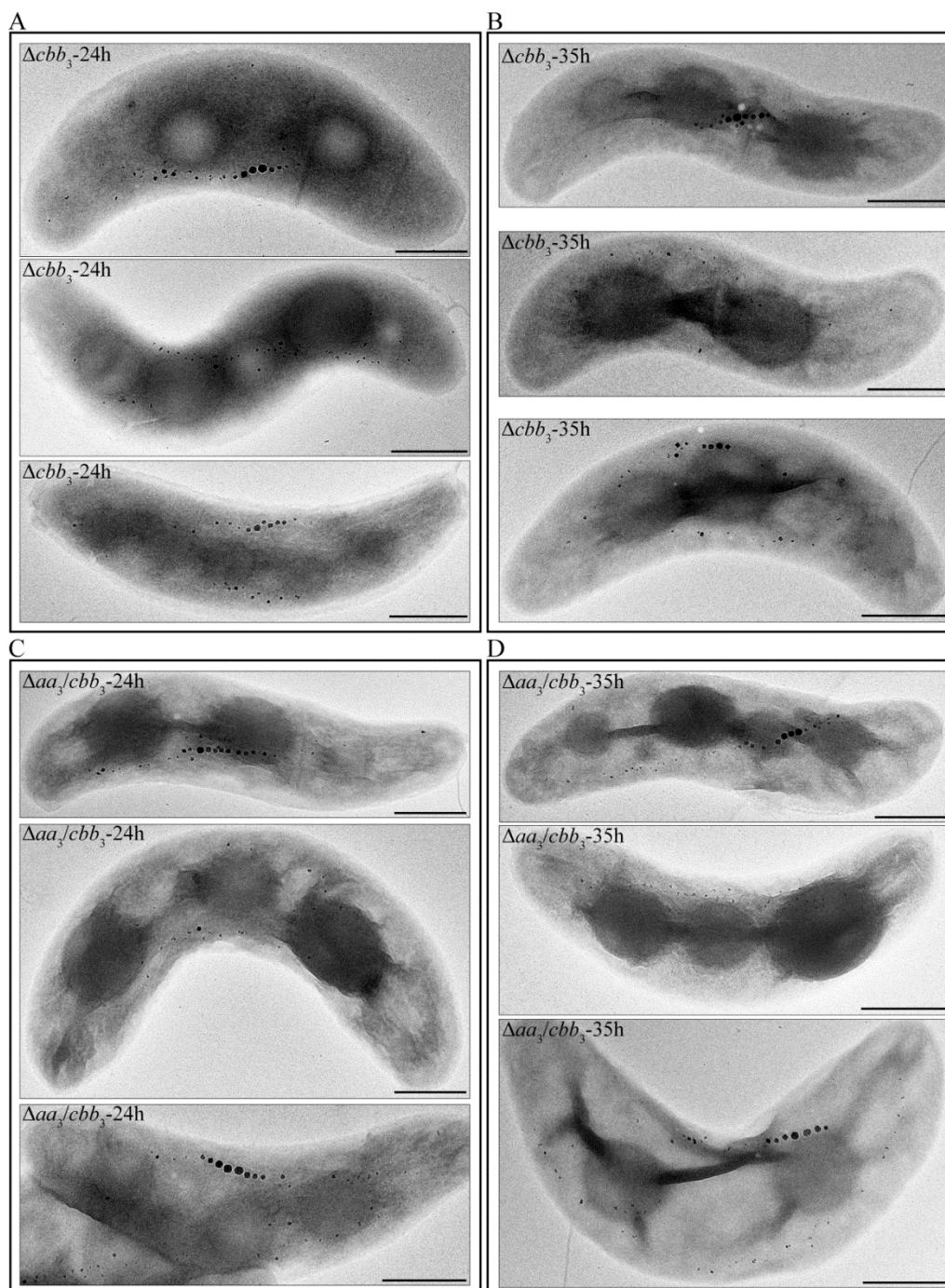


Fig. 5-S1 Biom mineralization phenotypes of Δcbb_3 and $\Delta aa_3\Delta cbb_3$ mutants incubated for 24 h (A and C) and 35 h (B and C) in microaerobic nitrate medium. Scale bar, 500 nm.

Table 5-S1 Bacterial strains and plasmids used in this work

Strain or plasmid	Description	Reference
Strains		
<i>E. coli</i> DH5 α	F ['] Φ 80d <i>lacZ</i> Δ M15 Δ (<i>lacZYA-argF</i>)U169 <i>deoR recA1 endA1 hsdR17</i> (r _k ⁻ , m _k ⁺) <i>phoA supE44 λ- thi-1 gyrA96 relA1</i>	Invitrogen
<i>E. coli</i> BW29427	<i>dap</i> auxotroph derivative of <i>E. coli</i> strain B2155	K. Datsenko and B. L. Wanner, unpublished
MSR-1 WT	Wild type R3/S1, but Rif ^r , Sm ^r	(1)
Δ <i>Mgfnr</i>	R3/S1, Δ <i>Mgfnr</i>	(Y. Li et al., submitted)
Δ <i>aa</i> ₃	R3/S1, Δ <i>aa</i> ₃	This study
Δ <i>bd</i>	R3/S1, Δ <i>bd</i>	This study
Δ <i>cbb</i> ₃	R3/S1, Δ <i>cbb</i> ₃	This study
Δ <i>bd</i> Δ <i>aa</i> ₃	R3/S1, Δ <i>bd</i> Δ <i>aa</i> ₃	This study
Δ <i>aa</i> ₃ Δ <i>cbb</i> ₃	R3/S1, Δ <i>aa</i> ₃ Δ <i>cbb</i> ₃	This study
Δ <i>bd</i> Δ <i>cbb</i> ₃	R3/S1, Δ <i>bd</i> Δ <i>cbb</i> ₃	This study
Plasmids		
pBBR1MCS-2	Km ^r , mobilizable broad-host-range vector	(2)
pOR093	<i>mamX</i> CXXCH (65,104)->AXXAH, pK19mobGII derivative, Km ^r	(3)
pLYJ97	pBBR1MCS-2 plus <i>gusA</i> from pK19mobGII	(4)
pLYJ115	pLYJ97 plus <i>aa</i> ₃ promoter region	This study
pLYJ128	pOR093 plus <i>cbb</i> ₃ 2-kb upstream and internal region	This study
pLYJ129	pOR093 plus <i>aa</i> ₃ 2-kb upstream region	This study
pLYJ130	pOR093 plus <i>bd</i> 2-kb downstream region	This study
pLYJ135	pLYJ97 plus <i>aa</i> ₃ promoter region	This study
pLYJ137	pLYJ97 plus <i>bd</i> promoter region	This study
pLYJ138	pBBR1MCS-2 plus <i>cbb</i> ₃ with its own promoter	This study
pLYJ139	pBBR1MCS-2 plus <i>aa</i> ₃ with its own promoter	This study
pLYJ140	pBBR1MCS-2 plus <i>bd</i> with its own promoter	This study

Table 5-S2 BlastP analyses of operons encoding terminal oxidases in MTB and non-MTB using MSR-1 as a query.

Protein in MSR-1	Encoded gene product (aa, kDa, pI)	AMB-1 (e-value, similarity)	MS-1 (e-value, similarity)	MC-1 (e-value, similarity)	RS-1 (e-value, similarity)	Best hit in non-MTB (e-value, similarity)
Mgr_2544	CcoN (532, 60.6, 9.09)	-	WP_009870373.1 (0.0, 93%)	Mmc1_2353 (0.0, 80%)	-	<i>Novispirillum itersonii</i> (0.0, 87%)
Mgr_2545	CcoO (243, 27.0, 6.30)	Amb4363 (4e-137, 86%)	WP_009870372.1 (7e-137, 86%)	Mmc1_2354 (1e-94, 70%)	-	<i>Novispirillum itersonii</i> (2e-124, 82%)
Mgr_2546	CcoQ (36, 4.4, 5.09)	Amb4364 (3e-09, 91%)	-	-	-	<i>Rhodospirillum rubrum</i> F11 (2e-11, 88%)
Mgr_2547	CcoP (291, 31.2, 5.90)	Amb4365 (8e-133, 76%)	WP_009870371.1 (1e-134, 77%)	Mmc1_2355 (4e-52, 49%)	-	<i>Phaeospirillum molischianum</i> (5e-123, 73%)
Mgr_0911	CoxB (269, 30.1, 6.29)	Amb2170 (1e-108, 76%)	WP_009868696.1 (3e-113, 77%)	-	-	<i>Novispirillum itersonii</i> (6e-105, 77%)
Mgr_0912	CoxA (526, 57.4, 7.96)	Amb2169 (0.0, 89%)	WP_009868695.1 (0.0, 89%)	-	-	<i>Novispirillum itersonii</i> (0.0, 88%)
Mgr_0913	CatG (180, 19.8, 8.93)	Amb2168 (2e-62, 68%)	WP_009868694.1 (2e-67, 72%)	-	-	<i>Azospirillum brasilense</i> Sp245 (3e-68, 75%)
Mgr_0914	CoxC (264, 29.5, 6.97)	Amb2168 (2e-115, 79%)	WP_009868693.1 (8e-104, 78%)	-	-	<i>Caenispirillum salinarum</i> (7e-105, 72%)
Mgr_0697	CydB (382, 41.3, 6.06)	-	-	-	DMR_06970 (1e-63, 54%) DMR_28310 (3e-23, 43%)	<i>Novispirillum itersonii</i> (0.0, 87%)
Mgr_0698	CydA (518, 57.6, 8.66)	-	-	-	DMR_06960 (2e-61, 46%) DMR_28300 (4e-108, 55%)	<i>Novispirillum itersonii</i> (0.0, 92%)

AMB-1: *Magnetospirillum magneticum*; MS-1: *Magnetospirillum magnetotacticum*; MC-1: *Magnetococcus marinus*; RS-1: *Desulfovibrio magneticus* strain RS-1. The *ccoN* gene encoding the catalytic subunit of *cbh*₃ oxidase is not found in *M. magneticum* while the *ccoQ* gene encoding a small membrane protein of unknown function is missing in *Ms. marinus* and the incomplete genome assembly of *M. magnetotacticum*. *D. magneticus* strain RS-1 harbors two *cydAB* operons as well as another operon *cyoABCDE* encoding a quinol oxidase *bo*₃ oxidase (DMR_14870, _14880, _14890, _14900, and _14910).

Table 5-S3 Growth (OD_{565 nm}), magnetic response (C_{mag}), and magnetosome crystal size of various terminal oxidase mutants under different conditions.

Strain	OD _{565 nm}	C _{mag}	Crystal size (nm)	<i>n</i>
0% O₂				
WT	0.13 ± 0.00	1.6 ± 0.1	38.0 ± 15.8	335
Δ <i>aa</i> ₃	0.13 ± 0.00	1.7 ± 0.0	38.4 ± 14.9	335
Δ <i>bd</i>	0.13 ± 0.00	1.6 ± 0.1	34.0 ± 18.2	427
Δ <i>bd</i> Δ <i>aa</i> ₃	0.14 ± 0.02	1.7 ± 0.1	35.9 ± 24.3	304
Δ <i>cbb</i> ₃	0.14 ± 0.01	1.7 ± 0.2	35.2 ± 23.4	300
Δ <i>aa</i> ₃ Δ <i>cbb</i> ₃	0.13 ± 0.00	1.7 ± 0.1	34.6 ± 16.6	470
Δ <i>bd</i> Δ <i>cbb</i> ₃	0.14 ± 0.01	1.6 ± 0.0	38.4 ± 19.9	318
2% O₂, +NO₃⁻				
WT	0.22 ± 0.01	1.6 ± 0.0	28.0 ± 15.3	337
Δ <i>aa</i> ₃	0.22 ± 0.01	1.6 ± 0.0	30.1 ± 15.0	334
Δ <i>bd</i>	0.20 ± 0.01	1.7 ± 0.0	30.1 ± 14.6	309
Δ <i>bd</i> Δ <i>aa</i> ₃	0.22 ± 0.01	1.7 ± 0.1	31.1 ± 13.0	319
2% O₂, +NH₄⁺				
WT	0.11 ± 0.00	1.5 ± 0.1	-	-
Δ <i>aa</i> ₃	0.12 ± 0.01	1.5 ± 0.0	-	-
Δ <i>bd</i>	0.10 ± 0.01	1.4 ± 0.1	-	-
Δ <i>bd</i> Δ <i>aa</i> ₃	0.11 ± 0.00	1.4 ± 0.1	-	-

Number of crystals measured for each strain (*n*) is presented in the last column.

REFERENCES

1. **Schultheiss D, Kube M, Schüler D.** 2004. Inactivation of the flagellin gene *flaA* in *Magnetospirillum gryphiswaldense* results in nonmagnetotactic mutants lacking flagellar filaments. *Appl. Environ. Microbiol.* **70**:3624-3631.
2. **Kovach ME, Elzer PH, Hill DS, Robertson GT, Farris MA, Roop RM, Peterson KM.** 1995. Four new derivatives of the broad-host-range cloning vector pBBR1MCS, carrying different antibiotic-resistance cassettes. *Gene* **166**:175-176.
3. **Raschdorf O, Müller FD, Posfai M, Plitzko JM, Schüler D.** 2013. The magnetosome proteins MamX, MamZ and MamH are involved in redox control of magnetite biomineralization in *Magnetospirillum gryphiswaldense*. *Mol. Microbiol.* **89**:872-886.
4. **Li Y, Katzmann E, Borg S, Schüler D.** 2012. The periplasmic nitrate reductase Nap is required for anaerobic growth and involved in redox control of magnetite biomineralization in *Magnetospirillum gryphiswaldense*. *J. Bacteriol.* **194**:4847-4856.

CHAPTER 6

DISCUSSION

6.1 Denitrification is involved in redox control of magnetite biomineralization

6.1.1 The periplasmic nitrate reductase Nap plays a role in anaerobic and aerobic growth and may poise optimum redox conditions for magnetite synthesis

In this work, we for the first time demonstrated that MSR-1 is capable of anaerobic growth and magnetite synthesis using nitrate as the only anaerobic electron acceptor. Our work indicates that the reduction of nitrate to nitrite catalyzed by the periplasmic nitrate reductase Nap is the primary energy-generating step for denitrification, whereas the subsequent reduction steps alone do not support anaerobic growth. WT cells did not synthesize magnetite when incubated in the absence of electron acceptors oxygen and nitrate, suggesting that magnetite biomineralization requires energy generated by respiratory activity.

Deletion of the entire *nap* cluster also severely impaired magnetite biomineralization under microaerobic conditions in the presence and absence of nitrate, resulting in the synthesis of fewer, smaller and misshapen magnetosome particles. This is in agreement with the finding by Taoka et al. that the abolishment of nitrate reductase activity by molybdenum deprivation led to an approximately 60% decrease of iron content, although they suggested that Nap is not essential to magnetite biomineralization (1). In some nonmagnetic bacteria, the Nap enzyme is also involved in redox balancing using nitrate as an ancillary oxidant to dissipate excess reductant which may cause lower growth rates (2, 3). Consistent with this, a significant delay of growth in Δnap mutant was observed under aerobic conditions. In addition, although the oxidation state of carbon sources did not affect the transcription of *nap*, the WT contained shorter chains with irregular crystals on the more reduced substrate acetate compared to the more oxidized substrate pyruvate, while in Δnap magnetite synthesis was equally low under both conditions. Therefore, similar to Nap in other bacteria, such as *P.*

pantotrophus (4) and various strains of *R. sphaeroides* (5-7), our data confirm a role of Nap of MSR-1 in the maintenance of the intracellular redox balance, thereby poising an optimum redox potential for magnetite synthesis. The lower C_{mag} even observed in acetate-grown WT cells might indicate that Nap activity is still insufficient to dispel all excess reductant originating from reduced carbon substrates.

6.1.2 Nitrite reductase NirS supports ferrous iron oxidation for anaerobic magnetite biomineralization

In contrast to Nap, we found that NirS is not absolutely required for anaerobic growth. The observed impairments in magnetite biomineralization in $\Delta nirS$ are not directly caused by the accumulation of nitrite as concluded from the following observations: (i) Although nitrite was built up to 1-2 mM when cells of WT and $\Delta nirS$ were incubated under a constant microaerobic atmosphere, no effect was observed on magnetite biomineralization; (ii) Added nitrate (20 mM) and nitrite (2.5 mM) were not completely reduced, but did not affect biomineralization in the WT and $\Delta nirS$; (iii) A $\Delta nirN$ culture still displayed defects in magnetite synthesis although all nitrite was completely depleted from the medium at the end of incubation. These data altogether suggest that the observed effects on magnetite synthesis in $\Delta nirS$ are directly associated with its enzymatic activity, which is in agreement with the proposed Fe(II):nitrite oxidoreductase function of NirS in magnetospirilla (8). However, different from the earlier assumption, our work demonstrated that the suspected iron-oxidizing activity is not confined to NirS of magnetotactic bacteria, but might be a common property of cytochrome *cd₁* nitrite reductases of all denitrifiers. The impaired magnetite synthesis in $\Delta nirS$ is probably a consequence of decreased oxidation of ferrous iron, which in the WT takes place in the periplasm and is catalyzed by NirS with nitrite as electron acceptor.

The conspicuous sequence similarity between NirS and NirN suggested a similar or related function of the two proteins and further raised the question whether NirN itself may catalyze nitrite reduction. However, despite of the superficially similar phenotypes in denitrifying growth and magnetosome formation, closer inspection revealed that deletion of *nirS* completely abolished nitrite reduction, whereas a $\Delta nirN$ mutant was still capable of reducing nitrite upon prolonged incubation. This proved that NirN is indirectly involved in nitrite reduction, and not sufficient to support nitrite reduction in the absence of NirS. Therefore, we concluded that in MSR-1 NirN is likely related to biomineralization only indirectly through

physiological functional interaction with NirS, and NirS is the only enzyme for nitrite reduction.

6.1.3 NorCB proteins are essential for growth by denitrification and involved in magnetite biomineralization by yet-unknown functions

In an earlier study poor growth and low C_{mag} values were described in a $\Delta norB$ mutant of *M. magneticum* grown under anaerobic conditions (9). However, no growth was observed in the $\Delta norCB$ mutant of MSR-1 under anaerobic and microaerobic conditions in the presence of nitrate. This may be caused by the toxicity of nitric oxide, which as the product of nitrite reduction was accumulated in the $\Delta norCB$ mutant while converted to non-toxic N_2O in the WT. The growth discrepancy between *nor* mutants of MSR-1 (no growth) and *M. magneticum* (poor growth) might be due to different genotypes: In MSR-1 *norCB* genes were completely eliminated, whereas in *M. magneticum* only *norB* (downstream of *norC*) was interrupted by transposon insertion, thereby possibly retaining some residual activity of the nitric oxide reductase. Among all denitrification genes, the *norCB-gusA* fusion showed the highest expression, suggesting that a high expression level of *norCB* in MSR-1 is mandatory to reduce all toxic NO to N_2O during denitrification.

Deletion of *norCB* also resulted in the formation of fewer magnetosome particles and slightly aberrant cell morphology in microaerobic ammonium medium. These relatively subtle effects are unlikely caused by limited energy yields during denitrification as speculated by Wang et al. (9), since there is no denitrification occurring in the absence of nitrate. On the other hand, the comparatively high expression levels of the *norCB-gusA* fusion indicate that under microaerobic and aerobic conditions in the absence of nitrate NorCB may be involved in further, yet unknown functions directly or indirectly linked to magnetite biomineralization. For example, it has been shown that Nor from *P. denitrificans* is able to reduce oxygen to water *in vitro* (10, 11), which might be a possible role of NorCB in MSR-1 in microaerobic respiration and magnetite biomineralization.

6.2 Oxygen respiration is linked to magnetite biomineralization

In addition to denitrification, MSR-1 is also capable of aerobic respiration using oxygen as terminal electron acceptor. In this work, three putative terminal oxidases (*cbb*₃-type, *aa*₃-type, and *bd*-type) were identified in MSR-1. Mutagenesis of different terminal oxidases demonstrated that only oxidases *cbb*₃ and *bd* are the functional enzymes for aerobic respiration, whereas *aa*₃ oxidase has no physiological significance for O₂ reduction under test conditions. In agreement with this, Δcbb_3 and $\Delta aa_3\Delta cbb_3$ mutants displayed identical phenotypes, further suggesting that the *aa*₃ oxidase does not participate in aerobic respiration in the laboratory. In natural habitats, MSR-1 cells are adapted to low O₂ conditions, under which high-affinity terminal oxidases like *cbb*₃ are favorable for O₂ respiration and energy conservation. In contrast, the *aa*₃ oxidase which has a low affinity for O₂ (12), is insufficient to utilize trace amount of O₂. Therefore, it is not surprising that the *aa*₃ oxidase does not show any activity for O₂ reduction.

Based on the observation that a $\Delta bd\Delta cbb_3$ double deletion mutant did not grow in the presence of oxygen, we concluded that aerobic respiration is a prerequisite for microaerobic denitrification. Loss of the *bd* oxidase alone did not affect growth and magnetite biomineralization, which indicates that when *cbb*₃ oxidase is present, the *bd* oxidase might only provide a minor contribution to aerobic respiration. However, it is also possible that the activity of *bd* oxidase is induced to compensate the activity of *cbb*₃ only when *cbb*₃ oxidase is eliminated. Unlike *cbb*₃ and *aa*₃ oxidases which are present in other magnetospirilla *M. magneticum* and *M. magnetotacticum*, the *bd* oxidase is completely absent in these strains. This implies that the *bd* oxidase is likely dispensable in various magnetotactic bacteria, while *aa*₃ probably acts as an alternative terminal oxidase in these two magnetospirilla. In magnetotactic bacterium *Ms. marinus* which is unable to grow aerobically, neither *bd* nor *aa*₃ oxidase is present. Nevertheless, the *bd* oxidase might have unknown functions in MSR-1 whereas the *cbb*₃ oxidase may also be the only functional enzyme used for aerobic respiration in *M. magneticum* and *M. magnetotacticum*.

Delayed growth in microaerobic ammonium medium was observed in Δcbb_3 and $\Delta aa_3\Delta cbb_3$ mutants. This might be caused by the low efficiency of *bd* oxidase, since *bd* oxidase does not pump protons but only accepts electrons directly from quinol for O₂ reduction (13). Δcbb_3 and $\Delta aa_3\Delta cbb_3$ mutants displayed an even larger delay of growth in microaerobic nitrate

medium, where mutant cells did not start to reduce nitrate until O₂ was completely depleted, suggesting that the *cbb*₃ oxidase *per se*, but not aerobic respiration, is crucial for simultaneous O₂ and nitrate reduction. Therefore, besides as a terminal oxidase, *cbb*₃ oxidase may be capable of sensing O₂ and have a further key function to activate denitrification and aerobic respiration simultaneously. In microaerobic nitrate medium during early growth phase only aerobic respiration occurred (similar to conditions in microaerobic ammonium medium), while during the later growth phase only denitrification occurred and mutant cells also showed similar growth rates as the anaerobically growing WT. However, the biomineralization phenotypes of Δcbb_3 and $\Delta aa_3\Delta cbb_3$ mutants under this condition were much different from those in either microaerobic ammonium medium or anaerobic nitrate medium. Thus, it can be ruled out that the severe defects in magnetite synthesis in Δcbb_3 and $\Delta aa_3\Delta cbb_3$ mutants were caused by the incapability of co-occurrence of denitrification and aerobic respiration. Instead, severely impaired magnetosome formation likely results from the loss of *cbb*₃ oxidase *per se*, which argues for a more direct role of *cbb*₃ oxidase in magnetite biomineralization. In *R. sphaeroides*, besides as a terminal oxidase, *cbb*₃ oxidase also functions as a redox sensor to repress the activity of photosynthesis genes under aerobic conditions by controlling the activity of transcriptional regulators of photosynthesis gene expression (14-17). Therefore, it can be assumed that the *cbb*₃ oxidase of MSR-1 may have a similar role in magnetite biomineralization. In agreement with this, in Δcbb_3 and $\Delta aa_3\Delta cbb_3$ mutants the NAD⁺/NADH ratio under microaerobic conditions was more reduced than that in the WT. This is not surprising since as a terminal oxidase, *cbb*₃ is capable of accepting electrons during O₂ reduction. However, an optimal redox state (i.e. balanced ratio of Fe²⁺/Fe³⁺) seems to be very important for microaerobic biomineralization of the mixed-valence iron oxide magnetite [Fe(II)Fe(III)₂O₄] especially in the presence of nitrate. The loss of *cbb*₃ oxidase may further affect some other factors which are involved in magnetite biosynthesis. For example, some proteins encoded by genes within the genomic magnetosome island of MSR-1, such as MamX, MamZ, and FtsZ-like protein FtsZm, displayed different effects on magnetosome formation between in the presence and absence of nitrate (18, 19). Also, magnetospirilla contain a unique set of redox active magnetosome-associated proteins, which share a novel configuration of two close CXXCH heme-binding motifs, the magnetochrome domain (18, 20, 21). Therefore, the change of intracellular redox state may affect the activity or conformation of these proteins and further impair the redox balance of ferrous and ferric iron for magnetite synthesis. More complex magnetosome phenotypes, such as the presence of two magnetosome chains in the mutants indicate that

magnetosome chain assembly might be also regulated by the cellular redox state. Besides magnetosome-related proteins, the nitrite reductase NirS which shows a Fe(II): nitrite oxidoreductase activity, plays a role in magnetite biomineralization only under low O₂ conditions in the presence of nitrate. However, more reduced conditions in Δcbb_3 and $\Delta aa_3\Delta cbb_3$ mutants likely limit the concentration of ferric iron and further prevent the oxidation of ferrous iron for magnetite synthesis, thereby resulting in severely impaired magnetosome formation in the presence of nitrate. In addition, variable cell morphologies of microaerobically growing Δcbb_3 and $\Delta aa_3\Delta cbb_3$ mutants in the presence of nitrate, which are likely caused by delayed growth as well as reduced intracellular redox conditions, might be used to adapt to a changed condition.

6.3 Regulation of respiration and magnetite biomineralization in response to different oxygen concentrations

The common observation that magnetosomes are only synthesized under suboxic conditions raised the possibility of protein-mediated regulation of magnetite biomineralization. As described in the previous section, denitrification and oxygen respiration are involved in redox control required for anaerobic and microaerobic magnetite biomineralization. In *E. coli* and other bacteria the switch between aerobic and microaerobic metabolism is primarily controlled by an Fnr regulator (12, 22). Therefore, in this work we identified a putative Fnr protein (named MgFnr) in MSR-1 and tested whether the MgFnr protein also plays a role in growth and magnetite biomineralization. In fact, deletion of *Mgfnr* only affected magnetosome formation under microaerobic conditions in the presence of nitrate (i.e. when denitrification was active) but not in its absence. This implies that MgFnr might be involved in magnetite synthesis by regulation of denitrification genes, whereas expression of the terminal oxidases for O₂ respiration is not under the control of MgFnr, similar to Fnr from *S. oneidensis* (23). In agreement with this, neither the rates of oxygen consumption nor transcription of terminal oxidase genes displayed any difference in between the WT and $\Delta Mgfnr$ mutant. The presence of putative Fnr binding sites in the promoter regions of all operons encoding for denitrification further indicates that MgFnr is capable of controlling the transcription of denitrification genes in response to different oxygen concentrations. Consistent with this, transcription patterns of denitrification genes in $\Delta Mgfnr$ mutant were different from those in the WT. For instance, in the $\Delta Mgfnr$ strain the expression of *nap* was

no longer upregulated by oxygen, the expression of *nirS* under aerobic conditions was much higher than that in the WT, and the aerobic expression of *nor* and *nosZ* was no longer repressed but upregulated by oxygen. Furthermore, we failed to identify a putative Fnr protein encoded in the non-denitrifying magnetotactic bacteria *Ms. marinus* or *D. magneticus*, which also suggests that Fnr of magnetotactic bacteria is likely only involved in regulating expression of genes encoding for denitrification, but not required for aerobic respiration.

The observation of significantly decreased N₂ evolution in $\Delta Mgfnr$ mutant raised the question which step(s) of denitrification is affected by the loss of MgFnr. This does not likely result from the reduction steps from NO₃⁻ to N₂O based on the following findings: (i) The consumption rate of NO₃⁻ and NO₂⁻ was not reduced in $\Delta Mgfnr$ mutant; (ii) NO is lethal to the cells while no growth defect was observed in $\Delta Mgfnr$ mutant; (iii) No NO emission was found during mass spectrometry experiments which also implies that the activity of NO reductase is not affected by the deletion of *Mgfnr*; (iv) The N₂O emission rate after addition of nitrate was similar for $\Delta Mgfnr$ mutant and WT. Therefore, it can be concluded that loss of MgFnr only affects the last step of denitrification, the reduction of N₂O to N₂. In agreement with this, the emission rate of N₂ was lower for $\Delta Mgfnr$ mutant than for the WT. However, it cannot be excluded that loss of MgFnr has an impact on other pathways involved in biomineralization. For instance, it has been shown that (i) besides acting as nitrate reductase, Nap also plays a role in redox control for magnetite biomineralization, (ii) nitrite reductase NirS is capable of oxidizing ferrous iron to ferric iron for magnetite synthesis, and (iii) NO reductase Nor also participates in magnetosome formation by yet unknown functions. In addition, deletion of *Mgfnr* caused different phenotypes under anaerobic and microaerobic conditions in the presence of nitrate. This indicates that MgFnr plays a more important role under conditions when O₂ respiration and denitrification occur simultaneously. In combination with the observation that maintaining a balance between aerobic respiration and denitrification is required for WT-like magnetite biomineralization, we propose that MgFnr might provide the main contribution to mediate the expression of denitrification genes, and thereby poise the redox state for magnetosome formation.

Although MgFnr was able to complement a $\Delta Ecfnr$ mutant (*E. coli* Δfnr mutant) back to WT-like growth, which indicates that MgFnr also has the common properties of EcFnr, significantly different phenotypes during anaerobic growth were observed between $\Delta Ecfnr$ mutant and $\Delta Mgfnr$ mutant, such as a largely decreased growth yield in $\Delta Ecfnr$ mutant, while

no impaired growth in $\Delta Mgfnr$ mutant. These differences might be due to different media used for cultivation because in *E. coli* deletion of *Ecfnr* only led to growth defects in some minimal media (24) while there is no minimal medium available, which provides reliable growth of MSR-1. In addition, not only deletion of *Mgfnr* but also overexpression of *Mgfnr* in WT affected anaerobic and microaerobic magnetite biomineralization in the presence of nitrate and caused the synthesis of smaller magnetosome particles, which indicates that the proper expression of MgFnr is crucial for WT-like magnetosome synthesis and the expression level is under precise control, being regulated by itself and oxygen. Therefore, MgFnr might play an important role in poising redox conditions for magnetite synthesis by controlling the expression of denitrification genes, and thus the expression of MgFnr is required to be strictly regulated. However, it is unknown whether the expression of MgFnr is also controlled by other yet unknown proteins, and whether the expression of other genes involved in magnetosome formation is also regulated by MgFnr.

In conclusion, our work for the first time revealed a complete respiratory system in magnetotactic bacteria (Fig. 6-1). In addition to the denitrification pathway, which is regulated by MgFnr, two different branches of the respiration chain occur for O₂ reduction: one is the cytochrome bc₁-c-cbb₃ branch, and the other is that quinol oxidase bd directly accepts the electrons from quinol. O₂ respiration is a prerequisite for microaerobic denitrification. The genetic and biochemical analyses provided evidence that in MSR-1 in addition to the various essential and accessory proteins encoded within the genomic magnetosome island, genes outside magnetosome island are also involved in magnetite biomineralization. By poising the redox state required for magnetite biomineralization, denitrification and aerobic respiration have a key role in the synthesis of WT-like magnetosomes.

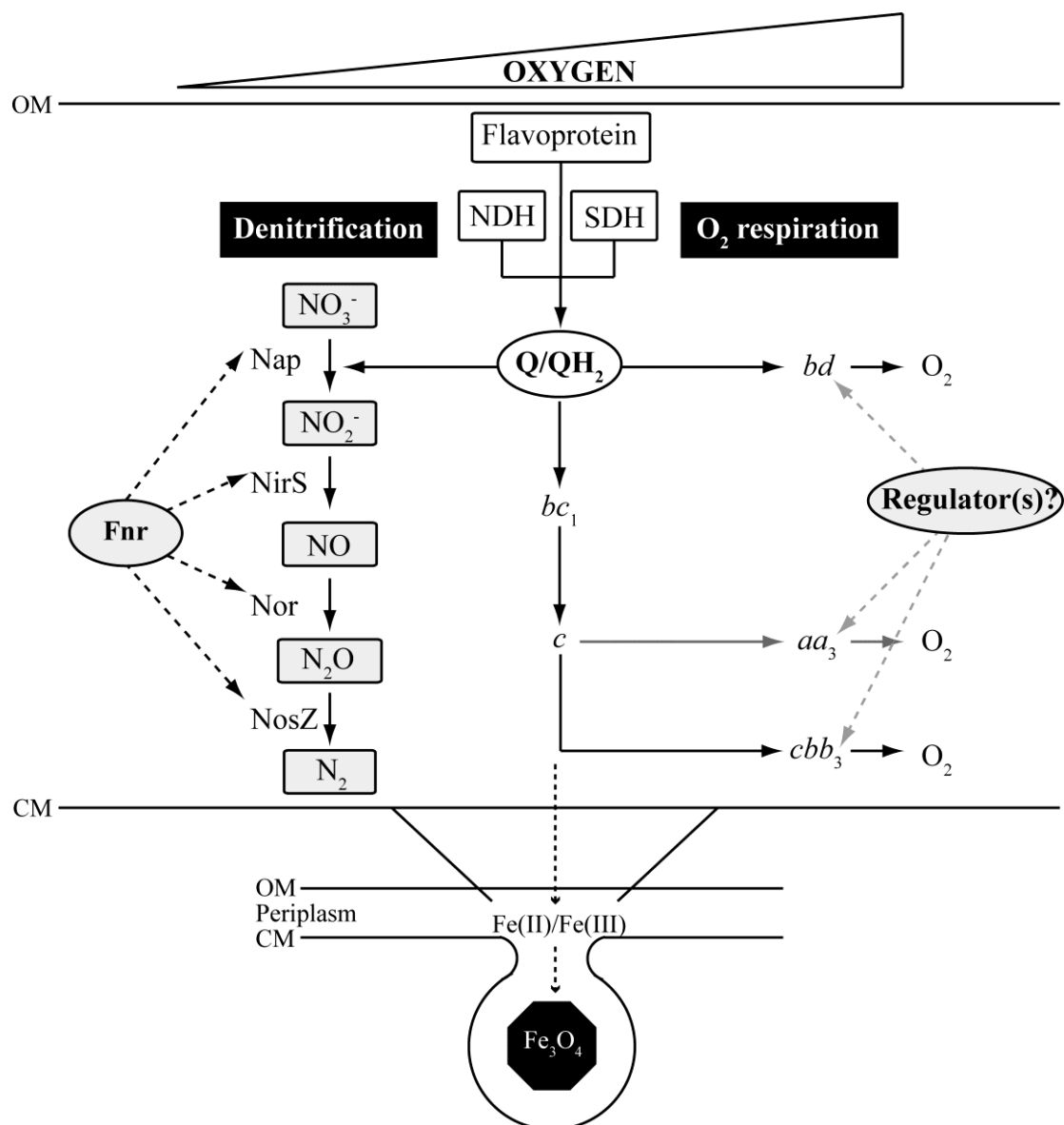


Fig. 6-1 Respiratory pathways in MSR-1. Two respiration pathways, denitrification and aerobic respiration, were identified in MSR-1. Two different branches of the respiration chain occur for O₂ reduction: one is the cytochrome *bc*₁-*c*-*cbb*₃ branch, and the other is that quinol oxidase *bd* directly accepts the electrons from quinol. O₂ respiration is a prerequisite for microaerobic denitrification. Besides used to generate energy for the growth, denitrification and oxygen respiration also play a role in poising the redox state required for magnetite biosynthesis. However, it is unknown whether enzymes acting upstream of the terminal oxidases, the redox state of the quinone pool, as well as the volume of electron flow through different branches of the electron transport chain, are also involved in the redox control required for magnetite biomineralization. Furthermore, it remains unclear whether terminal oxidases have other functions, such as participating in detoxification under O₂-rich growing conditions, or in aerotaxis or magnetotaxis to facilitate search for growth-favoring suboxic growing conditions. In addition to the oxygen sensor Fnr, which plays a role in controlling expression of denitrification genes and thus is involved in magnetite biomineralization, other unknown O₂ sensors probably occur to mediate the expression of genes encoding for aerobic respiration or to regulate the redox state for magnetite biomineralization in response to different oxygen concentrations. Solid-line arrows indicate the electron flow. SDH, succinate dehydrogenase; NDH, NADH dehydrogenase; Q/QH₂, quinone/quinol pool in the membrane; *bc*₁, cytochrome *bc*₁; *c*, cytochrome *c*. OM, outer membrane; CM, cytoplasmic membrane.

6.4 Open questions and further research

6.4.1 Which subunit(s) of Nap is involved in magnetite biomineralization?

Some organisms such as *Shewanella* and *Geobacter* species, respire mineral iron and are capable of formation of magnetite in the extracellular space (25). Since the ferric iron mineral as a respiratory electron acceptor, is an insoluble particle and thus cannot freely diffuse into bacterial cells, a cytochrome protein CymA is used to deliver the electron from the quinol pool to a MtrABC complex, which further transfers the electron to minerals located outside of the cell (26, 27). A CymA analogue NapC is found in magnetotactic bacteria, which is a subunit of the periplasmic nitrate reductase Nap encoded by the *nap* operon *napFDAGHBC*. Therefore, it is proposed that in addition to transferring the electron from the quinol pool for nitrate reduction, NapC probably plays a role in magnetite biomineralization by supplying the electron to magnetosome-associated proteins for the biosynthesis of magnetite (20). On the other hand, deletion of the whole *nap* operon severely impaired magnetite biomineralization and resulted in the biosynthesis of fewer, smaller and irregular crystals during denitrification and aerobic respiration. This raises the possibilities that impaired biomineralization in Δnap mutant is caused by the loss of NapC, or that other subunits of Nap are also required for the biosynthesis of WT-like magnetite particles. To this end, different single deletion mutants of *napFDAGHBC* have been constructed, including $\Delta napF$, $\Delta napD$, $\Delta napA$, $\Delta napH$, $\Delta napB$, and $\Delta napC$ (Y. Li, unpublished data). However, except for *napD*, deletion of any of other genes within the *nap* operon did not affect the synthesis of magnetite (Y. Li, unpublished data). Further analyses of these single *nap* deletion mutants on denitrifying growth and magnetite biomineralization will lead to a better understanding of the role of the Nap in biomineralization.

6.4.2 Do other proteins involved in electron transport play a role in magnetite biomineralization?

Despite the fact that terminal oxidase *cbb₃* acts as an O₂ sensor to poise the redox conditions for magnetite biomineralization, it will be interesting to know whether enzymes acting upstream of the *cbb₃* oxidase, the redox state of the quinone pool, as well as the volume of electron flow through different branches of the electron transport chain, are also involved in magnetite biomineralization. Therefore, by inhibition and mutagenesis, blocking and

impairing the electron transport chain will gain further insights into the relationship between respiration and magnetite biomineralization. On the other hand, although the *aa₃* oxidase does not show any physiological significance for O₂ reduction in the laboratory, it cannot be excluded that *aa₃* oxidase has some properties in nature. Furthermore, in addition to their essential role in aerobic respiration, the *bd* and *cbb₃* oxidases may have other yet-unknown functions. Therefore, more comprehensive analyses of terminal oxidases, such as the role in O₂-detoxification at O₂-rich environment and the role in aerotaxis and magnetotaxis to facilitate search for growth-favoring suboxic growing conditions, will be helpful to evaluate the functions of different terminal oxidases in magnetotactic bacteria.

6.4.3 Do other putative O₂ sensors occur in MSR-1 and control magnetite biomineralization by regulating the redox potential in response to different oxygen conditions?

As discussed above, although Fnr of MSR-1 mediates oxygen-dependent regulation, its relatively subtle and indirect effects on magnetite biomineralization cannot account for the observed complete inhibition of magnetite biosynthesis under aerobic conditions. Furthermore, since Fnr of MSR-1 only affects expression of denitrification genes but not genes encoding for O₂ respiration, some unknown O₂ regulators are probably present and mediate the expression of aerobic terminal oxidase genes in response to different oxygen concentrations, and magnetite biomineralization is also probably regulated by other unknown O₂ sensors through controlling intracellular redox conditions. Therefore, several potential regulators which have been described to be capable of acting as redox sensors in other bacteria, were identified in MSR-1 (Table 6-1) (Y. Li, unpublished data). In the future, by mutagenesis, a more expanded search for regulators involved in O₂ respiration may gain further insights into the mechanism of oxygen-dependent regulation of magnetite biomineralization.

Table 6-1 Identification of putative redox sensors in magnetospirilla

Putative sensor ^a	Function	MSR-1	Other magnetospirilla	
			AMB-1 ^b	MS-1 ^b
OxyR	Sensing oxidative stress ^c (<i>E. coli</i>)	MGR_2168	-	-
		MGR_2971	Amb0589	MTAC_1561
		MGR_1920	-	-
		MGR_1832	-	-
		MGR_0925	-	-

		MGR_3776	-	-
		MGR_0954	-	-
		MGR_1331	Amb4341	MTAC_1755
		MGR_3423	Amb0224	MTAC_0369
		MGR_3582	-	-
		MGR_2377	Amb0662	MTAC_4583
		MGR_1479	-	-
		MGR_1466	-	-
FixL	Regulation of nitrogen fixation (<i>Sinorhizobium meliloti</i>)	MGR_3308 ^d	Amb0896	MTAC_2889
		MGR_0571	-	-
NifL	Regulation of nitrogen fixation (<i>Azotobacter vinelandii</i>)	MGR_2943	-	-
		MGR_3433	-	-
HemAT	Chemotaxis (<i>Bacillus subtilis</i>)	MGR_2126	Amb2795	MTAC_0813
Aer	Aerotaxis (<i>E. coli</i>)	MGR_3404	-	-
		MGR_0403	-	-
ArcB	Regulation of respiration (<i>E. coli</i>)	MGR_0376	Amb1110	-

^a OxyR is a sensor of peroxide stress and able to mediate the cellular response to hydrogen peroxide. In response to peroxide treatment, OxyR activates the expression of detoxifying genes such as genes encoding hydroperoxidase I katG and alkylhydroperoxide reductase (28). FixL and NifL are regulators involved in controlling the expression of nitrogen fixation genes (29, 30). The HemAT protein is described to sense the presence of O₂ and modulate the activity of proteins which control flagella rotation (31), while Aer of *E. coli* participates in the regulation of the motility behavior in gradient of O₂, redox conditions and some nutrients (32). The ArcAB two-component system of *E. coli* is a global sensor of gene expression under suboxic growing conditions, which is achieved by sensing the redox state of the quinone pool (33).

^b AMB-1, *M. magneticum*; MS-1, *M. magnetotacticum*.

^c Organism used for reference protein sequences in BLASTP analyses.

^d One of genes encoding FixL protein (MGR_3308, indicated in gray box) has been deleted (Y. Li, unpublished data).

However, in addition to a possible effect caused by genetic regulation, alternatively, directly abiogenic perturbation of the redox balance of iron ions required for magnetite synthesis also probably exists in MSR-1. For example, ferrous iron can also be chemically oxidized by nitrite (34, 35), and nitrite and oxygen are potent oxidants for ferrous iron also in a chemical method for the preparation of magnetite films, ferrite plating (36). Therefore, magnetite biomineralization might be achieved by combined abiogenic oxidation and bioenzymatic catalysis.

6.4.4 How magnetotactic bacteria decompose the toxic products of O₂ respiration?

Magnetotactic bacteria can accumulate up to 3% intracellular iron content, which is 100-fold higher than that in *E. coli* (37). This high iron content in magnetotactic bacteria may lead to oxidative damage to DNA when free Fe²⁺ reacts with hydrogen peroxide via the Fenton reaction (38). To eliminate the toxic oxygen radicals such as hydrogen peroxide produced during respiration, an effective oxygen protective system is required to cope with the oxidative stress. The role in protecting cells against organic peroxides is exerted by different peroxide-scavenging enzymes. In the genome assembly of MSR-1, different genes encoding for decomposition of hydrogen peroxide are present (Table 6-2) (Y. Li, unpublished data). The function of different peroxide-scavenging enzymes should be tested, which may provide new insights to explain how magnetotactic bacteria are capable of utilizing such high amounts of iron for biomineralization.

Table 6-2 Putative enzymes involved in the decomposition of H₂O₂ in magnetospirilla

Putative enzyme	Function	MSR-1	Other magnetospirilla	
			AMB-1 ^b	MS-1 ^b
AhpC	Alkyl hydroperoxidase ^a (<i>Azospirillum brasilense</i>)	^c MGR_3748	-	-
		MGR_2378	Amb0663	-
		MGR_2380	Amb0664	MTAC_2744
		MGR_2715	Amb2684	MTAC_2431
KatG	Catalase (<i>E. coli</i>)	MGR_4274	-	-
Gpx	Glutathione peroxidase (<i>E. coli</i>)	MGR_2358	Amb3627	MTAC_4680
Tpx	Thiol peroxidase (<i>Rhodopirellula baltica</i>)	MGR_4262	Amb3876	MTAC_3424
CCP	Cytochrome <i>c</i> peroxidase (<i>Zymomonas mobilis</i>)	MGR_1307	Amb2882	-
		MGR_1787	-	-

^aOrganism used for reference protein sequences in BLASTP analyses.

^bAMB-1, *M. magneticum*; MS-1, *M. magnetotacticum*.

^cOne of genes encoding AhpC protein (MGR_3748, indicated in gray box) has been deleted (Y. Li, unpublished data).

6.5 REFERENCES

1. **Taoka A, Yoshimatsu K, Kanemori M, Fukumori Y.** 2003. Nitrate reductase from the magnetotactic bacterium *Magnetospirillum magnetotacticum* MS-1: purification and sequence analyses. *Can. J. Microbiol.* **49**:197-206.

2. **Richardson DJ, King GF, Kelly DJ, Mcewan AG, Ferguson SJ, Jackson JB.** 1988. The role of auxiliary oxidants in maintaining redox balance during phototrophic growth of *Rhodobacter capsulatus* on propionate or butyrate. *Arch. Microbiol.* **150**:131-137.
3. **Richardson DJ, Berks BC, Russell DA, Spiro S, Taylor CJ.** 2001. Functional, biochemical and genetic diversity of prokaryotic nitrate reductases. *Cell. Mol. Life Sci.* **58**:165-178.
4. **Sears HJ, Spiro S, Richardi J.** 1997. Effect of carbon substrate and aeration on nitrate reduction and expression of the periplasmic and membrane-bound nitrate reductases in carbon-limited continuous cultures of *Paracoccus denitrificans* Pd1222. *Microbiology* **143**:3767-3774.
5. **Gavira M, Roldan MD, Castillo F, Moreno-Vivian C.** 2002. Regulation of *nap* gene expression and periplasmic nitrate reductase activity in the phototrophic bacterium *Rhodobacter sphaeroides* DSM158. *J. Bacteriol.* **184**:1693-1702.
6. **Tabata A, Yamamoto I, Matsuzaki M, Satoh T.** 2005. Differential regulation of periplasmic nitrate reductase gene (*napKEFDABC*) expression between aerobiosis and anaerobiosis with nitrate in a denitrifying phototroph *Rhodobacter sphaeroides* f. *sp. denitrificans*. *Arch. Microbiol.* **184**:108-116.
7. **Hartsock A, Shapleigh JP.** 2011. Physiological roles for two periplasmic nitrate reductases in *Rhodobacter sphaeroides* 2.4.3 (ATCC 17025). *J. Bacteriol.* **193**:6483-6489.
8. **Yamazaki T, Oyanagi H, Fujiwara T, Fukumori Y.** 1995. Nitrite reductase from the magnetotactic bacterium *Magnetospirillum magnetotacticum* - a novel cytochrome *cd*₁ with Fe(II)-nitrite oxidoreductase activity. *Eur. J. Biochem.* **233**:665-671.
9. **Wang K, Ge X, Bo T, Chen Q, Chen G, Liu W.** 2011. Interruption of the denitrification pathway influences cell growth and magnetosome formation in *Magnetospirillum magneticum* AMB-1. *Lett. Appl. Microbiol.* **53**:55-62.
10. **Fujiwara T, Fukumori Y.** 1996. Cytochrome *cb*-type nitric oxide reductase with cytochrome *c* oxidase activity from *Paracoccus denitrificans* ATCC 35512. *J. Bacteriol.* **178**:1866-1871.
11. **Flock U, Watmough NJ, Adelroth P.** 2005. Electron/proton coupling in bacterial nitric oxide reductase during reduction of oxygen. *Biochemistry* **44**:10711-10719.
12. **Bueno E, Mesa S, Bedmar EJ, Richardson DJ, Delgado MJ.** 2012. Bacterial adaptation of respiration from oxic to microoxic and anoxic conditions: redox control. *Antioxid. Redox Signal.* **16**:819-852.
13. **VanOrsdel CE, Bhatt S, Allen RJ, Brenner EP, Hobson JJ, Jamil A, Haynes BM, Genson AM, Hemm MR.** 2013. The *Escherichia coli* CydX protein is a member of the CydAB cytochrome *bd* oxidase complex and is required for cytochrome *bd* oxidase activity. *J. Bacteriol.* **195**:3640-3650.

14. **O'Gara JP, Kaplan S.** 1997. Evidence for the role of redox carriers in photosynthesis gene expression and carotenoid biosynthesis in *Rhodobacter sphaeroides* 2.4.1. J. Bacteriol. **179**:1951-1961.
15. **O'Gara JP, Eraso JM, Kaplan S.** 1998. A redox-responsive pathway for aerobic regulation of photosynthesis gene expression in *Rhodobacter sphaeroides* 2.4.1. J. Bacteriol. **180**:4044-4050.
16. **Oh JI, Kaplan S.** 2001. Generalized approach to the regulation and integration of gene expression. Mol. Microbiol. **39**:1116-1123.
17. **Oh JI, Kaplan S.** 2002. Oxygen adaptation . The role of the CcoQ subunit of the *cbb₃* cytochrome *c* oxidase of *Rhodobacter sphaeroides* 2.4.1. J. Biol. Chem. **277**:16220-16228.
18. **Raschdorf O, Müller FD, Posfai M, Plitzko JM, Schüler D.** 2013. The magnetosome proteins MamX, MamZ and MamH are involved in redox control of magnetite biomineralization in *Magnetospirillum gryphiswaldense*. Mol. Microbiol. **89**:872-886.
19. **Müller FD, Raschdorf O, Nudelman H, Messerer M, Katzmann E, Plitzko JM, Zarivach R, Schüler D.** 2014. The FtsZ-Like protein FtsZm of *Magnetospirillum gryphiswaldense* likely interacts with its generic homolog and is required for biomineralization under nitrate deprivation. J. Bacteriol. **196**:650-659.
20. **Siponen MI, Adryanczyk G, Ginet N, Arnoux P, Pignol D.** 2012. Magnetochrome: a *c*-type cytochrome domain specific to magnetotactic bacteria. Biochem. Soc. Trans. **40**:1319-1323.
21. **Siponen MI, Legrand P, Widdrat M, Jones SR, Zhang WJ, Chang MCY, Faivre D, Arnoux P, Pignol D.** 2013. Structural insight into magnetochrome-mediated magnetite biomineralization. Nature **502**:681-684.
22. **Uden G, Becker S, Bongaerts J, Holighaus G, Schirawski J, Six S.** 1995. O₂-sensing and O₂-dependent gene regulation in facultatively anaerobic bacteria. Arch. Microbiol. **164**:81-90.
23. **Zhou G, Yin J, Chen H, Hua Y, Sun L, Gao H.** 2013. Combined effect of loss of the *caa₃* oxidase and Crp regulation drives *Shewanella* to thrive in redox-stratified environments. ISME J. **7**:1752-1763.
24. **Lambden PR, Guest JR.** 1976. Mutants of *Escherichia coli* K12 unable to use fumarate as an anaerobic electron acceptor. J. Gen. Microbiol. **97**:145-160.
25. **Bird LJ, Bonnefoy V, Newman DK.** 2011. Bioenergetic challenges of microbial iron metabolisms. Trends Microbiol. **19**:330-340.
26. **Clarke TA, Edwards MJ, Gates AJ, Hall A, White GF, Bradley J, Reardon CL, Shi L, Beliaev AS, Marshall MJ, Wang ZM, Watmough NJ, Fredrickson JK, Zachara JM, Butt JN, Richardson DJ.** 2011. Structure of a bacterial cell surface decaheme electron conduit. Proc. Natl. Acad. Sci. U. S. A. **108**:9384-9389.

27. **Okamoto A, Hashimoto K, Neilson KH, Nakamura R.** 2013. Rate enhancement of bacterial extracellular electron transport involves bound flavin semiquinones. *Proc. Natl. Acad. Sci. U. S. A.* **110**:7856-7861.
28. **Zheng M, Wang X, Templeton LJ, Smulski DR, LaRossa RA, Storz G.** 2001. DNA microarray-mediated transcriptional profiling of the *Escherichia coli* response to hydrogen peroxide. *J. Bacteriol.* **183**:4562-4570.
29. **Green J, Crack JC, Thomson AJ, LeBrun NE.** 2009. Bacterial sensors of oxygen. *Curr. Opin. Microbiol.* **12**:145-151.
30. **de Bruijn FJ, Rossbach S, Bruand C, Parrish JR.** 2006. A highly conserved *Sinorhizobium meliloti* operon is induced microaerobically via the FixLJ system and by nitric oxide (NO) via NnrR. *Environ Microbiol* **8**:1371-1381.
31. **Hou S, Freitas T, Larsen RW, Piatibratov M, Sivozhelezov V, Yamamoto A, Meleshkevitch EA, Zimmer M, Ordal GW, Alam M.** 2001. Globin-coupled sensors: a class of heme-containing sensors in Archaea and Bacteria. *Proc. Natl. Acad. Sci. U. S. A.* **98**:9353-9358.
32. **Rebbapragada A, Johnson MS, Harding GP, Zuccarelli AJ, Fletcher HM, Zhulin IB, Taylor BL.** 1997. The Aer protein and the serine chemoreceptor Tsr independently sense intracellular energy levels and transduce oxygen, redox, and energy signals for *Escherichia coli* behavior. *Proc. Natl. Acad. Sci. U. S. A.* **94**:10541-10546.
33. **Malpica R, Franco B, Rodriguez C, Kwon O, Georgellis D.** 2004. Identification of a quinone-sensitive redox switch in the ArcB sensor kinase. *Proc. Natl. Acad. Sci. U. S. A.* **101**:13318-13323.
34. **Moraghan JT, Buresh RJ.** 1977. Chemical reduction of nitrite and nitrous oxide by ferrous iron. *Soil Sci. Soc. Am. J.* **41**:47-50.
35. **Vancleemput O, Baert L.** 1983. Nitrite stability influenced by iron compounds. *Soil Biol. Biochem.* **15**:137-140.
36. **Abe M.** 2000. Ferrite plating: a chemical method preparing oxide magnetic films at 24-100 degrees C, and its applications. *Electrochim. Acta* **45**:3337-3343.
37. **Schüler D, Frankel R.** 1999. Bacterial magnetosomes: microbiology, biomineralization and biotechnological applications. *Appl. Microbiol. Biotechnol.* **52**:464-473.
38. **Imlay JA.** 2002. How oxygen damages microbes: Oxygen tolerance and obligate anaerobiosis. *Adv. Microb. Physiol.* **46**:111-153.

ACKNOWLEDGEMENTS

My first and sincere appreciation goes to Prof. Dr. Dirk Schüler, my supervisor for his continuous encouragement, help and support in all stages of my PhD studies. I would also like to thank him for helping me at the beginning of my study to get used to the life in Munich.

I would like to thank PD Dr. Susanne Gebhard for acting as the “Zweitgutachter”.

I would like to thank Prof. Stuart J. Ferguson, Dr. Shilpa Bali (University of Oxford), Prof. David Pignol, and Monique Sabaty (Aix-Marseille Université) for their fruitful collaborations.

I would also like to thank all the past and present members of the “Magnetolab” who are always willing to help me with experimental problems or difficulties in my daily life.

I am especially grateful to my office members, Dr. Emanuel Katzmann, Dr. René Uebe, and Felix Popp for their immense help to my personal and professional time in Munich. Also many thanks to Dr. Karen T. Silva and Oliver Raschdorf for reading, translating and correcting my thesis. Thank you!

I gratefully thank the funding source CSC program that made my PhD work possible.

I would like to thank all of my Chinese friends in Munich, especially Chong Fang for our time together in Munich.

Finally, and importantly, I would like to thank my parents, my younger sister, and my boyfriend Wenteng for their support, encouragement and unwavering love. Here I would like to express my appreciation in Chinese.

谢谢你们，我亲爱的爸爸，妈妈以及可爱的妹妹！是你们无私的爱给了我无限的勇气和动力。希望你们身体健康，万事如意！谢谢我亲爱的腾腾，谢谢你这十年的陪伴与照顾！希望我们未来的时光会更加美满幸福！

CURRICULUM VITAE

Personal data

Name: Li, Yingjie
Date of birth: 21.12.1982
Place of birth: Shandong, China
Nationality: Chinese
Family status: Single

Education

Since 10/2009

PhD studies in the research group of Prof. Dr. Dirk Schüler at the department of Biology, Microbiology, Ludwig-Maximilians-Universität München.

Topic of PhD thesis is “Oxygen regulation and redox control of magnetosome biomineralization in *Magnetospirillum gryphiswaldense*”.

09/2006-07/2009

Master studies in the research group of Prof. Dr. Weifeng Liu and Prof. Dr. Guanjun Chen, State Key Laboratory for Microbial Technology, Shandong University, Ji’nan.

Topic of Master thesis is “Mechanism of cellulose degradation in *Cytophaga hutchinsonii*”.

09/2002-07/2006

Bachelor studies at the department of Biology, Biotechnology, Shandong University, Ji’nan.

Publications

Li Y, Katzmann E, Borg S, Schüler D. 2012. The periplasmic nitrate reductase Nap is required for anaerobic growth and involved in redox control of magnetite biomineralization in *Magnetospirillum gryphiswaldense*. *J. Bacteriol.* **194**:4847-4856.

Li Y, Bali S, Borg S, Katzmann E, Ferguson SJ, Schüler D. 2013. Cytochrome *cd*₁ nitrite reductase NirS is involved in anaerobic magnetite biomineralization in *Magnetospirillum gryphiswaldense* and requires NirN for proper *d*₁ heme assembly. *J. Bacteriol.* **195**:4297-4309.

Li Y, Sabaty M, Borg S, Silva KT, Pignol D, Schüler D. 2014. The oxygen sensor MgFnr controls magnetite biomineralization by regulation of denitrification in *Magnetospirillum gryphiswaldense*. Submitted.

Li Y, Raschdorf O, Silva KT, Schüler D. 2014. The terminal oxidase *cbb*₃ functions as an O₂ sensor to control redox balance for magnetite biomineralization in *Magnetospirillum gryphiswaldense*. In preparation.

Posters and oral presentations

Li Y, Katzmann E, Schüler D. 2011. Denitrification is linked to magnetite biomineralization in *Magnetospirillum gryphiswaldense*. *Annual Conference of the Association for General and Applied Microbiology (VAAM)*, Karlsruhe (poster)

Li Y, Katzmann E, Borg S, Schüler D. 2012. Denitrification pathway is essential for complete functional magnetosome crystals for magnetic orientation in *Magnetospirillum gryphiswaldense*. *Annual Conference of the Association for General and Applied Microbiology (VAAM)*, Tübingen (poster)

Li Y, Katzmann E, Borg S, and Schüler D. 2012. A complete denitrification pathway is required for the biomineralization of functional magnetite crystals in *Magnetospirillum gryphiswaldense*. The 3rd International Magnetotactic Bacteria Meeting (MTB2012), Berkeley (oral presentation)

Li Y, Bali S, Borg S, Katzmann E, Ferguson SJ, Schüler D. 2013. A complete denitrification pathway is required for the biomineralization of functional magnetite crystals in *Magnetospirillum gryphiswaldense*. The 18th European Nitrogen Cycle Meeting, Darmstadt (oral presentation)

Declaration / Eidesstattliche Versicherung

Hiermit versichere ich, an Eidesstatt dass ich die vorliegende Arbeit selbständig und nur unter Verwendung der angegebenen Hilfsmittel und Quellen angefertigt habe. Der Autor hat zuvor nicht versucht, anderweitig eine Dissertation einzureichen oder sich einer Doktorprüfung zu unterziehen. Die Dissertation wurde keiner weiteren Prüfungskommission weder in Teilen noch als Ganzes vorgelegt.

München, 24th February 2014

Yingjie Li